UNIVERSIDAD DE GRANADA

FACULTAD DE FARMACIA

Departamento de Farmacología

Programa Oficial de Posgrado de Medicina Clínica y Salud Pública

Role of peroxisome proliferator activated receptor beta/delta (PPARβ/δ) agonists in the treatment of the vascular alterations in different experimental models of metabolic syndrome

Tesis Doctoral para aspirar al Grado de Doctor presentada por

Marta Toral Jiménez

Granada, 2017

Editor: Universidad de Granada. Tesis Doctorales
Autora: Marta Toral Jiménez
ISBN: 978-84-9163-170-5
URI: http://hdl.handle.net/10481/45938

UNIVERSIDAD DE GRANADA

FACULTAD DE FARMACIA

Departamento de Farmacología

Programa Oficial de Posgrado de Medicina Clínica y Salud Pública

Role of peroxisome proliferator activated receptor beta/delta (PPARβ/δ) agonists in the treatment of the vascular alterations in different experimental models of metabolic syndrome

Tesis Doctoral para aspirar al Grado de Doctor presentada por

Marta Toral Jiménez

Bajo la dirección de los Doctores:

Juan Manuel Duarte Pérez

Julio Juan Gálvez Peralta

Miguel Romero Pérez

Granada, 2017

Universidad de Granada

La Doctoranda Marta Toral Jiménez y los directores de la Tesis Juan Manuel Duarte Pérez, Julio Juan Gálvez Peralta y Miguel Romero Pérez garantizamos, al firmar esta Tesis Doctoral, que el trabajo ha sido realizado por la doctoranda bajo la dirección de los directores de la tesis y hasta donde nuestro conocimiento alcanza, en la realización del trabajo, se han respetado los derechos de otros autores a ser citados, cuando se han utilizado sus resultados o publicaciones.

Granada, 1 de Febrero de 2017

Director/es de la Tesis

Fdo.: Juan Manuel Duarte Pérez

Doctoranda

Fdo.: Marta Toral Jiménez

Fdo.: Julio Juan Gálvez Peralta

Fdo.: Miguel Romero Pérez

´

A mi Madre…

“Si os apasiona la ciencia haceros científicos. No penséis lo que va a ser de vosotros. Si trabajáis firme y con entusiasmo, la ciencia llenará vuestra vida”.

Severo Ochoa

INDEX

INDEX

FIGURE INDEX

TABLE INDEX

ABBREVIATIONS

ABBREVIATIONS

A23187
Calcium ionophore calimycin

ABCG1
ATP-binding cassette transporter G1

ABCA1
ATP-binding cassette transporter A1

ACh
Acetylcholine

Akt
Protein kinase B

AMPK
5′-adenosine monophosphate-activated protein kinase

AngII
Angiotensin II

AP-1
Activated protein-1

Apo
Apolipoprotein

Apo $E^{-/-}$
Apolipoprotein E deficient

AT1
Angiotensin II receptor type 1

ATF
Activating transcription factor

AU
Arbitrary units

AUC
Area under curve

BP
Blood pressure

BH_4
Tetrahydrobiopterin

BiP
Binding immunoglobulin protein

BSA
Bovine serum albumin

Ca^{2+}
Calcium

Cav-1
Caveolin-1

CCCP
Carbonyl cyanide m-chlorophenylhydrazone

cGMP
Cyclic guanosine monophosphate

CHOP
CCAAT/enhancer binding protein homologous protein

CM-H2DCFDA
5-(and-6) chloromethyl-2'-7'-dichlorodihydrofluorescein diacetate

CPT-1
Carnitine palmitoyl-transferase-1

Cu/ZnSOD
Copper/zinc superoxide dismutase

CVD
Cardiovascular diseases

DAF-2
Diaminofluorescein-2

db/db
Diabetic

DAG
Diacylglycerol

DAPI
4,6-diamidino-2-phenylindole dichlorohydrate

DHE
Dihydroethidium

DOCA
Deoxicorticosterone acetate

DMEM
Dulbecco's modified Eagle's médium

DMSO
Dimethylsulfoxide

DTPA
Diethylenetriaminepenta-acetic acid

EC
Endothelial cells

EC_{50}
Half maximal effective concentration

EDCF
Endothelium-derived contracting factors

EDHF
Endothelium-derived hyperpolarizing factor

eNOS
Endothelial nitric oxide synthase

ER
Endoplasmic reticulum

ERAD
ER-associated degradation

ERK
Extracellular-regulated kinase

ET-1
Endothelin-1

eIF2α
Eukaryotic initiation factor 2α

FBS
Fetal bovine serum

FFA
Free fatty acids

GADPH
Glyceraldehyde-3-phosphate dehydrogenase

GPx-1
Glutathione peroxidase-1

GTT
Glucose tolerance test

HDL
High-density lipoprotein

HEPES
4-(2-hydroxyethyl)-1-piperazineethanesulfonic acid

15-HETE
15-hydroxyeicosatetraenoic acid

HFD
High-fat diet

HOMA-IR
Homeostatic model assessment of insulin resistance

HO-1
Hemo-oxigenase-1

HUVEC
Human umbilical vein endothelial cells

ICAM-1
Intercellular adhesion molecule-1

IL
Interleukin

ip
Intraperitoneally

IR
Insulin resistance

IRE-1α
Inositol-requiring transmembrane kinase/endonuclease-1α

IRS-1
Insulin receptor substrate-1

JNK
c-Jun N-terminal kinase

KHS
Krebs–Henseleit solution

LDL
Low-density lipoprotein

LDLR$^{-/-}$
Low-density lipoprotein receptor knockout

L-NAME
N^G-nitro-L-arginine methyl ester

LPS
Lipopolysaccharides

MABP
Mean arterial blood pressure

MAEC
Mouse aortic endothelial cells

MAM
Mitochondria-associated ER membranes

MAPK
Mitogen-activated protein kinase

MCP-1
Monocyte chemoattractant protein-1

Mfn2
Mitofusin-2

mg/kg/d
mg kg^{-1} per day

MitoQ
Mitoquinone

MnSOD
Manganese superoxide dismutase

mRNA
Messenger RNA

MS
Metabolic syndrome

NADPH
Nicotinamide adenine dinucleotide phosphate

NCoR
Nuclear receptor co-repressor

NFAT
Nuclear factor of activated T cells

NF-κB
Nuclear factor-κB

NIH
National Institutes of Health

NO
Nitric oxide

O_2^-
Superoxide

ob/ob
Obese

2-OH-E^+
2-hydroxyethidium

$ONOO^-$
Peroxynitrite

PAGE
Polyacrilamide gel electrophoresis

4-PBA
4-phenyl butyric acid

PBS
Phosphate-buffered saline

PKC
Protein kinase C

PDK-4
Pyruvate dehydrogenase kinase- 4

PEG-SOD
Pegylated superoxide dismutase

PERK
Eukaryotic translation initiation factor-2α kinase 3

PGA1
Prostaglandin A1

PGD2
Prostaglandin D2

PGs
Prostaglandins

PKC
Phosphorylation of protein kinase C

Phe
Phenylephrine

PI3K
Phosphatidylinositide 3-kinase

PMSF
Phenylmethysulfonyl fluoride

PPAR
Peroxisome proliferator activated receptors

PPARα
PPAR alpha

PPARβ/δ
PPAR beta/delta

PPARγ
PPAR gamma

PPRE
Peroxisome proliferator-response elements

RAS
Renin-angiotensin system

RLU
Relative luminescence units

ROS
Reactive oxygen species

RPL13a
Ribosomal protein L13a

rpm
Revolutions per minute

RT-PCR
Reverse transcriptase-PCR

RXR
9-cis-retinoic acid receptor

SBP
Systolic blood pressure

SDS
Sodium dodecyl sulphate

SERCA
Sarco/endoplasmic reticulum Ca^{2+} ATPase

SHR
Spontaneously hypertensive rats

siRNA
Small interfering RNA

SNP
Nitroprusside sodium

SNPs
Single nucleotide polymorphisms

SNS
Sympathetic nervous system

STAT3
Signal transducer and activator of transcription 3

STZ
Streptozotocin

SUMO
Small ubiquitin-like modifiers

sXBP1
Spliced X-box binding protein 1

T2DM
Type 2 diabetes mellitus

TTFA
Thenoyltrifluoroacetone

TG
Triglycerides

TLR4
Toll-like receptor 4

TNF-α
Tumor necrosis factor-α

TUDCA
Tauroursodeoxycholic acid

UCP2
Uncoupling protein-2

UPR
Unfolded protein response

VCAM-1
Vascular cell adhesion molecule-1

VLDL
Very low density lipoprotein

VSMC
Vascular smooth muscle cells

WKY
Wistar-Kyoto

XBP1
X-box binding protein 1

XBP1s
spliced X-box binding protein 1

RESUMEN

RESUMEN

La disfunción endotelial desempeña un papel clave en el riesgo de desarrollo de enfermedad cardiovascular inducido por uno de los componentes esenciales del síndrome metabólico, la obesidad. El **objetivo general** de esta Tesis Doctoral es analizar el efecto del compuesto GW0742, agonista de receptores activados por proliferador de peroxisomas beta/delta (PPARβ/δ), sobre la función endotelial en un modelo experimental de síndrome metabólico en ratón obeso inducido por una dieta rica en grasa (HFD, *high-fat diet*). Para alcanzar este objetivo se han realizado varios experimentos:

1. Estudiar el efecto in vivo de la administración crónica de GW0742

Se han utilizado ratones macho de 5 semanas de edad que fueron divididos aleatoriamente en los siguientes grupos: control, control tratado con GW0742 (3mg/kg/día, mediante sonda gastroesofágica), ratones que consumen HFD, HFD-GW0742, HFD más el antagonista de PPARβ/δ, GSK0660 (1mg/kg/día, intraperitoneal) o HFD-GW0742-GSK0660. Los tratamientos se mantuvieron durante 11 ó 13 semanas. Los resultados mostraron que la administración de GW0742 previene la menor vasodilatación dependiente de endotelio y de óxido nítrico (NO, *nitric oxide*) inducida por acetilcolina (ACh, *acetylcholine*) en los anillos aórticos de los ratones que consumen HFD. Además, el GW0742 incrementa la fosforilación de protein cinasa B (Akt, *protein kinase B*) y óxido nítrico sintasa endotelial (eNOS, *endothelial nitric oxide synthase),* e inhibe el incremento de la interacción caveolina-1/eNOS, la fluorescencia de etidio, la expresión de NOX-1, del receptor tipo Toll 4 (TLR4, *Toll-like receptor 4*), factor de necrosis tumoral-α (TNF-α, *tumor necrosis factor-α*) e interleucina-6 (IL-6, interleukin-6), y la fosforilación de IκB-α en la aorta del grupo HFD. Estos cambios vasculares se acompañan con la prevención de la ganancia de peso, la hipertensión, la hipertrofia cardiaca y renal, y la acumulación de grasa inducida por el consumo de HFD. Este compuesto también suprime el incremento de los niveles plasmáticos de glucosa y triglicéridos (TG, *triglycerides*), la intolerancia a la

glucosa y la resistencia a la insulina (determinado mediante el cálculo de HOMA-IR, *homeostatic model assessment of insulin resistance*) inducidos por la HFD. El GW0742 incrementa los niveles plasmáticos de lipoproteínas de alta densidad (colesterol HDL, *high-density lipoprotein*) y restaura los niveles de TNF-α y adiponectina en la grasa. El GSK0660 previene todos los cambios inducidos por GW0742. Se concluye que la activación PPARβ/δ reduce la obesidad y ejerce efectos protectores sobre la hipertensión y sobre manifestaciones tempranas de la aterosclerosis, incluyendo la disfunción endotelial y el estado pro-oxidante y pro-inflamatorio vascular en ratones que consumen HFD.

2. Estudiar los efectos del GW0742, independientes de sus efectos metabólicos sistémicos, sobre la disfunción endotelial inducida por lípidos

Un aumento de especies reactivas de oxígeno (ROS, *reactive oxygen species*) y una reducida biodisponibilidad de NO están involucrados en la disfunción endotelial inducida por los ácidos grasos. En esta Tesis se demuestra que en células endoteliales de aorta de ratón (MAEC, *mouse aortic endothelial cells*) el GW0742 previene la disminución de la producción de NO estimulada por el ionóforo de calcio A23187 y de la fosforilación de la eNOS en la Ser^{1177}, y el incremento de los niveles intracelulares de ROS causados por la exposición a palmitato *in vitro*. Este agonista PPARβ/δ también restaura la relajación dependiente de endotelio inducida por ACh en aorta de ratón incubada con palmitato. *In vivo*, el tratamiento durante 3 semanas con GW0742 (3mg/kg/día) previene la reducción de la relajación de ACh y de la fosforilación de eNOS en la Ser^{1177}, y el incremento de la producción de ROS y de la actividad del sistema nicotinamín adenín dinucleótido fosfato (NADPH, *nicotinamide adenine dinucleotide phosphate*) oxidasa en la aorta de ratones que consumen una HFD. El antagonista de PPARβ/δ GSK0660 suprimió todos los efectos protectores inducidos por el GW0742. El GW0742 aumenta la expresión vascular de carnitina palmitoil transferasa-1 (CPT-1, *carnitine palmitoyltransferase-1*). Los efectos del GW0742 sobre la relajación inducida por ACh en aorta y sobre la producción de NO y ROS en MAEC expuestas a palmitato se suprimen por el inhibidor de CPT-1 etomoxir

y por silenciamiento de CPT-1. El GW0742 también inhibe el aumento de diacilgicerol (DAG, *diacylglycerol*), la activación de la protein cinasa Cα/βII (PKCα/βII, *protein kinase Cα/βII*) y la fosforilación de eNOS en la Thr^{495} inducido por palmitato en MAEC, efectos que se suprimen con etomoxir. Todos estos hallazgos indican que la activación PPARβ/δ abole la disfunción endotelial inducida por lípidos por una sobreexpresión de CPT-1 en las MAEC, lo que reduce la acumulación de DAG y la subsiguiente producción de ROS e inhibición de la eNOS mediada por PKC.

La resistencia a insulina inducida por ácidos grasos en células endoteliales se caracteriza por un aumento de ROS y una reducida biodisponibilidad de NO. En esta Tesis se demuestra que, en células endoteliales de vena de cordón umbilical humano (HUVEC, *human umbilical vein endothelial cells*), el GW0742 previene la disminución de la producción de NO y de la fosforilación de la eNOS en la Ser^{1177} estimulada por insulina, y el incremento de los niveles intracelulares de ROS causados por la exposición a palmitato *in vitro*. Los efectos protectores del GW0742 se suprimen tanto por el antagonista PPARβ/δ GSK0660 como por el inhibidor de CPT-1 etomoxir. De todo ello se concluye que la activación PPARβ/δ *in vitro* previene el deterioro de la señalización de la insulina inducida por palmitato, lo que conduce a un aumento de la producción de NO estimulada por insulina en HUVEC. Este efecto protector podría ser debido al aumento de la expresión de CPT-1, que normaliza la producción de ROS y restaura la vía de señalización de la insulina IRS (*insulin receptor substrate*)-Akt-eNOS.

3. Estudiar los efectos del GW0742 sobre la disfunción endotelial inducida por lipopolisacarido (LPS, lipopolysaccharides)

La endotoxina bacteriana LPS activa vías inflamatorias, induce la expresión de citocinas en el endotelio, aumenta la producción de ROS en la pared vascular e induce disfunción endotelial. Los niveles plasmáticos de LPS están aumentados en individuos obesos y en ratones con obesidad inducida por HFD (endotoxemia metabólica). El tratamiento crónico con GW0742 no modifica los niveles plasmáticos de LPS. En esta Tesis también hemos analizado si la activación PPARβ/δ modifica la inflamación, el

estrés oxidativo y la disfunción endotelial inducidos por LPS en ratón. Se ha encontrado que el tratamiento *in vivo* con GW0742 previene la reducción de la relajación dependiente de endotelio, el incremento de la producción vascular de ROS, la regulación al alza de los niveles vasculares de mRNA de NOX-1, NOX-2, $p47^{phox}$ y $p22^{phox}$, y de los marcadores de estrés de retículo endoplasmático (ER, *endoplasmic reticulum*) inducidos por LPS en ratón. En MAEC, el GW0742 previene la disminución de la producción de NO estimulada por A23187 y el incremento de los niveles intracelulares de ROS causados por la exposición a LPS *in vitro*. El antagonista de PPARβ/δ GSK0660 suprime todos los efectos protectores *in vivo* e *in vitro* provocados por el GW0742. Este agonista también normalizó la reducida expresión de la proteína desacoplante-2 (UCP2, *uncoupling protein-2*) y de la proteína de fusión mitocondrial, mitofusin-2, inducida por LPS. Los efectos del GW0742 sobre la producción de NO y de ROS en MAEC expuestas a LPS se suprimen por el inhibidor de UCP2 genipín y por el silenciamiento de UCP2. El genipín también suprime los cambios en la expresión de las subunidades de la NADPH oxidasa y de los marcadores de estrés del ER inducidos por GW0742. En conjunto se observa que la activación PPARβ/δ reduce la disfunción endotelial inducida por LPS mediante la regulación al alza de UCP2 endotelial, con la subsiguiente inhibición del estrés del ER y de la actividad NADPH oxidasa, lo que conduce a la reducción de la producción de ROS y al aumento de la biodisponibilidad de NO.

Todos estos experimentos indican que la activación de PPARβ/δ previene la aparición de uno de los acontecimientos iniciales en el desarrollo de la placa de ateroma, la disfunción endotelial. La aterogénesis es la base patológica sobre la que se sustenta la enfermedad cardiovascular (angina, infarto), que es primera causa de muerte de los pacientes con síndrome metabólico. La mejora de factores que deterioran la función endotelial, tales como parámetros metabólicos sistémicos (hiperglucemia, intolerancia a la glucosa, HOMA-IR, trigliceridemia, niveles de HDL), citocinas pro-inflamatorias y presión arterial elevada contribuye a este efecto protector en situación de obesidad. Además, la activación PPARβ/δ en el lecho vascular

(acciones vasculares directas) también está involucrada en la mejora de la disfunción endotelial asociada al síndrome metabólico. Así, el incremento de la oxidación de ácidos grasos en el endotelio, mediada por el gen diana de PPARβ/δ, CPT-1, mejora no solo la respuesta relajante inducida por activación calcio-dependiente de eNOS, sino también la producción de NO provocada por fosforilación de la eNOS mediante insulina. La activación de otro gen PPARβ/δ como el UCP2 protege al endotelio del efecto deletéreo de la endotoxemia metabólica.

Estos hallazgos sugieren que los agonistas PPARβ/δ, como el GW0742, poseen un potencial terapéutico en la prevención de la disfunción endotelial, y en consecuencia de la enfermedad cardiovascular, en situaciones de obesidad.

INTRODUCTION

INTRODUCTION

1. Metabolic syndrome

1.1. Definition

Hypertension, diabetes and obesity are common cardiovascular risk factors, but not independent in humans and their combination is referred to as metabolic syndrome (MS) (Panchal and Brown, 2011).

The term MS was originally coined in 1970s (Jay and Ren, 2007) and also is recognized by other names such as MS X, cardio-MS, syndrome X, insulin resistance (IR) syndrome (Grewal *et al.,* 2016).

Since it was first described in the 1920s, the MS has appeared to be one of the most important problems of worldwide public health in the 21st century, taking into account its growing prevalence in developed and developing countries (Eckel *et al.,* 2010). The MS, which clusters as the main metabolic abnormalities central obesity, low concentrations of plasma high-density lipoprotein (HDL)-cholesterol, high levels of triglycerides (TG), hypertension and hyperglycemia, together with IR (Grundy *et al.,* 2005; Grundy, 2008; Bruce and Byrne, 2009), is associated with an increased risk of both cardiovascular diseases (CVD) (Kaur, 2014) and type 2 diabetes mellitus (T2DM) (Grundy *et al.,* 2004).

Many definitions of this syndrome have been proposed by different health organizations (Table 1) during all these years, and although they provide different clinical and epidemiological criteria to identify the components of the metabolic disturbances that are clustered in this syndrome, they agree on its core components (Azhar, 2010).

Table 1. Historical definitions of the metabolic syndrome.

	Definition	Central obesity	Dyslipidemia	Blood pressure	Renal dysfunction	Fasting plasma glucose	Reference
WHO (1998)	High insulin levels, IFG or IGT and two or more of the following:	WHR > 0.9 (men) 0.85> (women) or BMI >30 kg/m^2	TG ≥150 mg/dL HDL<35 mg/dL (men) HDL<39 mg/dL (women)	≥140/90 mmHg	Urinary albumin excretion rate ≥20µg/min or albumin: creatine ratio ≥30 mg/kg	-	Alberti and Zimmet, 1998
EGIR (1999)	Top 25% of the fasting insulin values among nondiabetic individuals and two or more of the following:	WC ≥94 cm (men), ≥80 cm (women)	TG ≥20 mmol/L and HDL< 1.0 mg/dL	≥140/90 mmHg or antihypertensive medication	-	≥ 6.1 mmol/L	Balkau and Charles, 1999
NCEP-ATPIII (2001, 2004 and 2005)	Three or more of the following:	WC ≥ 102 cm (40 men), ≥88 cm (35 women)	TG ≥150 mg/dL or HDL<40 mg/dL (men), HDL<50 mg/dL (women)	≥130/85 mmHg	-	≥110 mg/dL†	Grundy *et al.*, 2004 Grundy *et al.*, 2005
AACE-ACE (2003)	IGT and two or more of the following:	-	TG ≥150 mg/dL or HDL<40 mg/dL (men), HDL<50 mg/dL (women)	≥130/85 mmHg	-	-	Einhorn *et al.*, 2003
IDF (2005)	Central obesity as defined by ethnic/racial, specific WC and two or more of the following:	-	TG ≥150 mg/dL or specific treatment for this abnormality HDL<40 mg/dL (men), HDL<50 mg/dL(women) or specific treatment for this abnormality	≥130/85 mmHg or treatment of previously diagnosed hypertension	-	≥100 mg/dL	Alberti *et al.*, 2005

† 2003, the American Diabetic Association changed the criteria for IFG from ≥110 to <100mg/dL. Abbreviations: AACE-ACE: The American Association of Clinical Endocrinologists-American College of Endocrinology; BMI: body mass index; EGIR: The European Group for the Study of Insulin Resistance; HDL: high-density lipoprotein; IDF: The International Diabetes Federation; IGF: Impaired fasting glucose; IGT: Impaired glucose tolerance; NCEP-ATPIII: The National Cholesterol Education Program Adult Treatment Panel III; TG: triglycerides; WC: Waist circumference; WHO: World Health Organization; WHR: Waist hip ratio (table modified from Azhar, 2010).

Currently, prevalence of this syndrome is increasing dramatically, not only in adult or older populations (Meigs *et al.,* 2003; Ford *et al.,* 2004), but also in children and young people (Cook *et al.,* 2003; Weiss *et al.,* 2004), running in parallel with the worldwide epidemic of obesity and diabetes (Zimmet *et al.,* 2001). Because of the elevated risk it presents of developing CVD and T2DM, the MS has become an important public health problem that demands urgent therapeutic attention and interventional approaches (Alberti *et al.,* 2009).

The MS occurs commonly throughout the world, ranging in prevalence from 10% to 40% (Grundy, 2008). This syndrome is present most often in populations characterized by excessive nutrient intake and physical inactivity (Alberti *et al.,* 2009), but underlying metabolic and genetic susceptibilities are critical factors as well.

Nowadays, several attempts have been made to develop a clinical definition of the MS, the most commonly accepted is a recent consensus definition, which includes abdominal obesity as a key (but not necessary) component, elevations in serum TG and glucose, increased BP, and reduced levels of HDL-cholesterol. The presence of three or more of these constitutes a clinical diagnosis of MS (Grundy, 2016) (Table 2).

Table 2. Criteria for clinical diagnosis of metabolic syndrome.

	Categorical cut points
Increased waist circumference*	Population-specific and country specific definitions
Increased TG (drug treatment for elevated TG alternate indicator†)	≥150 mg/dL (1.7 mmol/L)
Reduced HDL-cholesterol (drug treatment for reduced HDL-cholesterol is alternative indicator†)	<40 mg/dL (1.0 mmol/L) in men; <50 mg/dL (1.3 mmol/L) in women
Increased BP (antihypertensive drug treatment in patient with history of hypertension is alternative indicator)	Systolic ≥130 and/or diastolic ≥85 mmHg
Increased fasting glucose‡ (drug treatment of increased glucose is alternative indicator)	>100 mg/dL (5.5 mmol/L)

**It is recommended that the IDF cut points be used for non-Europeans and either the IDF or AHA/NHLBI cut points used for people of European origin until more date are available. †Most commonly used drugs for increased TG and reduced HDL cholesterol are fibrates and nicotic acid. A patient on one of these drugs can be presumed to have high TG and low HDL. Use of high-dose ω-3 fatty acids presumes high TG. ‡Most patients with type 2 diabetes will have the metabolic syndrome by the proposed criteria. Abbreviations: AHA/NHLBI: The American Heart Association and the National Heart, Lung, and Blood Institute; BP: blood pressure; HDL: high-density lipoprotein; IDF: The International Diabetes Federation; TG: triglycerides (table modified from Eckel et al., 2010; Grundy, 2016).*

1.2. Pathogenesis

The pathogenesis of the MS is complex and not fully elucidated. Central obesity and adipose tissue disorders together with IR appear to stand out as the main potential etiologic factors (Grundy *et al.,* 2004; Licata *et al.,* 2006; Meshkani and Adeli, 2009), although other causes that play a main role in the development of MS include genetic profile and other acquired factors such as physical inactivity, ageing, pro-inflammatory and pro-thrombotic states and hormonal dysregulation (Kaur, 2014).

The MS consists of five factors: atherogenic dyslipidemia, elevated BP, IR resulting in hyperglycemia, a pro-thrombotic state, and a pro-inflammatory state. All often are commonly present in in obese subjects (Grundy, 2016) (Figure 1).

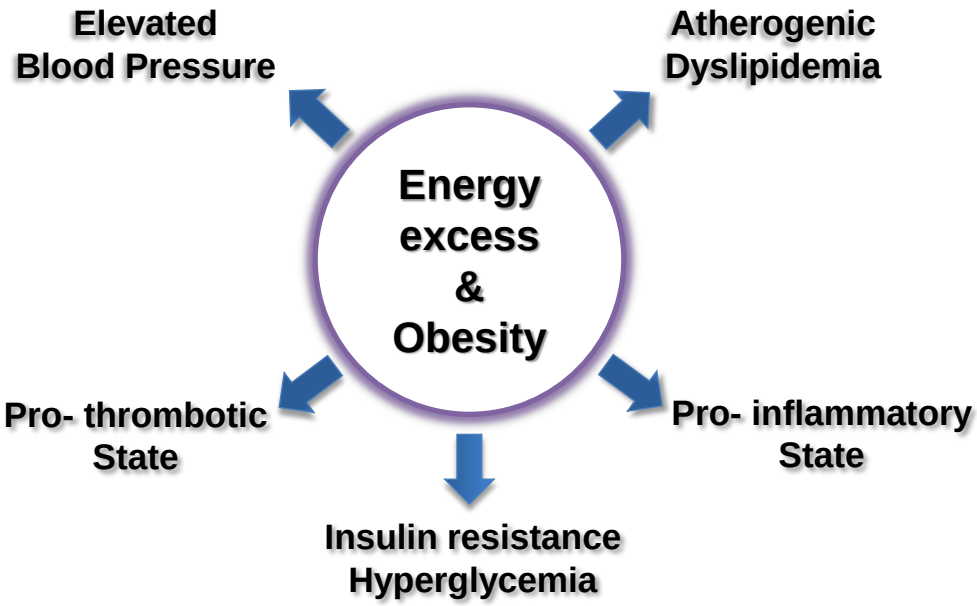

Figure 1. Relation between energy excess/obesity and risk factors of the metabolic syndrome *(modified from Grundy, 2016).*

The contribution of each of these components to cardiovascular risk indubitably varies among individuals but, in combination, they double the risk for atherosclerotic CVD (Grundy, 2016).

In addition, it has been reported that this pathology is often associated to non-alcoholic fatty liver disease (Khashab *et al.,* 2008), polycystic ovary syndrome (Apridonidze *et al.,* 2005), cholesterol gallstone (Grundy, 2008), protease inhibitor therapy for HIV (Jerico *et al.,* 2005) and cancer (Pothiwala *et al.,* 2009).

1.2.1. Features of the metabolic syndrome

a) Atherogenic dyslipidemia

Most individuals with MS show atherogenic dyslipidemia, characterized by low levels of HDL-cholesterol and high concentration of TG in plasma, a profile that constitutes an important risk factor for CVD. The major component of atherogenic dyslipidemia is elevation of apolipoprotein (Apo)-B containing lipoproteins. These include elevated levels of low-density lipoprotein (LDL), and very low density lipoprotein (VLDL) (Kaur, 2014; Grundy, 2016).

b) Elevated blood pressure

Hypertension is another core component of the MS and an important risk factor for coronary heart disease, stroke, and renal disease (Chobanian *et al.,* 2003). Essential hypertension is frequently associated with the several metabolic abnormalities, of which obesity, glucose intolerance, and dyslipidemia are the most common (Bruce and Byrne, 2009). Different studies suggest that both hyperglycemia and hyperinsulinemia activate the renin-angiotensin system (RAS) by increasing the expression of angiotensinogen and angiotensin II (AngII) (Malhotra *et al.,* 2001). There is also evidence that IR and hyperinsulinemia lead to sympathetic nervous system (SNS) activation, and, as a result, the kidneys increase sodium reabsorption, the heart

increases cardiac output, and arteries respond with vasoconstriction resulting in hypertension (Morse *et al.,* 2005). It has been recently discovered that adipocytes also produce aldosterone in response to AngII (Briones *et al.,* 2012). In this regard, the adipocyte may be considered a miniature renin-angiotensin aldosterone system.

c) Pro-inflammatory state

Elevated levels of inflammatory markers, including pro-inflammatory cytokines, support the implication of an inflammatory state in the MS. Among acute phase response markers and inflammatory cytokines, interleukin (IL)-6, C-reactive protein and tumor necrosis factor-α (TNF-α) have been directly related to the MS and most of its features, i.e., obesity and IR (Matsuzawa *et al.,* 2004; Dandona *et al.,* 2005; Khera *et al.,* 2009). A link between inflammation and metabolic diseases has been increasingly recognized. In fact, obesity may underlie a low-grade systemic inflammation where macrophages invade excess adipose tissue, resulting in the release of cytokines and promoting systemic inflammation (Weisberg *et al.,* 2006; Lumeng and Saltiel, 2011; Johnson *et al.,* 2012). Although an excess of adipose tissue *per se* may be responsible for low-grade inflammation, overnutrition independent of obesity may also engender inflammatory responses (Tam *et al.,* 2010; Laugerette *et al.,* 2014). Cytokines released from adipose tissue may induce IR in skeletal muscle (Wieser *et al.,* 2013), alter the pituitary-adrenal axis, and may accelerate loss of pancreatic β-cells (Oh *et al.,* 2011). Finally, low-grade inflammation within atherosclerotic lesions may increase the probability of plaque rupture, causing acute CVD (Libby *et al.,* 2002).

Recent studies have established a hypothesis to explain MS pathogenesis from a pro-inflammatory state that induces IR and leads to clinical and biochemical manifestations of the MS. This resistance to insulin action promotes inflammation further through an increase in free fatty acids (FFA) concentration and interference with the anti-inflammatory effect of insulin (Dandona *et al.,* 2005, Galisteo *et al.,* 2008).

d) Hyperglycemia/ Insulin resistance

As another main component and causative factor of the MS, IR, accompanied or not by hyperglycemia, is an essential target in the therapeutic approach of this syndrome (Grundy, 2012). The primary cause of hyperglycemia in patients with MS is IR which is defined as the failure of cells to respond normally to insulin's glucose-lowering effects, resulting in hyperglycemia (Rieusset, 2015).

e) Pro-thrombotic state

Individuals with obesity and MS appear to have multiple abnormalities in the hemostatic system that may well predispose to atherosclerotic CVD. Among these are endothelial dysfunction, enhanced coagulation, impaired fibrinolysis, and platelet dysfunction (Alessi and Juhan-Vague, 2006; Kostapanos *et al.,* 2013). Specific abnormalities include elevated levels of inhibitor of plasminogen activator type 1 (Kraja *et al.,* 2007), tissue factor (Samad and Ruf, 2013; Rao *et al.,* 2014), fibrinogen (Kraja *et al.,* 2007) and factor VII and VIII activity (Ay *et al.,* 2007). Finally, it seems likely that patients with this syndrome are higher risk for venous thrombosis (Ay *et al.,* 2007).

1.3. Cardiovascular and metabolic alterations in metabolic syndrome

During the past two decades, considerable attention has been given to the clustering of cardiovascular risk factors and metabolic abnormalities that markedly increase the risk for development of T2DM and CVD (Azhar, 2010).

1.3.1. Metabolic endotoxemia

Recent evidences have shown that obesity is associated with metabolic disorders in multiple tissues, which contribute to the progression of IR and the MS.

It has been demonstrated that an excess of dietary lipid intake not only increases systemic exposure to potential pro-inflammatory FFA and their derivatives, but, more

specifically, facilitates the absorption of endotoxins, leading to higher lipopolysaccharides (LPS) plasma levels, defined as 'metabolic endotoxemia' (Cani *et al.,* 2007). In this way, the gut microbiota appears to be involved in the development of obesity and related metabolic disorders (Turnbaugh *et al.,* 2006; Turnbaugh *et al.,* 2009). Particularly, specific compounds derived from the gut microbiota, such as LPS from Gram-negative bacteria, could act as triggers in the development of IR, T2DM and inflammation (Cani *et al.,* 2007; Cani *et al.,* 2008; Cani *et al.,* 2009).

A moderate increase in the plasma concentration of the inflammatory mediator LPS occurs during a fat-enriched diet (Cani *et al.,* 2007). In turn, this low-grade chronic systemic inflammation initiates IR (Cani *et al.,* 2007). In fact, it has been shown that the strategies that reduce endotoxemia or impair LPS/ toll-like receptor 4 (TLR4) signaling are able to improve glucose homoeostasis (Cani *et al.,* 2007; Cani *et al.,* 2008).

In addition, an increase in intestinal permeability has been proposed as a crucial mechanism in the development of metabolic endotoxemia (Brun *et al.,* 2007; Cani *et al.,* 2007; Cani *et al.,* 2008). Thus, obese mice exhibit an altered gut barrier, characterized by the disruption of tight-junction proteins between epithelial cells. Among the mechanisms involved in this phenomenon, excessive TNF-α production was proposed to help to propagate the extension of local inflammation, which would trigger the alteration of tight-junction proteins (Mazzon and Cuzzocrea, 2008).

Besides, increased expression of pro-inflammatory markers has been observed in visceral and subcutaneous adipose tissue of lean mice after chronic low dose LPS injection, with concomitant increases in weight gain, visceral and subcutaneous adipose tissue size, and increased liver weight (Cani *et al.,* 2007). Furthermore, LPS can initiate systemic and local inflammation and also result in reactive oxygen species (ROS) production upon binding with TLR4 and subsequent activation of nuclear factor-κB (NF-κB) (Asehnoune *et al.,* 2004; Lu *et al.,* 2008). TLR4 is abundant on immune cells, liver (Gustot *et al.,* 2006), adipose tissue (Song *et al.,* 2006) and skeletal muscle (Frost *et al.,* 2002). Collectively, these tissues play an important role in the regulation of glucose and lipid homeostasis, and it has been demonstrated that pro-inflammatory

cytokines and ROS production interfere with normal metabolism in these tissues (Boutagy *et al.,* 2016).

Finally, in a series of studies, such as Toral *et al.* (2014) showed that the changes induced in the gut microbiota by the chronic consumption of a probiotic, *Lactobacillus coryniformis,* in high-fat diet (HFD)-fed mice in favor of *Lactobacillus* spp. are associated with a significant improvement in gut inflammation and gut barrier disruption, as shown by the increase in the intestinal mucus glycoprotein mucin-3 and tight-junction protein expression, thus, promoting a healthier microvilli environment, which is correlated with lower plasma LPS levels (Figure 2).

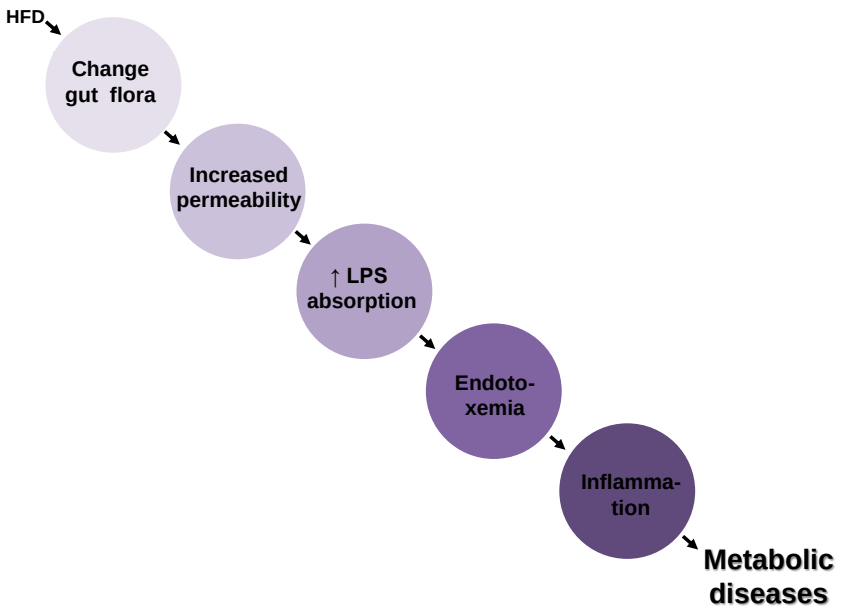

Figure 2. Scheme representing the mechanisms involved in bacteria-induced metabolic disease. *Excessive high-fat feeding changes intestinal microflora. This is associated with an increased intestinal permeability. Consequently, endotoxemia increases and triggers inflammation and metabolic disorders. Abbreviations: HFD: high-fat diet; LPS: lipopolysaccharides.*

1.3.2. Endoplasmic reticulum stress

The link among metabolism, inflammation, and endoplasmic reticulum (ER) stress is not surprising when one considers how the function of each intersects with the others. All three processes are tightly regulated adaptive responses that are fundamental to survival and dependent on the availability of sufficient energy for appropriate function (Hummasti and Hotamisligi, 2010).

It is now evident that the ER is an organelle impaired in MS. This organelle plays a major role in calcium (Ca^{2+}) homeostasis, and the synthesis, maturation and folding of both secretory and membrane proteins. However, when the folding capacity of the ER cannot cope with the high load of unfolded and misfolded proteins, ER homeostasis is disturbed and the ER sets up a physiological process termed ER stress, which leads to activation of the unfolded protein response (UPR) pathway, which aims to reduce protein synthesis, synthesize new chaperone proteins to degrade misfolded proteins and, ultimately, trigger apoptosis (Rieusset, 2015). When these unfolded or misfolded protein load increases, these proteins are directed to the cytoplasm and degraded by the ER-associated degradation (ERAD) process (Salvadó *et al.,* 2015).

UPR pathway is mediated by three transmembrane ER proteins: inositol-requiring transmembrane kinase/endonuclease-1α (IRE-1α), eukaryotic translation initiation factor-2α kinase 3 (PERK) and activating transcription factor (ATF)-6 (Rieusset, 2015). Under non-stress conditions, the N-terminal of these trans-membrane proteins are bound to the intra-luminal binding immunoglobulin protein (BiP) (Palomer *et al.,* 2014), the master regulator of the UPR (Rieusset, 2015). After stress exposure, the large excess of unfolded proteins sequesters BiP from trans-membrane ER proteins, thereby inducing the UPR (Palomer *et al.,* 2014). In particular, ATF-6 is transported from the ER to the Golgi complex, where proteolytic cleavage releases a soluble fragment that it translocates to the nucleus, in which it acts as a transcription factor for ER chaperones (Xu *et al.,* 2012). In addition, the endoribonuclease activity of IRE-1α cleaves a 26-base-pair segment from the messenger RNA (mRNA) of X-box binding protein 1 (XBP1), creating the active or spliced (XBP1s) form of the transcription factor XBP1 (Salvadó *et al.,* 2014). XBP1s up-regulates ER chaperones and components of

ERAD mechanism (Rieusset, 2015). Finally, PERK phosphorylates and inhibits the eukaryotic initiation factor 2α (eIF2α), and by this means inhibits the translation of most mRNA (Hetz *et al.,* 2011). However, some mRNA escape this translational control, for example transcription factor ATF-4, a master regulator of the ER stress response that is capable of inducing the expression of ATF-3, BiP, CCAAT/enhancer binding protein homologous protein (CHOP) and genes involved in autophagy, antioxidant responses and apoptosis (Ma *et al.,* 2002) (Figure 3).

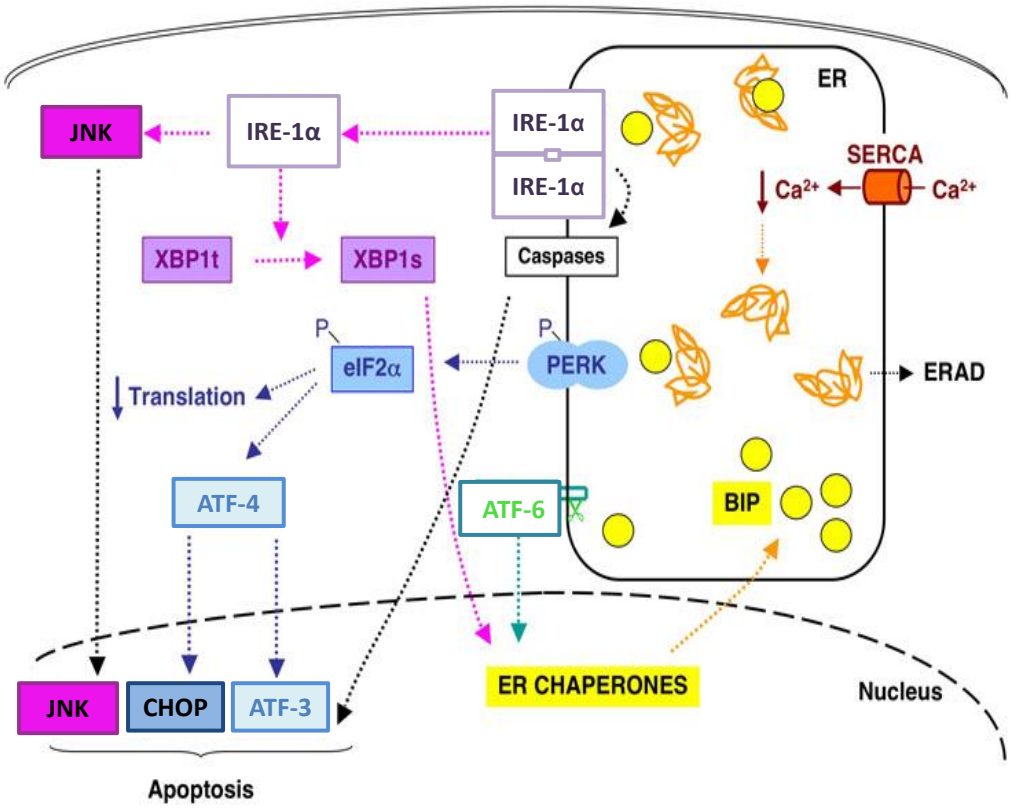

Figure 3. Schematic presentation of unfolded protein response signal transduction machinery. *Illustration showing the factors and pathways that function in the unfolded protein response induced by non-esterified fatty acid and hyperglycemia that drives the induction of genes involved in apoptosis. Abbreviations: ATF, activating transcription factor; BiP: binding immunoglobulin protein; CHOP:CCAAT/enhancer binding protein homologous protein; eIF2α: eukaryotic initiation factor 2α; ER: endoplasmic reticulum; ERAD: ER-associated degradation; IRE-1α: inositol-requiring transmembrane kinase/endonuclease-1α; JNK: c-Jun N-terminal kinase; PERK: eukaryotic translation initiation factor-2α kinase 3; SERCA: Sarco/endoplasmic reticulum Ca^{2+} ATPase; XBP: X-box binding protein (Cnop et al., 2008).*

This UPR in eukaryotic cells consists of three different mechanisms: (1) translational attenuation to limit further protein loads, (2) transcriptional activation of genes encoding factors involved in ER protein folding and degradation, and (3) ERAD, which serves to restore the folding capacity through the clearance of unfolded or

misfolded proteins by retro-translocating these proteins from the ER into the cytosol via the ubiquitin-proteasome system (Kadowaki and Nishitoh, 2013).

Together, these pathways work to decrease translation and increase protein folding (Eizirik *et al.,* 2008). The three branches of the canonical UPR intersect with a variety of inflammatory and stress signaling systems, including the NF-κB pathway (Hotamisligil, 2010).

A large number of groups have described the relation between ER stress response and a variety of human diseases, including neurodegenerative disease, metabolic disease, inflammatory disease, diabetes mellitus, cancer, and CVD (Kadowaki and Nishitoh, 2013). Recent evidences suggest that dysfunction of the UPR, or prolonged ER stress has emerged as a key player in the progression of IR and intersects with many different inflammatory and stress signaling pathways that disrupt insulin signaling (Hotamisligil, 2010) (Figure 4).

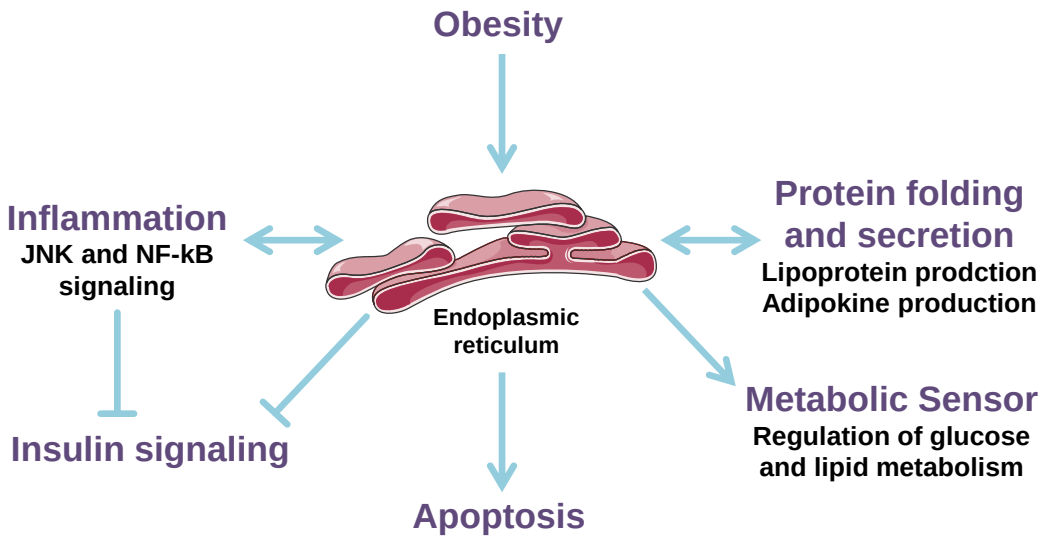

Figure 4. ER stress and metabolic dysfunction. *Induction of ER stress under conditions of obesity has the potential to impact metabolic regulation at multiple levels. This includes direct effects of UPR signaling on insulin action, glucose and lipid metabolism, and inflammatory signaling but also possibly other aspects of metabolic dysfunction.*

Specifically, obesity results in chronic ER stress in adipose tissue (Salvadó *et al.,* 2015) and liver of mice (Hotamisligil, 2010). Indeed, *in vivo* experiments have demonstrated an important role for ER stress in HFD-induced inflammation (Kawasaki *et al.,* 2012), increasing the expression of cytokines such as IL-6 and TNF-α through a PERK-dependent mechanism, perpetuating the process and the development of IR (Jiao *et al.,* 2011).

These perturbations in ER homeostasis can result in the dysregulation of lipid and glucose metabolism in the liver and adipose tissue**,** leading to a number of metabolic diseases such as hepatic steatosis and dyslipidemia. ER stress is also known to contribute to lipogenesis and inactivate lipoprotein secretion (Hotamisligil, 2010). Mice with XBP1 haploinsufficiency develop IR when placed on a HFD, despite being on a genetic background normally resistant to diet-induced obesity and diabetes. This was attributable, at least in part, to ER stress-mediated induction of c-Jun N-terminal kinase (JNK) activity and inhibition of insulin action (Ozcan *et al.,* 2004). Mice heterozygous for a non-phosphorylable eIF2α allele develop normally, but become obese and IR in response to HFD. These mice also exhibit defects in insulin secretion (Scheuner *et al.,* 2001).

Increased expression of UPR mediators and ER chaperones was significantly correlated with patient body mass index and modestly correlated with insulin sensitivity in adipose tissue of lean rats compared to their obese littermates (Sharma *et al.,* 2008), while in atherosclerosis, chronic ER stress activates inflammatory signaling in macrophages. Deletion of CHOP reduces apoptosis in macrophages and plaque necrosis, leading to suppression of atherosclerotic progression in both apolipoprotein E deficient (Apo $E^{-/-}$) and low-density lipoprotein receptor knockout $(LDLR)^{-/-}$ mice, which are two common animal models of atherosclerosis (Thorp *et al.,* 2009).

Recent evidences suggest that treatment with chemical ER chaperones reduces both obesity/IR and atherosclerosis in mice that could protect in the context of metabolic disease (Ozcan *et al.,* 2006). In fact, treatment of IR humans with tauroursodeoxycholic acid (TUDCA), a conjugated bile acid derivative that inhibits ER stress-induced apoptosis, results in increased insulin sensitivity (Kars *et al.,* 2010).

Under pathological conditions such as hypertension, ER stress was reported to be involved in endothelial dysfunction induced by AngII infusion (Kassan *et al.,* 2012). More recently, Galán *et al.* (2014) have demonstrated that chemical induction of ER stress with tunicamycin is associated with endothelial dysfunction and increased oxidative stress in arterial wall.

In addition, some studies support that alterations of ER homoeostasis are able to promote mitochondrial dysfunction, thus establishing the link between mitochondrial dysfunction and cardiovascular complications associated with MS (Rieusset, 2015). Additional data have suggested that the PERK signaling pathway of the UPR regulates mitochondrial function during ER stress (Rainbolt *et al.,* 2014), and mitochondrial dysfunction was associated with increased ROS production, suggesting a potential role of oxidative stress in the ER stress response.

Finally, the mitochondria-associated ER membranes (MAM), which are considered the contact points between the ER and mitochondria, might be participating in altered insulin action in peripheral tissue. Several lines of evidence demonstrated that the ablation in the liver of regulator of mitochondrial fusion, mitofusin-2 (Mfn2), which has been identified at the MAM interface (de Brioto and Scorrano, 2008), induces mitochondrial dysfunction, ER stress, IR and impaired glucose tolerance (Sebastian *et al.,* 2012). Moreover, an important increase in ER-mitochondria contact sites via MAM has been described during HFD-induced obesity leading to a significant increased mitochondrial oxidative function (Arruda *et al.,* 2014).

1.3.3. Endothelial dysfunction

Endothelial dysfunction participates actively in the development of CVD associated with MS (Liao, 2013).

Endothelium is the biological active inner layer of the blood vessels, which controls vascular functions. The arterial vessel is outlined by three distinct layers; tunica intima, a single layer of endothelial cells (EC); tunica media, which comprises the vascular

smooth muscle cells (VSMC) and tunica adventitia, an elastic lamina with terminal nerve fibers and surrounding connective tissue (Dhananjayan *et al.,* 2016).

The endothelium plays an important role in vascular homeostasis by modulating blood flow, delivery of nutrients, VSMC proliferation and migration, fibrinolysis and coagulation, inflammation, platelet and leukocyte adherence (Szmitko *et al.,* 2003).

Vascular EC not only provide a physical barrier between the vessel wall and lumen, but also maintain vascular homeostasis and facilitate the passage of substances such as nutrients and leukocytes across the vessel wall (Lenna *et al.,* 2014). To carry out the above functions, the endothelium secretes numerous mediators, including nitric oxide (NO), prostanoids, endothelin-1 (ET-1), AngII, tissue-type plasminogen activator, plasminogen activator inhibitor-1, von Willebrand factor, adhesion molecules and cytokines. The production of these moieties in response to various stimuli (Quyyumi, 1998) are necessary for normal vascular function including the regulation of vascular tone and coagulation, immune responses, and vascular cell growth. Under physiological conditions, the endothelium maintains a fine balance between vasodilation and vasoconstriction (Lenna *et al.,* 2014).

EC constitutively express endothelial nitric oxide synthase (eNOS) that after Ca^{2+}/calmodulin binding generates NO using L-arginine as a substrate together with cofactors as tetrahydrobiopterin (BH_4). NO then rapidly diffuses into VSMC, resulting in the formation of cyclic guanosine monophosphate (cGMP) (Li and Forstermann, 2014), and activating a cGMP dependent protein kinase, which leads to an increased extrusion of Ca^{2+} from cytosol in VSMC, thus inhibiting the contractile machinery and initiating vasodilation (Mombouli and Vanhoutte, 1999).

The term endothelial dysfunction is most often used to denote impairment of endothelium-dependent vasodilatation in favor of vasoconstriction, including pro-inflammatory and pro-thrombotic effects. Part of the dysfunction is related to decreased eNOS activity, reduced anticoagulant properties, increased adhesion molecule expression, chemokine and cytokine release, as well as ROS production by the endothelium. A key mechanism of endothelial dysfunction involves the vascular

production of ROS, particularly superoxide (O_2^-), which reacts rapidly with NO and inactivates it (Tschudi *et al.,* 1996).

The impairment of endothelium dependent relaxation observed in obesity involves inactivation of NO by O_2^- (Roberts *et al.,* 2006; Kobayasi *et al.,* 2010) due to an increase of ROS generation in vascular cells. This has been attributed to an enhancement of nicotinamide adenine dinucleotide phosphate (NADPH) oxidase activity (Roberts *et al.,* 2006; Bourgoin *et al.,* 2008), xanthine oxidase protein content (Erdei *et al.,* 2006) and mitochondrial ROS production (Tian *et al.,* 2012b), as well as to a decrease in antioxidant enzymes (Roberts *et al.,* 2006; Kobayasi *et al.,* 2010). Also, various stimuli such as high glucose levels, IR and disturbed blood flow can lead to endothelial dysfunction in part through the activation of ER stress (Lenna *et al.,* 2014).

Endothelial dysfunction is considered an early event involved in the initiation and progression of atherosclerosis that can be detected at early stages of development of the MS. The basic elements that correlate the establishment of MS and an accelerated phase of atherogenesis are often silent triggers that are present many years before the beginning of T2DM and CVD (McVeigh and Cohn, 2003). Over time, IR is associated with more components of the MS including, low HDL-cholesterol level, hypertension, increased vascular production of ROS, platelet activation, high TG and elevation of oxidation-prone LDL-cholesterol level, as previously described (Dhananjayan *et al.,* 2016) (Figure 5).

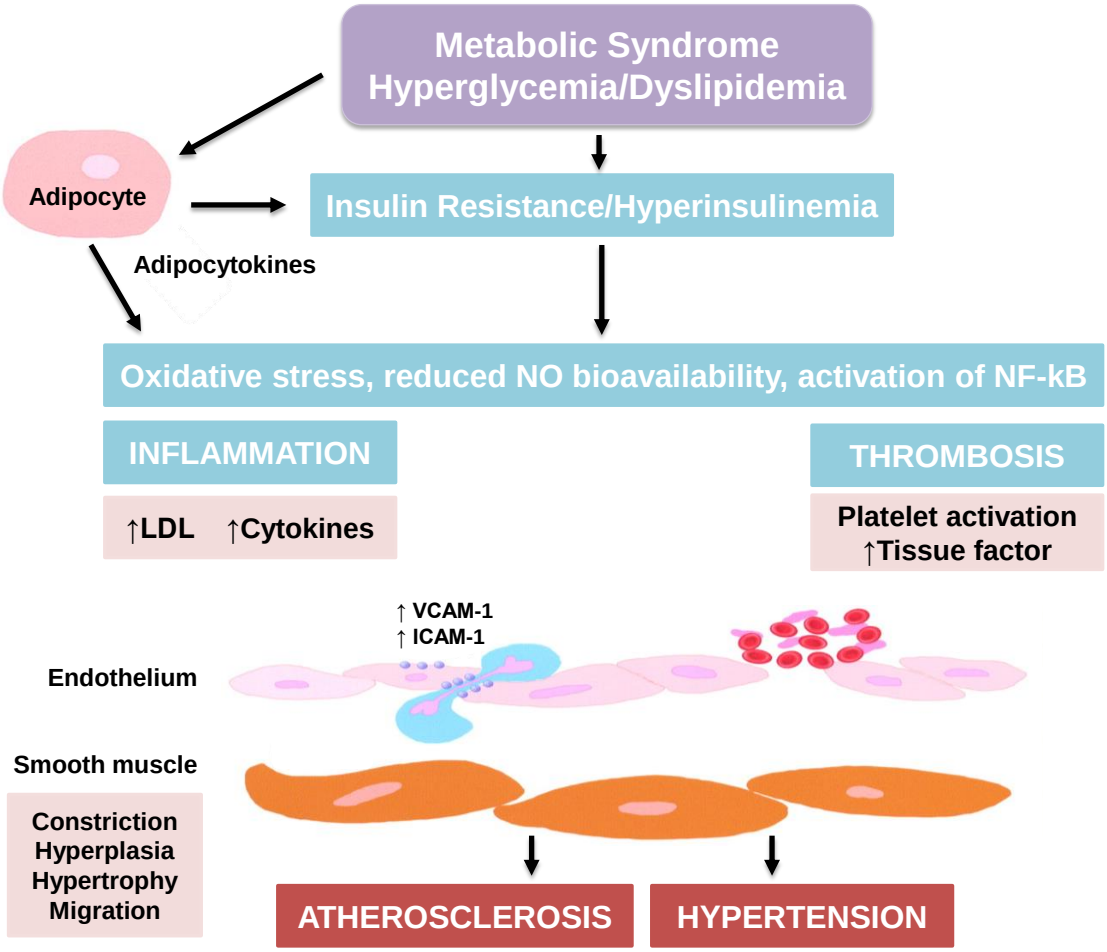

***Figure 5. Pathophysiology of cardiovascular disease in metabolic syndrome**. Abbreviations: ICAM-1: intercellular adhesion molecule-1; LDL: low-density lipoprotein; NF-κB: nuclear factor-κB; VCAM-1: vascular cell adhesion molecule-1 (modified from Prasad and Quyyumi, 2004).*

In obesity, this enhancement of ROS bioavailability, in particular O_2^-, affects endothelial function not only by reducing NO bioavailability, but also by promoting inflammation (Vila and Salaices, 2005). Obesity impairs endothelial function by inducing changes in BP, glucose levels, lipid metabolism and systemic inflammation (Avogaro and Kreutzenberg, 2005).

In addition, during obesity induced by HFD feeding, the vasculature is more susceptible than other tissues to the deleterious effects of nutrient overload, inflammation and endothelial dysfunction, including decreased aortic NO levels (Kim *et al.,* 2008). Both, LPS and FFA such as palmitate, stimulate TLR4 in the vasculature, which results in increased NADPH oxidase dependent O_2^- production and inflammation (Kim *et al.,* 2007; Maloney *et al.,* 2009; Liang *et al.,* 2013). Supporting this, it has been reported that HFD was able to increase arterial BP in mice, and the improvement in endothelial function by a probiotic, *Lactobacillus coryniformis*, as a result of reduced TLR4 activation and signaling, prevents obesity-induced hypertension, without showing any significant effect on BP in mice receiving the standard diet (Toral *et al.,* 2014).

This impaired endothelium-dependent vasodilation, a characteristic hallmark of endothelial dysfunction, is an underlying factor in the pathogenesis of CVD (Campia *et al.,* 2012). Endothelium-dependent vasodilation is markedly impaired in obese adults with MS compared with metabolically healthy obese adults (Schinzari *et al.,* 2015). Individuals with metabolic disorders exhibit higher degree of endothelial dysfunction (Kwaśniewska *et al.,* 2015) probably due to reduced plasmatic levels of NO in these patients (Ahirwar *et al.,* 2015).

This finding underscores the role of MS in endothelial vasodilator dysfunction. However, the influence of MS on endothelium-dependent vasodilation is currently unknown (Dow *et al.,* 2016), and its incidence continues to increase, despite enormous therapeutic advancements. For this reason, intensive efforts are necessary to develop new drugs involving new mechanisms to treat MS.

1.4. Mouse models for metabolic syndrome

The widespread impact of MS in humans means that there is an urgent need to study relevant causes and progression of the signs. These studies require experimental models in laboratory animals that adequately mimic all the aspects of the human disease, thus developing all major features of MS, especially obesity, diabetes, dyslipidemia, hypertension and possibly fatty liver disease and kidney dysfunction

(Panchal and Brown, 2011). Among these, murine models have become quite useful tools in recent years because the entire mouse genome is now sequenced, and a large number of transgenic and knockout models are readily available (Cornier *et al.,* 2008).

1.4.1. Genetic models of obesity and type 2 diabetes mellitus

These models are useful for evaluating specific molecular mechanisms that may be involved in the development of obesity and T2DM in mice. Within these genetic models are included:

a) Obese (ob/ob) mice

This was one of the first models for the study of diabetes (Enser, 1972). These mice inherited a monogenetic autosomal recessive mutation in the leptin gene on chromosome 6, this allows the development of different of signs MS with the age. In this way, at week 4 of age these mice can develop hyperinsulinemia, obesity and hyperglycemia. After 12 week of age, impaired glucose tolerance, hepatic steatosis and inflammation can be found (Dubuc, 1976). At week 24 of age, these mice developed left ventricular hypertrophy with decreased cardiac function (Mark *et al.,* 1999). Unlike humans with MS, these mice showed reduced BP and did not develop dyslipidemia even after the age of 36 weeks (Mark *et al.,* 1999; van den Bergh *et al.,* 2008).

b) Diabetic (db/db) mice

These mice have inherited an autosomal recessive mutation in the leptin receptor gene present on chromosome 4 (Chen *et al.,* 1996), leading to higher body weights than their lean littermates after 6 weeks of age (Dong *et al.,* 2010). After 8 weeks of age, fasting blood glucose concentrations are increased. These mice show high plasma concentrations of TG, total cholesterol and FFA along with reduced HDL/LDL-cholesterol ratio after 13 weeks of age (Ae Park *et al.,* 2006). Impaired glucose tolerance and hyperinsulinemia can be also observed after 12 weeks of age (Dong *et al.,* 2010; Winzell *et al.,* 2010) showing vascular endothelial dysfunction, although BP

was unchanged (Dong *et al.,* 2010). They develop hepatic steatosis after 20 weeks of age (Ge *et al.,* 2010). Of note, *db/db* mice fail to show hepatic inflammation and fibrosis (Sahai *et al.,* 2004).

1.4.2. Diet-induced models of metabolic syndrome

Diet plays an important role in growth and development as a source of nutrition, but the composition of the diet decides its nutritional status. The modern diet, especially in western countries, is rich in carbohydrates such as fructose and sucrose as well as in saturated fat, which results in an increased caloric intake that has been associated with many diet-induced complications including MS, CVD and non-alcoholic fatty liver disease (Lim *et al.,* 2010; Massiera *et al.,* 2010). Combinations of carbohydrate and fat-rich dietary components have been used in rodents to mimic these features and symptoms of human MS (Panchal and Brown, 2011).

a) Fructose-induced metabolic syndrome

As commented, fructose has become an important ingredient in western diets (Tappy and Lê, 2010). The main sources of fructose in the diet are sucrose, high-fructose corn syrup, fruits and honey. Unlike glucose, high-fructose feeding to rodents induces the development of MS symptoms including high BP, IR, impaired glucose tolerance and dyslipidemia (Lê and Tappy, 2006; Tran *et al.,* 2009). Fructose feeding promotes ventricular hypertrophy, ventricular dilatation, decreased ventricular contractile function, infiltration of inflammatory cells in heart and hepatic steatosis (Chang *et al.,* 2007; Patel *et al.,* 2009). Fructose has been reported to induce obesity (Bocarsly *et al.,* 2010) in rodents and it is accompanied by leptin resistance (Shapiro *et al.,* 2008). In addition, it has been reported that fructose increases plasmatic TG concentrations without changes in plasma cholesterol concentrations (Miatello *et al.,* 2005). Unlike glucose, fructose does not elicit insulin secretion from pancreatic β-cells, possibly due to the absence of the fructose transporter in pancreatic β-cells, and it also lacks the ability to stimulate the secretion of leptin (Bray *et al.,* 2004).

b) Sucrose-induced metabolic syndrome

Sucrose feeding has been also used to mimic human MS in laboratory animals (Tappy and Lê, 2010). Similar to fructose, sucrose feeding has shown variable results, especially with obesity (Santuré *et al.,* 2002). It is described that sucrose induces lipogenesis in rodents along with increased plasma concentrations of insulin, leptin, TG, glucose and FFA, and impaired glucose tolerance (Coelho *et al*., 2010). As a result, sucrose promotes an IR state without change in fasting plasma insulin and glucose concentrations, but showing higher postprandial plasma concentrations of insulin and glucose (Santuré *et al.,* 2002). Sucrose feeding increases systolic BP (SBP) in rodents (Sharma *et al.,* 2008) and can develop hepatic steatosis (Huang *et al.,* 2010).

c) High fat diet-induced metabolic syndrome

HFD has been commonly used as an experimental model of obesity, dyslipidemia and IR in rodents for many decades. The complications developed by HFD resemble the human MS. These complications may extend to cardiac hypertrophy, cardiac fibrosis, myocardial necrosis and hepatic steatosis (Panchal and Brown, 2011). HFD feeding to mice increases SBP and induces endothelial dysfunction (Kobayasi *et al.,* 2010). Besides, HFD-fed mice also shows albuminuria, increased glomerular tuft area, mesangial expansion, renal lipid accumulation, collagen deposition in glomeruli and increased infiltration of macrophages in renal medulla (Deji *et al.,* 2009).

Different types of HFD have been used, ranging the fat fractions between 20% and 60% as energy fat. Also, it has been used animal-derived fats, such as lard or beef tallow, or plant oils such as olive or coconut oil (Buettner *et al.,* 2006). Long-term feeding with HFD increases body weight (Lei *et al.,* 2007; Sutherland *et al.,* 2008) plasma TG, FFA and insulin levels and decreases plasma adiponectin concentrations, leading to moderate hyperglycemia and impaired glucose tolerance in most mouse strains (Kim *et al.,* 2010). Finally, long-term with HFD can also be able to develop hepatic steatosis (Hsu *et al.,* 2009).

2. Peroxisome proliferator activated receptor beta/delta (PPARβ/δ)

Peroxisome proliferator activated receptors (PPAR) are non-steroidal receptors belonging to type I nuclear hormone receptors superfamily that are involved in the regulation of multiple processes in living systems. They play protective and homeostatic roles in CVD, metabolism disorders, inflammation and immune responses, thrombosis, angiogenesis and cancer (Duez *et al.,* 2001; Daynes and Jones, 2002; Michalik *et al.,* 2004; Hamblin *et al.,* 2009; Azhar, 2010; Barlaka *et al.,* 2016).

PPAR are composed of three member isoforms encoded by separate genes and with a high degree of interspecies sequence conservation, which include PPAR alpha (PPARα), PPAR beta/delta (PPARβ/δ), and PPAR gamma (PPARγ). Each PPAR subtype has different functions determined by their level of expression, ligand specificity and its activity, which are both tissue and metabolic pathway dependent (Chen *et al.,* 2008; Oyekan, 2011) (Figure 6).

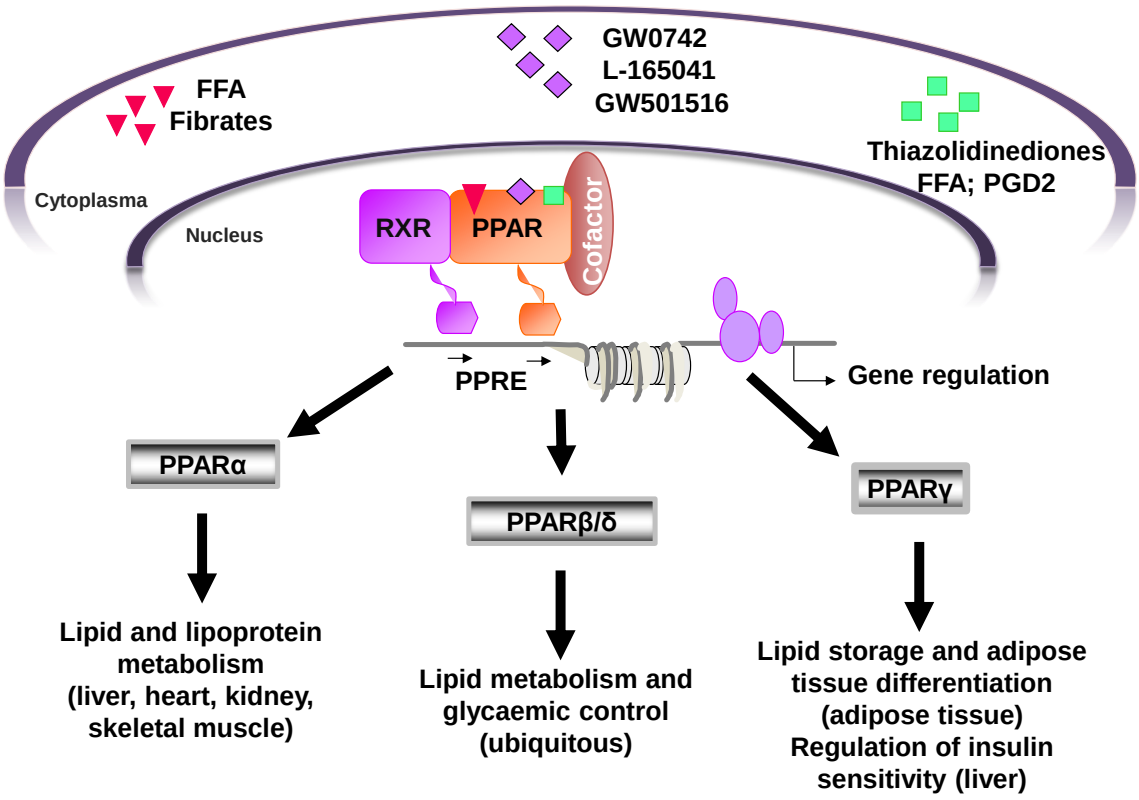

Figure 6. Localization and biological functions of peroxisome proliferator activate receptors (PPAR). *Three members of the PPAR family have been identified: alpha, gamma and beta/delta. PPARα is activated by natural ligands such as free fatty acids (FFA) as well as synthetic compounds like the lipid-lowering fibrates. PPARγ is activated by natural ligands include FFA and prostaglandins (PGs), such as prostaglandin D2 (PGD2) derivatives and synthetic ligands which include the thiazolidinediones which are insulin sensitizers used for treatment of diabetes mellitus. The least well-known receptor in the PPAR family is PPARβ/δ. The development of specific and high-affinity ligands (GW0742, L-165041 or GW501516) for this receptor have shown that PPARβ/δ is a potential molecular target to prevent or treat several metabolic disorders.*

In the cardiovascular system, it is well established that PPAR are involved in many functions, especially those involved in the regulation of vascular tone, inflammation, and energy homeostasis. PPAR are expressed in EC, VSMC and macrophages. Increasing evidences suggest that activation of PPAR in the vasculature exerts

cardiovascular protection due to their anti-atherosclerotic, anti-inflammatory and vasodilatory effects (Schiffrin *et al.,* 2003; Harrington *et al.,* 2010), together with its ability to inhibit proliferation of VSMC and EC (Benkirane *et al.,* 2006; Lee *et al.,* 2006), to reduce cardiac hypertrophy (Asakawa *et al.,* 2002; Smeets *et al.,* 2008), to inhibit platelet aggregation (Moraes *et al.,* 2007) and to lower BP (Iglarz *et al.,* 2003; Khan *et al.,* 2005; Zarzuelo *et al.,* 2011).

2.1. Structure

PPARβ/δ was initially described as PPARβ in *Xenopus laevis* (Dreyer *et al.,* 1992) and then it was found that this receptor shares 90% sequence homology with PPARδ from mice (Takada *et al.,* 2000). Though it was not originally certain whether PPARβ from Xenopus was identical to murine PPARδ, now both are recognised as homologues for each other, hence the terminology PPARβ/δ. In contrast to PPARα and PPARγ, which are expressed mainly in tissues with high fatty acid catabolism, vascular and immune cells, PPARβ/δ is expressed ubiquitously in almost every tissues with particular abundance in the skeletal muscle, liver, intestine, kidney and abdominal adipose tissues, where it is often expressed at higher levels than PPARα and PPARγ (Braissant *et al.,* 1996; Cimini *et al.,* 2005; Feige *et al.,* 2006; Zarzuelo *et al.,* 2011; Mandard and Patsouris, 2013).

2.2. Transcriptional regulation mechanisms

PPAR can be activated by a large variety of endogenous ligands, such as long-chain dietary fatty acids and their oxidized derivatives (Forman *et al.,* 1997; Feige *et al.,* 2006). However, each PPAR isoform exhibits high affinity for specific fatty acids due to the dimension of their ligand-binding domain (Xu *et al.,* 1999). Therefore, 15-hydroxyeicosatetraenoic acid (15-HETE), prostaglandins (PGs), such as prostaglandin A1 (PGA1) and prostaglandin D2 (PGD2), and carbaprostacyclin are the most potent endogenous agonists of PPARβ/δ (Kersten and Wahli, 2000; Naruhn *et al.,* 2010). However, given the variety and anatomic distribution of endogenous PPAR ligands and

the grade of expression of the receptor in each tissue, and also the combinations in which they occur depending on physiological and pathophysiological conditions is a major challenge to know the role of each endogenous ligand in a given cell at a fixed time-point. For example, the expression of PPARβ/δ in aorta and in kidney is increased in spontaneously hypertensive rats (SHR), but its target genes are decreased. This might be related to a limited uptake of PPARβ/δ endogenous ligands (i.e. fatty acids) in SHR, which are genetically deficient in CD36, a membrane fatty acid transporter (Zarzuelo *et al.,* 2011).

PPAR may also be activated by synthetic ligands: fibrates and thiazolidinediones are well known selective synthetic agonists for PPARα and PPARγ respectively, while several selective PPARβ/δ agonists have been recently designed, including GW0742, GW501516 and L-165041 (Bishop-Bailey and Bystrom, 2009) (Figure 7). In 2003, GW501516 (Endurobol) and GW0742, were developed by Glaxo Smith Kline, which showed high affinity and more than 1000-fold selectivity for PPARβ/δ compared to the other PPAR subtypes (Grewal *et al.,* 2016). The use of these agonists has contributed to clarify the role of PPARβ/δ activation under pathophysiological conditions, including MS.

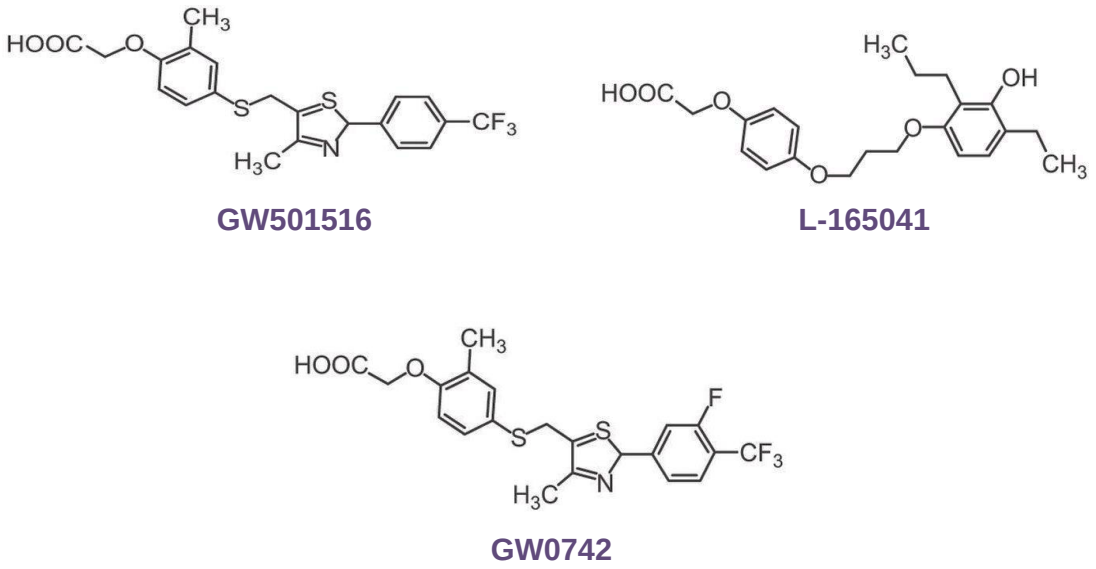

Figure 7. Chemical structure of main PPARβ/δ synthetic agonists used in research and clinical trials.

The PPARβ/δ activation includes at least two different molecular mechanisms: transcriptional transactivation and transcriptional transrepression. After ligand binding, PPARβ/δ undergoes conformational changes, which lead to the release of co-repressors and recruitment of co-activators and the 9-cis-retinoic acid receptor (RXR), thereby forming a PPAR/RXR heterodimer. This PPAR/RXR complex then interacts with specific DNA sequences called peroxisome proliferator-response elements (PPRE) in the promoter areas of the target genes, leading to the activation of target gene transcription in a ligand-dependent way. Moreover, PPARβ/δ can negatively regulate the expression of genes by a ligand-dependent or ligand independent transrepression mechanism. Transrepression may occur either through directly binding of PPAR/RXR heterodimer to transcription factors, such as activated protein-1 (AP-1), NF-κB, nuclear factor of activated T cells (NFAT), and signal transducer and activator of transcription 3 (STAT3), or through taking co-repressors, such as nuclear receptor co-repressor (NCoR), in the absence of ligands and fully prevent the activation of

PPAR-mediated transactivation (Kota *et al.*, 2005; Usuda and Kanda, 2014). These transcriptional regulation mechanisms are summarized in (Figure 8).

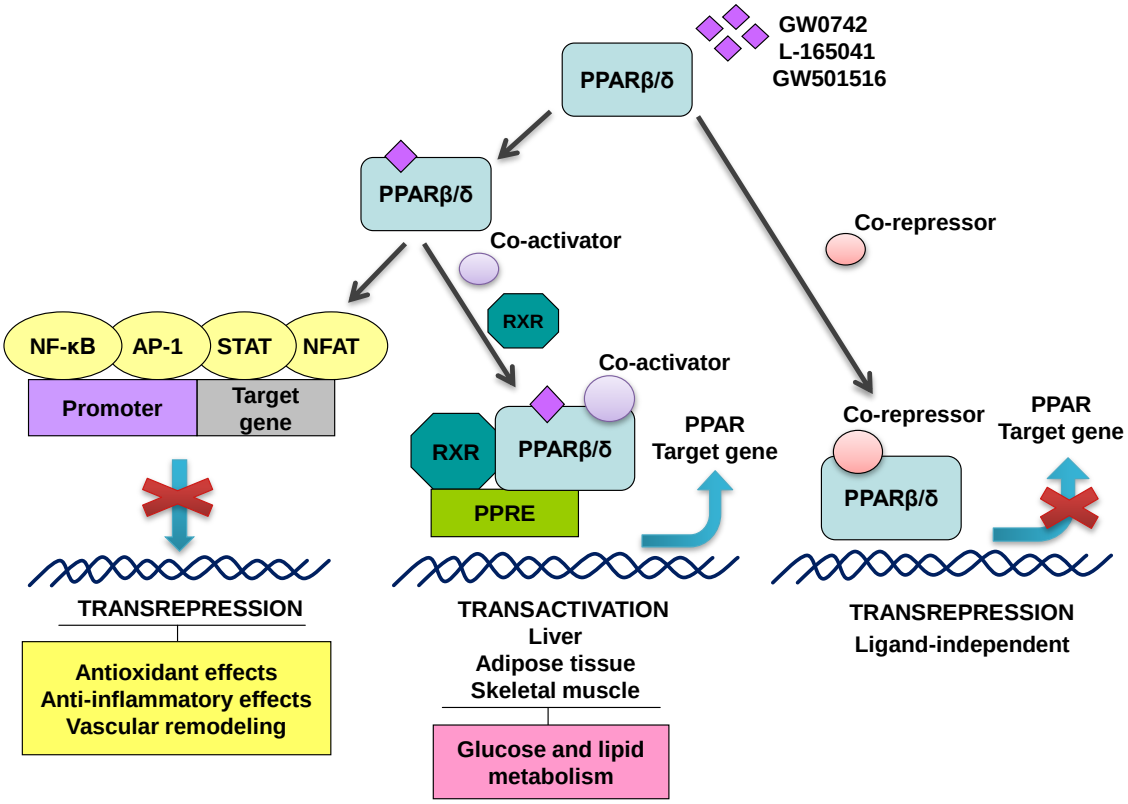

Figure 8. Molecular mechanisms of PPAR activation. *In transactivation, PPAR-RXR heterodimers bind to DNA-specific sequences called peroxisome proliferator-response elements (PPRE), which are located in the promoter regions of genes involved in glucose and fatty acid metabolism. A second mechanism, transrepression involves interfering with other transcription-factors such as NF-κB, activator protein-1 (AP-1), signal transducer and activator of transcription (STAT), and nuclear factor of activated T-cells (NFAT), thereby represses transcription of pro-inflammatory and pro-oxidant genes. Lastly, PPAR may repress the transcription of direct target genes in the absence of ligand (ligand-independent transrepression) recruiting corepressor complexes that mediate active repression.*

Furthermore, post-translational modifications by phosphorylation, ubiquitination, addition of small ubiquitin-like modifiers (SUMO)ylation are also involved in the regulation of PPAR activity and functions (Burns and Vanden Heuvel, 2007; Wadosky and Willis, 2012). Ubiquitination and SUMOylation decrease the expression of PPAR target genes, either by promoting PPAR degradation (via ubiquitination) or recruiting additional proteins to PPAR promoter sequences that increase PPAR transrepression function via SUMOylation or inhibit PPAR transactivation function. PPARβ/δ is regulated by posttranslational regulatory mechanisms that partly may serve to protect the cell against deregulated PPARβ/δ expression.

The effects of PPAR agonist treatment on post-translational changes of PPAR are complex. In fact, PPARβ/δ agonists may stimulate, inhibit or have no effect on PPAR activity depending on the cell type and PPAR concentration (Wadosky and Willis 2012). For instance, under conditions of moderate PPARβ/δ expression the ubiquitination and degradation of the receptor is not significantly influenced by the agonist GW501516 (Rieck *et al.,* 2007). However, the overexpression of PPARβ/δ severely increases its degradation, concomitant with its polyubiquitination and the formation of high molecular mass complexes containing multiple, most likely oligomerized PPARβ/δ molecules that lacked stoichiometrical amounts of the obligatory PPARβ/δ dimerization partner, RXR. However, further investigations are required to clarify these post-translational modifications for PPARβ/δ.

2.3. Clinical implications of PPARβ/δ agonists

Although PPAR were originally identified in the '90s, the physiological function of PPARβ/δ is much less studied and understood than the other two PPAR isoforms. However, in recent years the development of synthetic ligands with enhanced affinity, and also the availability of various models of PPARβ/δ knockout and transgenic mice have allowed a better understanding of metabolic functions of PPARβ/δ (Balakumar *et al.,* 2007; Bishop-Bailey and Bystrom, 2009). The use of PPARβ/δ agonists in preclinical models of MS have also played a major role in advancing our understanding

of the mechanisms and pathway involved in PPARβ/δ activation, which in turn would help to identify new drugs in MS treatment.

2.3.1. Metabolic functions of PPARβ/δ activation

PPARβ/δ is critically involved in the regulation of lipid, lipoprotein and glucose metabolism in multiple tissues including adipose tissue, skeletal muscle and heart (Azhar, 2010).

PPARβ/δ has been identified as a key regulator of adipocyte proliferation and differentiation, as well as in and cholesterol homeostasis. The first biological effect described for a PPARβ/δ agonist was an increase in serum HDL-cholesterol in diabetic mice following administration of L-165041 (Leibowitz *et al.,* 2000). The number of HDL particles (Apo A-I, Apo A-II and Apo A-III) are all increased with PPARβ/δ receptor activation (Oliver *et al.,* 2001). The mechanism by which PPARβ/δ activation raises HDL-cholesterol levels remains to be elucidated, although accumulating evidence has defined a role of PPARβ/δ in cholesterol ATP-binding cassette transporter A1 (ABCA1); in mice knockout for the expression of ABCA1, this increase was not observed, this may serve as possible explanation for PPARβ/δ mediated increase in HDL (Oliver *et al.,* 2001).

Studies in obese mice have shown that PPARβ/δ activation increased the expression of enzymes catabolizing FFA in skeletal muscle and decreased serum glucose concentrations (Tanaka *et al.,* 2003; Wang *et al.,* 2003). Also, it has been described that mice fed a HFD exhibited an improvement in insulin sensitivity in response to PPARβ/δ ligand activation, and, interestingly, this effect was not found in PPARβ/δ-null mice (Lee *et al.,* 2006). Similarly, PPARβ/δ activation for three months in *db/db* mice reduces glycemia in association with improved insulin sensitivity and improved islet function (Winzell *et al.,* 2010). Moreover, it is shown that PPARβ/δ agonist, GW501516 improves hyperglycemia by attenuating hepatic glucose production, promoting glucose disposal and preventing fatty acid release from adipose tissue deposits.

The role of PPARβ/δ in glucose metabolism has not been precisely delineated. It appears that PPARβ/δ ligands may improve insulin sensitivity by facilitating FFA oxidation in the adipose, skeletal and cardiac tissues (Gilde *et al.,* 2003; Tanaka *et al.,* 2003). More recently, there has been reported that PPARβ/δ activates β-oxidation respect of its targeting on gene pyruvate dehydrogenase kinase-4 (PDK-4) that inhibits pyruvate dehydrogenase complex which decreases glucose oxidation (Planavila *et al.,* 2005). PDK-4 is a key enzyme that mediates the shift from glycolytic to fatty acid oxidative metabolism via pyruvate dehydrogenase phosphorylation and subsequent inactivation (Patel and Korotchkina, 2006).

2.3.2. Effects of PPARβ/δ activation on elevated arterial blood pressure

Accumulating evidence demonstrates that PPARβ/δ is an important modulator of the MS and may be a therapeutic target for treating most of its features, including hypertension (Benetti *et al.,* 2011). It has become evident in recent years that individuals with MS have an increased burden of CVD that remains the leading cause of morbidity and mortality for these patients.

The first study to report the effects of pharmacological PPARβ/δ activation on elevated arterial BP was carried out in SHR (Zarzuelo *et al.,* 2011), an established animal model for human hypertension. In this study, long-term administration of PPARβ/δ agonist GW0742 induced a progressive reduction in SBP and heart rate in SHR, but it had no effect in normotensive Wistar-Kyoto (WKY) rats. This latter observation is supported by previous reports showing that GW0742 treatment does not influence in SBP in normotensive rats (Harrington *et al.,* 2010). Subsequently, other studies confirmed these antihypertensive effects in other experimental models, such as AngII-infused mice (Neels and Grimaldi, 2014; Romero *et al.,* 2016) and ET-1-dependent and AngII-independent hypertension induced by deoxicorticosterone acetate (DOCA)-salt in rats (Zarzuelo *et al.,* 2013a). Interestingly, PPARβ/δ blockade with an antagonist of this receptor, GSK0660, reversed the beneficial effects induced by GW0742 on arterial BP and arterial reactivity in AngII-infused mice (Romero *et al.,*

2016). However, in the ET-1-dependent model, the antihypertensive effect seems to be independent of PPARβ/δ activation (Xu *et al.,* 2006). Thus, a direct vasodilator effect, which is in part independent of receptor activation, could also collaborate to reduce SBP.

2.3.3. Effects of PPARβ/δ activation on cardiac and vascular structure

Sustained elevated BP is associated with changes in cardiovascular structure, including ventricular hypertrophy and increased vascular wall thickness/lumen diameter ratio (Prewitt *et al.,* 2002; Santos and Shah, 2014). The antihypertensive effects induced by PPARβ/δ agonists were accompanied in some experimental models by reduced vascular remodeling and cardiac hypertrophy (Zarzuelo *et al.,* 2011; Zarzuelo *et al.,* 2013a; Neels and Grimaldi, 2014). However, it has been shown a clear dissociation between the effects on BP and those in cardiac and vascular structures, which seem to be related with the experimental model of hypertension. Moreover, PPARβ/δ activation inhibits the hypertrophic effects of several stimuli (pressure, AngII, etc) in hypertension, but it has also direct pro-hypertrophic effects.

Several studies based on treatment with synthetic agonists have shown that PPARβ/δ activation exerts beneficial effects to prevent cardiac hypertrophy and vascular remodeling by inhibiting cardiomyocytes and VSMC proliferation, cytokines and growth factors release and extracellular matrix deposition due to its anti-inflammatory and antioxidant properties (Planavila *et al.,* 2005; Liu *et al.,* 2013; Galatou *et al.,* 2014; Barlaka *et al.,* 2016). Furthermore, a PPARβ/δ agonist reduced the right heart hypertrophy and right ventricular systolic pressure in an experimental model of pulmonary arterial hypertension induced by chronic hypoxia (Harrington *et al.,* 2010). However, chronic GW0742 treatment has mild inhibitory effects in cardiac hypertrophy despite intense reduction of BP (Zhang *et al.,* 2007; Zarzuelo *et al.,* 2011). It is well known that drugs that decrease BP and/or reduce the renin-angiotensin system activity (i.e. angiotensin converting enzyme inhibitors, AngII receptor type 1 (AT1) antagonist and direct renin inhibitors) reduce cardiac hypertrophy in hypertension (including SHR). This lack of inhibitory effects may be explained by the induction of rapid cardiac growth,

mediated via calcineurin-A/NFAT, as previously described in mice with PPARβ/δ agonists GW0742 and GW501516 (Wagner *et al.,* 2009), that counterbalances the effects of reduced BP and AngII pathway activity.

However, in SHR, GW0742 reduced both the increased cardiomyocyte size and collagen accumulation indicating that it prevents the histopathological consequences of hypertension, which is in agreement with inhibition of AngII induced collagen synthesis in response to PPARβ/δ activation (Lee *et al.,* 2003; Zhang *et al.,* 2007). By contrast, in AngII-infused mice the reduction in left ventricular hypertrophy was higher than the reduction in BP reduction, indicating direct protective effects independent of BP reduction (Romero *et al.,* 2016).

In addition, chronic treatment with GW0742 strongly reduced vascular remodeling in mesenteric arteries from SHR (Zarzuelo *et al.,* 2011), and AngII-infused mice (Neels and Grimaldi, 2014; Romero *et al.,* 2016), which may contribute to reduce BP. In both models of hypertension the reduction of vascular remodeling was higher than the change in BP, indicating a protective local effect, mainly in the vasculature. The fate of VSMC, i.e. the maintenance of a differentiated contractile phenotype or the dedifferentiation into a proliferative phenotype, may be determined by the balance between the protein kinase B (Akt) and the extracellular-regulated kinase (ERK) pathways. PPARβ/δ activation by GW0742 induced a change in the balance between Akt/ERK pathways (Zarzuelo *et al.,* 2011), which may participate in the regulation of VSMC phenotypic change in SHR, leading to reduced vascular remodeling. However, further studies implicating PPARβ/δ in the pathogenesis of cardiac hypertrophy and vascular remodeling are necessary to elucidate its role in hypertension.

2.3.4. Effects of PPARβ/δ activation on endothelial dysfunction

Endothelial dysfunction is well thought out as the first step in the development of the pathogenesis of hypertension, atherosclerosis and other CVD. Therefore, independently of other cardiovascular risk factors, there is an inverse association between endothelial dysfunction and future cardiovascular outcomes (Bonetti *et al.,*

2003; Endemann and Schiffrin, 2004). There is increasing evidence that endothelial dysfunction and hypertension are involved in a vicious cycle which culminates in progressive target organ injury and dysfunction (Félétou *et al.,* 2010). It has been described that those antihypertensive treatments augmenting the bioavailability of NO, which contributes to restoring proper endothelial function, give extra beneficial effects in ameliorating target organ damage in hypertension (Portaluppi *et al.,* 2004). The pharmacological activation of PPARβ/δ prevents the endothelial dysfunction and downregulates inflammatory responses. Endothelial dysfunction is characterized by impaired endothelium-dependent vasodilation, reduced NO bioavailability, increased vascular O_2^- production and pro-thrombotic and pro-inflammatory state (Kodja and Harrison, 1999; Endemann and Schiffrin, 2004; Bauersachs and Widder, 2008).

Our research group has reported that PPARβ/δ activation by GW0742 improved endothelial dysfunction by increasing eNOS activation and lowering ROS levels in animal models of hypertension and diabetes (Zarzuelo *et al.,* 2011; Quintela *et al.,* 2012; Zarzuelo *et al.,* 2013a). Briefly, the chronic administration of GW0742 restored the impaired endothelial vasodilator function as measured by the endothelium-dependent relaxation to acetylcholine (ACh) in SHR and DOCA-salt rats, through a direct PPARβ/δ activation in the vascular wall via induced phosphorylation phosphatidylinositide 3-kinase (PI3K)-Akt-eNOS pathway and reduced caveolin-1 (Cav-1)/eNOS interaction (Zarzuelo *et al.,* 2011; Zarzuelo *et al.,* 2013a). Furthermore, this restoration of endothelial dysfunction by GW0742 was also attributed to a reduction in oxidative stress and particularly to diminished O_2^- driven NO inactivation.

Excessive production of ROS is a hallmark of CVD, including hypertension. In fact, it has been suggested that increased oxidative stress is a pathogenic factor in the development of essential hypertension and endothelial dysfunction (Lima *et al.,* 2009; Gómez-Guzmán *et al.,* 2011). Long-term administration of PPARβ/δ agonist GW0742 induced a significant decrease on vascular O_2^- production attributed to downregulated $p22^{phox}$ and $p47^{phox}$ expression and it decreased both basal and AngII or ET-1-stimulated NADPH oxidase activity, which is the main source of vascular O_2^- (Zarzuelo

et al., 2011; Zarzuelo *et al.,* 2013a). Similar results were observed in experimental models of diabetes (Quintela *et al.,* 2012).

IR is also implicated in the mechanism underlying endothelial dysfunction associated to metabolic-related cardiovascular disorders. Recent studies have shown that in human EC under high glucose conditions, PPARβ/δ activation by GW0742 and L-165041 prevented the impairment of insulin-stimulated NO production via PDK-4 up-regulation, with the subsequent inhibition of both mitochondrial ROS production and ERK1/2 activation. These effects improved insulin signaling by reducing ERK1/2-mediated insulin receptor substrate-1 (IRS-1) phosphorylation at Ser^{636} and Ser^{270} (Quintela *et al.,* 2014). Furthermore, chronic administration of GW0742 increased Akt and eNOS phosphorylation and improved NO-dependent insulin relaxation in aorta and mesenteric arteries from streptozotocin (STZ)-induced type 1 diabetic rats. These beneficial effects were abolished in the presence of the specific PDK-4 inhibitor dichloroacetate, showing the critical role of PDK-4 in the improvement of insulin signaling induced by PPARβ/δ activation in the endothelium under hyperglycemic conditions (Quintela *et al.,* 2014). In addition, ET-1 is involved in the development of O_2^- production and endothelial dysfunction in type 1 diabetic rats. Chronic GW0742 administration also improves Ca^{2+}-mediated eNOS activation and relaxation induced by ACh in aorta and mesenteric arteries from STZ-induced diabetic rats, by reducing vascular ET-1 overproduction (Quintela *et al.,* 2012). Furthermore, in mesenteric arteries the endothelium-derived hyperpolarizing factor (EDHF) also participates in the endothelium-dependent relaxation and is essential for the physiological control of resistance artery tone. During diabetes an impairment of its pathway has been reported (Wigg *et al.,* 2001; Leo *et al.,* 2011). However, GW0742 chronic treatment has not effect on the EDHF-dependent vasodilation in mesenteric arteries from STZ-induced diabetic rats (Quintela *et al.,* 2012). Similar results showing that PPARβ/δ activation by agonist GW1516 protects endothelial function and improves insulin-induced relaxation in diabetic and obese mice have also been described (Tian *et al.,* 2012a). In addition, the antidiabetic drug metformin restores endothelial function through inhibiting ER stress and increasing NO bioavailability on activation of 5′-adenosine monophosphate-

activated protein kinase (AMPK)/PPARβ/δ pathway in obese diabetic mice (Cheang *et al.,* 2014). All these results showed that PPARβ/δ controls glucose metabolism directly in EC, exerting protective effects against endothelial dysfunction induced by these metabolic disorders.

2.3.5. Effects of PPARβ/δ activation on vascular inflammation

Vascular inflammation contributes to vascular dysfunction in hypertension, which is a core component of the MS. In addition, the end-organ damage associated with hypertension is mediated, at least in part, by inflammation (Duan *et al.,* 2009) Pharmacological PPARβ/δ activation exhibits anti-inflammatory and anti-atherogenic properties in vascular wall. Vascular inflammation has been considered as a main mechanism that participates in the progression of vascular injury associated to MS and has gained increasingly strong to explain the link between increased BP and atherosclerosis (Collins *et al.,* 1995; Cines *et al.,* 1998; Rival *et al.,* 2002). The expression of pro-inflammatory genes, including IL-1β, IL-6, TNF-α, was reduced by PPARβ/δ selective agonists in aorta from hypertensive animals (Zarzuelo *et al.,* 2011). The enhancement of ROS production, in particular O_2^-, affects endothelial function not only by reducing NO bioavailability, but also by promoting inflammation (Vila and Salaices, 2005). In addition, cytokines are capable to act synergistically to initiate the inflammatory cascade, resulting in other cytokines, cytokine receptor, and genes involved in inflammation, all of which can damage vascular function (Vila and Salaices, 2005). Mitogen-activated protein kinase (MAPK) signaling pathways are associated with the vascular inflammation that is modulated by ROS (Griendling *et al.,* 2000). Thus, PPARβ/δ activation by specific agonists reduced vascular O_2^- levels in hypertensive animals contributing to reduce vascular inflammation. This protective effect on vascular inflammation was also related to prevention in the progression of endothelial dysfunction and vascular remodeling associated to hypertension.

2.4. Clinical evidences

Based on the beneficial effects shown by pharmacological PPARβ/δ activation in experimental animal models of metabolic-related CVD, several clinical trials have been conducted to evaluate the protective effects against metabolic and vascular diseases of selected PPARβ/δ agonists in the last years (Ooi *et al.,* 2011; Choi *et al.,* 2012; Olson *et al.,* 2012). Some studies have analyzed a possible association of single nucleotide polymorphisms (SNPs) in the human PPARβ/δ gene with metabolic and CVD. However, a SNPs located at in the 5'- untranslated region (5'-UTR) of the human PPARβ/δ (+294T/C) (Skogsberg *et al.,* 2003; Chia *et al.,* 2015) was not associated with obesity, MS (Grarup *et al.,* 2007; Lagou *et al.,* 2008), or increased risk coronary heart disease (Skogsberg *et al.,* 2003).

Although no severe side effects have been described so far, none of the PPARβ/δ agonists tested has been approved for clinical use yet. Thus, Endurobol (GW501516), in healthy volunteers, reduced plasma TG and increased plasma HDL-cholesterol concentration (Sprecher, 2007). In another study with healthy overweight men with moderate dyslipidemia, GW501516 treatment resulted in significant reductions in plasma TG, LDL-cholesterol, Apo B and insulin levels, while HDL-cholesterol level was unchanged (Risérus *et al.,* 2008), being proposed as a pharmacological candidate for the treatment of MS, diabetes mellitus, dyslipidemia and atherosclerosis (Risérus *et al.,* 2008; Ooi *et al.,* 2011; Olson *et al.,* 2012), but unfortunately its development was stopped when the agonist was related to induction of tumours in several organs in rodents (Gupta *et al.,* 2004; Pollock *et al.,* 2010).

Safety issues have been raised regarding the role of PPARβ/δ ligands in carcinogenesis, with conflicting studies indicating that PPARβ/δ activation can both inhibit and promote tumorigenesis, the latter particularly in animal models (Peters *et al.,* 2015). This is of interest given that PPAR are known to be expressed at lower levels in human cells than they are in rodent cells, and gene expression is also differentially regulated by PPAR in human versus rodent cells (Neels and Grimaldi, 2014). For instance, synthetic PPARα ligands induce carcinogenesis in rodents. However, human subjects receiving fibrates for the treatment of dyslipidemia are resistant to the

carcinogenic effects of these PPARα ligands (Youssef and Badr, 2011). Similarly, the PPARγ ligand pioglitazone was associated with a higher incidence of bladder cancer in preclinical studies whereas, in humans, although conflicting results have been reported, the latest large-scale studies indicate that pioglitazone use was not associated with the incidence of bladder cancer (Levin *et al.,* 2015; Lewis *et al.,* 2015).

MBX-8025, another PPARβ/δ agonist, has shown to normalize lipid profiles and C-reactive protein levels in patients with MS and has ended a phase II clinical trial (Choi *et al.,* 2012). Several mild side effects such as increased creatinine kinase levels, decreases in red blood cell count and haematocrit and a modest increase in platelet count have been described in the clinical trials with this drug (Bays *et al.,* 2011). However, no clinical trials have been performed in essential hypertensive patients.

Because most side effects of these selective PPARβ/δ agonists are related to ubiquitously expression of PPARβ/δ and the dosing regimen used (Mackenzie and Lione, 2013), further pharmacokinetic studies of PPARβ/δ agonists are required to adjust the concentration levels in the blood to that which is selective to PPARβ/δ and define a therapeutic window and a safe dose.

Finally, a novel class of dual PPARα/β/δ (Wallace *et al.,* 2005; Cariou *et al.,* 2011), PPARγ/β/δ (Liu *et al.,* 2001; Xu *et al.,* 2006; Gonzalez *et al.,* 2007) and PPARα/γ/β/δ pan agonists (Tenenbaum *et al.,* 2005a; Tenenbaum *et al.,* 2005b; Ramachandran *et al.,* 2006; Shearer and Billin, 2007) are currently in various stages of development in clinical trials due to their promising results in preclinical studies to treat all of the clinical disorders of the MS including IR, hyperglycemia and dyslipidemia. In fact, in abdominally obese patients and IR patients, with or without diabetes, GFT505, a dual PPARα/β/δ agonist, improved several metabolic parameters, including hepatic and peripheral IR, inflammation and dyslipidemia (Cariou *et al.,* 2011; Cariou *et al.,* 2013). GFT505 was well tolerated and safe, with mild adverse reactions, such as headache, gastrointestinal intolerance and back pain. Furthermore, it has been assessed the safety and efficacy of GFT505 in patients with non-alcoholic steatohepatitis and was well tolerated although a few patients had an increase in creatinine, which is not estimated to be related with renal insufficiency (Ratziu *et al.,* 2016).

It has become evident in recent years supports, the hypothesis that PPARβ/δ activation represents an attractive therapeutic strategy for the treatment and prevention of MS. Thanks to this potential interest, PPARβ/δ agonists have reached clinical trials. However, the number of clinical trials performed to study the efficacy and safety of PPARβ/δ ligands in humans remains small, and several questions need to be answered (Vázquez-Carrera, 2016) and further investigation into the mechanism of this pleiotropic effect of PPARβ/δ agonist is necessary to be considered as a novel therapeutic target in treating this pathology.

GLOSSARY

GLOSSARY

Adipokine: any protein (cytokine, growth factor, hormone, etc.) secreted from adipocytes.

Atherogenic dyslipidemia: the presence of high levels of TG, LDL-cholesterol, and low levels of HDL-cholesterol. It is often observed in patients with IR and T2DM.

Cardiac hypertrophy: is a thickening of the heart muscle (myocardium) which results in a decrease in size of the chamber of the heart, including the left and right ventricles. A common cause of cardiac hypertrophy is high blood pressure (hypertension) and heart valve stenosis

Chaperone: a molecule that prevents protein misfolding by stabilizing folding intermediates and preventing their aggregation in the cell. It can be an endogenous protein such as BiP, or pharmacological compounds such as 4-PBA or TUDCA.

Chemokine: secreted chemotactic cytokines that can induce directed chemotaxis in the responsive cells.

Cytokine: small protein molecules secreted that function is predominantly in immunological intercellular communication. These include IL and interferons.

Endothelial dysfunction: a key event in the development of atherosclerosis that compromises the normal function of EC, leading to the inability of arteries and arterioles to dilate fully in response to an appropriate stimulus.

ER stress: a consequence of any perturbation that results in high load of unfolded and misfolded proteins in the ER. The ER stress activates the UPR.

4-PBA: chemical chaperone that inhibits ER stress by improving ER protein folding capacity.

Glucose intolerance: an umbrella term referring to metabolic conditions characterized by the presence of higher than normal blood glucose levels (hyperglycemia). Hyperglycemia patients usually exhibit either impaired fasting glucose or impaired glucose tolerance.

Hyperinsulinemia: is a condition in which there are excess levels of insulin circulating in the blood relative to the level of glucose.

IR: a condition in which the cells of an organism become resistant to the effects of insulin. Due to this, higher levels of insulin are required to have an effect. This resistance is manifested against both endogenously produced and exogenously injected insulin.

Insulin signaling: insulin is a hormone produced by the β-cells in the pancreas. It regulates carbohydrate and fat metabolism by causing cells in the muscles, liver, and fat tissue to take up glucose from blood and store it as glycogen. Insulin signaling is the intracellular events stimulated after insulin receptor activation.

Lipogenesis: a process by which acetyl-CoA, an intermediate in the metabolism of simple sugars such as glucose, is converted in fat.

Lipotoxicity: a process that results from the accumulation of lipid intermediates in non-adipose tissues.

Low-grade systemic inflammation: obesity-induced inflammation differs from inflammation in classical immunity in that it is a low-grade inflammation than produces much lower levels of circulating cytokines. It is also a chronic inflammation because it requires a relatively long HFD treatment (> 8 weeks in animal models) before inflammation is observed in adipose tissue. Obesity- induced inflammation is the result of exposure to nutrient excess, resulting in adipocyte hypertrophy, macrophage infiltration and polarization, and activation of inflammatory pathways.

MAM: are functional domains that represent close contact sites through which ER communicates with mitochondria supporting the transfer not only of lipids but also the exchange of Ca^{2+} ions and other molecules, and regulating energy metabolism.

SUMOylation: is a post-translational modification process. It is analogous to ubiquitination in terms of the reaction scheme and enzyme classes used, but rather than conjugation by ubiquitin, involves addition of SUMO. SUMOylation can affect a protein's structure and subcellular localization.

TUDCA: bile acid derivate that acts as chemical chaperone to enhance protein folding and ameliorate ER stress.

Thapsigargin: ER stressor which induces ER stress by inhibiting the SERCA and, consequently, blocking the Ca^{2+} entry into the ER lumen.

Tunicamycin: ER stressor that disrupts glycosylation of newly synthesized protein resulting in ER stress.

Ubiquitination: Process for a protein is inactivated by attaching ubiquitin to it. Ubiquitin is a small molecule, which acts as a tag that signals the protein-transport machinery to ferry the protein to the proteasome for degradation.

UPR: adaptive (defensive) ER stress response that involves the activation of a signaling pathway to restore the folding capacity. If ER homeostasis cannot be restored apoptosis is induced.

JUSTIFICATION AND OBJETCTIVES

JUSTIFICATION AND OBJECTIVES

The MS is a cluster of metabolic and cardiovascular disorders associated with IR, where obesity is considered a complex chronic disease whose prevalence is steadily increasing (Bray, 2004). Consequently, the prevalence of obesity-related disorders, such as T2DM and CVD, is also increasing. The mechanisms by which obesity increases the risk of CVD are incompletely understood, but endothelial dysfunction seems to play a key role, that can subsequently promote the development of atherosclerosis and hypertension.

Many factors may impair endothelial function in obesity, including changes in BP, glucose levels, and lipid metabolism (Avogaro and Kreutzenberg, 2005). Furthermore, obesity is characterized by a chronic immune-mediated low-grade systemic inflammation (Hotamisligil, 2006). Oxidative stress has also been implicated in endothelial dysfunction. Obesity-induced increase in ROS in vascular cells has been attributed to an enhancement of ROS-generating systems, such as NADPH oxidase (Roberts *et al.,* 2006), xanthine oxidase (Erdei *et al.,* 2006) and mitochondria (Tian *et al.,* 2012b), or to a decrease in antioxidant enzymes (Roberts *et al.,* 2006; Kobayasi *et al.,* 2010). In vascular cells, the redox-sensitive NF-κB regulates the transcription of genes that encode inflammatory cytokines, which in turn, can activate NF-κB, stimulating further ROS and cytokine production and promoting more inflammation (De Martin *et al.,* 2000). Increased NF-κB activation in obesity is involved in the impaired endothelium-dependent relaxation in human (Pierce *et al.,* 2009) and obese mice (Kobayasi *et al.,* 2010).

As previously explained, the PPAR, PPARα, PPARβ/δ, and PPARγ are members of the nuclear hormone receptor superfamily. PPARβ/δ is the least studied isoform of PPAR, and it is ubiquitously expressed in tissues. The role of PPARβ/δ in obesity has been examined by the loss-of-function approach or by using synthetic PPARβ/δ ligands. PPARβ/δ knockout mice are more prone to weight gain on a HFD, whereas the PPARβ/δ transgenic mice are protected against obesity and lipid accumulation (Wang *et al.,* 2003). Moreover, PPARβ/δ agonists can improve the lipid profile by

increasing the levels of HDL-cholesterol and decreasing LDL-cholesterol and TG in obese animal models (Leibowitz *et al.,* 2000; Oliver *et al.,* 2001) and obese men (Risérus *et al.,* 2008). In addition, PPARβ/δ regulates glucose homeostasis and insulin sensitivity in various tissues (Lee *et al.,* 2006).

The improvement of systemic lipid and glucose metabolism by PPARβ/δ activation is associated with vascular protection in obesity. In fact, the PPARβ/δ agonist GW0742 reduced atherosclerosis in $LDLR^{-/-}$ mice (Graham *et al.,* 2005), and substantially attenuated AngII-accelerated atherosclerosis and the associated arterial inflammatory and atherosclerotic gene expression (Takata *et al.,* 2008).

However, PPARβ/δ agonists may also exert protective effects independently of their metabolic actions. Thus, chronic GW0742 treatment reduced BP and improved endothelial function in aortae from SHR (Zarzuelo *et al.,* 2011) and DOCA-salt hypertensive rats (Zarzuelo *et al.,* 2013a), independently of the systemic metabolic state. This ligand also increased ACh-induced relaxation in aorta and small mesenteric arteries from STZ-induced diabetic rats (Quintela *et al.,* 2012) without altering blood glucose levels. Moreover, direct effects of these agonists on vascular cells in culture have also been described.

Activation of PPARβ/δ exhibits anti-inflammatory properties in EC by inhibiting the expression of vascular cell adhesion molecule-1 (VCAM-1) and monocyte chemoattractant protein-1 (MCP-1) (Rival *et al.,* 2002). PPARβ/δ activation restored the high glucose-induced impairment of insulin signaling in EC (Quintela *et al.,* 2014) and the impaired endothelium-dependent relaxation induced by high glucose in mouse aortae (Tian *et al.,* 2012a). In addition, activation of PPARβ/δ significantly reduced AngII-induced ROS generation in VSMC by inhibiting the activation of NADPH oxidase (Lee *et al.,* 2012) and by up-regulation of antioxidant genes (Kim *et al.,* 2011a; Kim *et al.,* 2011b).

While PPARβ/δ activation has been reported to improve obesity-induced endothelial dysfunction (Tian *et al.,* 2012a), the role of oxidative stress and vascular

inflammation as well as the consequences on BP and left ventricular hypertrophy are unknown.

Therefore, *the first aim of this Doctoral Thesis* was to analyze the effects of chronic treatment with the highly selective PPARβ/δ agonist GW0742 on metabolic and vascular function in obese mice fed a HFD.

Endothelial dysfunction is an early event involved in the development of atherosclerosis. HFD impairs endothelial function in animals and humans (Vogel *et al.,* 1997; Esposito *et al.,* 2004). One of the characteristic abnormalities of the MS is the elevated circulating concentrations of FFA (Creager *et al.,* 2003) which are implicated in the mechanism underlying endothelial dysfunction associated to lipid metabolic disorders. Potential mechanisms whereby exposure to saturated FFA induces changes in the endothelium include impairment of eNOS activity, and increased ROS such as O_2^- production (Bedard and Krause, 2007), that can be generated by both mitochondrial electron transport (Nishikawa and Araki, 2007) and by cytosolic enzymes such as the NOX family of NADPH oxidase (Inoguchi *et al.,* 2000). These enzymes transfer electrons from NAD(P)H across cell membranes and are a major source of vascular ROS.

Decreasing lipotoxicity may be a key component to prevent and treat cardiovascular complications of lipid metabolic disorders. Accumulation of fatty acid derivatives can be attenuated by their metabolism via mitochondrial β-oxidation. The rate-limiting step for β-oxidation of long-chain fatty acids is their transport into mitochondria via carnitine palmitoyl-transferase-1 (CPT-1). Activation of fatty acids oxidation by overexpressing CPT-1 in skeletal muscle improves lipid-induced IR (Sebastián *et al.,* 2007; Bruce *et al.,* 2009; Coll *et al.,* 2010).

PPARβ/δ is expressed in multiple cell types including adipose and EC (Piqueras *et al.,* 2007). PPARβ/δ activation promotes fatty acid β-oxidation in adipocytes and skeletal muscle, decreases lipid accumulation, and reduces obesity (Wang *et al.,* 2003). Lipid metabolism in EC also involves conventional pathways, with functional

rates much slower than in hepatocytes or in cardiomyocytes (Héliès-Toussaint *et al.,* 2006), which might be regulated by PPARβ/δ activation, as in other metabolic tissues (Tanaka *et al.,* 2003; Bruce *et al.,* 2009; Coll *et al.,* 2010; Alvarez Guardia *et al.,* 2011).

In the present Doctoral Thesis we hypothesized that PPARβ/δ activation would protect against endothelial dysfunction and vascular inflammation induced by lipids as a result of increased FFA β-oxidation in blood vessel.

This justifies that *the second aim of this Doctoral Thesis* was to examine whether PPARβ/δ activation would protect against endothelial dysfunction and vascular inflammation induced by palmitate both, *in vitro*, in isolated vessels and cultured EC, and *in vivo*, in mice fed a HFD.

Insulin has multiple biological actions not only on metabolism but also on cardiovascular functions. Insulin exerts desirable effects on the vasculature, primarily by enhancing eNOS activation and expression and thus endothelial NO bioavailability, which in turn engenders a wide array of anti-atherogenic actions. IR is characterized by reduced insulin-induced NO from the endothelium, which may contribute to increased risk of vascular diseases (Boden, 2011). The impaired insulin signaling in EC causes attenuation of insulin-induced capillary recruitment and insulin delivery, which, in turn, leads to a further reduction in glucose uptake by skeletal muscle (Kubota *et al.,* 2011).

Studies in cultured cells (Xiao-Yun *et al.,* 2009; Wang *et al.,* 2013), isolated arteries (Symons *et al.,* 2009), animal models (Du *et al.,* 2006; Symons *et al.,* 2009), and humans (Steinberg *et al.,* 2000) demonstrate that elevated FFA cause impairing of the insulin signaling creating continuous and progressive damages to the vascular wall and resulting in endothelial dysfunction.

Recent evidence suggests that oxidative stress may contribute to alter insulin sensitivity in the vascular endothelium. Studies have shown that exposure to FFA increases ROS such as O_2^-, thus triggering molecular pathways of insulin-mediated production NO. Therefore, decreasing this lipotoxicity may also prevent IR at the endothelium.

PPAR play a pivotal role in regulating dietary lipid metabolism and fat storage in mammals (Watt *et al.,* 2004; Arck *et al.,* 2010). PPARβ/δ activation reduces weight gain and circulating TG level, while increasing HDL-cholesterol in HFD-induced obese mice, *db/db*, and *ob/ob* mice through stimulating fatty acid β-oxidation (Cheang *et al.,* 2013). An overexpression of PPARβ/δ significantly reduces the plasma level of FFA as well as the consequent lipotoxicity and improves insulin secretion in pancreatic β-cells by modulating the oxidation of FFA (Martinez *et al.,* 2008). PPARβ/δ also regulates glucose homeostasis in EC, preventing glucose-induced impairment of endothelial insulin signaling in diabetic rodents (Tian *et al.,* 2012a; Quintela *et al.,* 2014). However, there no data showing if PPARβ/δ activation would protect insulin signaling impaired by FFA in EC.

Consequently, *the third aim of this Doctoral Thesis* was to examine the possible protective effect of a PPARβ/δ agonist, GW0742, on endothelial dysfunction induced by palmitate in primary cultures of human umbilical vein endothelial cells (HUVEC) with a focus on impaired insulin signaling.

Obesity and diabetes mellitus are associated with augmented circulating levels of FFA, low-grade chronic inflammation (Antuna-Puente *et al.,* 2008), and endothelial dysfunction attributable to impaired release of endothelium-derived relaxing (mainly, NO) and augmented production of endothelium-derived contracting factors (EDCF) (Vanhoutte *et al.,* 2009). The bioavailability of NO is reduced by obesity and diabetes mellitus (Gruber *et al.,* 2008; Toral *et al.,* 2014). Increased release of ROS also contributes to this endothelial dysfunction (Shi and Vanhoutte, 2008), primarily through reducing NO bioavailability via the direct chemical reaction of O_2^- with NO, resulting in the formation of peroxynitrite ($ONOO^-$). Furthermore, $ONOO^-$ formation may result in further impairment of NO levels and enhanced oxidative stress by inhibiting eNOS activity through oxidation of BH_4, a cofactor of endothelial eNOS. This leads to eNOS uncoupling, where eNOS produces O_2^- instead of NO (Li and Forstermann, 2014).

Pro-inflammatory cytokines (TNF-α, IL-6, resistin, and lipocalin-2) link obesity to metabolic and vascular dysfunction (Antuna-Puente *et al.,* 2008). In this way, LPS and saturated FFA share as pattern recognition target TLR4, which activate inflammatory pathways, induce cytokine expression in the endothelium (Kim *et al.,* 2005; Shi *et al.,* 2006), augment ROS production in the vascular wall (Toral *et al.,* 2014), and induce endothelial dysfunction (Liang *et al.,* 2013; Toral *et al.,* 2014). Both NADPH oxidase (Somers *et al.,* 2000; Brandes and Kreuzer, 2005), and mitochondria (Doughan *et al.,* 2008; Tian *et al.,* 2012b) are major sources of vascular ROS, which are activated by LPS (Emre *et al.,* 2007; Duarte *et al.,* 2013; Liang *et al.,* 2013). Targeting ROS by antioxidants, such as tempol or mitochondrial targeted antioxidant, improve endothelium-dependent vasodilation in hypertensive and diabetic rodents (Minamiyama *et al.,* 2007; Dikalova *et al.,* 2010).

The uncoupling protein-2 (UCP2) is an anion transporter in the inner membrane, which reduces the electromechanical gradient and thus attenuates mitochondrial ROS production (Krauss *et al.,* 2005). In EC, UCP2 overexpression preserves endothelial function through increasing NO bioavailability secondary to the inhibition of ROS production in the endothelium of obese diabetic mice (Tian *et al.,* 2012b). LPS down-regulates UCP2, which was required to increase mitochondrial ROS production and $UCP2^{-/-}$ macrophages exhibited increased inflammatory response induced by LPS (Emre *et al.,* 2007), suggesting a protective role of UCP2. Moreover, UCP2 up-regulation reduced ER stress in macrophages (Xu *et al.,* 2015).

PPARβ/δ modulates LPS-induced inflammation in cultured cardiomyocytes (Ding *et al.,* 2006), adipocytes (Rodriguez-Calvo *et al.,* 2008), and astrocytes (Chistyakov *et al.,* 2014) and protects against multiple organ caused by endotoxin shock (Kapoor *et al.,* 2010). In addition, activation of PPARβ/δ exhibits anti-inflammatory properties in EC (Rival *et al.,* 2002) and protects endothelial function in diabetic mice (Tian *et al.,* 2012a; Cheang *et al.,* 2014) and rats (Quintela *et al.,* 2012; Quintela *et al.,* 2014). PPARβ/δ activation restores endothelial functions through inhibiting ER stress in obese mice by mechanisms incompletely understood (Cheang *et al.,* 2014).

Activation of PPARβ/δ increases UCP2 gene expression in cardiac fibroblast (Teunissen *et al.,* 2007), soleus muscle (Oishi *et al.,* 2008) and pancreatic β-cells (Wan *et al.,* 2010), and would be involved in its protective effects on endothelial function. However, it remains unclear if PPARβ/δ activation modulates endothelial dysfunction induced by LPS, and if UCP2 play a role in this effect.

For this reason, *the last aim of this Doctoral Thesis* was to investigate the protective effects of PPARβ/δ activation on LPS-induced oxidative stress and endothelial dysfunction and determined whether or not UCP2 could contribute to the endothelial benefit of PPARβ/δ activation.

MATERIALS AND METHODS

MATERIALS AND METHODS

1. Animals and experimental groups

Male C57BL/6J mice were obtained from Janvier (St Berthevin Cedex, France). All mice were maintained at a constant temperature (24 ± 1ºC), with a 12-hour dark/light cycle, and they were provided with free access to tap water and food. Animal body weight, food and water intake were controlled regularly. All experiments were performed in accordance with the Guide for the Care and Use of Laboratory Animals (National Institutes of Health (NIH) publication no. 85-23, revised 1996) and approved by our Institutional Committee for the ethical care of animals. Four different experiments were performed, at the end of each one, mice were sacrificed to collect blood and tissue samples for further processing.

1.1. Effects of chronic GW0742 treatment in hypertension, vascular inflammatory, oxidative status and endothelial dysfunction in diet-induced obesity

To study these effects, we performed 2 experiments.

1.1.1. Experiment 1: Five-week old male C57BL/6J mice were randomly assigned to four different groups of 9-10 animals each.

a) Control.
b) Control-treated.
c) HFD.
d) HFD-treated.

Treated mice received GW0742 (Tocris Bioscience, Bristol, UK) by oral gavage 3 mg kg^{-1} per day (mg/kg/d), mixed in 0.1 mL of 1% methylcellulose, and non-treated mice only the vehicle. GW0742 treatment was followed for 13 weeks.

GW0742 is a highly potent and selective PPARβ/δ agonist with a 200-fold higher affinity toward PPARβ/δ than other PPAR isotypes with a half maximal effective concentration (EC_{50}) value of 50 nM for PPARβ/δ. The plasma concentration of GW0742 was not determined in the present study; however, it has been shown that mice treated with 1 and 10 mg/kg/d of GW0742 for 4 weeks showed plasma concentrations of 440.7 and 2,270 nM, respectively (Takata *et al.,* 2008), and $LDLR^{-/-}$ mice treated with 6 mg/kg/d for 16 weeks showed concentrations in the range of 805-1,250 nM (Graham *et al.,* 2005). Notably, the plasma concentration of the ligand at the 3 mg/kg/d dose would be expected to specifically activate PPARβ/δ without any cross-reactivity with other PPAR isoforms because the expected levels (<805 nM) are below the reported EC_{50} values for murine PPARα (8,900 nM) and PPARγ (>10,000 nM) (Graham *et al.,* 2005).

Control mice received standard chow diet (13% calories from fat, 20% calories from protein, 67% calories from carbohydrate) (Global diet 2014, Harlan Laboratories, Barcelona, Spain), whereas obese mice were fed a western-type HFD in which 60% of its caloric content were derived from fat (60.3% calories from fat (lard), 18.4% calories from protein, 21.3 % calories from carbohydrate) (Purified diet 230 HF, Scientific Animal Food & Engineering, Augy, France)

1.1.2. Experiment 2: To determine whether PPARβ/δ is involved on the effects induced by GW0742 in hypertension, vascular inflammatory and oxidative status, and endothelial dysfunction in HFD-fed mice, the PPARβ/δ antagonist GSK0660 was co-administered along with GW0742. Briefly, five-week old male C57BL/6J mice were randomly assigned to five different groups of 8-9 animals each.

a) Control.
b) HFD.
c) HFD-GSK0660.
d) HFD- treated.
e) HFD-treated- GSK0660.

Treated mice received GW0742 by oral gavage 3 mg/kg/d, mixed in 0.1 mL of 1% methylcellulose, whereas non-treated mice only the vehicle. GSK0660 (Tocris Bioscience, Bristol, UK) was injected intraperitoneally (ip) (0.1 mL) at 1 mg/kg/d (Sanchez-Siles *et al.,* 2011). GSK0660 was diluted first in dimethylsulfoxide (DMSO) and later in NaCl 0.9% (DMSO less than 1%). Non-treated mice received the corresponding oral and intraperitoneal vehicles of the active treatments. Treatments were followed for 11 weeks. Control mice received standard chow diet, whereas obese mice were fed with a western-type HFD.

1.2. Experiment 3: Effects of three weeks GW0742 treatment on lipid-induced endothelial dysfunction

Five-week old male C57BL/6J mice were divided into four different groups of 8-9 animals each.

a) Control.
b) HFD.
c) HFD-treated.
d) HFD-treated-GSK0660.

As mentioned above, treated mice received GW0742 by oral gavage 3 mg/kg/d, mixed in 0.1 mL of 1% methylcellulose, and GSK0660 was injected ip (0.1 mL) at 1 mg/kg/d. Mice were treated with the corresponding oral and intraperitoneal vehicles of the substances given to the other groups.

In this experiment, treatments were followed by three weeks in order to study the specific effects of lipid-induced endothelial dysfunction on the vessels, while avoiding other confounding factors such as obesity and established IR.

Control mice received standard chow diet, whereas HFD mice were fed a western-type diet.

1.3. Experiment 4: Effects of GW0742 on LPS-induced endothelial dysfunction

Ten-week old male C57BL/6J mice were randomly divided into four groups (n=10):

1) Control.
2) LPS.
3) LPS-treated.
4) LPS-treated-GSK0660.

In this experiment, treated mice received GW0742 by oral gavage 3 mg/kg/d, mixed in 0.1 mL of methylcellulose and GSK0660 was administrated with 0.1mL of NaCl 0.9% at 1 mg/kg/d. Non-treated mice received the corresponding oral and intraperitoneal vehicles of the substances given to the other groups. After 3 days of treatment, LPS (10 mg/kg) or vehicle (saline) was given ip with four hours prior to sacrifice.

2. Blood pressure measurements

SBP was determined once a week, in the morning, 18-20 h after administration of the drugs in conscious, pre-warmed, restrained mice by tail-cuff plethysmography (digital pressure meter, LE 5001; Letica S.A., Barcelona, Spain). At least seven determinations were made in every session and the mean of the lowest three values within 5 mmHg was taken as the SBP level (Toral *et al.,* 2014).

In experiment 2, at the end of the experimental period, mice were subjected to isofluorane anesthesia, a polyethylene catheter containing 100U heparin in isotonic, sterile NaCl solution was inserted in the left carotid artery to monitor intra-arterial BP in conscious, unrestrained conditions. Direct BP was recorded continuously (MacLab; AD Instruments, Hastings, UK). Twenty-four hours after implantation of the catheter, intra-arterial BP was recorded continuously for 60 min with a sampling frequency of 400/s (McLab; AD Instruments, Hastings, UK). Mean arterial blood pressure (MABP) values

obtained during the last 30 min were averaged for intergroup comparisons (Gómez-Guzmán *et al.,* 2014).

3. Glucose tolerance test

A glucose tolerance test (GTT) was carried on according to the method described by Barroso *et al.* (2011). One week before the sacrifice of the mice, GTT was performed on mice fasted for 18 h. Animals received a 50% glucose solution in water at a dose of 2 g/kg body weight by intraperitoneal injection, and blood was collected from the tail vein after 0, 15, 30, 60 and 120 min.

4. Plasma determinations

At the end of the treatment, mice were killed under isoflurane anesthesia. Blood samples were chilled on ice and centrifuged for 10 min at 3,500 revolutions per minute (rpm) at 4 ºC, and the plasma frozen at -80 °C. Plasma glucose, TG, HDL and total cholesterol concentrations were measured by colorimetric methods using Spinreact kits (Spinreact, S.A., Spain). Plasma insulin concentration was quantified using a mice insulin ELISA kit (Alpco Diagnosis, Salem, USA). Homeostatic model assessment of insulin resistance (HOMA-IR) was calculated using the formula: fasting glucose (mM) x fasting insulin (μU/mL)/22.5. Plasma LPS concentration was measured using the Pierce LAL chromogenic endotoxin quantitation Kit (Thermo Fisher Scientific S.L.U, Alcobendas, Madrid, Spain). Plasma FFA concentration was determined using a Wako NEFA C test kit (Wako Chemicals, Richmond, VA, USA).

5. Morphological variables

The heart, kidney, liver and epididymal and mesenteric fat were excised, cleaned and weighed. The heart, kidney, liver and fat weight indices were calculated by dividing

the heart, kidney, liver and fat weight by the tibia length. All tissue samples were frozen in liquid nitrogen and then stored at -80ºC.

6. Vascular reactivity studies

Descending thoracic aortic rings were dissected from animals and were suspended in a wire myograph (model 610M, Danish Myo Technology, Aarhus, Denmark) for isometric tension measurement as previously described (Toral *et al.,* 2014). The organ chamber was filled with Krebs solution (composition in mM: 118 NaCl, 4.75 KCl, 25 $NaHCO_3$, 1.2 $MgSO_4$, 2 $CaCl_2$, 1.2 KH_2PO_4 and 11 glucose) at 37ºC and gassed with 95% O_2 and 5% CO_2 (pH ~7.4). Length-tension characteristics were obtained via the myograph software (Myodaq 2.01) and the aortae were loaded to a tension of 5 mN.

In endothelium-intact aorta, cumulative concentration-response curves to phenylephrine (Phe) (1 nM - 1 µM) were performed in the absence or in the presence of N^G-nitro-L-arginine methyl ester (L-NAME, 100 µM). The concentration-relaxation response curves to ACh (1 nM - 10 µM) were performed in intact rings pre-contracted by Phe or the thromboxane A_2 analogous U46619 (10 nM) to obtain similar level of pre-contraction in both control and L-NAME treated aortic rings. The relaxant responses to sodium nitroprusside (SNP) (1 nM - 10 µM) were studied in the dark in endothelium-denuded vessels pre-contracted by Phe (1 µM).

In some experiments, responses to ACh were studied after incubation with 10 µM of NADPH oxidase inhibitor apocynin (added 30 min before of U46619) or 10 µM of the UCP2 inhibitor genipin for 60 min before the addition of U46619.

Relaxant responses to ACh and SNP were expressed as a percentage of pre-contraction.

7. *Ex vivo* culture of mouse aortic rings

In order to study lipid-induced endothelial dysfunction, specific, we employed palmitic acid, which is considered as a major component of dietary saturated fat and 20 percent of the total serum FFA, and it is often used to induce endothelial dysfunction (Kim *et al.,* 2005; Maloney *et al.,* 2009; Contreras *et al.,* 2011).

With this purpose, mouse thoracic aortic rings (2 mm in length) were dissected in sterile phosphate-buffered saline (PBS) and incubated in Dulbecco's modified Eagle's medium (DMEM) supplemented with 10% fetal bovine serum (FBS), plus 100 U/mL penicillin, and 100 µg/mL streptomycin. Lipid-containing media were prepared by conjugation of palmitic acid with fatty acid-free bovine serum albumin (BSA), using a method modified from that described previously (Chavez and Summers, 2003). Briefly, palmitic acid was dissolved in ethanol and diluted 1:100 in DMEM containing 2% (w/v) fatty acid-free BSA. Aortic rings were incubated for 24 h in serum-free DMEM containing 2% fatty acid-free BSA (control) or palmitate (100 µM)-conjugated BSA in either the presence or absence of GW0742 (1 µM). In some experiments, the rings were co-incubated with GSK0660 (1 µM) or with CPT-1 irreversible inhibitor etomoxir (40 µM). After the incubation period the rings were transferred to a chamber filled with fresh Krebs solution and mounted in the myograph for measurement of changes in isometric force or used to western blot.

Responses to ACh were studied after incubation with apocynin (10 µM), or the mitochondrial antioxidant mitoquinone (mitoQ, generously given by Dr. MP Murphy, Medical Research Council Mitochondrial Biology Unit, Cambridge, UK, 0.1 µM), incubated for 60 min before the addition of U46619.

8. Primary culture of mouse aortic endothelial cells (MAEC)

MAEC were isolated from mouse thoracic aortae using a previously reported method with several modifications (Kobayashi *et al.,* 2005). The aortae were isolated from male C57BL/6J mice (8-12 weeks of age). Fat and connecting tissues were

rapidly removed. A 24-gauge cannula was inserted into the proximal portion of the aorta. After ligation at the site with silk thread, the inside of the lumen is briefly washed with PBS. The other side is bound and filled with collagenase (type P) solution (2mg/mL, dissolved in serum-free Medium 199). After incubation for 40 min at 37ºC, EC are removed from the aorta by flushing with 1 mL of medium 199 containing 20% FBS. EC should be collected by centrifugation at 2,300 rpm for 5 minutes. Then, the precipitate is gently resuspended with 2 mL of 20% FBS-medium 199 and cultured in a 35mm pretreated with 0.2% gelatin disk. To remove smooth muscle cells, after 2 hours incubation at 37ºC, the medium is removed, the cells were washed with warmed PBS and culture medium was added.

The cells were cultured (medium 199 (Lonza, Basel, Switzerland) + 20% FBS + 2 mM penicillin/streptomycin + 2 mM amphotericin B + 2 mM glutamine + 10 mM 4-(2-hydroxyethyl)-1-piperazineethanesulfonic acid (HEPES) + 30 µg/mL endothelial cell growth supplement + 100 mg/mL heparin) under 5% CO_2 at 37°C. All the cells used in the experiments from passages 2 to 5 were starved in serum-free medium for 2 h before the experiments.

MAEC were incubated with GW0742 (1 µM), during 15 hours, and in the last 3 hour in serum-free medium 199 containing 2% fatty acid-free BSA (control cells) or palmitate (100 µM)-conjugated BSA. In some experiments, cells were co-incubated with the PPARβ/δ antagonist GSK0660 (1 µM), 1 hour before the addition of GW0742, with etomoxir (40 µM), or with the non-selective protein kinase C (PKC) inhibitor chelerythrine (1 µM) during palmitate incubation. In other experiments, apocynin (10 µM), or mitoQ (0.1 µM), were added during palmitate incubation.

In another set of experiments, MAEC were incubated with GW0742 (1 µM), during 16 hours, and in the last 4 hour in LPS-free (control cells) or LPS-containing (10 µg/mL) serum-free medium 199. In some experiments, cells were co-incubated with the PPARβ/δ antagonist GSK0660 (1 µM), or with the UCP2 inhibitor genipin (10 µM) 1 hour prior the addition of GW0742. In other experiments apocynin (10 µM), the ER stress inhibitor 4-phenylbutyric acid (4-PBA, 0.1 mM), the mitochondrial antioxidant

mitoQ (0.1 μM), or the AMPK inhibitor compound C (10 μM) were added during LPS incubation.

9. Primary culture of human umbilical vein endothelial cells (HUVEC)

EC were isolated from human umbilical cord veins using a previously reported method with several modifications (Jimenez *et al.,* 2010). After ligation at the site with silk thread, the inside of the lumen is briefly washed with PBS solution with 2 mM penicillin/streptomycin and 2 mM amphotericin B. HUVEC were isolated by filling the lumen of fresh umbilical veins with 0.1% collagenase (type P) in PBS during incubation for 20 min at 37ºC, inverting the umbilical cord and washing the vein with culture medium. HUVEC should be collected by centrifugation at 2,300 rpm for 5 minutes. Then, the precipitate is gently resuspended with 1 mL of 20% FBS-medium 199 and the collected cells were seeded in culture flasks pre-treated with 0.2% gelatin containing culture medium.

The cells were cultured in medium 199 supplemented with 20% FBS, 2 mM penicillin/streptomycin, 2 mM amphotericin B, 2mM glutamine, 10 mM HEPES, 30 μg/mL endothelial cell growth supplement and 100 mg/mL heparin, in a humidified 5% CO_2 atmosphere at 37°C. All the cells used in the experiments from passages 2 to 5 were starved in serum-free medium for 2 h before the experiments.

HUVEC were incubated with GW0742 (1 μM), during 15 hours, and in the last 3 hour in serum-free medium 199 containing 2% fatty acid-free BSA (control cells) or palmitate (100 μM)-conjugated BSA. In some experiments, cells were co-incubated with GSK0660 (1 μM), 1 hour before the addition of GW0742, or with etomoxir (40 μM) during palmitate incubation. In other experiments, the inhibitor of complex I rotenone (5 μM), the inhibitor of complex II, thenoyltrifluoroacetone (TTFA, 10 μM), the uncoupler of oxidative phosphorylation, carbonyl cyanide m-chlorophenylhydrazone (CCCP, 0.5

μM), the non-selective NADPH oxidase inhibitor diphenyliodonium chloride (DPI, 10 μM), apocynin (10 μM) or mitoQ (0.1 μM) were added during palmitate incubation.

10. Transfection of CPT-1 and UCP2 small interfering RNA (siRNA)

Confluent MAEC were transfected with control, CPT-1-specific siRNA or UCP2-specific siRNA (pooled, validated siRNA from Dharmacon, Lafayette, CO, USA) using lipofectamine RNAiMAX (Invitrogen Life Technologies, Carlsbad, CA, USA) for 48 h, essentially as described previously (Quintela *et al.,* 2014). For that, MAEC were seed to a 60-80% confluent at the time of transfection in antibiotics- and serum-free medium 199. siRNA-lipid complexes were prepared adding specific siRNA to lipofectamine, both previously diluted in medium 199, and incubating for 20 minutes at room temperature, then, these complexes were added to cells, which were incubated for 3 hours at 37°C. Finally, MAEC were washed and incubated with complete medium 199. After 48 hours, cells were used to measure NO or ROS production, gene and protein expression.

To check efficiency of transfection, protein and gene expression of CPT-1 and UCP2 were analyzed by western blot and real-time RT-PCR, respectively.

11. Quantification of NO released by diaminofluorescein-2 (DAF-2)

Quantification of NO released by MAEC and HUVEC was performed using the NO-sensitive fluorescent probe DAF-2 as described previously (Quintela *et al.,* 2014). Briefly, cells were incubated as mentioned above. After this period, cells were washed with PBS and then were pre-incubated with 100 μM L-arginine in PBS for 5 min at 37ºC. Subsequently, 0.1 μM DAF-2 was incubated for 2 min and then 1 μM calcium ionophore calimycin (A23187) or 100 nM insulin were added for 30 min. Then the

fluorescence intensity (arbitrary units, AU) was measured at 5, 15 and 30 min using a spectrofluorimeter (Fluorostart, BMG Labtechnologies, Offenburg, Germany) with excitation wavelength set at 490nm and emission wavelength at 510 nm. The autofluorescence was subtracted from each value. In some experiments, 100 μM L-NAME was added 15 min before the addition of L-arginine. The difference between fluorescence signal without and with L-NAME was considered NO production.

12. In situ detection of vascular ROS content

Unfixed thoracic aortic rings were cryopreserved (0.1 M PBS plus 30% sucrose for 1-2h), included in optimum cutting temperature compound medium (Tissue-Tek; Sakura Finetechnical, Tokyo, Japan), frozen (-80ºC), and 10 μm cross-sections were obtained in a cryostat (Microm International Model HM500 OM). Sections were incubated for 30 min in HEPES buffer solution, containing dihydroethidium (DHE, 10 μM), counterstained with the nuclear stain 4,6-diamidino-2-phenylindoledichlorohydrate (DAPI, 300 nM) and in the following 24 h examined on a fluorescence microscope (Leica DM IRB, Wetzlar, Germany). Sections were photographed and ethidium and DAPI fluorescence were quantified using ImageJ (version 1.32j, NIH, http://rsb.info.nih/ij/). ROS production was estimated from the ratio of ethidium/DAPI fluorescence (Toral e*t al.,* 2014). In preliminary experiments, before incubation with DHE, serial sections were treated with either the O_2^- scavenger tiron (10 μM), or pegylated superoxide dismutase (PEG-SOD, 250 U/mL) for 30 min at 37ºC, indicating the specificity of this reaction.

13. Measurement of intracellular ROS concentrations

Endothelial ROS production was measured using two independent methods:

A. The fluorescent probe 5-(and-6-)chloromethyl-2'-7'-dichlorodihydrofluorescein diacetate (CM-H2DCFDA) (Invitrogen Life Technologies, Carlsbad, CA, USA) was used to determine the intracellular generation of ROS in EC. This reagent enters into cells and reacts with ROS to generate the fluorescent product 2'-7'-dichlorofluorescein.

In some experiments, cells were pre-incubated either with the mitochondrial antioxidant mitoQ (0.1 μM) or the membrane-permeable superoxide dismutase mimetic tempol (50 μM) for 60 min prior the addition of GW0742.

From there on, confluent MAEC or HUVEC in 96-well plates, incubated as previously explained, were then incubated with 5 μM CM-H2DCFDA for 30 min at 37ºC. After removal the media and washing of the cells, the fluorescent intensity (relative fluorescent units) was measured at an excitation and emission wavelength of 490 nm and 545 nm, respectively, using a spectrofluorimeter (Fluorostart, BMG Labtechnologies, Offenburg, Germany).

B. The O_2^- production in intact EC was also measured by DHE fluorescence HPLC assay as described previously (Fernandes *et al.,* 2007; Laurindo *et al.,* 2008). After incubations described above, MAEC were washed with PBS/diethylenetriaminepentaacetic acid (DTPA) two to three times. All subsequent steps were done under dim light. PBS/DTPA and DHE (50 μM) was added to each well and plates were kept in an incubator (at 37ºC under 5% CO_2) for 30 min. Thereafter, cells were washed two to three times with PBS/DTPA. Acetonitrile (500 μL) was added to each well and the cells were immediately harvested and the lysate was kept over ice. The lysates were centrifuged at 12,000 g for 10 min at 4 ºC, and supernatants were dried under vacuum. For HPLC analysis, pellets were resuspended in 120 μL PBS/DTPA, and a volume of

50 µl was injected. Samples were analyzed by HPLC (Varian 920 LC series), using a 4 µm C_{18} reverse-phase column (Synergi 150 x 4.6 mm, Phenomenex, Torrance, CA, USA) and a gradient of solutions A (pure acetonitrile) and B (water/10% acetonitrile/0.1% trifluoroacetic acid, by vol.) at a flow rate of 1 mL/min, and run as described by Laurindo *et al. (*2008). Ethidium and 2-hydroxyethidium (2-OH-E^+) were monitored by fluorescence detection with excitation at 510 nm and emission at 595 nm. The 2-OH-E^+ peak reflect the amount of O_2^- formed in the cells during the incubation. Values were normalized per µg of protein and the increase of 2-OH-E^+ peak was represented as an increase (n-fold) compared with control. To optimize the HPLC analysis, 50 µM DHE was incubated with xanthine/xanthine oxidase (0-50 µM and 0.1 U/mL) in Krebs-Henseleit solution (KHS)/HEPES/DTPA at 37°C for 30 min. 2-OH-E^+ was separated by HPLC as described above.

14. Measurement of mitochondrial ROS production

Mitochondrial O_2^- production was measured using a previously reported method with several modifications (Wojtala *et al.,* 2014), employing the MitoSOX™ Red (Invitrogen Life Technologies, Carlsbad, CA, USA), a mitochondrial O_2^- indicator.

Confluent MAEC grown in multi-well plates were incubated as mentioned above. Subsequently, MitoSOX™ Red (5 µM) was added and cells were incubated in the dark, 30 min at 37ºC (needed to allow the probe to enter the cell and start the reaction within the mitochondria). After removal the media and washing of the cells with PBS, the fluorescent intensity (relative fluorescent units) was measured at an excitation and emission wavelength of 490 nm and 590 nm, respectively, using a spectrofluorimeter (Fluorostart, BMG Labtechnologies, Offenburg, Germany).

15. NADPH oxidase activity

NADPH-enhanced O_2^- release in homogenates from cultured MAEC and HUVEC or intact aortic rings was quantified by lucigenin-enhanced chemiluminescence, as previously described (Sanchez *et al.,* 2007).

On the one hand, cells were incubated as mentioned in section 8 and 9. After this period, cells were washed with cold PBS and homogenized in lysis buffer composed of 20 mM KH_2PO_4, 1 mM EGTA, 10 µg/mL aprotinin, 0.5 µg/mL leupeptin, 0.75 µg/mL pepstatin, 0.5 mM phenylmethysulfonyl fluoride (PMSF) (pH~7.4).

Whereas, aortic rings from all experimental groups were incubated for 30 min at 37°C in HEPES-containing physiological salt solution (pH~7.4) of the following composition (in mM): 119 NaCl, 20 HEPES, 4.6 KCl, 1 $MgSO_4$, 0.15 Na_2HPO_4, 0.4 KH_2PO_4, 1 $NaHCO_3$, 1.2 $CaCl_2$ and 5.5 glucose.

Then NADPH (100 µM) was added to the buffer containing the MAEC or HUVEC homogenate suspension (30 µg of protein in 500 µL) or aortic rings, and lucigenin (5 µM) was injected automatically. NADPH oxidase activity was determined by measuring luminescence over 200 s in a scintillation counter (Lumat LB 9507, Berthold, Germany) in 5-s intervals and was calculated by subtracting the basal values from those in the presence of NADPH and expressed as RLU (relative light units)/min per µg of protein for cells or RLU/min per mg of tissue for aortic rings.

The NADPH oxidase activity in intact MAEC was also measured by DHE fluorescence assay in the microplate reader, as described previously (Fernandes *et al.,* 2007). Confluent MAEC grown in 6-well dishes (well area of 9.6 cm^2) incubated as previously described were washed with ice-cold PBS, harvested, homogenized in lysis buffer composed of 50 mM Tris-HCl (pH 7.4) containing 0.1 mM EDTA, 0.1 mM EGTA, 10 µg/mL aprotinin, 10 µg/mL leupeptin and 1 mM PMSF, sonicated (10s of 3 cycles al 8W). Fresh homogenates (10 µg of protein) were incubated with DHE (10 µM) and DNA (1.25 µg/mL) in PBS (100 mM), pH 7.4, containing 100 µM DTPA with the addition of NADPH (50 µM), at a final volume of 120 µL. Incubations were performed for 30 min at 37ºC, in the absence or presence of SOD conjugated to PEG-SOD (25

U/mL), in the dark. Total fluorescence was followed in a microplate reader using a rhodamine filter (excitation 490 nm and emission 590 nm) in a spectrofluorometer (Fluorostart, BMG Labtechnologies, Offenburg, Germany).

16. Reverse transcriptase-polymerase chain reaction (RT-PCR) analysis

For RT-PCR analysis, total RNA was extracted from liver, fat, aorta or MAEC and HUVEC by homogenization and converted to cDNA using standard methods. PCR was performed with a Techne Techgene thermocycler (Techne, Cambridge, UK). A quantitative real-time RT-PCR technique was used to analyse mRNA expression. The sequences of the sense and antisense primers used for amplification are described in Table 3 (for mouse) and Table 4 (for human). Preliminary experiments were carried out with various amounts of cDNA to determine non-saturating conditions of PCR amplification for all the genes studied. Therefore, under these conditions, relative quantification of mRNA was assessed by the SYBR Green based-RT-PCR method. The efficiency of the PCR reaction was determined using a dilution series of a standard tissue sample. Quantification was performed using the $\Delta\Delta$Ct method. The housekeeping genes ribosomal protein L13a (RPL13a), β-actin or glyceraldehyde-3-phosphate dehydrogenase (GADPH) were used for internal normalization.

Table 3. Oligonucleotides for mouse used in real-time RT-PCR.

mRNA targets	Descriptions	Sense	Antisense
p47phox	P47phox subunit of NADPH oxidase	ATGACAGCCAGGTGAAGAAGC	CGATAGGTCTGAAGGCTGATGG
p22phox	P22phox subunit of NADPH oxidase	GCGGTGTGGACAGAAGTACC	CTTGGGTTTAGGCTCAATGG
Cav-1	Caveolin-1	TCTACAAGCCCAACAACAAGG	AGGAAAGAGAGGATGGCAAAG
eNOS	Endothelial nitric oxide synthase	ATGGATGAGCCAACTCAAGG	TGTCGTGTAATCGGTCTTGC
NOX-1	NOX-1 subunit of NADPH oxidase	TCTTGCTGGTTGACACTTGC	TATGGGAGTGGGAATCTTGG
NOX-2	NOX-2 subunit of NADPH oxidase	ATGCAGGAAAGGAACAATGC	TTGCAATGGTCTTGAACTCG
NOX-4	NOX-1 subunit of NADPH oxidase	ACAGTCCTGGCTTACCTTCG	TTCTGGGATCCTCATTCTGG
IL-6	Interleukin-6	GATGGATGCTTCCAAACTGG	AGGAGAGCATTGGAAGTTGG
TNF-α	Tumor necrosis factor-alpha	ACGATGCTCAGAAACACACG	CAGTCTGGGAAGCTCTGAGG
IL-1β	Interleukin-1 beta	GTCACTCATTGTGGCTGTGG	GCAGTGCAGCTGTCTAATGG
JNK-1	c-JunN-terminal kinase- 1	GATTTTGGACTGGCGAGGACT	TAGCCCATGCCGAGAATGA
Adiponectin	Adiponectin	GATGGCAGAGATGGCACTCC	CTTGCCAGTGCTGCCGTCAT
TLR4	Toll-like receptor 4	GCCTTTCAGGGAATTAAGCTCC	AGATCAACCGATGGACGTGTAA
ABCG1	ATP-Binding Cassette Transporter G1	AAGGCCTACTACCTGGCAAAGA	GCAGTAGGCCACAGGGAACA
CPT-1	Carnitine palmitoyl transferase-1	GGACCGTGAAGAGATCAAGC	CGAGGATTCTCTGGAACTGC
UCP2	Uncoupling protein -2	GCCACTTCACTTCTGCCTTC	GAAGGCATGAACCCCTTGTA
PDK-4	Pyruvate dehydrogenase kinase-4	CACATGCTCTTCGAACTCTTCAAG	TGATTGTAAGGTCTTCTTTCCCAAG
Cu/ZnSOD	Copper/zinc superoxide dismutase	CAATGTGACTGCTGGAAAGG	AATCCCAATCACTCCACAGG

mRNA targets	Descriptions	Sense	Antisense
MnSOD	Manganese superoxide dismutase	ACGTTTCTTTGGCTCATTGG	GCGCCTCTCAGATAAACAGG
GPx-1	Glutathione peroxidase	GCTGCTCATTGAGAATGTCG	CAGGTCGGACGTACTTGAGG
HO-1	Hemo-oxigenase-1	ACAGCCCCACCAAGTTCAAA	GCCAGGCAAGATTCTCCCTT
Mfn2	Mitofusin-2	GGGGCCTACATCCAAGAGAG	GCAGAACTTTGTCCCAGAGC
BiP	Binding immunoglobulin protein	CAAAGAGCGCATTGACAC	TCTTCAATGTCCGCATCC
IRE-1α	Inositol-requiring 1 transmembrane Kinase/endonuclease-1α	AAGATGGACTGGCGGGAGAAC	GGGAAGCGGGAAGTGAAGTAG
PERK	Eukaryotic translation initiation factor-2α kinase 3	ATGCACAGGGACCTCAAG	CTGCTCTGGGCTCATGTATAG
ATF-6	Activating transcription factor-6	TTCGAGGCTGGGTTCATAG	GGGAGGCGTAATACACTT
CHOP	CCAAT/enhancer binding protein homologous protein	CAGGAGAACGAGCGGAAAGTGG	TGCTGGGTACACTTCCGGAGAG
PPARα	Peroxisome proliferator-activated receptor alpha	AGGCTGTAAGGGCTTCTTTCG	GGCATTTGTTCCGGTTCTTC
PPARβ/δ	Peroxisome proliferator-activated receptor beta	TAGGACTGGTGATCTGTGAG	TACAAGTGAGTGGGAGAGAG
PPARϒ	Peroxisome proliferator-activated receptor gamma	CATGGTGCCTTCGCTGAT	CAATGGCCATGAGGGAGTTA
Actb	Beta actin	AATCGTGCGTGACATCAAG	ATGCCACAGGATTCCATACC
RPL13a	Ribosomal protein L13a	CCTGCTGCTCTCAAGGTTGTT	TGGTTGTCACTGCCTGGTACTT
GADPH	Glyceraldehyde-3-phosphate dehydrogenase	TGCACCACCAACTGCTTAGC	GGATGCAGGGATGATGTTCT

Table 4. Oligonucleotides for human used in real-time RT-PCR.

mRNA targets	Descriptions	Sense	Antisense
CPT-1	Carnitine palmitoyl transferase-1	TTCTTCTTCCGCCAAACC	GAAGGCGGATACACATAGC
HPRT-1	Hypoxanthine phosphoribosyltransferase-1	TGACACTGGCAAAACAATGCA	GGTCCTTTTCACCAGCAAGTC
Actb	Beta actin	CGGTGAAGGTGACAGCAG	TGTGTGGACTTGGGAGAGG

17. Western blotting analysis

Aortic ring were homogenized in cold lysis buffer (pH~7,4) containing: 50 mM Tris-HCl, 150 mM NaCl, 2 mM EDTA, 50 mM NaF, 0.1 % sodium dodecyl sulphate (SDS), 0.5% Na-deoxycholate, 1% Triton X-100, 1 mM PMSF, 0.5 µg/mL aprotinin, 0.5 µg/mL leupeptin and 0.2 mM Na_3VO_4. Whereas, confluent MAEC or HUVEC were washed with cold PBS, harvested, homogenized in cold lysis buffer composed of 20 mM HEPES (pH~7.9), 100 mM NaCl, 1 mM Na_3VO_4, 4 mM $Na_4P_2O_7$, 10 mM EDTA, 1 mM PMSF, 10 mM NaF, 0.1 mM okadaic acid and 1% Triton X-100.

Aortic, MAEC or HUVEC homogenates were run on a SDS-polyacrilamide gel electrophoresis (PAGE) (40 µg of protein per lane). Then, proteins were transferred to polyvinylidene difluoride membranes, incubated overnight at 4°C with primary antibodies (1:1000) (Table 5). Afterwards, the membranes were washed three times for 10 min in Tris-buffered saline (containing 0.1% Tween 20) and were incubated with the correspondent secondary peroxidase conjugated antibodies (1:3000) (Table 5) at room temperature for 2 h. After washing the membranes, antibody binding was detected by an electrochemiluminescent (ECL) system (Amersham Pharmacia Biotech, Amersham, UK). Films were scanned and densitometric analysis was performed using Scion Image-Release Beta 4.02 software (http://www.scioncorp.com) (Quintela *et al.,* 2014).

For phosphorylated proteins, abundance ratio was calculated and data are expressed as a percentage of the values in control aorta or cells from the same gel. Aortic, MAEC or HUVEC samples were re-probed for expression of α-actin or β-actin, respectively.

Table 5. Antibodies used in western blot.

Primary antibody (supplier)	**Secondary antibody (supplier)**	**% SDS-polyacrilamide gel electrophoresis**	**kDa**
Mouse monoclonal **anti-p-eNOS (Ser^{1177})** (Cell Signaling Technology, MA, USA)	Goat anti-mouse (Santa Cruz Biotechnology, Santa Cruz, USA)	8%	140
Rabbit monoclonal **anti-p-eNOS (Thr^{495})** (Merck Millipore, Darmstadt, Germany)	Goat anti-rabbit (Santa Cruz Biotechnology, Santa Cruz, USA)	8%	140
Mouse monoclonal **anti-eNOS** (Transduction Laboratories, California, USA)	Goat anti-mouse (Santa Cruz Biotechnology, Santa Cruz, USA)	8%	140
Rabbit monoclonal **anti-p-Akt (Ser^{473})** (Cell Signaling Technology, MA, USA)	Goat anti-rabbit (Santa Cruz Biotechnology, Santa Cruz, USA)	10%	60
Rabbit monoclonal **anti-Akt** (Cell Signaling Technology, MA, USA)	Goat anti-rabbit (Santa Cruz Biotechnology, Santa Cruz, USA)	10%	60
Rabbit monoclonal **anti-TNF-α** (Cell Signaling Technology, MA, USA)	Goat anti-rabbit (Santa Cruz Biotechnology, Santa Cruz, USA)	12%	17-28
Rabbit monoclonal **anti-IL-6** (Cell Signaling Technology, MA, USA)	Goat anti-rabbit (Santa Cruz Biotechnology, Santa Cruz, USA)	12%	24

Primary antibody (supplier)	**Secondary antibody (supplier)**	**% SDS-polyacrilamide gel electrophoresis**	**kDa**
Rabbit polyclonal **anti-TLR4** (Cell Signaling Technology, MA, USA)	Goat anti-rabbit (Santa Cruz Biotechnology, Santa Cruz, USA)	10%	110
Rabbit polyclonal **anti-p-IκB-α (Ser$^{32/36}$)** (Santa Cruz Biotechnology, Santa Cruz, USA)	Goat anti-rabbit (Santa Cruz Biotechnology, Santa Cruz, USA)	10%	40
Rabbit polyclonal **anti-PPARβ/δ** (Transduction Laboratories, California, USA)	Goat anti-rabbit (Santa Cruz Biotechnology, Santa Cruz, USA)	10%	52
Rabbit polyclonal **anti-NOX-1** (Novus Biological, Cambridge, UK)	Goat anti-rabbit (Santa Cruz Biotechnology, Santa Cruz, USA)	10%	65
Goat polyclonal **anti-CPT-1** (Santa Cruz Biotechnology, Santa Cruz, USA)	Rabbit anti-goat (Santa Cruz Biotechnology, Santa Cruz, USA)	10%	80/82
Rabbit polyclonal **anti-p-PKCα/βII (Thr$^{638/641}$)** (Cell Signaling Technology, MA, USA)	Goat anti-rabbit (Santa Cruz Biotechnology, Santa Cruz, USA)	10%	86/94
Rabbit polyclonal **anti-PKCα** (Cell Signaling Technology, MA, USA)	Goat anti-rabbit (Santa Cruz Biotechnology, Santa Cruz, USA)	10%	80
Rabbit polyclonal **anti-Mfn2** (Sigma-Aldrich, Barcelona, Spain)	Goat anti-rabbit (Santa Cruz Biotechnology, Santa Cruz, USA)	10%	86
Goat polyclonal **anti-UCP2** (R&D Systems, Minneapolis, USA)	Rabbit anti-goat (Santa Cruz Biotechnology, Santa Cruz, USA)	10%	33

Primary antibody (supplier)	Secondary antibody (supplier)	% SDS-polyacrilamide gel electrophoresis	kDa
Rabbit polyclonal **anti-p-IRS-1 (Ser^{307})** (Bioworld Technology,MN, USA)	Goat anti-rabbit (Santa Cruz Biotechnology, Santa Cruz, USA)	8%	180
Rabbit polyclonal **anti-IRS-1** (Bioworld Technology,MN, USA)	Goat anti-rabbit (Santa Cruz Biotechnology, Santa Cruz, USA)	8%	180

18. Co-immunoprecipitation

Aortic homogenates were immunoprecipitated, as previously described (Zarzuelo *et al.,* 2013b), by using a Cav-1 antibody (Transduction Laboratories, San Diego, California, USA) and analyzed by western blot using antibodies against eNOS (Transduction Laboratories, San Diego, California, USA). Briefly, aortic homogenates were brought to a final volume of 0.5 mL with buffer containing 10 mM PBS, 50 mM KCl, 0.05 mM EDTA, 2.5 mM $MgCl_2$, 8.5% glycerol, 1 mM dithiothreitol, 0.1% Triton X-100, 2% BSA and 1 mg/mL non-fat milk for 6 h at 4 °C, and incubated with 3 µg of Cav-1. Immunocomplex was captured by incubating the samples with protein A-agarose suspension overnight at 4 °C on a rocking platform. Agarose beads were collected by centrifugation and washed three times with PBS containing protease inhibitors. After centrifugation, the pellet was washed with 60 µL of SDS-PAGE sample buffer and boiled for 5 min at 100 °C. An aliquot of the supernatant was subjected to electrophoresis on 10% SDS-PAGE and immunoblotted with an antibody against eNOS.

19. Measurement of diacylglycerol (DAG)

DAG levels in MAEC were measured by the DAG kinase assay method as previously described (Coll *et al.,* 2010). Briefly, confluent MAEC incubated were washed with cold PBS, harvested and homogenized in PBS. Then, lipids were extracted from approximately 50 µg of MAEC with 600 µL of chloroform, methanol, 1 N HCl in a proportion of 100:100:1. After agitation and centrifugation, the lower phase containing the chloroform-extracted lipids was transferred to a new microfuge tube. Chloroform was evaporated under a N_2 stream. Dried lipids were resuspended in 300 µL of 0.1 N KOH in methanol and incubated for 1 h at 37°C to eliminate DAG. Then, 300 µL of PBS was added, and lipid extraction was repeated as indicated above. Lipids were resuspended in 100 µL of reaction buffer (150 ng/100 µL cardiolipin, 280 µM DTPA, 51 mM octyl β-d-glucopyranoside, 50 mM NaCl , 51 mM imidazole, 1 mM EDTA, 12.5 mM $MgCl_2$, 2 mM dithiothreitol, 0.7% glycerol, 70 µM β-mercaptoethanol, 500 µM ATP, 5 µCi/100 µL [γ-^{32}P]ATP), and 35 ng of DAG kinase was added to each sample. Reactions were incubated at 30 °C for 30 min and stopped by the addition of 170 µL of stop buffer (135 mM NaCl, 1.5 mM $CaCl_2$, 0.5 mM glucose, 10 mM HEPES, pH 7.2) and 30 µL of 100 mM EDTA. Lipids were extracted again with 1 mL chloroform, methanol, HCl 1 N (100:100:1), resuspended in 40 µL of chloroform, spotted onto silica gel TLC plates (Whatman Inc.), and resolved using chloroform: methanol: acetic acid (65:15:5) as a solvent. Plates were measured in a PhosphoImager (BioRad). Quantification of DAG mass was obtained by comparison with a standard curve ranging from 0 to 1000 pmoL of ceramide-1-phosphate, which was processed in parallel to the samples.

20. Reagents

All chemicals were obtained from Sigma-Aldrich (Barcelona, Spain), unless otherwise stated.

21. Statistical analysis

Results are expressed as means ± SEM. Statistical analyses were performed using Graph Pad Prism 5 software. A two-factor ANOVA was used to test for drug or group interactions. When a significant interaction was detected, one-way ANOVA with a Student Newman-Keuls post hoc test was used to discern individual differences between groups. Significance was accepted at $P<0.05$.

RESULTS

RESULTS

1. Chronic peroxisome proliferator-activated receptorβ/δ agonist GW0742 prevents hypertension, vascular inflammatory and oxidative status, and endothelial dysfunction in diet-induced obesity

1.1. Effects of GW0742 treatment on morphological variables, plasma determinations, and blood pressure

As expected, body weight increased steadily over the 13-weeks study period among mice fed HFD compared to low-fat-fed control mice, and this effect became statistically significant after 1 week of HFD feeding (Figure 9A). Similarly, energy intake was higher in the HFD-fed group when compared with control mice (Figure 9B). GW0742 treatment of mice feeding control or HFD significantly reduced body weight gain when compared with the vehicle-treated mice. Statistical differences were observed as early as 4 weeks after initiation of the treatment. Importantly, daily energy intake of GW0742-treated mice was similar to that of vehicle-treated mice. Anatomical analysis (Figure 9C and D) revealed that mesenteric and epididymal adipose depots were also increased after HFD intake. Again, long-term administration of GW0742 significantly reduced fat depots in mice fed control and HFD.

Analysis of metabolic plasma variables (Table 6) showed that fasted glycemia, the area under curve (AUC) 120 min after GTT, HOMA-IR, plasma TG and plasma cholesterol were higher in HFD-fed mice when compared with control mice. Long-term GW0742 treatment reduced basal glycemia, IR and plasma TG, improved glucose tolerance, increased HDL but it was without effect on fasting plasma insulin and cholesterol. LPS plasma levels were also significantly higher in HFD than in control mice, thus revealing the existence of endotoxemia, which was unaffected after GW0742 treatment (Table 6). SBP was increased in HFD fed mice as compared to

control group, and this change was prevented by chronic GW0742 treatment (Figure 10A). Similarly, heart and kidney hypertrophy, which were also found in obese mice, was prevented by the drug (Figure 10B and C).

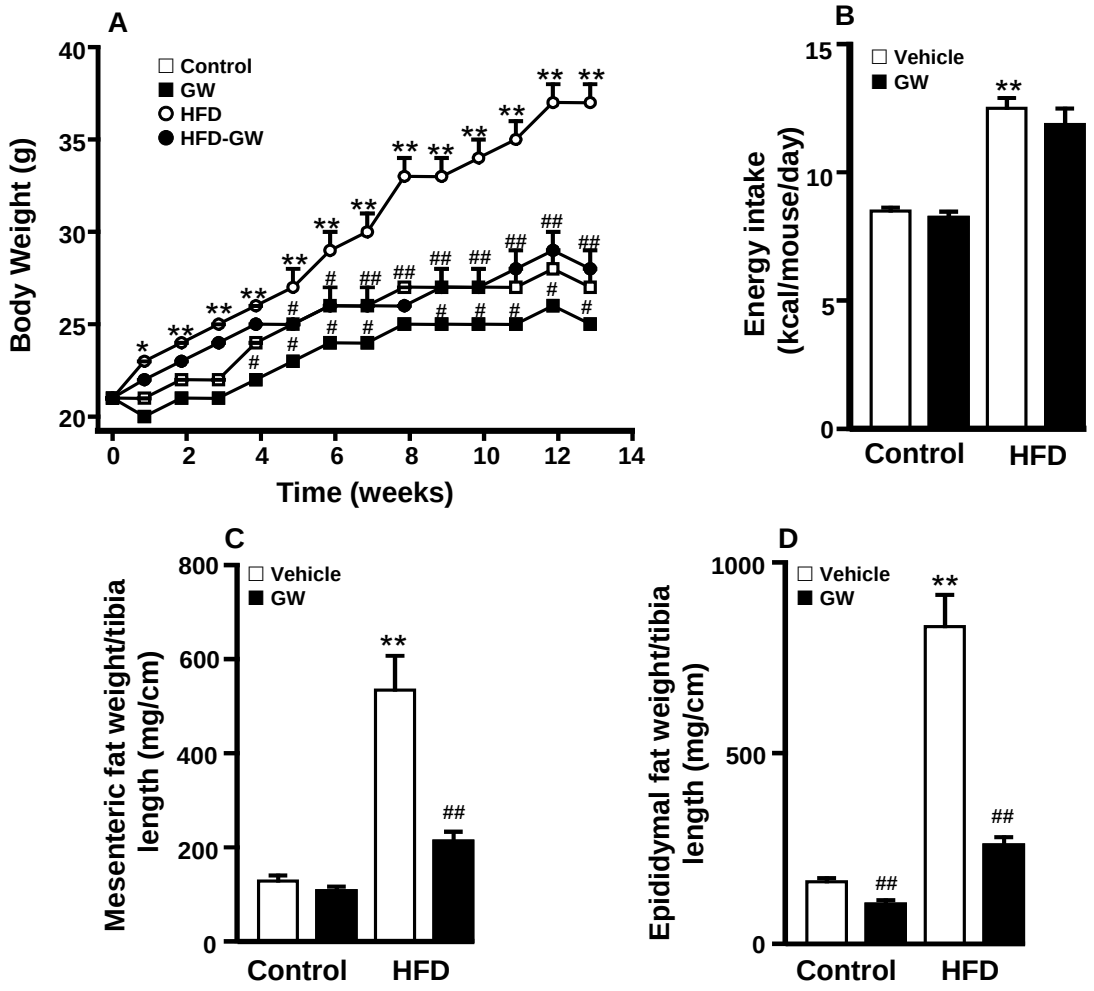

Figure 9. Effects of GW0742 (GW) administration on the morphological changes*. Body weight evolution (**A**), energy intake (**B**), mesenteric fat (**C**), and epididymal fat (**D**) in control and high fat diet (HFD)-fed mice. Values are means ± SEM (n= 9-10). *P<0.05 and **P<0.01 vs control; #P<0.05 and ##P<0.01 vs non-treated HFD-fed mice.*

Table 6. Plasma determinations in all experimental groups (Experiment 1).

	Control (n = 10)	Control-GW (n = 10)	HFD (n = 9)	HFD-GW (n = 10)
Fasting glucose (mg/dL)	88.5 ± 5.6	89.7 ± 2.5	136.9 ± 10.6**	105.6 ± 4.2$^{\#}$
Total cholesterol (mg/dL)	84.9 ± 3.6	102.1 ± 2.7	125.3 ± 10.7*	121.1 ± 4.0
TG (mg/dL)	51.6 ± 3.9	51.0 ± 3.3	86.7 ± 11.2*	60.7 ± 9.2$^{\#}$
HDL (mg/dL)	87.6 ± 5.1	98.1 ± 3.7	85.2 ± 4.4	133.3 ± 15.4$^{\#}$
Fasting insulin (ng/mL)	0.48 ± 0.08	0.60 ± 0.13	0.59 ± 0.05	0.53 ± 0.03
HOMA-IR	2.5 ± 0.5	3.2 ± 0.7	4.6 ± 0.6*	3.3 ± 0.2$^{\#}$
AUC GTT (mg/dL/min)	169 ± 8	180 ± 14	285 ± 14**	205 ± 10$^{\#\#}$
LPS (EU/mL)	0.43 ± 0.04	0.40 ± 0.05	0.83 ± 0.03**	0.86 ± 0.05

*AUC, area under curve; GTT, glucose tolerance test; HDL, high-density lipoprotein; HFD, high fat diet; HOMA-IR, homeostatic model assessment of insulin resistance; LPS, lipopolysaccharides; TG, triglycerides. Results are shown as mean ± SEM. All parameters were assessed in mice fed a control diet (control), or HFD treated with vehicle or GW0742 (GW). *P<0.05 and **P<0.01 vs control-vehicle; $^{\#}$P<0.05 and $^{\#\#}$P<0.01 vs vehicle-treated HFD mice.*

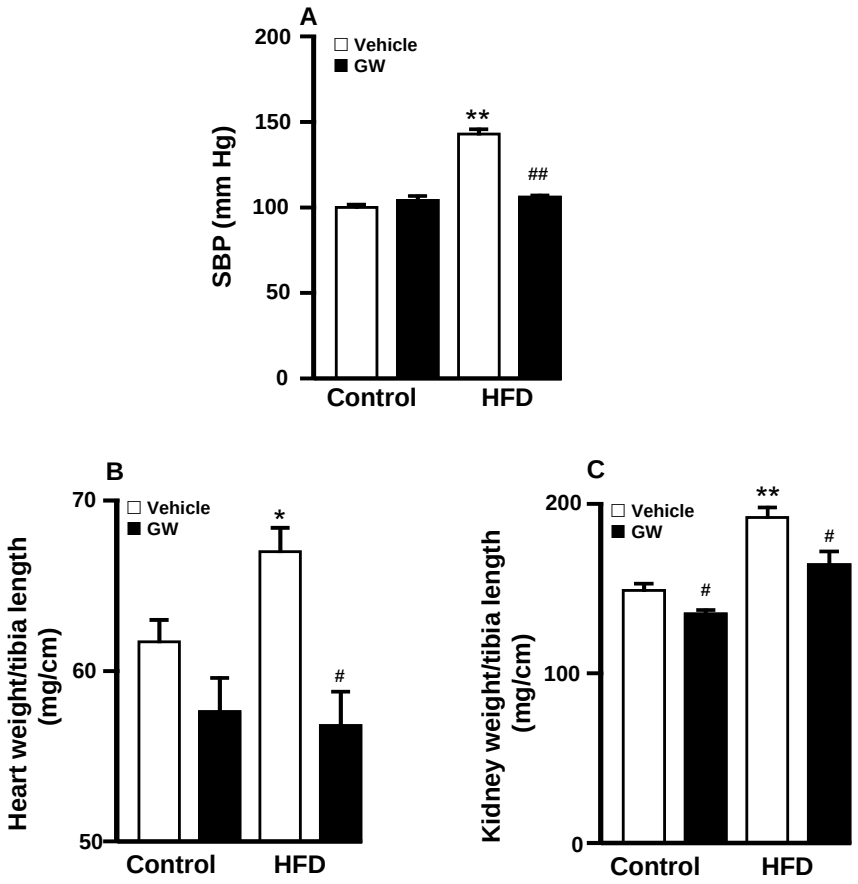

Figure 10. Effects of GW0742 (GW) administration on blood pressure and morphological changes*. Systolic blood pressure (SBP), measured by tail-cuff plethysmography (**A**), and heart (**B**) and kidney (**C**) hypertrophy in control and high fat diet (HFD)-fed mice. Values are means ± SEM (n= 9-10). *P<0.05 and **P<0.01 vs control; $^{\#}$P<0.05 and $^{\#\#}$P<0.01 vs non-treated HFD-fed mice.*

1.2. GW0742 treatment improves endothelial function in obese mice

Aortae from mice fed a HFD showed significant reduced endothelium-dependent vasodilator responses to ACh (considered as an index of endothelial function) as compared with aortae from the control group (maximal effect = 31.8 ± 6.0% and 74.0 ± 11.6%, respectively, $p<0.01$) (Figure 11A). GW0742 administration produced a significant increase in the endothelium-dependent relaxation induced by ACh in mice fed HFD (maximal effect = 66.5 ± 6.8%, $p<0.01$ vs HFD group), being without effect in control mice. The relaxant response induced by ACh was almost fully inhibited by L-NAME in all experimental groups (Figure 11B), showing that, in this vessel, ACh-induced relaxation in both control and HFD groups was almost entirely dependent of endothelium-derived NO. To analyze whether the impaired response to endothelial-derived NO is due to a reduced bioavailable NO or due to a defect in the signalling of NO in vascular smooth muscle, we analyzed the effects of SNP, which directly activates soluble guanylyl cyclase in vascular smooth muscle, mimicking the effects of endogenous NO. The endothelium-independent vasodilator responses to SNP were not different among groups (Figure 11C).

Moreover, eNOS, (Figure 12A) and Cav-1 (Figure 12B), an allosteric negative regulator of eNOS, gene expression was similar in the aortae from all experimental groups. However, HFD promotes the inhibitory interaction between eNOS and Cav-1, which was prevented by GW0742 (Figure 12C). In addition, phosphorylation of eNOS at Ser^{1177} and Akt at Ser^{473} were reduced in HFD-vehicle and restored in aortae from GW0742-treated mice (Figure 12D), as previously described by another PPARβ/δ agonist GW1516 (Tian *et al.,* 2012a).

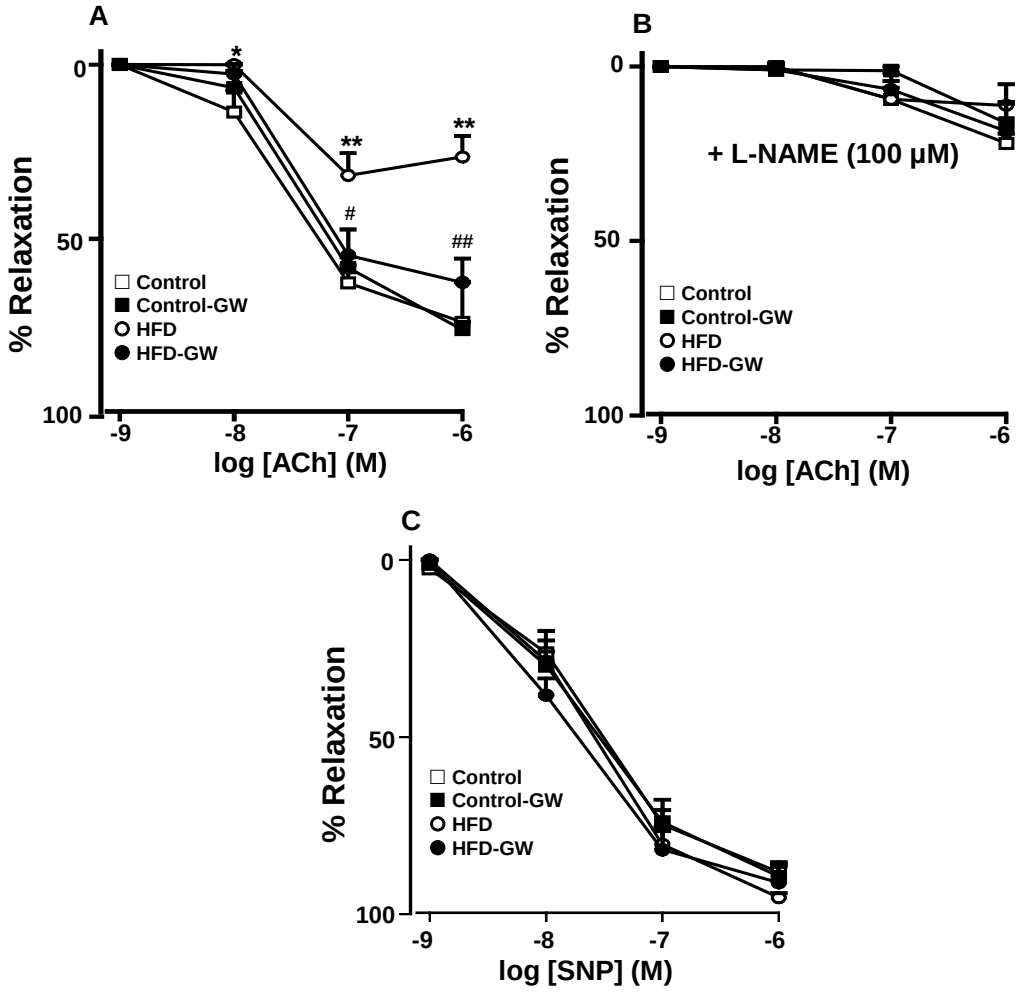

Figure 11. Effects of GW0742 (GW) on endothelial function and NO-mediated relaxation. *Vascular relaxant responses induced by acetylcholine (ACh), in endothelium-intact aortae pre-contracted by phenylephrine in the absence (**A**) and in the presence of L-NAME (100 µM), (**B**) and vascular relaxant responses induced by sodium nitroprusside (SNP) (**C**), in endothelium-denuded aortae pre-contracted by phenylephrine, in control and high diet fat (HDF)-fed mice. Values are expressed as mean ± SEM (n= 8-10 rings from different rats). *P<0.05 and **P<0.01 vs control; #P<0.05 and ##P<0.01 vs non-treated HFD-fed mice.*

.

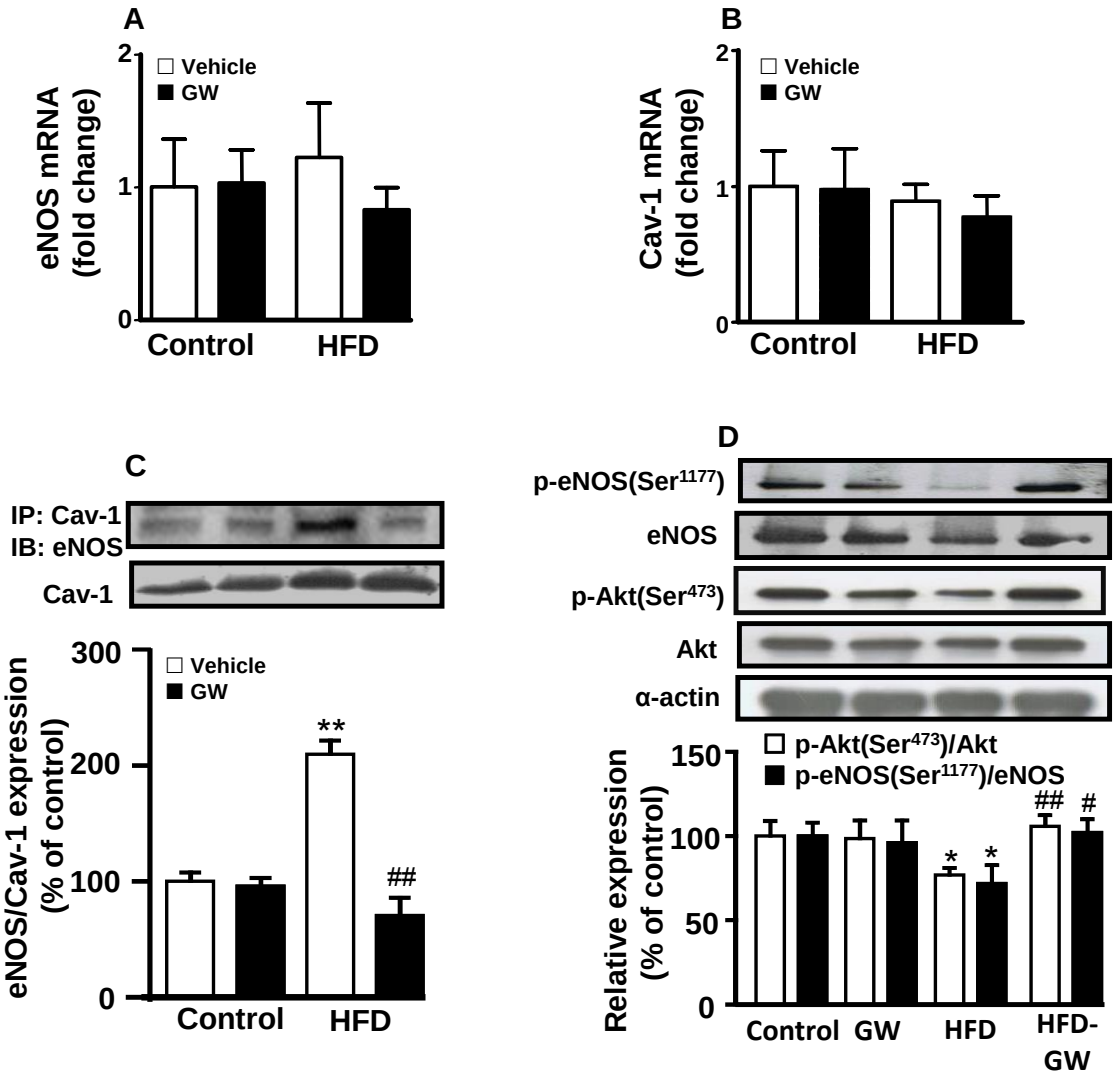

Figure 12. Effects of GW0742 (GW) on the NO pathway in the mouse aorta. *mRNA levels of eNOS (**A**) and caveolin-1(Cav-1) (**B**) by RT-PCR, Cav-1/eNOS interaction by western blot (IB) analysis of amount of eNOS co-immunoprecipitated (IP) with Cav-1 (**C**), and protein expressions (**D**) of phospho-eNOS(Ser^{1177})/eNOS and phospo-Akt(Ser^{473})/Akt by western blot in control and high fat diet (HDF)-fed mice. Results are shown as mean ± SEM, derived from 9-10 separate experiments for RT-PCR and 4-5 for western blot. *P<0.05 and **P<0.01 vs control; $^{\#}$P<0.05 and $^{\#\#}$P<0.01 vs non-treated HFD-fed mice.*

1.3. GW0742 reduces vascular ROS levels in obese mice by reducing NADPH oxidase activity and by down-regulation of inflammatory genes

To characterize and localize ROS levels within the vascular wall, ethidium red fluorescence was analyzed in sections of aorta incubated with DHE. Positive red nuclei could be observed in adventitial, medial and endothelial cells from sections of aorta incubated with DHE (Figure 13A). Staining was almost abolished by the O_2^- scavenger tiron and PEG-SOD (Figure 13A). Nuclear red ethidium fluorescence was quantified and normalized to the blue fluorescence of the nuclear stain DAPI, allowing comparisons between different sections. Rings from mice fed HFD showed marked increased staining in adventitial, medial and EC as compared with control mice, which was significantly reduced by GW0742 treatment (Figure 13A and B). Since NADPH oxidase is the major source of ROS in the vascular wall, we investigated the effect of GW0742 on gene expression of the main subunits in aortae from all experimental groups. Significant mRNA up-regulation of the NADPH oxidase subunit NOX-1 (Figure 13C) and NOX-1 protein (Figure 13D) were detected in rings from HFD as compared to control mice, without changes in NOX-4 (Figure 13E), $p47^{phox}$ (Figure 13F), and $p22^{phox}$ (Figure 13G) mRNA. Again, GW0742 reduced mRNA overexpression of NOX-1 subunits in HFD-fed mice.

Since oxidative stress induces inflammation and viceversa, the IκB-α phosphorylation (an index of NF-κB activation), and the mRNA levels of pro-inflammatory cytokines TNF-α, IL-1β and IL-6 were analyzed. We found that in aortic homogenates p-IκB-α (Figure 14A) and the mRNA level and protein expression of TNF-α (Figure 14B, 14C) and IL-6 (Figure 14E, 14F) were higher in HFD group as compared with control group, without showing any change when IL-1β was evaluated (Figure 14D). GW0742 significantly reduced IκB-α phosphorylation and the mRNA levels of pro-inflammatory cytokines in mice fed HFD. GW0742 treatment also prevented the up-regulation of TLR4 induced by HFD at mRNA (Figure 14G) and protein levels (Figure 14H).

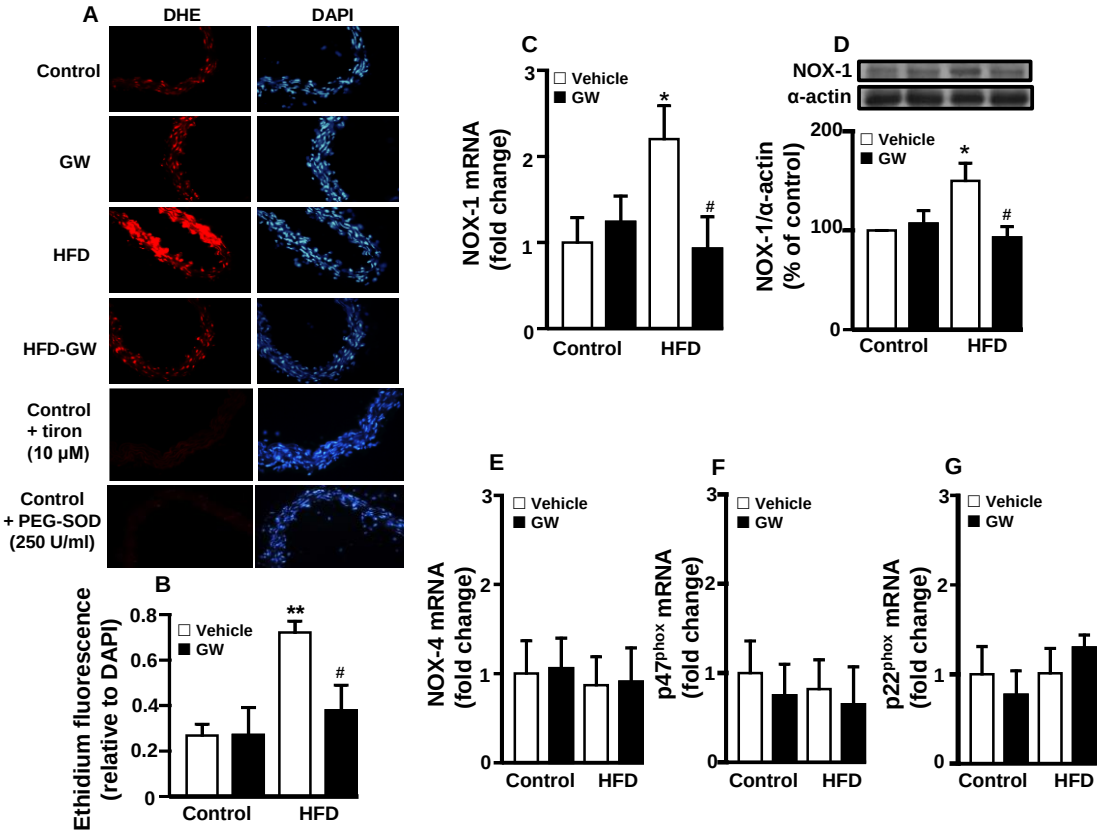

Figure 13. Effects of GW0742 (GW) on ROS production and NADPH oxidase pathway. *Left pictures show arteries incubated in the presence of DHE, which produces a red fluorescence when oxidized to ethidium by ROS. Right pictures show blue fluorescence of the nuclear stain DAPI (x 400 magnification) (**A**) Averaged values, mean ± SEM (n= 8-10 rings from different mice) of the red ethidium fluorescence normalized to the blue DAPI fluorescence (**B**). Expression of NADPH oxidase subunits NOX-1 (**C**), NOX-4 (**E**), p47^{phox} (**F**) and p22^{phox} (**G**) at the level of mRNA by RT-PCR, and NOX-1 protein expression (**D**) in control and high fat diet (HDF)-fed mice. For western blot histograms represent densitometric values normalized to the corresponding α-actin (n= 3-5), expressed as percentage of control vehicle group. Results are shown as mean ± SEM, derived from 9-10 rings. *P<0.05 and **P<0.01 vs control; $^{\#}$P<0.05 vs non-treated HFD-fed mice.*

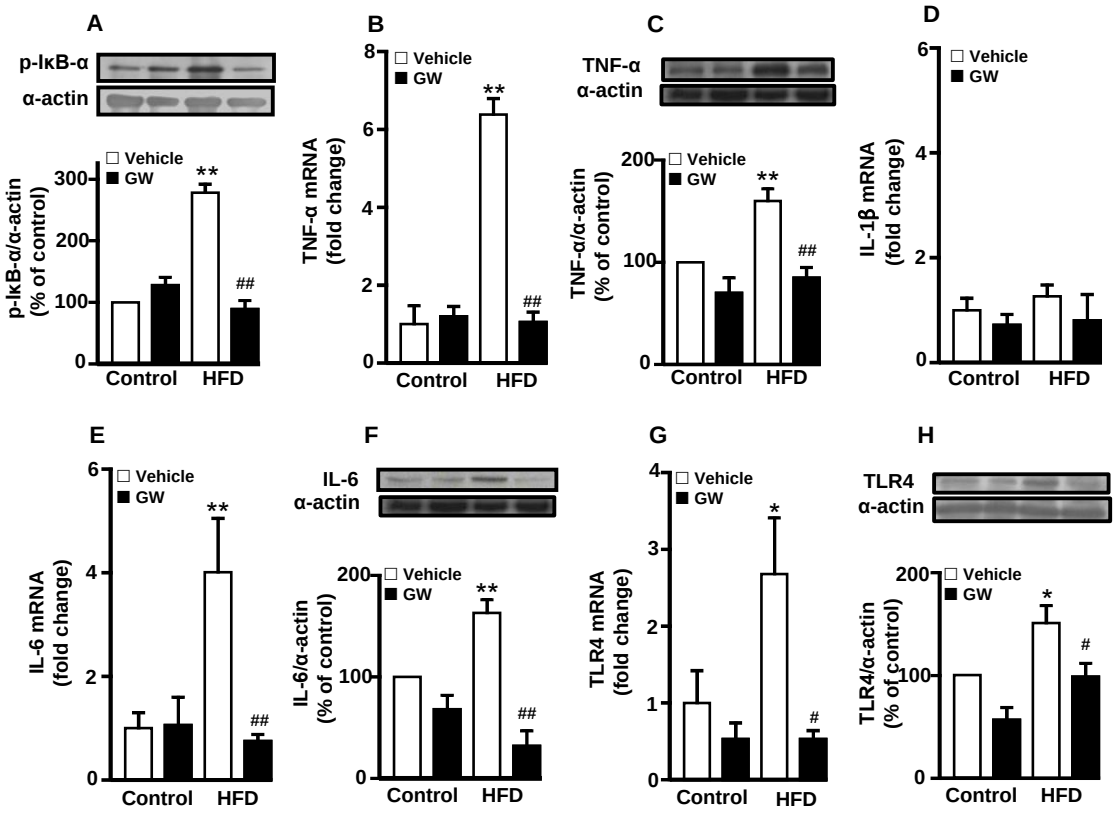

Figure 14. Effects of GW0742 (GW) administration on IκB-α phosphorylation, pro-inflammatory cytokines, and TLR4 expression. *Aortic IκB-α phosphorylation (**A**) and levels of mRNA by RT-PCR and protein by western blot of TNF-α (**B, C**), IL-1β (**D**), IL-6 (**E, F**), and TLR4 (**G, H**), in control and high fat diet (HDF)-fed mice. For western blot histograms represent densitometric values normalized to the corresponding α-actin (n= 3-5), expressed as percentage of control vehicle group. Results are shown as mean ± SEM, derived from 9-10 rings. *P<0.05 and **P<0.01 vs control; #P<0.05 and ##P<0.01 vs non-treated HFD-fed mice.*

1.4. GW0742 reduced hepatic and fat inflammation

Obesity is frequently associated with hepatic and fat inflammation (Cani *et al*., 2007). Accordingly, mice fed a HFD showed increased mRNA levels of the pro-inflammatory cytokine TNF-α in both liver (Figure 15A) and fat (Figure 15C), which were reduced GW0742-treated HFD-fed mice. The c-Jun N-terminal kinases are key regulators of inflammation. Obesity increases total activity JNK, and deficiency in JNK-1, but not JNK-2, results in reduced adiposity and improved insulin sensitivity (Tuncman *et al.,* 2006). We found that the raise in JNK-1 mRNA levels (Figure 15B) detected in the livers from HFD group was abolished by GW0742. We also found decreased adiponectin (Figure 15D) mRNA levels in adipose depots in the HFD group, which were ameliorated by GW0742.

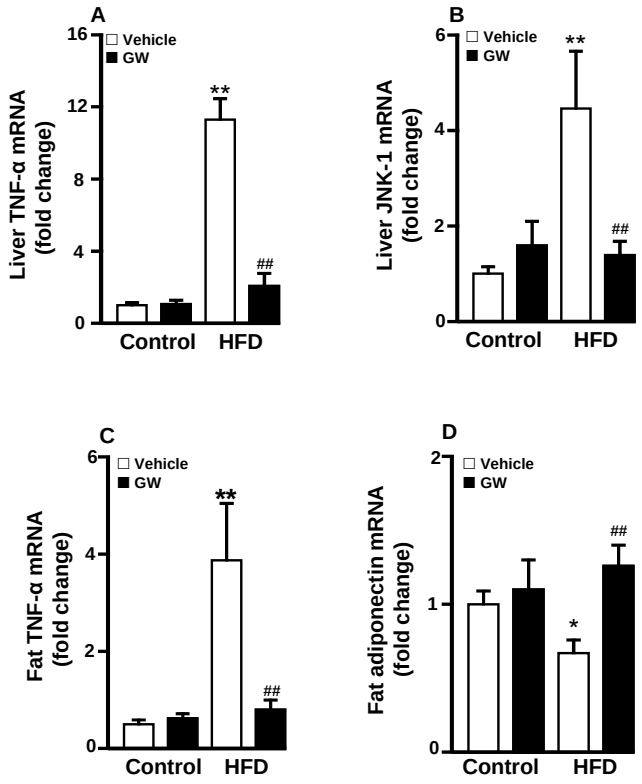

***Figure 15**. **Effects of GW0742 (GW) administration on inflammatory genes.** Liver TNF-α (**A**) and JNK-1 (**B**) and fat TNF-α (**C**) and adiponectin (**D**) mRNA levels of control and high fat diet (HDF)-fed mice. Results are shown as mean ± SEM, derived from 8-10 separate experiments. *P<0.05 and **P<0.01 vs control; ##P<0.01 vs non-treated HFD-fed mice.*

1.5. GW0742 increased mRNA expression of PPARβ/δ-target genes in aorta

The gene expression of PPARβ/δ (Figure 16A, 16B), PPARα (Figure 16C), and PPARγ (Figure 16D) were unchanged in the aortae from all experimental groups. Chronic treatment with GW0742 increased the mRNA levels of three well-known PPARβ/δ-target genes, CPT-1 (Figure 16E), PDK-4 (Figure 16F), UCP2 (Figure 16G), and ATP-binding cassette transporter G1 (ABCG1; Figure 16H) in both mice fed normal and HFD.

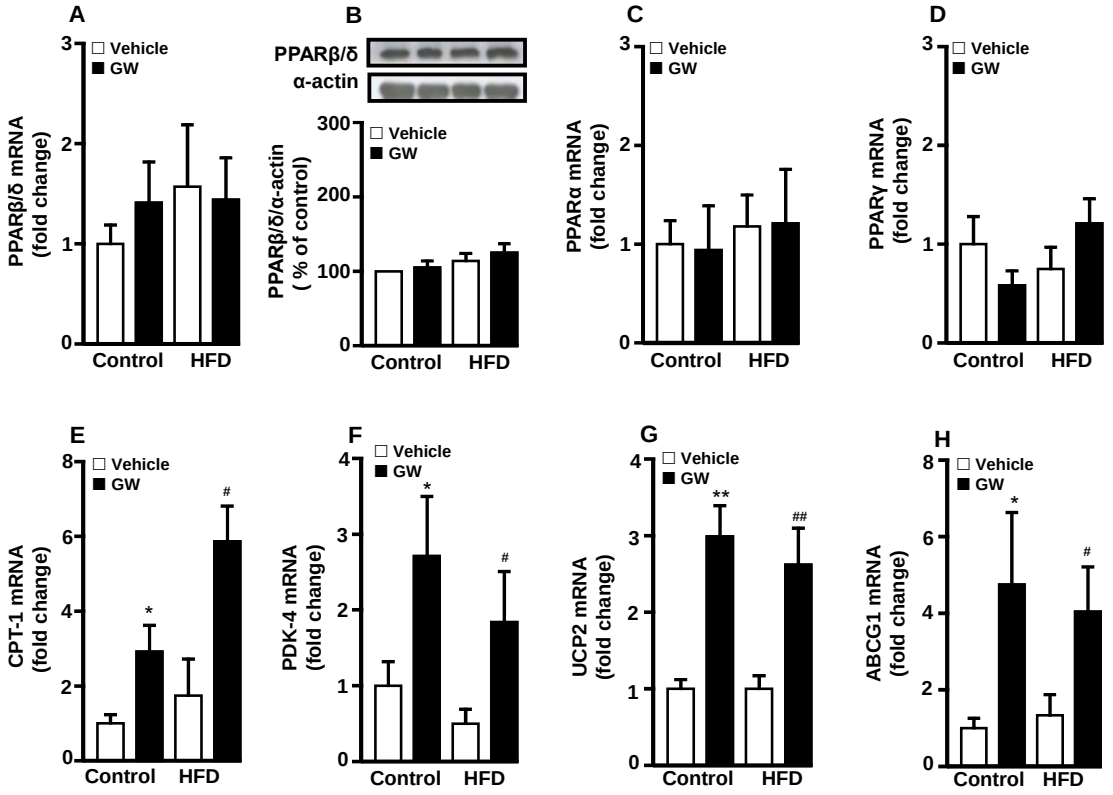

Figure 16. Effects of GW0742 (GW) administration on PPAR and PPARβ/δ-target genes in aorta. *mRNA (**A**) and protein (**B**) PPARβ/δ levels, mRNA levels of PPARα (**C**), and PPARγ (**D**), CPT-1 (**E**), PDK-4 (**F**), UCP2 (**G**) and ABCG1 (**H**) in aortae from control and high fat diet (HFD)-fed mice. For western blot histograms represent densitometric values normalized to the corresponding α-actin (n= 3-5), expressed as percentage of control vehicle group. Results are shown as mean ± SEM, derived from 8-10 separate experiments. *P<0.05 and **P<0.01 vs control; #P<0.05 and ##P<0.01 vs non-treated HFD-fed mice*.

1.6. Role of PPARβ/δ on the effects of GW0742

To determine whether PPARβ/δ is involved in the effects induced by GW0742, the PPARβ/δ antagonist GSK0660 was administered in addition to GW0742. All changes induced by GW0742 in body weight gain, fat accumulation, heart and kidney hypertrophy and SBP were prevented by GSK0660 (Figure 17). The antihypertensive effects were observed using direct intra-arterial recordings in conscious mice, ruling out possible artefacts of tail-cuff based BP determinations in obese animals. GSK0660 also abolished the effects induced by GW0742 on metabolic plasma variables (Table 7) and mRNA levels of liver TNF-α and JNK-1, and fat TNF-α and adiponectin (Figure 18). In addition, the increased relaxation to ACh induced by GW0742 in HFD fed mice was abolished by GSK0660 (Figure 19A). Furthermore, PPARβ/δ blockade suppressed the reduction induced by GW0742 in aortic DHE staining (Figure 19B, 19C), and NOX-1 (Figure 19D), TNF-α (Figure 19E), IL-6 (Figure 19F), and TLR4 (Figure 19G) mRNA levels. GSK0660 did not modify all these parameters in HFD fed mice when administered alone.

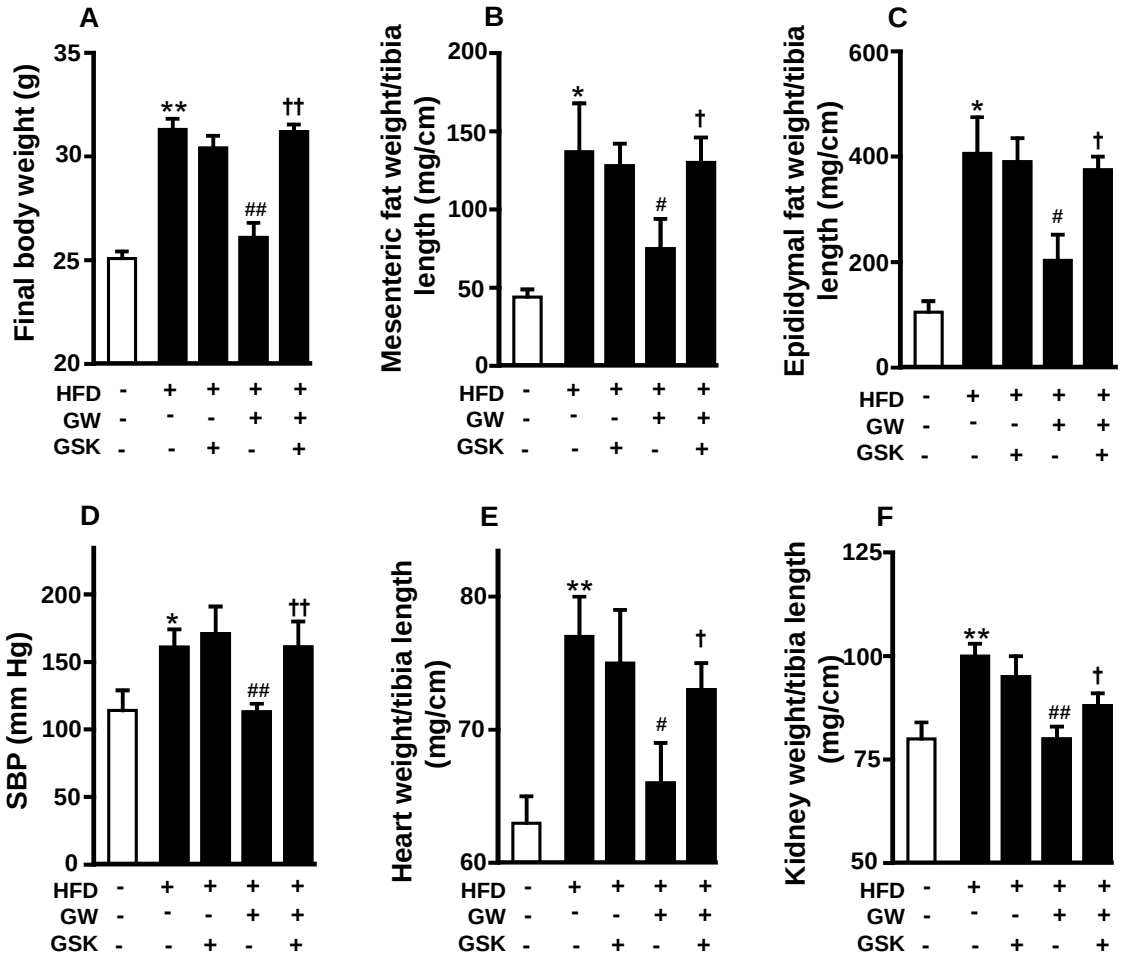

Figure 17. Effects of the PPARβ/δ antagonist GSK0660 (GSK) on the morphological changes, and blood pressure induced by GW0742 (GW). *Final body weight (**A**), mesenteric fat (**B**), and epididymal fat (**C**), systolic blood pressure (SBP), measured by intra-arterial catheter (**D**), and relative heart (**E**) and kidney weight (**F**) to tibia length. Values are expressed as mean ± SEM (n= 8-9). *P<0.05 and **P<0.01 vs control; $^{\#}$P<0.05 and $^{\#\#}$P<0.01 vs non-treated high fat diet (HFD)-fed mice; † P<0.05 and †† P<0.01 vs HFD-treated with GW.*

Table 7. Plasma determinations in all experimental groups (Experiment 2).

	Control (n = 8)	HFD (n = 8)	HFD-GSK (n = 8)	HFD-GW (n = 8)	HFD-GW-GSK (n = 9)
Fasting glucose (mg/dL)	94.6 ± 11.6	152.5 ± 7.4**	168.1 ± 21.6*	128.4 ± 5.7$^{\#}$	183.7 ± 9.4††
Total cholesterol (mg/dL)	69.7 ± 7.4	109.8 ± 12.5*	133.7 ± 8.0**	119.8 ± 12.5	139.6 ± 12.4
TG (mg/dL)	44.4 ± 3.2	66.7 ± 8.7*	69.1 ± 5.7*	44.7 ± 5.2#	60.9 ± 5.8†
HDL (mg/dL)	55.2 ± 8.2	61.2 ± 5.2	69.2 ± 5.3	117.3 ±12.2$^{\#\#}$	73.3 ± 16.0†
AUC GTT (mg/dL/min)	269 ± 10	328 ± 14**	337 ± 21**	286 ± 11#	350 ± 18††

*AUC, area under curve; GTT, glucose tolerance test; HDL, high-density lipoprotein; HFD, high fat diet; TG, triglycerides. Values are expressed as mean ± SEM. All parameters were assessed in mice fed a control diet (control), or HFD treated with vehicle or GW0742 (GW) or GW plus GSK0660 (GSK). *P<0.05 and **P<0.01 vs control; $^{\#}$P<0.05 and $^{\#\#}$P<0.01 vs HFD; †P<0.05 vs HFD-GW group.*

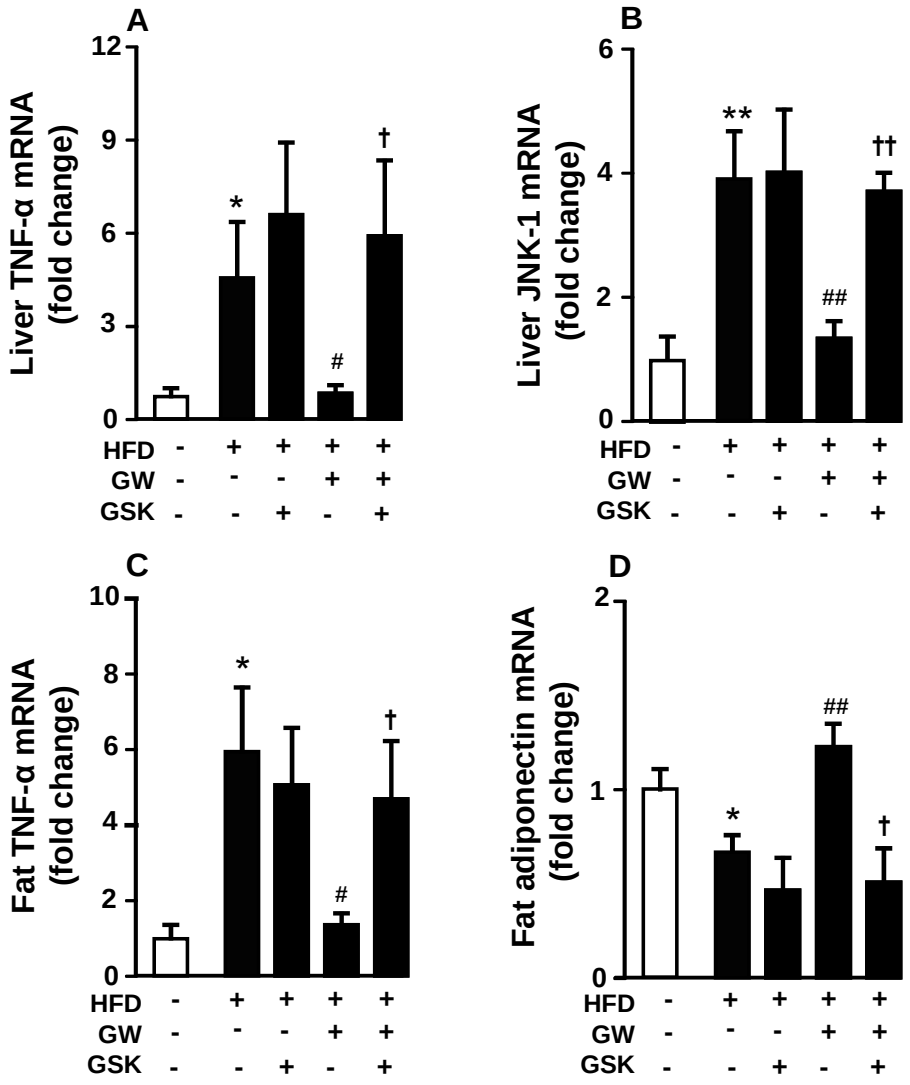

Figure 18*. *Effects of the PPARβ/δ antagonist GSK0660 (GSK) on inflammatory genes. *Liver TNF-α (**A**) and JNK-1 (**B**) and fat TNF-α (**C**) and adiponectin (**D**) mRNA levels of control and non-treated high fat diet (HDF)-fed mice treated with vehicles or GW0742 (GW). Values are expressed as mean ± SEM (n= 8-9). *P<0.05 and **P<0.01 vs control; $^{\#}$P<0.05 and $^{\#\#}$P<0.01 vs non-treated HFD-fed mice; †P<0.05 and ††P<0.01 vs HFD-treated with GW.*

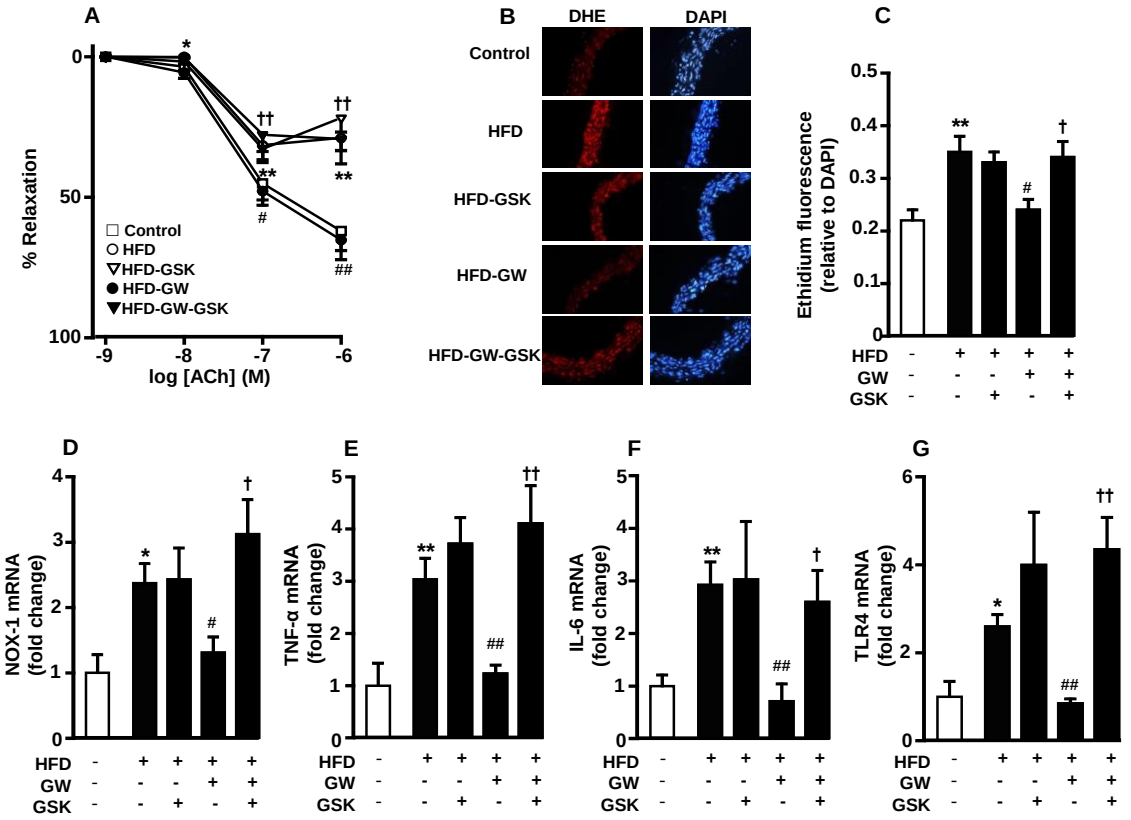

Figure 19. Effects of the PPARβ/δ antagonist GSK0660 (GSK) on the changes in endothelial function, aortic oxidative and inflammatory level induced by GW0742 (GW). *Vascular relaxant responses induced by acetylcholine (ACh) (**A**) in endothelium-intact aortae pre-contracted by phenylephrine. ROS content measured by ethidium fluorescence (**B**, **C**), and expression of NOX-1 (**D**), TNF-α (**E**), IL-6 (**F**), and TLR4 (**G**) at the level of mRNA by RT-PCR in aortic rings. Values are expressed as mean ± SEM (n= 8-9 rings from different mice). *P<0.05 and **P<0.01 vs control; #P<0.05 and ##P<0.01 vs non-treated high fat diet (HFD)-fed mice; †P<0.05 and ††P<0.01 vs HFD-treated with GW.*

2. Carnitine palmitoyl-transferase-1 up-regulation by PPARβ/δ prevents lipid-induced endothelial dysfunction

2.1. PPARβ/δ activation restores the palmitate-induced impairment of endothelium-dependent vasodilatation and NO production

Incubation of mice isolated aortae with palmitate inhibited the endothelium-dependent relaxation to ACh (Figure 20A) and the phosphorylation of eNOS at the activation site Ser^{1177} (Figure 20B). In MAEC, palmitate reduced the A23187-stimulated NO production (Figure 20C) and eNOS at Ser^{1177} phosphorylation (Figure 20D). The PPARβ/δ agonist GW0742 (1 μM) restored the aortic relaxation to ACh, eNOS phosphorylation at Ser^{1177} and the level of NO production induced by A23187 in aorta and MAEC exposed to palmitate. All the effects of GW0742 were abolished by co-incubation with PPARβ/δ antagonist GSK0660 (1 μM). GW0742 did not modify either the aortic relaxation to ACh or A23187-stimulated NO production in MAEC incubated in control conditions (data not shown).

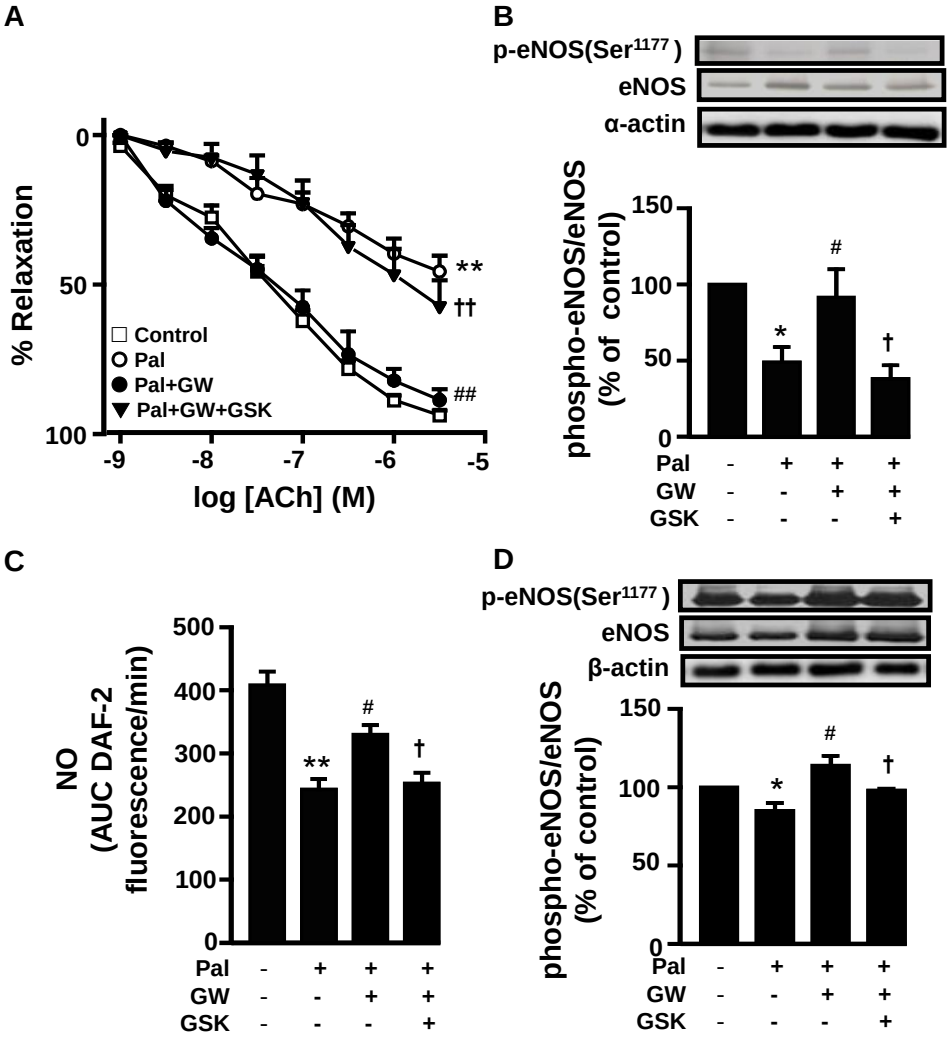

Figure 20. The PPARβ/δ agonist prevents palmitate (Pal)-induced endothelial dysfunction in vitro*. Vascular relaxant responses induced by acetylcholine (ACh) (**A**) in mouse aortae pre-contracted by U46619 (10 nM), and eNOS(Ser^{1177}) phosphorylation (**B**) after incubation for 24 h in the absence (control) or presence of Pal (100 µM), GW0742 (GW, 1 µM), or GSK0660 (GSK, 1 µM). Results are shown as mean ± SEM, derived from 9-11 different rings. Immunoblots from 7 separate experiments were quantified. NO release (**C**) and eNOS(Ser^{1177}) phosphorylation (**D**) in MAEC incubated with GW (1 µM) for 15 hours, and in the last 3 hours in the absence (control cells) or presence of Pal (100 µM). In some experiments, cells were co-incubated with GSK (1 µM). Results are mean ± SEM (n= 7-15). Immunoblots from 3 separate experiments were quantified. *P<0.05 and **P<0.01 vs control; $^{\#}$P<0.05 and $^{\#\#}$P<0.01 vs Pal; †P<0.05 and ††P<0.01 vs Pal+GW group.*

2.2. PPARβ/δ activation *in vivo* improves endothelial dysfunction in aortae from HFD mice

To examine the effects of PPARβ/δ activation *in vivo*, GW0742 was given by oral gavage (3 mg/kg/d, for 3 weeks) to mice fed a HFD. GW0742 treatment was unable to prevent the changes induced by HFD on body weight (Figure 21A), energy intake (Figure 21B), heart and kidney weight, and the higher plasmatic fasting glucose, cholesterol, TG, HDL, the GTT, and FFA (Table 8). However, GW0742 reduced significantly fat accumulation, an effect that was inhibited by co-administration with the PPARβ/δ antagonist GSK0660 (Table 8).

Aortae from mice fed a HFD showed significantly reduced endothelium-dependent vasodilator responses to ACh as compared with aortae from the control group (Figure 22A). GW0742 administration produced a significant increase in the endothelium-dependent relaxation induced by ACh in mice fed HFD, being without effect in control mice. The increased relaxation to ACh induced by GW0742 treatment in HFD fed mice was abolished by co-administration with GSK0660 (1 mg/kg/d ip). The relaxant response induced by ACh was almost fully inhibited by the eNOS inhibitor L-NAME in all experimental groups (Figure 22B), involving eNOS activation, and the endothelium-independent vasodilator responses to SNP were not different among groups (Figure 22C). SBP significantly increased in mice fed a HFD. GW0742 prevented the raise in SBP and this effect was abolished by GSK0660 (Figure 22D). Phosphorylation of eNOS at Ser^{1177} and Akt at Ser^{473} were reduced in the aortae from mice fed a HFD. GW0742 restored the phosphorylation of both targets and these effects were suppressed by GSK0660 (Figure 22E).

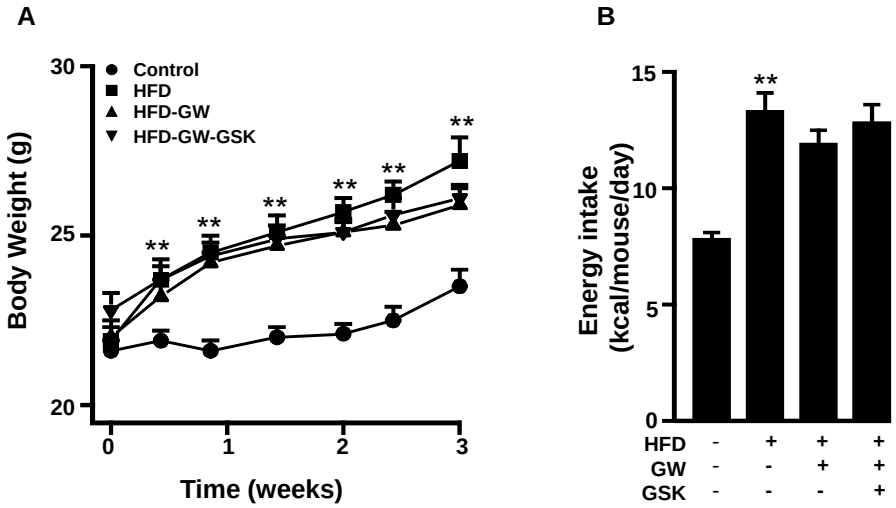

***Figure 21**. **Effects of GW0742 (GW) treatment on the morphological changes**. Body weight evolution (**A**) and mean energy intake (**B**) in mice fed a control diet (control), or a high fat diet (HFD) treated with vehicle or GW or GW plus GSK0660 (GSK). Results are shown as mean ± SEM, n= 10. **P<0.01 vs control group.*

Table 8. Morphological and plasma determinations in all experimental groups.

	Control (n = 9)	HFD (n = 10)	HFD-GW (n =10)	HFD-GW-GSK (n =10)
Body weight (g)	23.4 ± 0.5	27.2 ± 0.7**	25.9 ± 0.5	26.1 ± 0.4
Heart weight/tibia length (mg/cm)	60.5 ± 1.5	62.2 ± 1.3	62.7 ± 2.0	63.1 ± 1.7
Mesenteric fat weight/ Body weight (%)	0.12 ± 0.3	0.93 ± 0.08**	0.31 ± 0.04$^{\#}$	0.48 ± 0.04†
Epididymal fat weight/ Body weight (%)	1.01 ± 0.17	2.58 ± 0.22**	1.50 ± 0.07$^{\#\#}$	1.94 ± 0.19†
Kidney weight/tibia length (mg/cm)	66.6 ± 1.3	76.0 ± 2.4**	71.4 ± 2.0	70.8 ± 2.2
Fasting glucose (mg/dL)	102.3 ± 8.2	140.7 ± 14.9*	149.7 ± 9.9	168.7 ± 10.0
Total cholesterol (mg/dL)	69.2 ± 4.3	86.6 ± 4.0*	93.0 ± 5.8	112.0 ± 6.2
TG (mg/dL)	71.8 ± 4.9	93.0 ± 7.6*	99.6 ± 8.8	96.5 ± 5.7
HDL (mg/dL)	73.7 ± 3.7	83.5 ± 4.4	95.5 ± 5.7	95.1 ± 10.6
AUC GTT (mg/dL/min)	237 ± 15	318 ± 15**	290 ± 16	287 ± 16
FFA (mM)	0.36 ± 0.03	0.46 ± 0.04*	0.45 ± 0.03	0.47 ± 0.04

*AUC, area under curve; FFA, free fatty acid; GTT, glucose tolerance test; HDL, high-density lipoprotein; HFD, high fat diet; TG, triglycerides. Results are shown as mean ± SEM. All parameters were assessed in mice fed a control diet (control), or HFD treated with vehicle or GW0742 (GW) or GW plus GSK0660 (GSK). *P<0.05 and **P<0.01 vs control; $^{\#}$P<0.05 and $^{\#\#}$P<0.01 vs HFD; †P<0.05 vs HFD-GW group.*

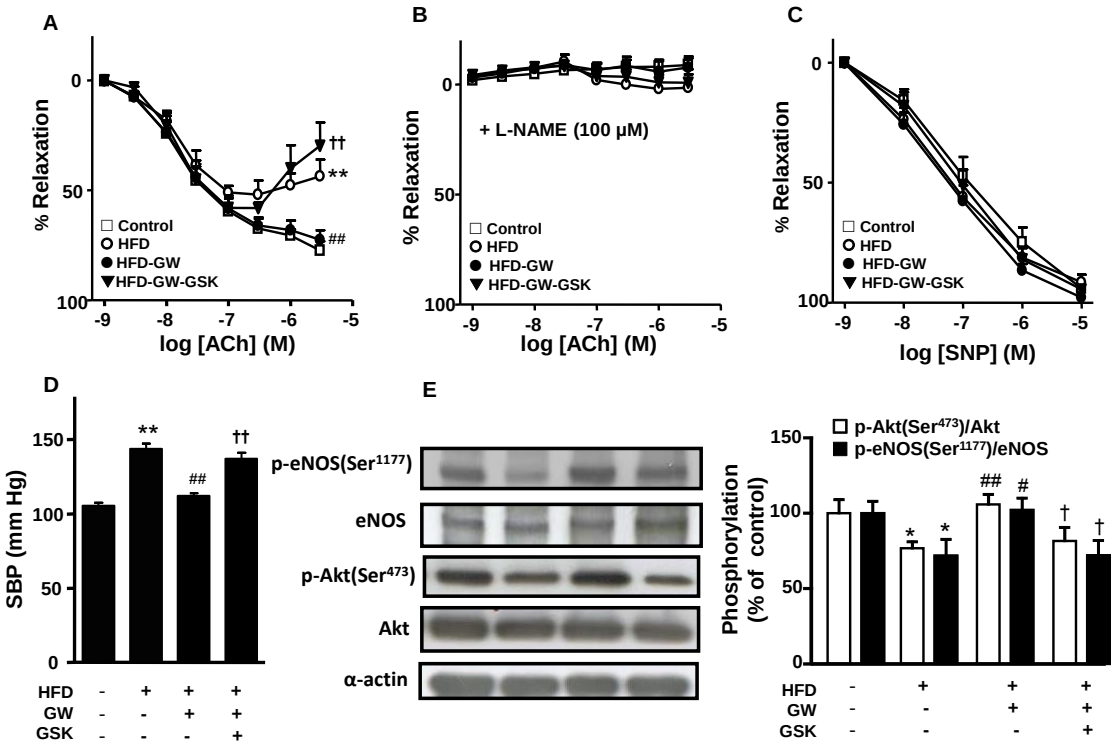

Figure 22. The PPARβ/δ agonist prevents high fat diet (HFD)-induced endothelial dysfunction in vivo. *Vascular relaxant responses induced by acetylcholine (ACh) in the absence (**A**) or in the presence of L-NAME (100 µM) (**B**), and endothelium-independent relaxant response to nitroprusside (SNP) (**C**) in aortae pre-contracted by U46619 (10 nM). Systolic blood pressure (SBP) in mice fed a control diet (control), or a HFD treated with vehicle, GW0742 (GW) or GW plus GSK0660 (GSK) (**D**). Values are expressed as mean ± SEM (n= 6-8 rings from different mice). Phosphorylation of eNOS and Akt in aorta (**E**) from all experimental groups. Immunoblots from 6 separate experiments were quantified. *P<0.05 and **P<0.01 vs control; $^{\#}$P<0.05 and $^{\#\#}$P<0.01 vs HFD; †P<0.05 and †† P<0.01 vs HFD-GW group.*

2.3. PPARβ/δ activation reduces the increased ROS production induced by palmitate

To examine whether ROS are involved on endothelial dysfunction induced by palmitate in mouse aorta, we analyze the endothelium-dependent relaxant response to ACh in the presence of the mitochondrial antioxidant mitoQ, or the NADPH oxidase inhibitor apocynin. Both, mitoQ (Figure 23A) and apocynin (Figure 24A) significantly improved the impaired aortic relaxation to ACh induced by palmitate. Intracellular ROS production measured by CM-H2DCFDA in MAEC was increased after palmitate incubation (Figure 23B). The increase in intracellular O_2^- levels induced by palmitate incubation in MAEC was then confirmed by determination of 2-OH-E^+ levels by HPLC (Figure 23C). This ROS increase was inhibited by mitoQ and GW0742. The effect of GW0742 was abolished by blockade of PPARβ/δ by GSK0660. NADPH oxidase activity, measured by both lucigenin-enhanced chemiluminescence (Figure 24B) and DHE fluorescence in the microplate reader (Figure 24C), was also increased by palmitate, while apocynin and GW0742 inhibited this increase. Again, GSK0660 suppressed the effect of GW0742. Similarly, this PPARβ/δ agonist abolished the up-regulation of NOX-4 mRNA in MAEC incubated with palmitate, but not in those co-incubated with GSK0660 (Figure 24D).

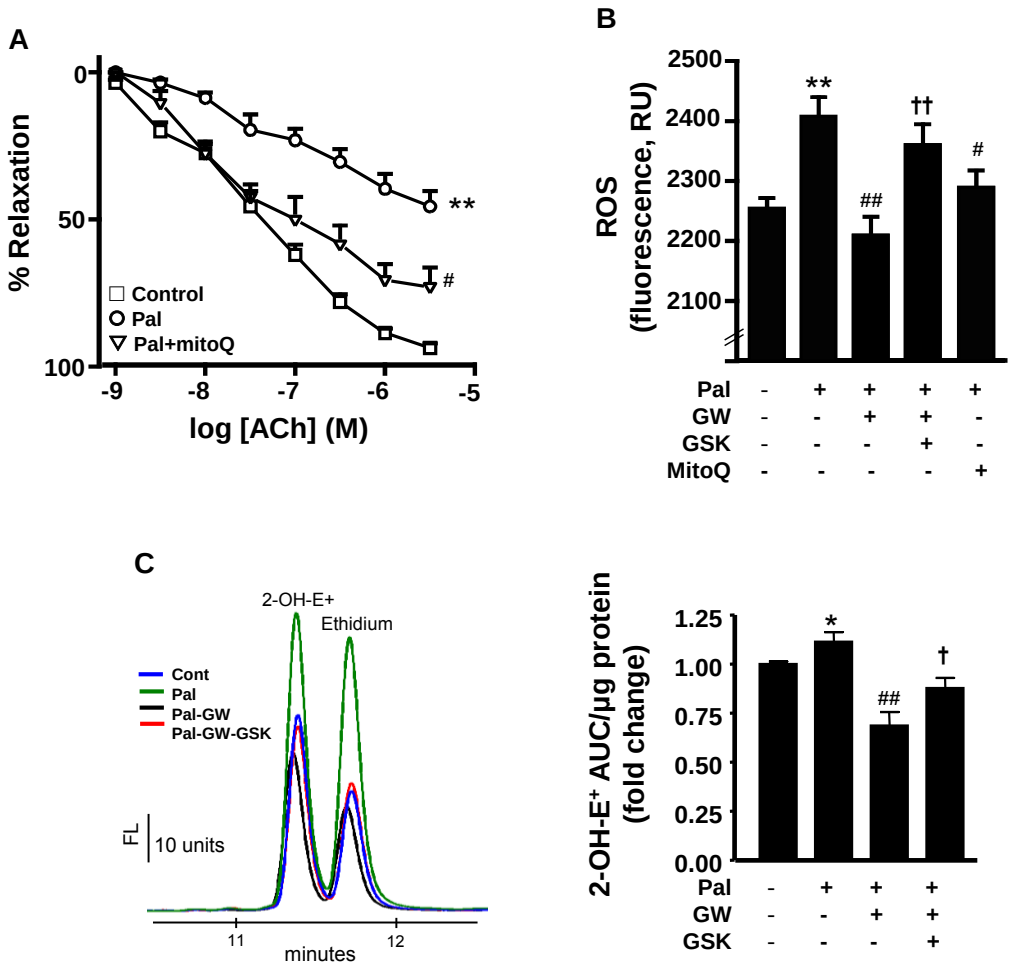

Figure 23. Role of ROS production in palmitate (Pal)-induced endothelial dysfunction. *Vascular relaxant responses induced by acetylcholine (ACh) (**A**) in intact aortae pre-contracted by U46619 (10 nM), after incubation for 24 h in the absence (control) or presence of Pal (100 µM). In some experiments, responses to ACh were studied after incubation with mitoQ (0.1 µM) (**A**) incubated for 60 min before the addition of U46619. Results are shown as mean ± SEM, derived from 9-11 different rings. ROS measured by fluorescence in CM-H2DCFDA-loaded cells (**B**), and O_2^- production detected by 2-hydroxyethidium (2-OH-E^+) fluorescence HPLC (**C**). Left, Representative example. Right, quantification of 2-OH-E^+ peak, expressed in area under curve (AUC)/µg protein. (**B, C**) MAEC were incubated with GW0742 (GW, 1 µM) for 15 hours, and in the last 3 hour in the absence (control cells) or presence of Pal (100 µM). In some experiments, cells were co-incubated with mitoQ (0.1 µM) added with Pal. Results are mean ± SEM (n= 6-15). *P<0.05 and **P<0.01 vs control; $^{\#}$P<0.05 and $^{\#\#}$P<0.01 vs Pal; †P<0.05 and ††P<0.01 vs Pal+GW group.*

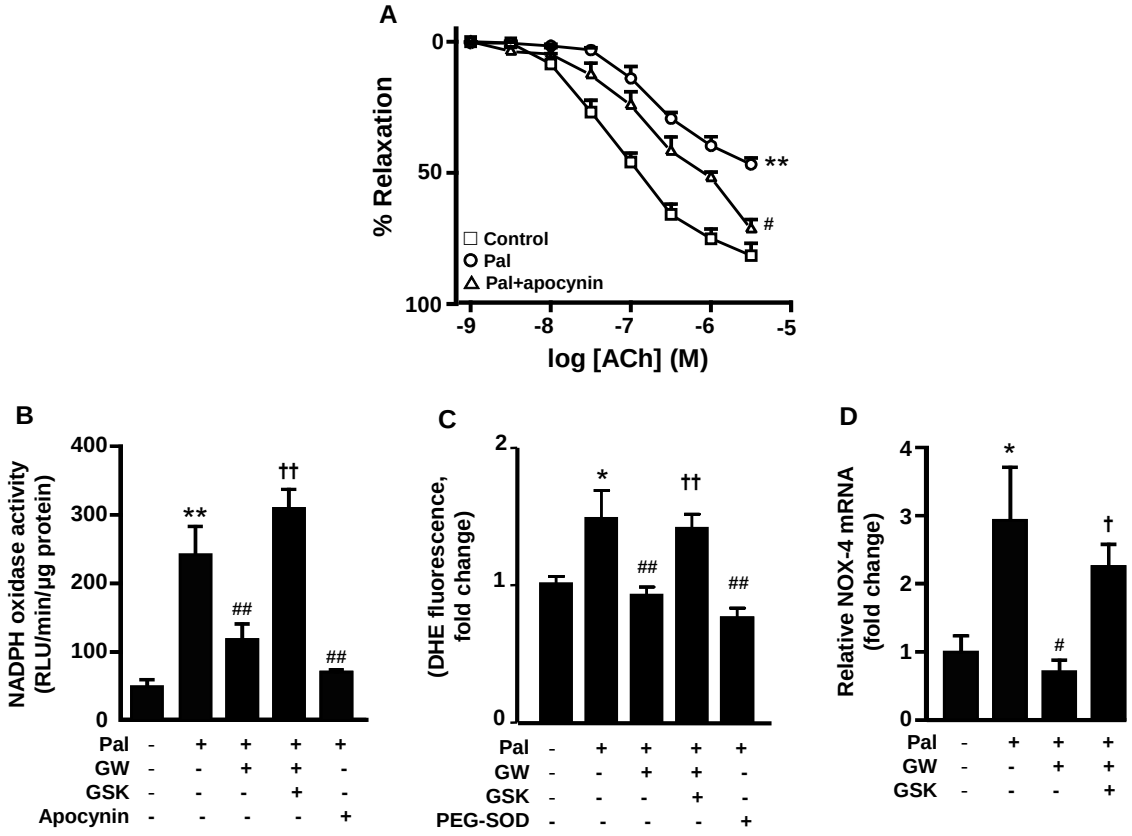

Figure 24. Role of NADPH oxidase in palmitate (Pal)-induced endothelial dysfunction. *Vascular relaxant responses induced by acetylcholine (ACh) (**A**) in intact aortae pre-contracted by U46619 (10 nM), after incubation for 24 h in the absence (control) or presence of Pal (100 µM). In some experiments, responses to ACh were studied after incubation with apocynin (10 µM) (**A**) incubated for 60 min before the addition of U46619. Results are shown as mean ± SEM, derived from 9-11 different rings. NADPH oxidase activity measured by lucigenin-enhanced chemiluminescence (**B**), or DHE fluorescence measured in the microplate reader (**C**), and mRNA levels of NOX-4 (**D**) in MAEC incubated with GW0742 (GW,1 µM) for 15 hours, and in the last 3 hour in the absence (control cells) or presence of Pal (100 µM). In some experiments, cells were co-incubated with apocynin (10 µM) added with Pal, or incubations were performed for 30 min in the absence or presence of SOD conjugated to polyethylene glycol (PEG-SOD, 25 U/mL). Results are mean ± SEM (n= 6-15). *P<0.05 and **P<0.01 vs control; $^{\#}$P<0.05 and $^{\#\#}$P<0.01 vs Pal; †P<0.05 and ††P<0.01 vs Pal+GW group.*

2.4. PPARβ/δ activation *in vivo* reduced vascular ROS levels in HFD fed mice by reducing NADPH oxidase activity and mitochondrial sources and by up-regulation of antioxidant genes

To characterize and localize ROS levels within the vascular wall, red fluorescence was analyzed in sections of aorta incubated with DHE. Rings from mice fed a HFD showed marked increased staining in adventitial, medial and EC as compared with control mice, which was significantly reduced by GW0742 administration. The increased red fluorescence induced by HFD was abolished by PEG-SOD, indicating its specificity for O_2^- (Figure 25A). GW0742 treatment also prevented the raise in vascular NADPH oxidase activity (Figure 25B) and the up-regulation of the NADPH oxidase subunits NOX-4, NOX-1, $p47^{phox}$, and $p22^{phox}$ (Figure 25C) induced by the HFD. The increase in the pro-oxidant NADPH oxidase subunits induced by the HFD was accompanied by reduced mRNA levels of mitochondrial and cytoplasmic antioxidant enzymes (Figure 26), such as manganese superoxide dismutase (MnSOD), UCP2, and glutathione peroxidase (GPx-1). The mRNA levels of hemo-oxigenase-1 (HO-1) and CPT-1 were increased, and copper/zinc superoxide dismutase (Cu/ZnSOD) was not significantly affected by the HFD. GW0742 administration prevented the HFD-induced changes in MnSOD and GPx-1 and did not affect Cu/ZnSOD. The PPARβ/δ agonist increased UCP2, CPT-1 and HO-1 mRNA levels above control levels. PPARβ/δ blockade with GSK0660 inhibited the effects of GW0742 on aortic ROS levels, NADPH oxidase activity and changes in gene expression (Figures 25 and 26).

Since oxidative stress induced inflammation and viceversa, the mRNA expression of pro-inflammatory cytokines TNF-α, IL-1β and IL-6 was analyzed. We found that in aortic homogenates the expression of these cytokines was higher in HFD group as compared with the control group (Figure 27). As expected, GW0742 administration significantly reduced the mRNA levels of these pro-inflammatory cytokines in mice fed HFD, and this effect was prevented by GSK0660.

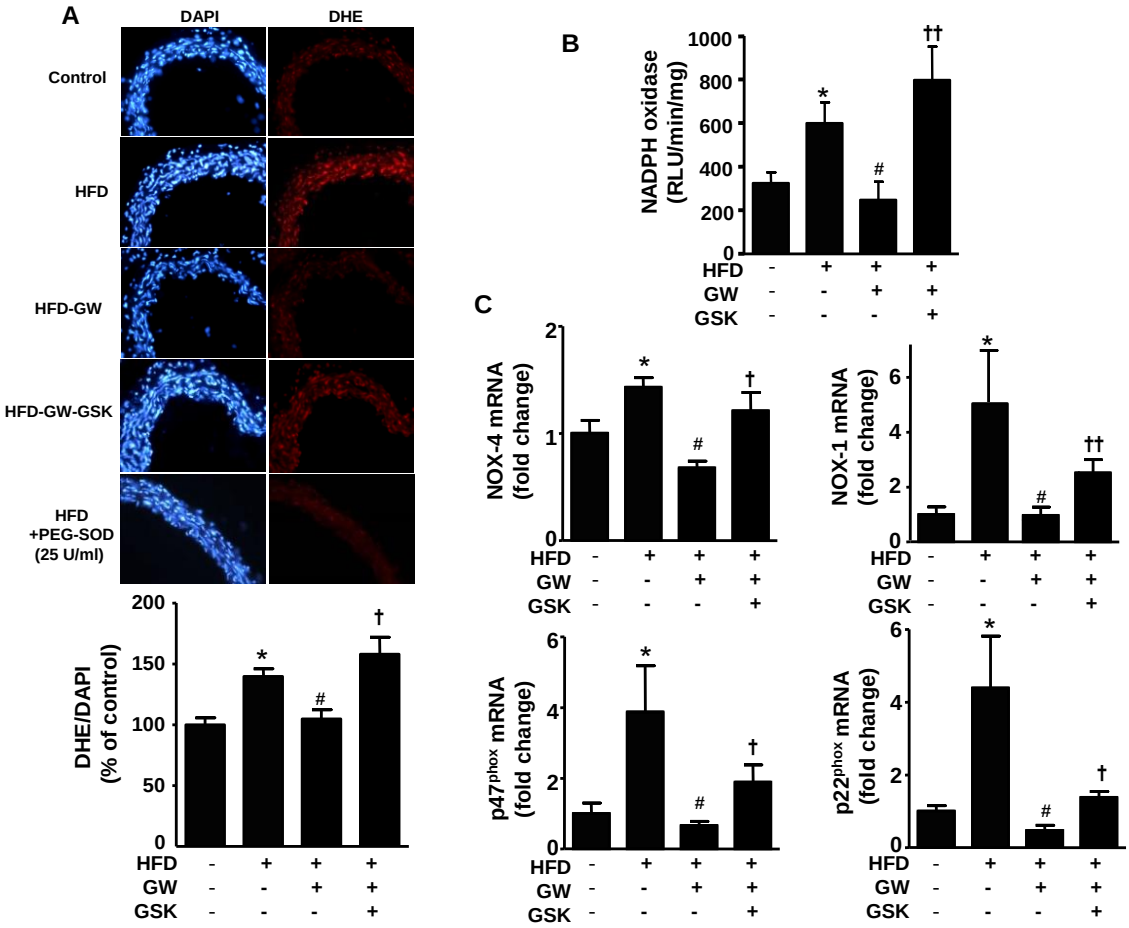

Figure 25. Role of ROS production in high fat diet (HFD)-induced endothelial dysfunction*. Right pictures show arteries incubated in the presence of DHE which produces a red fluorescence when oxidized to ethidium by ROS. Left pictures show blue fluorescence of the nuclear stain DAPI (x 400 magnification) (**A**). Bottom shows red ethidium fluorescence intensity normalized to the blue DAPI fluorescence (mean ± SEM, n= 5-7 rings from different mice). NADPH oxidase activity measured by lucigenin-enhanced chemiluminescence (n= 7-9) (**B**) and expression of NADPH oxidase subunits NOX-4, NOX-1, p47^{phox} and p22^{phox} (**C**) at the level of mRNA by RT-PCR. Results are shown as mean ± SEM. All parameters were assessed in aortae from mice fed a control diet (control), or a HFD treated with vehicle or GW0742 (GW) or GW plus GSK0660 (GSK). *P<0.05 vs control; $^{\#}$P<0.05 vs HFD; †P<0.05 and ††P<0.01 vs HFD-GW group.*

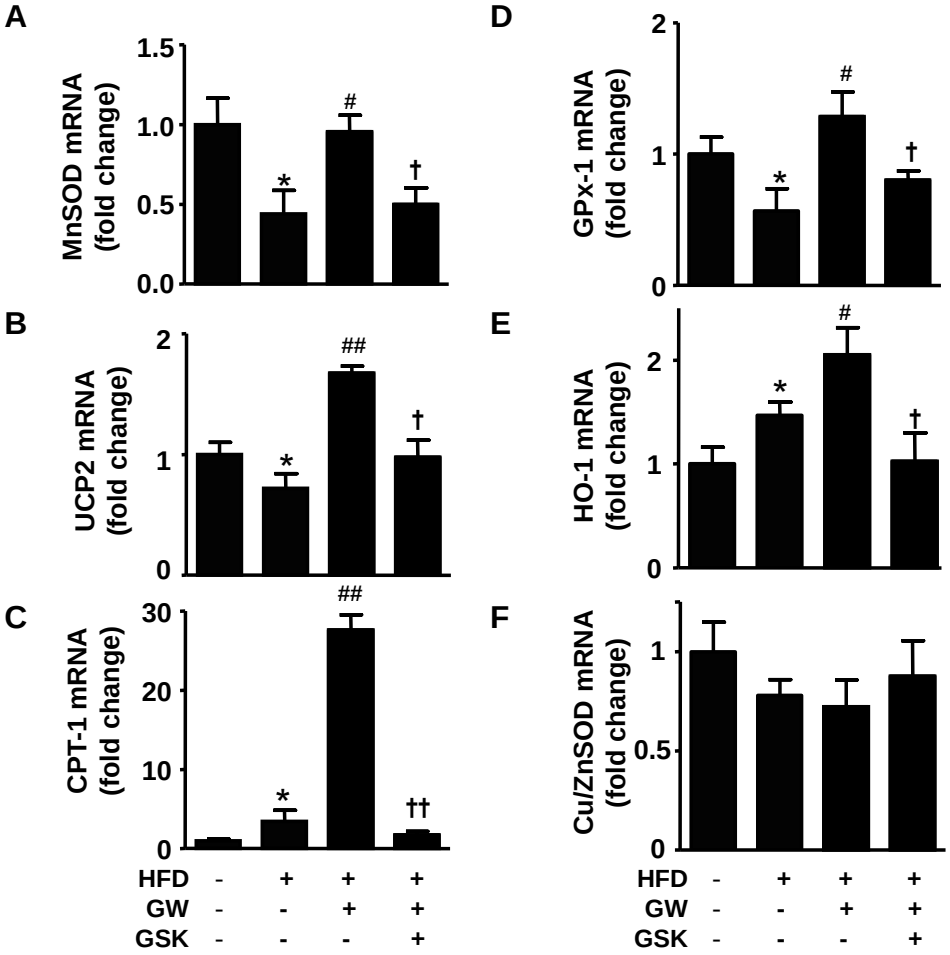

Figure 26. Effects of GW0742 (GW) on gene expression. *MnSOD (**A**), UCP2 (**B**), CPT-1 (**C**), GPx-1 (**D**), HO-1 (**E**), and Cu/ZnSOD (**F**) mRNA expression. Results are shown as mean ± SEM in aortae from mice fed a control diet (control), or a high fat diet (HFD) treated with vehicle or GW0742 (GW) or plus GSK0660 (GSK). *P<0.05 vs control; $^{\#}$P<0.05 and $^{\#\#}$P<0.01 vs HFD; †P<0.05 and ††P<0.01 vs HFD-GW group.*

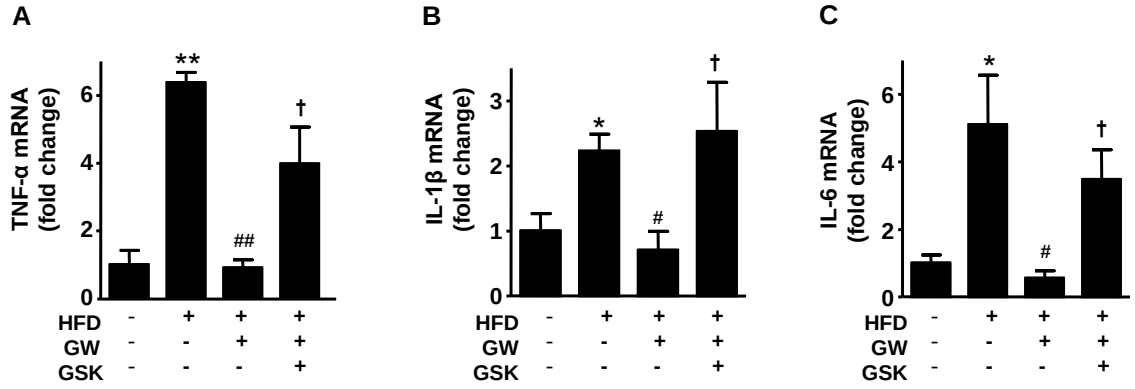

Figure 27. Effects of GW0742 (GW) on inflammatory genes. *mRNA levels of TNF-α (**A**), IL-1β (**B**), and IL-6 (**C**) of aorta from mice fed a control diet (control), or a high fat diet (HFD) treated with vehicle or GW0742 (GW) or GW plus GSK0660 (GSK). Results are shown as mean ± SEM, n= 5. *P<0.05 and **P<0.01 vs control; #P<0.05 and ##P<0.01 vs HFD; †P<0.05 vs HFD-GW group.*

2.5. Role of CPT-1 in the preventive effects of PPARβ/δ activation on palmitate-induced endothelial dysfunction

GW0742 induced a marked increase in the mRNA and protein levels of CPT-1 in MAEC that was sensitive to PPARβ/δ blockade and independent of the presence of palmitate (Figure 28A). The preventive effects induced by GW0742 on the impaired A23187-stimulated NO production (Figure 28B), the increased ROS generation (Figure 28C) in MAEC and the reduced ACh relaxation in aorta (Figure 28D) incubated with palmitate were abolished by the CPT-1 irreversible inhibitor etomoxir. Moreover, siRNA targeting CPT-1 in MAEC, which effectively down-regulated CPT-1 mRNA and protein (Figure 28E), also blunted the increase in NO production (Figure 28F), and the reduction in ROS generation (Figure 28G) induced by GW0742 in MAEC incubated with palmitate.

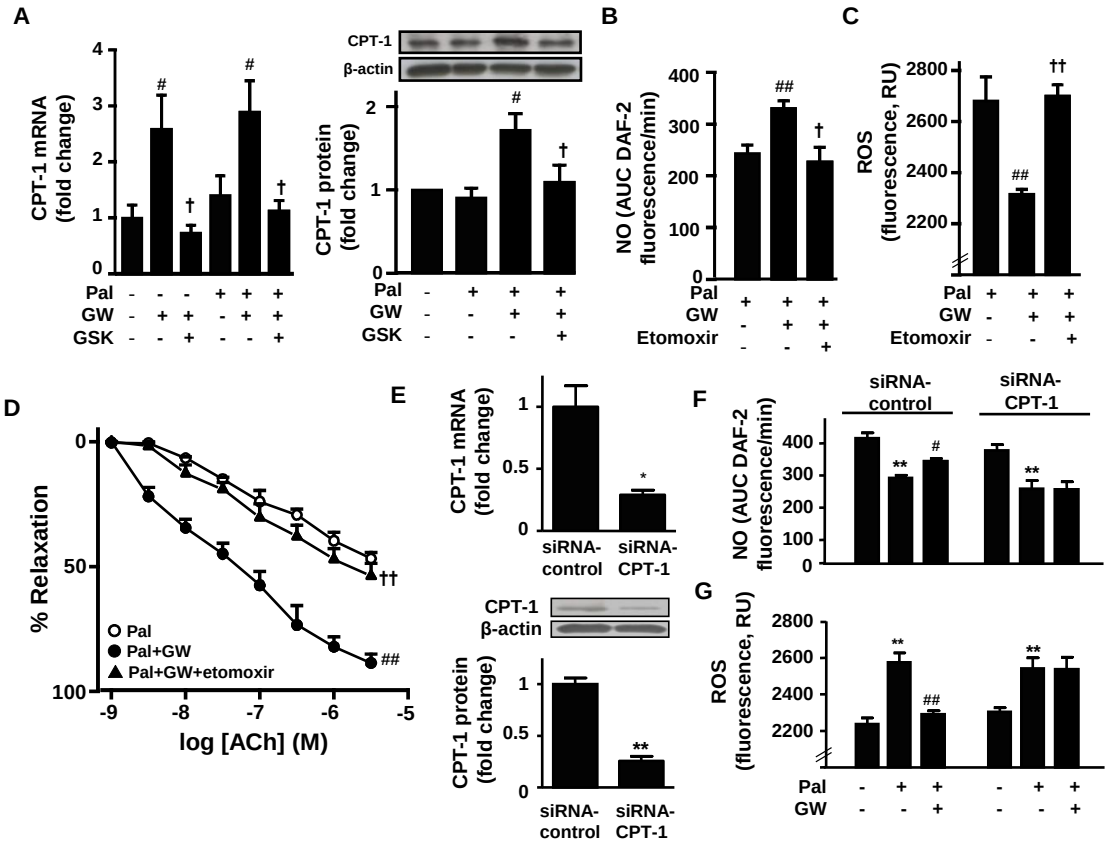

Figure 28. Role of CPT-1 in the preventive effects of PPARβ/δ activation on palmitate (Pal)-induced endothelial dysfunction. *mRNA and protein expression of CPT-1 (**A**) in MAEC incubated with GW0742 (GW, 1 μM), during 15 hours, and in the last 3 hour in the absence (control cells) or presence of Pal (100 μM). In some experiments, cells were co-incubated with GSK0660 (GSK, 1 μM), 1 hour prior the addition of GW. Results are mean ± SEM (n= 7-15). Immunoblots from 4 separate experiments were quantified. A23187-stimulated NO production (**B**) and CM-H2DCFDA-detected intracellular ROS (**C**) in MAEC (incubated as in panel A) with or without etomoxir (40 μM) during Pal incubation. Vascular relaxant responses induced by acetylcholine (ACh) (**D**) in mouse aortae pre-contracted by U46619 (10 nM), after incubation for 24 h in the presence of Pal (100 μM), GW (1 μM), or with etomoxir (40 μM). Results are shown as mean ± SEM, derived from 9-11 different rings. mRNA and protein levels of CPT-1 (**E**) after CPT-1-specific siRNA transfection in MAEC for 48 h, and A23187-stimulated NO production (**F**) and CM-H2DCFDA-detected intracellular ROS (**G**) in MAEC incubated GW (1 μM), during 15 hours, and in the last 3 hour in the absence (control cells) or presence of Pal (100 μM) in control siRNA and siRNA-CPT-1 transfected cells. *P<0.05 and **P<0.01 vs control; $^{\#}$P<0.05 and $^{\#\#}$P<0.01 vs Pal; †P<0.05 and ††P<0.01 vs Pal+GW group.*

2.6. PPARβ/δ activation prevents DAG accumulation and PKCα/βII and Thr^{495}-eNOS phosphorylation in palmitate-exposed MAEC

Since the exposure of EC to palmitate increased ROS production, which was concomitant with increases in DAG level and PKC activity in these cells (Inoguchi *et al.,* 2000), we next assessed the capacity of GW0742 to prevent DAG accumulation and the role of the PKC pathway. As expected, MAEC exposed to palmitate showed enhanced DAG levels compared with control cells (Figure 29A). When palmitate-exposed cells were treated with the PPARβ/δ-specific agonist DAG levels decreased. The mechanism by which GW0742 prevented DAG accumulation appears to involve increased fatty acid oxidation because the effect of this PPARβ/δ agonist was blunted by etomoxir (Figure 29A). The non-selective PKC inhibitor chelerythrine reversed the impaired A23187-stimulated NO production (Figure 29B), and the increased ROS production (Figure 29C) induced by palmitate in MAEC. Exposure to palmitate increased the phosphorylated levels of PKCα/βII (Figure 29D). GW0742 and the selective PKC inhibitor chelerythrine prevented the increase in PKCα/βII phosphorylation. The effects of GW0742 were prevented by etomoxir. Moreover, eNOS phosphorylation at Thr^{495}, which reduces eNOS activity, was increased by palmitate and reversed after GW0742 or chelerythine pretreatment (Figure 29E). Again, the effect of GW0742 was suppressed by co-incubation with etomoxir.

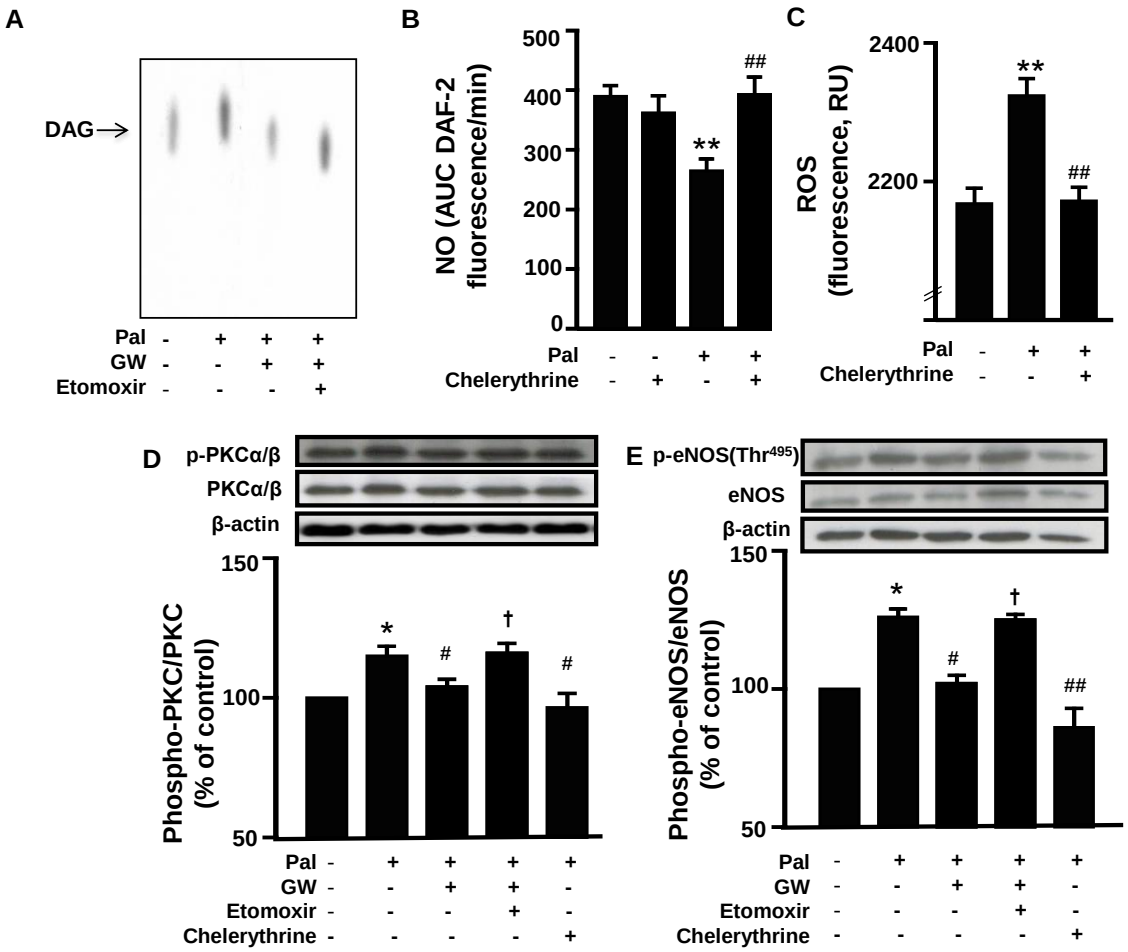

Figure 29. Role of PKC on the protective effects of PPARβ/δ activation in endothelial dysfunction-induced by palmitate (Pal). *DAG accumulation (**A**) in MAEC incubated with GW0742 (GW, 1 μM), during 15 hours, and in the last 3 hour in the absence (control cells) or presence of Pal (100 μM) or with etomoxir (40 μM) during Pal incubation. A23187-stimulated NO production (**B**), and CM-H2DCFDA-detected intracellular ROS (**C**) in MAEC incubated GW (1 μM), during 3 hour in the absence (control cells) or presence of Pal (100 μM) or with chelerythrine (1 μM). PKCα/βII (**D**) and Thr^{495}-eNOS (**E**) phosphorylation in MAEC (incubated as above). Results are mean ± SEM (n= 7-15). Immunoblots from 7 separate experiments were quantified. *P<0.05 and **P<0.01 vs control; $^{\#}$P<0.05 and $^{\#\#}$P<0.01 vs Pal; †P<0.05 vs Pal+GW group.*

3. PPARβ/δ activation attenuates palmitate-induced endothelial insulin resistance via carnitine palmitoyl-transferase-1 up-regulation in human endothelial cells

3.1. GW0742 restored NO production in the presence of palmitate

Incubation of HUVEC in lipid-containing media reduced significantly insulin-stimulated NO production (Figure 30A) and eNOS at Ser^{1177} and Akt at Ser^{473} phosphorylation but not IRS-1 at Ser^{307} phosphorylation (Figure 30B). PPARβ/δ agonist, GW0742 (1 μM), restored eNOS phosphorylation at Ser^{1177} and Akt at Ser^{473} and also the level of NO production induced by insulin in HUVEC exposed to palmitate. Moreover, we analyzed the direct effect of GW0742 (without palmitate treatment) on NO production in response to insulin, and no significant alteration was observed (data not shown). These results suggested that the increased NO bioavailability induced by PPARβ/δ agonist is just an action from its protective effect against palmitate insult. Interestingly, the effect of GW0742 was abolished in the presence of GSK0660 (1 μM), indicating that this beneficial effect was PPARβ/δ dependent (Figure 30).

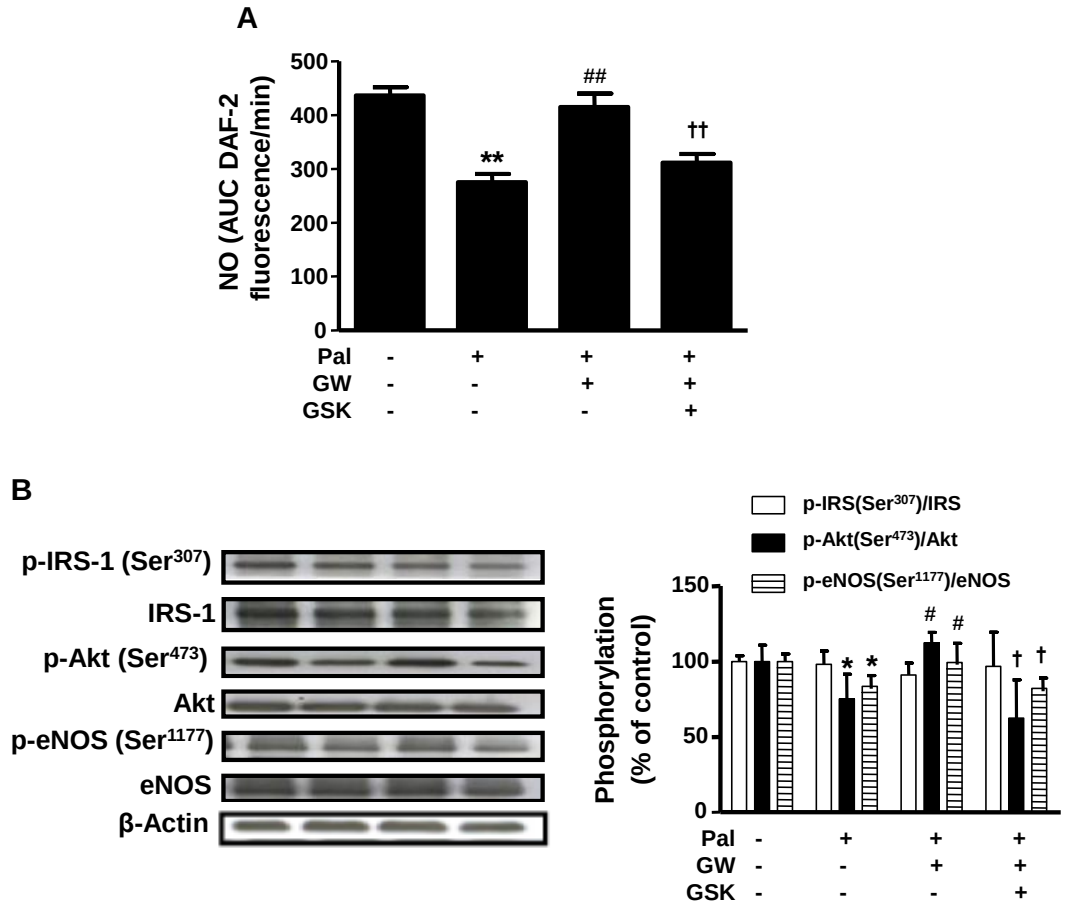

Figure 30. The PPARβ/δ agonist restores NO production in the presence of palmitate (Pal). *NO release induced by insulin (100 nM) (**A**) in HUVEC incubated with GW0742 (GW, 1 μM) for 15 hours, and in the last 3 hours in the absence (control cells) or presence of Pal (100 μM). In some experiments, cells were co-incubated with GSK0660 (GSK, 1 μM) 1 hour before the addition of GW. Results are mean ± SEM (n= 7-15). Expressions of phospho-IRS, phospho-Akt and phospho-eNOS by western blot (**B**) in insulin-stimulated HUVEC. Immunoblots from 4 separate experiments were quantified. *P<0.05 and **P<0.01 vs control; $^{\#}$P<0.05 and $^{\#\#}$P<0.01 vs Pal; †P<0.05 and ††P<0.01 vs Pal+GW group.*

3.2. GW0742 reduced the increased ROS production induced by palmitate

Because ROS is tightly associated with endothelial dysfunction, we analyzed the NO generation in the presence of mitoQ in HUVEC. The mitoQ (Figure 31A) significantly improved the impaired NO production in response to insulin in EC incubated with palmitate.

After a 3 hours treatment with palmitate, intracellular oxidative stress was measured using a CM-H2DCFDA fluorescent probe. Compared with the control, the fluorescence intensity in palmitate-exposed cells was significantly higher (Figure 31B), indicating that intracellular ROS production was enhanced in EC. CCCP did not reduce this increased ROS production, whereas rotenone, TTFA, and mitoQ significantly prevented the effect of palmitate treatment, which indicates that mitochondrial ROS production is markedly increased in palmitate stimulated HUVEC (Figures 31B and 31C), which might be related to impairment NO production. Incubation with GW0742 abolished lipid-induced intracellular ROS production. Co-incubation of this PPARβ/δ agonist with GSK0660 suppressed the inhibition of ROS (Figure 31B). NADPH oxidase activity, measured by lucigenin-enhanced chemiluminescence, and ROS production (Figure 32A and 32B) were also increased by palmitate, whereas DPI, apocynin and GW0742 inhibited this increase. Again, GSK0660 suppressed the effects of GW0742.

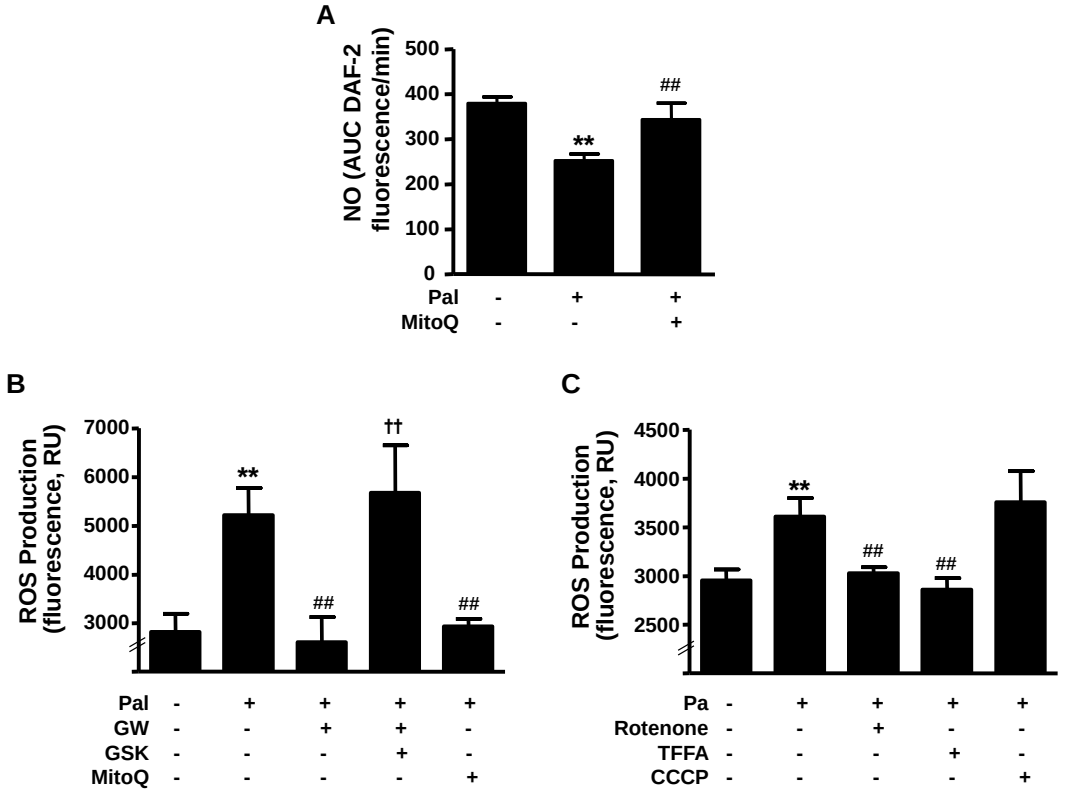

Figure 31. Role of ROS production in palmitate (Pal)-induced impaired NO production by insulin. *NO release induced by insulin (100 nM) (**A**) in HUVEC incubated for 3 hours in the absence (control cells) or presence of Pal (100 μM). In some experiments, cells were co-incubated with mitoQ (0.1 μM) added with pal. ROS measured by fluorescence with CM-H2DCFDA (**B, C**) in HUVEC were incubated with GW0742 (GW, 1 μM) for 15 hours, and in the last 3 hour in the absence (control cells) or presence of Pal (100 μM). In some experiments, cells were co-incubated with GSK0660 (GSK, 1 μM), 1 hour prior the addition of GW, or either with mitoQ (0.1 μM) or the inhibitor of complex I rotenone (5 μM), or the inhibitor of complex II, TTFA (10 μM), or the uncoupler of oxidative phosphorylation, CCCP (0.5 μM) during Pal incubation. Results are mean ± SEM (n= 6-15). **P<0.01 vs control; ##P<0.01 vs Pal; ††P<0.01 vs Pal+GW group.*

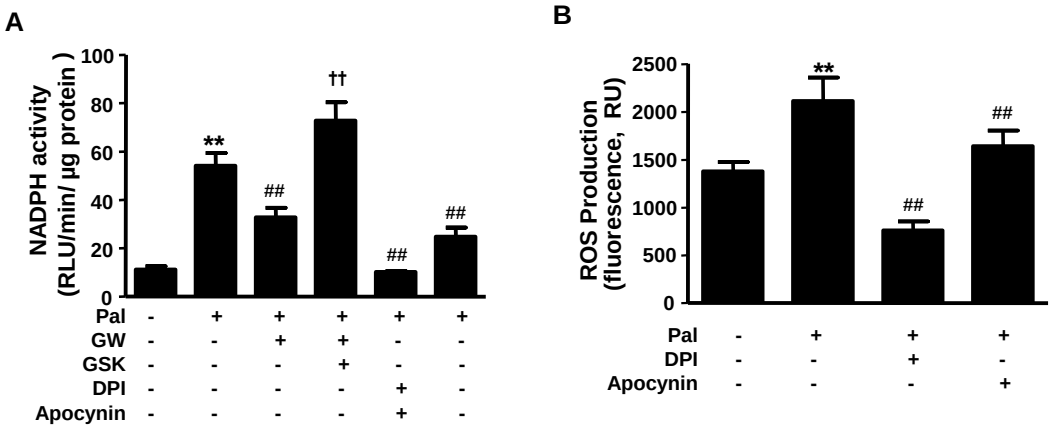

Figure 32. Role of NADPH oxidase in palmitate (Pal)-induced impaired NO production. *NADPH oxidase activity measured by lucigenin-enhanced chemiluminescence (**A**) and ROS measured by fluorescence with CM-H2DCFDA (**B**) in HUVEC were incubated with GW0742 (GW, 1 µM) for 15 hours, and in the last 3 hour in the absence (control cells) or presence of Pal (100 µM). In some experiments, cells were co-incubated with GSK0660 (GSK, 1 µM), 1 hour prior the addition of GW, or either with DPI (10 µM) or apocynin (10 µM) added with Pal. Results are mean ± SEM (n= 6-15). **P<0.01 vs control; ##P<0.01 vs Pal; ††P<0.01 vs Pal+GW group.*

3.3. Role of CPT-1 in the preventive effects of PPARβ/δ activation on impairment of endothelial action of insulin induced by palmitate

We assessed the expression of CPT-1, a well-known PPARβ/δ target gene involved in fatty acid oxidation (Wan *et al.,* 2010), which catalyzes the rate-limiting step in mitochondrial fatty acid oxidation and mitigates mitochondrial ROS production. GW0742 induced a marked increase in the mRNA of the PPARβ/δ target gene CPT-1 in HUVEC that was sensitive to PPARβ/δ blockade and independent of the presence of palmitate (Figure 33A). The preventive effects induced by GW0742 on the impaired insulin-stimulated NO production (Figure 33B), the increased ROS generation (Figure 33C) and the NADPH activity (Figure 33D) in HUVEC incubated with palmitate, were abolished by the CPT-1 irreversible inhibitor etomoxir.

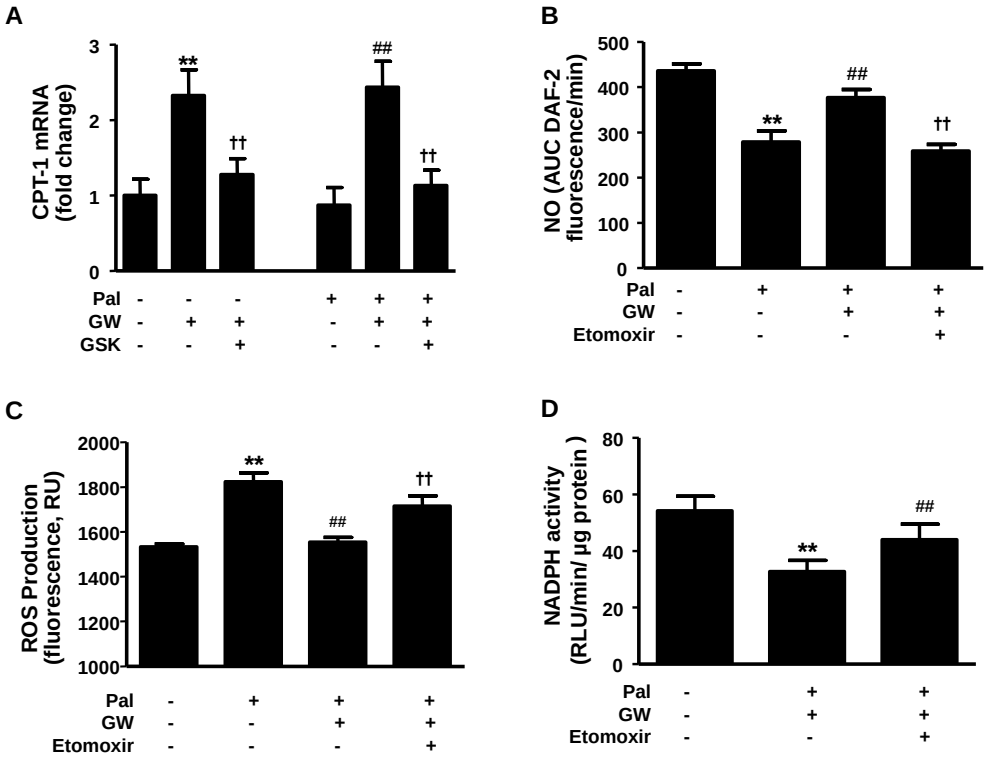

Figure 33. Role of CPT-1 in the preventive effects of PPARβ/δ activation on palmitate (Pal)-induced impaired NO production. *mRNA of CPT-1 (**A**) in HUVEC incubated with GW0742 (GW, 1 µM) for 15 h, and in the last 3 h in the absence (control cells) or presence of Pal (100 µM). In some experiments, cells were co-incubated with PPARβ/δ antagonist GSK0660 (GSK, 1 µM), 1 h before the addition of GW. Insulin (100 nM)-stimulated NO production (**B**), and CM-H2DCFDA-detected intracellular ROS (**C**) and NADPH oxidase activity measured by lucigenin-enhanced chemiluminescence (**D**) in HUVEC (incubated as in A) with or without etomoxir (40 µM) during Pal incubation. Results are mean ± SEM (n= 6-15). **P<0.01 vs control; ##P<0.01 vs Pal; ††P<0.01 vs Pal+GW group.*

4. Role of UCP2 in the protective effects of PPARβ/δ activation on lipopolysaccharides-induced endothelial dysfunction

4.1. PPARβ/δ activation *in vivo* improves endothelial function and vascular oxidative stress in LPS injected mice

To examine whether *in vivo* PPARβ/δ activation had protective effects in endothelial function, after 3 days of oral GW0742 treatment, LPS was given ip 4 hours prior to sacrifice. In these experimental conditions, GW0742 did not alter the aortic mRNA levels of PPARβ/δ (Figure 34A), but, as expected, it increased the expression of two well-known PPARβ/δ-target genes, PDK-4 (Figure 34B) and CPT-1 (Figure 34C). This increase was abolished by co-administration of the PPARβ/δ antagonist GSK0660. These results demonstrate the PPARβ/δ activation exerted by GW0742 in the vascular wall. The *in vivo* injection of LPS did not modify the aortic mRNA levels of PPARβ/δ (Figure 34A), PDK-4 (Figure 34B) and CPT-1 (Figure 34C), but significantly attenuated the relaxation to ACh, as compared to vehicle injected in control mice (Figure 34D). However, when mice were treated with GW0742 the impaired ACh relaxation induced by LPS was significantly improved. The increased relaxation to ACh induced by GW0742 treatment was prevented by GSK0660 (Figure 34D). The relaxant response induced by ACh was almost fully inhibited by the eNOS inhibitor L-NAME in all experimental groups (Figure 34E), whereas the endothelium-independent vasodilator responses to SNP were not different among groups (Figure 34F).

ROS production has been involved in endothelial dysfunction induced by LPS (Liang *et al.,* 2013; Toral *et al.,* 2014). Thus, we analyzed firstly vascular ROS content in aorta from all experimental groups. Rings from mice injected with LPS showed a marked increased staining in ethidium fluorescence as compared with control mice, which was significantly reduced by GW0742 administration (Figure 35A). PEG-SOD incubation suppressed this increase, thus involving O_2^- as main ROS in the vasculature. NADPH oxidase (Somers *et al.,* 2000; Brandes and Kreuzer, 2005), mitochondria (Doughan *et al.,* 2008; Tian *et al.,* 2012b), and ER (Cheang *et al.,* 2014)

are major sources of endothelial ROS, which are activated by LPS (Emre *et al.,* 2007; Duarte *et al.,* 2013; Liang *et al.,* 2013). To test the role of NADPH oxidase in endothelial dysfunction induced by LPS we used the NADPH oxidase inhibitor apocynin. In the presence of apocynin, the impairment of ACh induced-relaxation induced by LPS injection was almost abolished, suggesting a key role of NADPH oxidase in endothelial dysfunction induced by LPS (Figure 35B). In addition, LPS also increased the vascular mRNA levels of the NADPH oxidase subunits NOX-1 (Figure 35C), NOX-2 (Figure 35D), $p47^{phox}$ (Figure 35E), and $p22^{phox}$ (Figure 35F). GW0742 treatment prevented the increased aortic mRNA levels of these subunits induced by LPS (Figure 35C-F), which was inhibited by co-administration with the PPARβ/δ antagonist GSK0660.

UCP2 is involved in the increased mitochondrial ROS production induced by LPS in macrophages (Emre *et al.,* 2007). Aorta from LPS-injected mice showed reduced mRNA levels (Figure 36A) and protein expression (Figure 36B) of UCP2 as compared to control group. GW0742 treatment restored these expressional changes induced by LPS to values similar to the control group. Previous studies also implicated ER stress in oxidative stress, which seems to be reduced by PPARβ/δ activation with metformin (Cheang *et al.,* 2014). We found that LPS injection increased ER stress markers, such as BiP (Figure 36C), IRE-1α (Figure 36D), PERK (Figure 36E), ATF-6 (Figure 36F), and CHOP (Figure 36G) mRNA levels compared with control group. GW0742 treatment diminished ER stress induced by LPS (Figure 36C-G). Of note, the beneficial effect of GW0742 on UCP2 expression and ER stress was suppressed by co-administration with GSK0660.

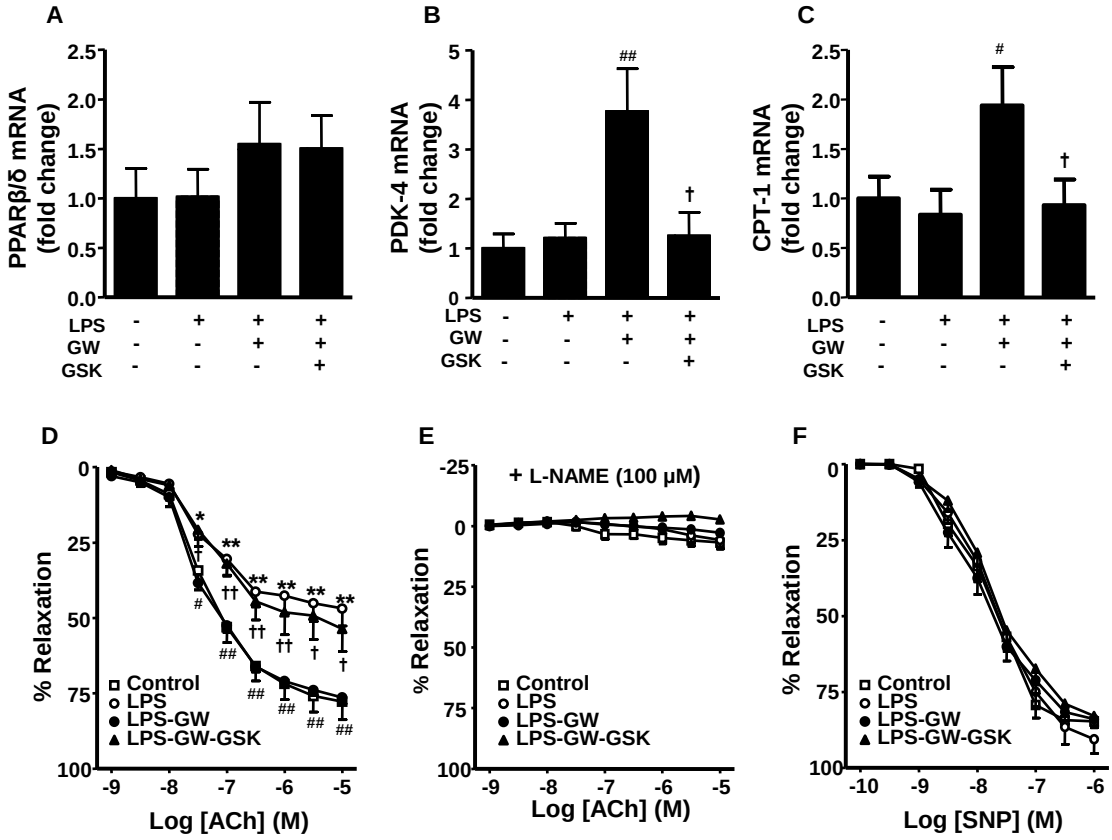

Figure 34. PPARβ/δ activation prevents LPS-induced endothelial dysfunction in vivo. *Aortic expressional changes induced by LPS and GW0742 (GW) on PPARβ/δ (**A**) and its target genes PDK-4 (**B**) and CPT-1 (**C**). Vascular relaxant responses induced by acetylcholine (ACh) in the absence (**D**) or in the presence (**E**) of L-NAME (100 μM), and endothelium-independent relaxant responses to nitroprusside (SNP) (**F**) in aortae pre-contracted by U46619 (10 nM) from all experimental groups: 1) control, 2) LPS, 3) LPS-treated with GW, and 4) LPS plus GW plus GSK0660 (GSK). Values are expressed as mean ± SEM (n= 6-8 rings from different mice). *P<0.05 and **P<0.01 vs control; #P<0.05 and ##P<0.01 vs LPS; †P<0.05 and ††P<0.01 vs LPS-GW group.*

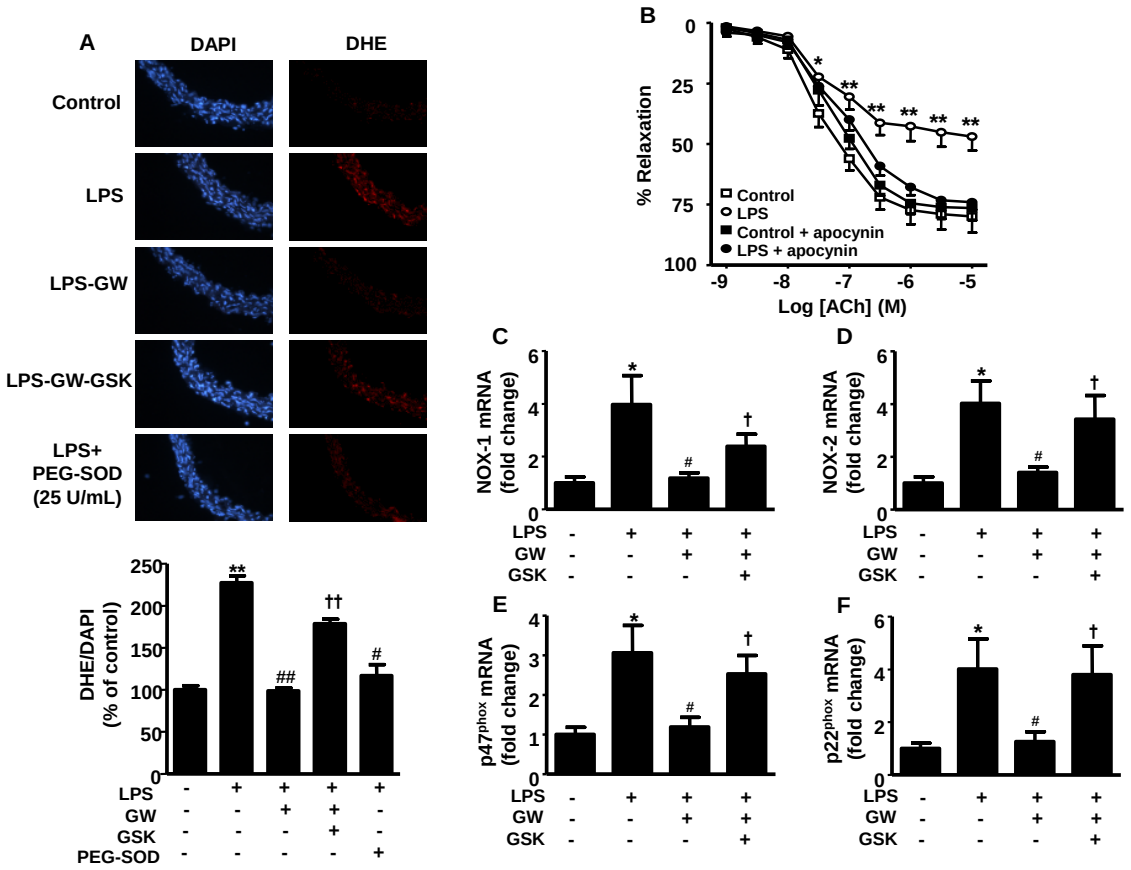

Figure 35. Role of ROS and NADPH oxidase on LPS-induced endothelial dysfunction. *Right pictures show arteries incubated in the presence of DHE which produces a red fluorescence when oxidized to ethidium by ROS. Left pictures show blue fluorescence of the nuclear stain DAPI (x 400 magnification). Bottom shows red ethidium fluorescence intensity normalized to the blue DAPI fluorescence (mean ± SEM, n= 6-8 rings from different mice). Some aortic rings from LPS group were incubated with PEG-SOD (25 U/mL) (**A**). Endothelium-dependent relaxation induced by acetylcholine (ACh) in the absence or in the presence (added 30 min before of U46619) of the NADPH oxidase inhibitor apocynin (10 μM) (**B**) in aortae pre-contracted by U46619 (10 nM) from control and LPS groups (n = 6-8). Expression of NADPH oxidase subunits NOX-1 (**C**), NOX-4 (**D**), p47^{phox} (**E**) and p22^{phox} (**F**) at the level of mRNA by RT-PCR. Results are shown as mean ± SEM (n= 6-8). ROS production and NADPH oxidase expression were assessed in aortae from all experimental groups: 1) control, 2) LPS, 3) LPS-treated with GW0742 (GW) and 4) LPS plus GW plus GSK0660 (GSK). *P<0.05 and **P<0.01 vs control; $^{\#}$P<0.05 and $^{\#\#}$P<0.01 vs LPS; †P<0.05 and ††P<0.01 vs LPS-GW group.*

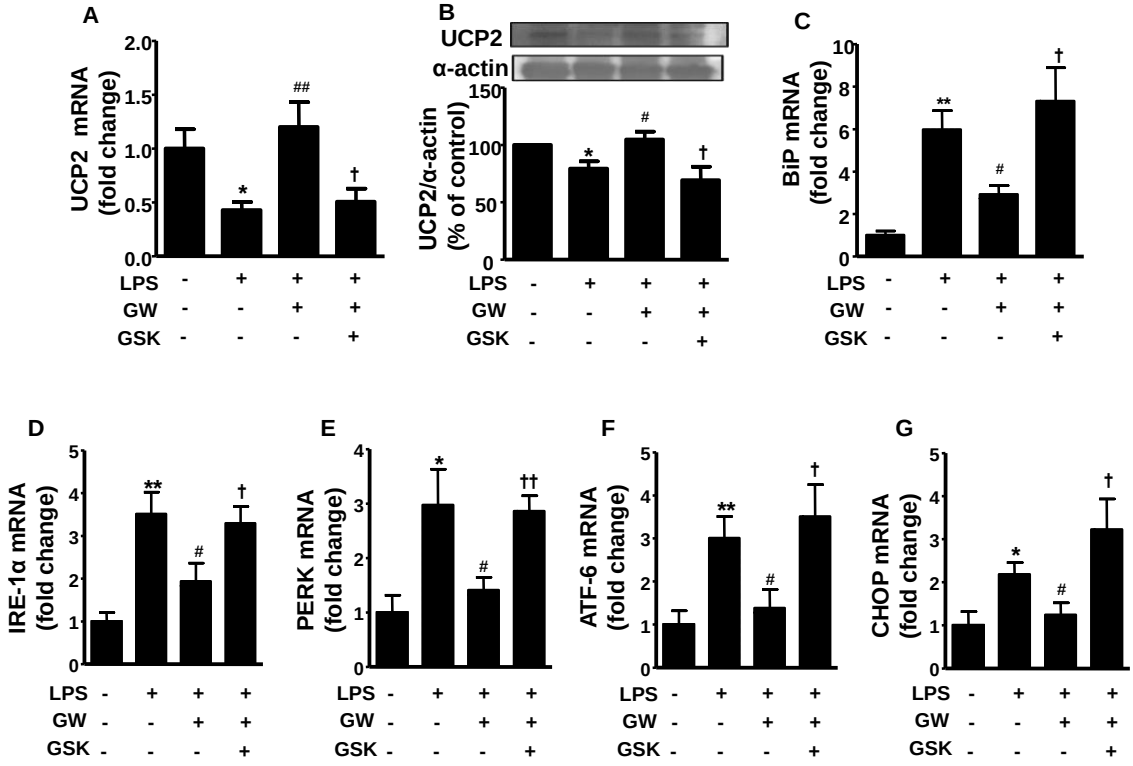

Figure 36. PPARβ/δ activation prevents the effects of LPS on UCP2 expression and on ER stress in vivo. *UCP2 (**A**), BiP (**C**), IRE-1α (**D**), PERK (E), ATF-6 (**F**), and CHOP (**G**) mRNA levels, and UCP2 protein expression (**B**) in aortae from all experimental groups: 1) control, 2) LPS, 3) LPS-treated with GW0742 (GW), and 4) LPS plus GW plus GSK0660 (GSK).The specify of the antibody for UCP2 was confirmed by siRNA experiments as shown below in Figure 39E. Results are shown as mean ± SEM (n= 6-8). *P<0.05 and **P<0.01 vs control; #P<0.05 and ##P<0.01 vs LPS; †P<0.05 and ††P<0.01 vs LPS-GW group.*

.

4.2. PPARβ/δ activation prevents the impairment of NO production and the increased ROS production induced by LPS in MAEC

Reduced A23187-stimulated NO production (Figure 37A) and increased intracellular ROS levels, measured by CMH2DCFDA fluorescence (Figure 37B), were observed in MAEC incubated for 4 hours with LPS. The PPARβ/δ agonist GW0742 (1 μM) restored the levels of both NO production-induced by A23187 and intracellular ROS levels in MAEC exposed to LPS. All the effects of GW0742 were abolished by co-incubation with PPARβ/δ antagonist GSK0660 (1 μM), but were unaffected by the AMPK inhibitor compound C (5 μM; data not shown). The reduced NO production induced by LPS was inhibited by co-incubation with the NADPH oxidase inhibitors apocynin, the mitochondrial antioxidant mitoQ, and the ER stress inhibitor 4-PBA (Figure 37C). These inhibitors also decreased the ROS production induced by LPS (Figure 37D), showing the involvement of ROS from NADPH oxidase, mitochondria and ER on the reduced NO production after LPS incubation. In fact, LPS increased the mRNA levels of NOX-2 (Figure 38A), and ER stress markers (Figure 38B-F) in MAEC, and this effect was prevented by PPARβ/δ activation.

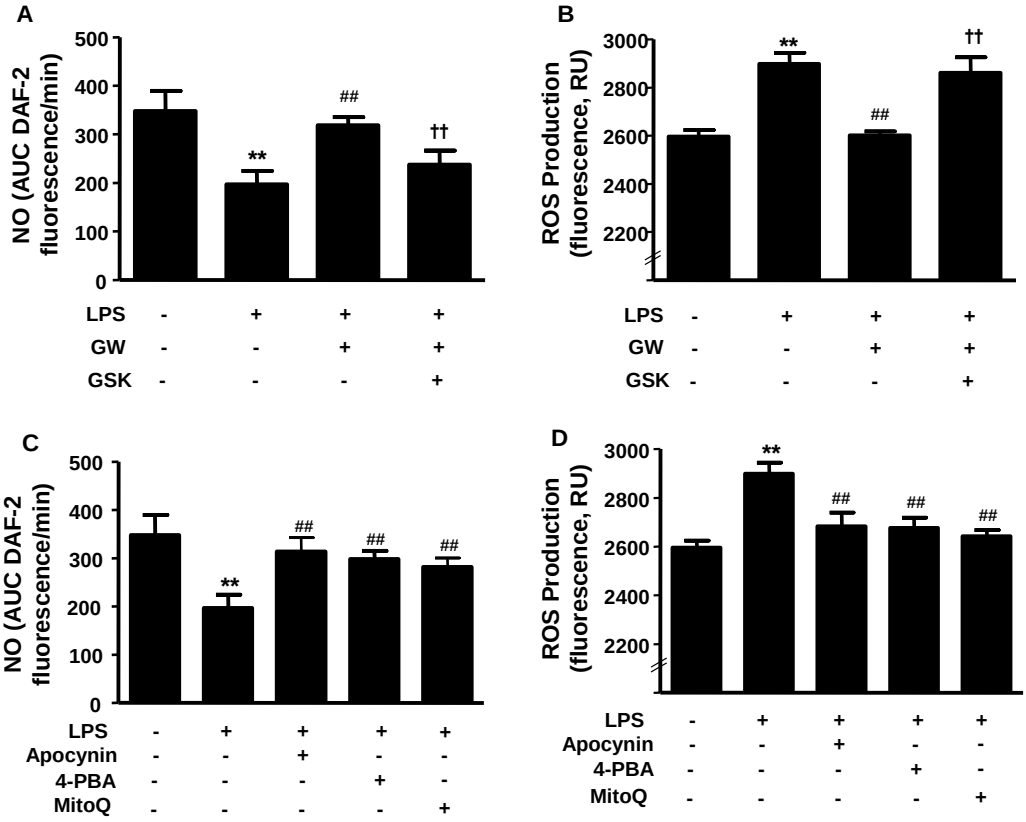

Figure 37. The PPARβ/δ agonist prevents LPS-induced endothelial dysfunction in vitro. *A23187-NO stimulated NO production (**A, C**) and CM-H2DCFDA-detected intracellular ROS (**B, D**) in MAEC. MAEC were incubated with GW0742 (GW, 1 μM), during 16 hours, and in the last 4 hour in LPS-free (control cells) or LPS-containing (10 μg/mL) serum-free medium 199. In some experiments, cells were co-incubated with GSK0660 (GSK 1 μM), 1 hour prior the addition of GW or with mitoQ (0.1 μM), apocynin (10 μM), or 4-PBA (0.1 mM) during LPS incubation. Results are mean ± SEM (n= 7-20). Values were obtained in 3 different determinations. **P<0.01 vs control; ##P<0.01 vs LPS; ††P<0.01 vs LPS-GW group.*

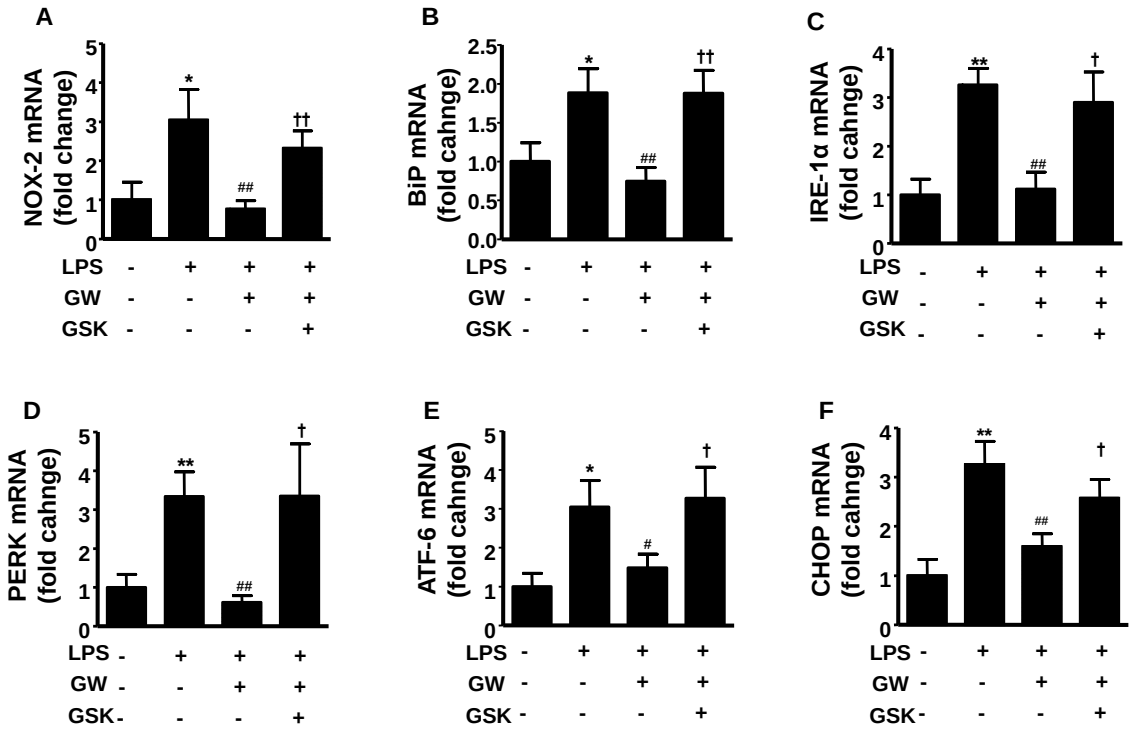

Figure 38. The PPARβ/δ agonist prevents LPS-up-regulation of NADPH oxidase and ER stress in vitro. *NOX-2 (**A**), BiP (**B**), IRE-1α (**C**), PERK (**D**), ATF-6 (**E**), and CHOP (**F**) mRNA levels. MAEC were incubated with GW0742 (GW, 1 μM), during 16 hours, and in the last 4 hour in LPS-free (control cells) or LPS-containing (10 μg/mL) serum-free medium 199. In some experiments, cells were co-incubated with GSK0660 (GSK, 1 μM). Results are mean ± SEM (n= 6-9). Values were obtained in 3 different determinations. *P<0.05 and **P<0.01 vs control; #P<0.05 and ##P<0.01 vs LPS; †P<0.05 and ††P<0.01 vs LPS-GW group.*

4.3. Role of UCP2 in the preventive effects of PPARβ/δ activation on LPS-induced endothelial dysfunction

In EC, UCP2 overexpression reduced mitochondrial ROS and improved endothelial function (Lee *et al.,* 2005). UCP2 is a well-known PPARβ/δ target gene, which was up-regulated in the vascular wall by chronic treatment with GW0742 as previously described in this Doctoral Thesis. In MAEC, GW0742 also increased the mRNA levels of UCP2 and abolished the down-regulation induced by LPS (Figure 39A). To determine if changes in UCP2 expression were responsible for the observed beneficial effects of GW0742 we used the UCP2 inhibitor genipin. This agent reduced the NO production stimulated by A23187 in control cells and abolished the improvement in NO production induced by GW0742 in LPS treated cells (Figure 39B). Similarly, genipin increased intracellular ROS in control cells and suppressed the effect induced by GW0742 in cells incubated with LPS (Figure 39C). To confirm the involvement of mitochondria as a source of intracellular ROS, we performed measures of mitochondrial ROS production using MitoSOX^{TM} Red, a mitochondrial O_2^- indicator. LPS increased MitoSOX^{TM} fluorescence (Figure 39D), which was abolished by mitoQ (data not shown). Activation of PPARβ/δ with GW0742 also suppressed the increase in mitochondrial ROS production induced by LPS, which was inhibited by genipin (Figure 39D), involving mitochondrial UCP2 in this effect. Genipin also increased mitochondrial ROS in control cells. Moreover, siRNA targeting UCP2 in MAEC, which effectively down-regulated UCP2 mRNA and protein (Figure 39E), also blunted the increase in NO production, and the reduction in ROS generation induced by GW0742 in MAEC incubated with LPS (Figure 39F). In addition, the improvement of endothelial-dependent relaxation to ACh induced by GW0742 treatment in LPS injected mice was suppressed by genipin (Figure 39G).

Furthermore, genipin also suppressed the effects of GW0742 on NADPH oxidase activity (Figure 40A), mRNA levels of NOX-2 (Figure 40B) and ER stress markers (Figure 40C-G), showing the key role of UCP2 mitochondrial in the control of ROS sources, such as NADPH oxidase and ER. In fact, silencing UCP2 or inhibition with genipin increased both NOX-2 mRNA level (Figure 40B) and ER stress markers

(Figure 40C-G). Mitochondrial ROS seems to be involved on the increased NADPH oxidase activity induced by LPS, since the mitochondrial antioxidant mitoQ normalized this effect, being without effect ER stress alleviation with 4-PBA (Figure 40A).

Shimasaki *et al*. (2013), demonstrated that UCP2 silencing in murine lung EC reduced the expression of genes required for fusion of mitochondria, such as Mfn2, which also modulates the UPR of ER (Sebastián *et al.,* 2012). We confirm that Mfn2 expression in siRNA targeting UCP2 or UCP2 inhibition in MAEC was reduced as compared to control (Figure 41A). We also found that LPS incubation reduced Mfn2 mRNA levels in MAEC (Figure 41B). This effect was prevented by GW0742, and UCP2 inhibition with genipin abolished the effect of GW0742, showing the critical role of UCP2 in the control of Mfn2 up-regulation induced by GW0742. In addition, we found that aortic Mnf2 mRNA (Figure 41C) and protein (Figure 41D) levels were reduced after LPS injection in mice. Again, PPARβ/δ activation abolished the effects of LPS.

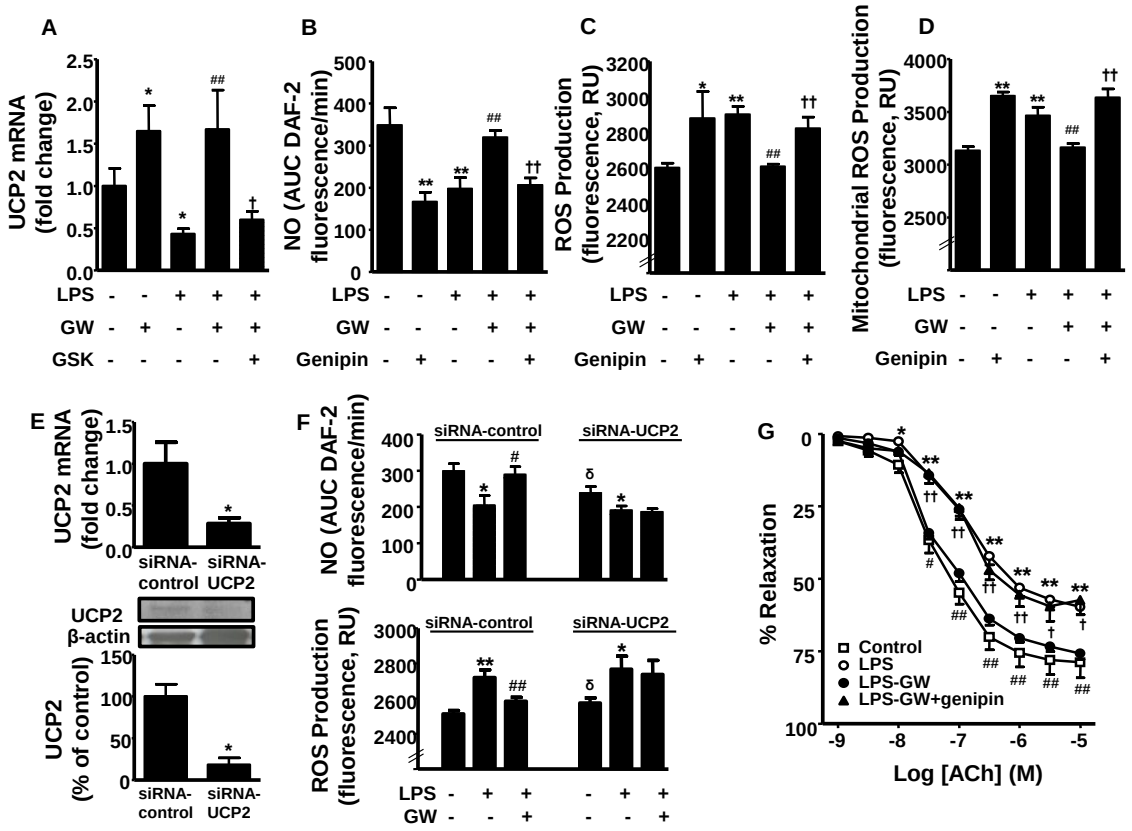

Figure 39. Role of UCP2 in the effects of PPARβ/δ activation on ROS, NO and endothelial dysfunction. *Changes in UCP2 expression (**A**) in MAEC. Results are mean ± SEM (n = 9-12). A23187-stimulated NO production (**B**), intracellular ROS (**C**), and mitochondrial ROS (**D**) in MAEC. MAEC were incubated with GW0742 (GW, 1 μM), during 16 hours, and in the last 4 hour in LPS-free (control cells) or LPS-containing (10 μg/mL) serum-free medium 199. In some experiments, cells were co-incubated with GSK0660 (GSK, 1 μM), or with genipin (10 μM) 1 hour prior the addition of GW. Values were obtained in 3 different determinations. mRNA (top) and protein (bottom) levels of UCP2 (**E**) after UCP2-specific siRNA transfection in MAEC for 48 h. A23187-stimulated NO production (top) and CM-H2DCFDA-detected intracellular ROS (bottom) (**F**) in MAEC control siRNA and siRNA-UCP2 transfected cells incubated with GW (1 μM), during 16 hours, and in the last 4 hour in LPS-free (control cells) or LPS-containing (10 μg/mL) serum-free medium 199. Vascular relaxant responses induced by acetylcholine (ACh) (**G**) in mouse aortae pre-contracted by U46619 (10 nM) from all experimental groups: 1) control, 2) LPS, 3) LPS-treated with GW. Some rings from the group LPS-GW were incubated for 1 h prior U46619 addition with genipin (10 μM). Values are expressed as mean ± SEM (n= 6-9 rings from different mice). *P<0.05 and **P<0.01 vs control; $^{\#}$P<0.05 and $^{\#\#}$P<0.01 vs LPS; †P<0.05 and ††P<0.01 vs LPS-GW group; $^{\delta}$P<0.05 control siRNA-UCP2 vs control siRNA-control.*

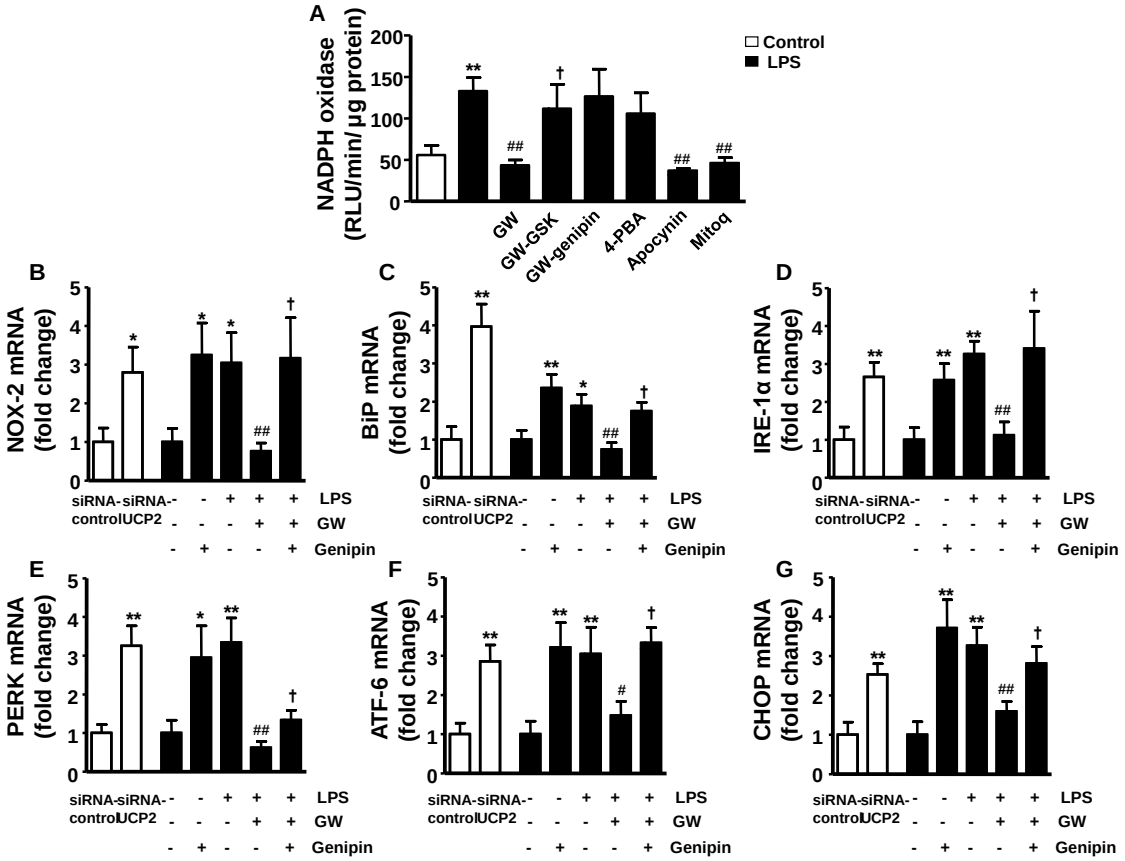

Figure 40. Role of UCP2 in the effects of PPARβ/δ activation on NADPH oxidase activity and ER stress in MAEC. *NADPH oxidase activity (**A**) and mRNA level of NOX-2 (**B**), BiP (**C**), IRE-1α (**D**), PERK (**E**), ATF-6 (**F**), and CHOP (**G**) in different experimental conditions. MAEC were incubated with GW0742 (GW, 1 μM), during 16 hours, and in the last 4 hour in LPS-free (control cells) or LPS-containing (10 μg/mL) serum-free medium 199. In some experiments, cells were co-incubated with GSK0660 (GSK, 1 μM), or with the UCP-2 inhibitor genipin (10 μM) 1hour prior the addition of GW. In another experiments apocynin (10 μM), 4-PBA (0.1 mM), or mitoQ (0.1 μM), were added during LPS incubation. In addition, mRNA expression of NOX-2 and ER stress markers in MAEC control siRNA and siRNA-UCP2 transfected cells was determined. Results are mean ± SEM (n= 9-12). Values were obtained in 3 different determinations. * P<0.05 and **P<0.01 vs control; $^{\#}$P<0.05 and $^{\#\#}$P<0.01 vs LPS; †P<0.05 vs LPS-GW group.*

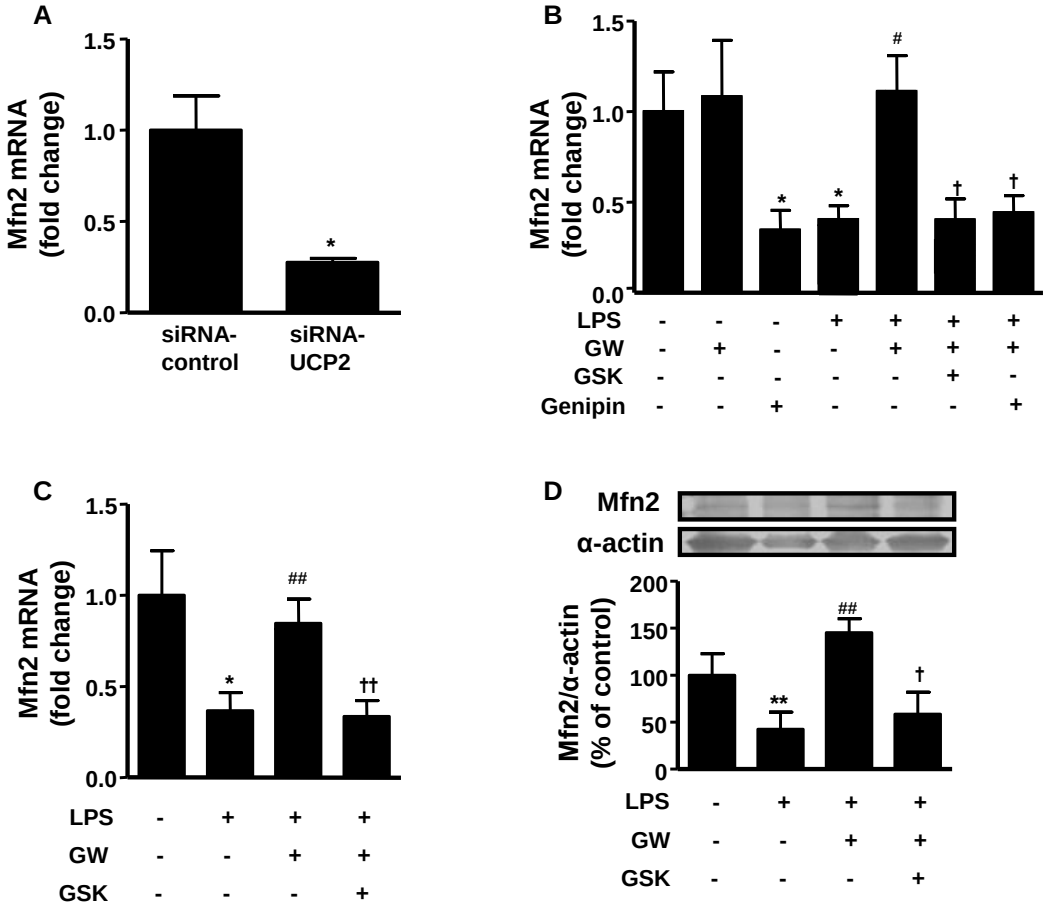

Figure 41. Effects of PPARβ/δ activation on Mitofusin-2 (Mfn2) gene expression in vitro and in vivo. *mRNA level of Mfn2 in MAEC control siRNA and siRNA-UCP2 transfected cells (**A**), and in MAEC exposed at different experimental conditions (**B**). MAEC were incubated with GW0742 (GW, 1 μM), during 16 hours, and in the last 4 hour in LPS-free (control cells) or LPS-containing (10 μg/mL) serum-free medium 199. In some experiments, cells were co-incubated with GSK0660 (GSK, 1 μM), or with the UCP2 inhibitor genipin (10 μM) 1 hour prior the addition of GW. Mfn2 mRNA levels (**C**), and protein expression (**D**) in aortae from all experimental groups (n= 6-8): 1) control, 2) LPS, 3) LPS-treated with GW and 4) LPS plus GW plus GSK. Results are shown as mean ± SEM. *P<0.05 and **P<0.01 vs control; $^{\#}$P<0.05 and $^{\#\#}$P<0.01 vs LPS; †P<0.05 and ††P<0.01 vs LPS-GW group.*

DISCUSSION

DISCUSSION

1. Chronic peroxisome proliferator-activated receptorβ/δ agonist GW0742 prevents hypertension, vascular inflammatory and oxidative status, and endothelial dysfunction in diet-induced obesity

In this Doctoral Thesis, it has been shown that chronic treatment with the highly selective PPARβ/δ agonist GW0742 restores the vascular oxidative and pro-inflammatory status and the endothelium-dependent relaxation in aorta from mice fed a HFD. Notably, the drug prevented the dietary fat-induced increase in BP, and the consequent cardiac and renal hypertrophy. All these changes were abolished by co-administration of the PPARβ/δ antagonist GSK0660, confirming the involvement of PPARβ/δ activation.

Endothelial dysfunction is a hallmark of vascular disease. In the aorta, NO is the major factor accounting for endothelium-dependent relaxation (Vanhoutte and Miller, 1985), as denoted by the almost full inhibitory action of L-NAME in this study. Thus, the diminished ACh-induced relaxation indicates an impaired agonist-induced NO bioactivity. Chronic GW0742 treatment prevented the altered responses to ACh in aortae from HFD-fed mice, indicating a protective role on agonist-induced NO bioactivity, as previously reported for another PPARβ/δ agonist (Tian *et al.,* 2012a). This effect was suppressed by PPARβ/δ blockade. In the present Thesis, the relaxant response to the activator of soluble guanylyl cyclase SNP was similar in aortae from all experimental groups, indicating that alterations in cGMP do not seem to contribute to endothelial dysfunction in HFD-fed mice. Thus, the functional changes observed in endothelium-dependent relaxation should be attributed to an alteration in NO synthesis or its bioavailability. There are controversial data about the role of NO production in endothelial dysfunction found in HFD-fed mice, since increase (Beyer *et al.,* 2008), decrease (Roberts *et al.,* 2005; Kobayasi *et al.,* 2010; Shen *et al.,* 2011), or no change (Noronha *et al.,* 2005; Sansbury *et al.,* 2012; Tian *et al.,* 2012b) in eNOS expression

have been described. In our experimental conditions, the expression of eNOS, and its negative modulator Cav-1, were similar among all experimental groups. However, HFD caused an inhibitory interaction between Cav-1 and eNOS, which possibly impaired NOS release. Furthermore, activation of Akt and eNOS by phosphorylation at Ser^{473} and Ser^{1177}, respectively, was reduced by HFD, and restored by chronic GW0742 (present results and Tian *et al.,* 2012a), suggesting that the impaired relaxation to ACh is related, at least in part, to a reduction of NO production.

A key mechanism of endothelial dysfunction involves the vascular production of ROS, particularly O_2^-, which reacts rapidly with NO and inactivates it (Tschudi *et al.,* 1996). The impairment of endothelium-dependent relaxation seen in obesity involves inactivation of NO by O_2^- (Noronha *et al.,* 2005; Kobayasi *et al.,* 2010). In aortae from HFD control group incubated with DHE, there was a marked increase in red fluorescence. DHE can react with O_2^- and other cellular oxidants to generate the two fluorescent products 2-OH-E^+ and ethidium, respectively (Zielonka and Kalyanaraman, 2010). However, the inhibitory effect of the O_2^- scavengers tiron and PEG-SOD in red staining of control rings suggests that the primary source of oxidant stress is likely to be O_2^-. Chronic GW0742 treatment abolished this increase in obese mice, which was suppressed by PPARβ/δ blockade.

Vascular NADPH oxidase is the main source of increased ROS in HFD-fed rodents (Roberts *et al.,* 2000; Roberts *et al.,* 2006) and in obese humans (Silver *et al.,* 2007). We found a marked increase in the expression of the catalytic NADPH oxidase subunit NOX-1 in aortae from HFD-fed mice, which was prevented by PPARβ/δ activation with GW0742, since it was prevented by GSK0660 co-administration, and this could be involved in the reduction of vascular ROS level induced by this drug. All the results suggest that the reduction of O_2^- levels in vascular wall, and the subsequent prevention of NO inactivation, constitute the main mechanisms involved in its protective effects on endothelial function.

The enhancement of ROS bioavailability, in particular O_2^-, affects endothelial function in obesity not only by reducing NO bioavailability, but also by promoting inflammation (Vila and Salaices, 2005). The NF-κB is an important redox-sensitive

transcriptional factor that regulates transcription of the genes that encode inflammatory cytokines. The NF-κB is found in the cytoplasm of cells in an inactive form in association with members of a family of inhibitory proteins referred to as IκB, including IκB-α (Bowie and O'Neill, 2000). Upon stimulation, IκB-α is phosphorylated and degraded, thus allowing the translocation of active NF-κB to the nucleus. The results of this Thesis show that increased vascular ROS is associated with amplified pro-inflammatory vascular status, since IκB-α phosphorylation and the mRNA levels of the pro-inflammatory cytokines TNF-α and IL-6 were higher in the aortae from the HFD control group than in non-obese mice. Moreover, PPARβ/δ activation, which reduced ROS level, also prevented the HFD-induced NF-κB activation and the increase in the mRNA and protein levels of these cytokines in the vascular wall.

The present study confirms that HFD increased arterial BP in mice. Interestingly, GW0742 prevented the hypertension observed in this animal model as previously found in genetic and DOCA-salt induced hypertension in rats (Zarzuelo *et al.,* 2011; Zarzuelo *et al.,* 2013a). However, it had no significant effect on BP in the normotensive mice receiving standard diet. Sustained high BP is one of the most powerful determinants of renal and cardiac hypertrophy development, critical risk factors for major cardiovascular events. Herein, we show that, in parallel with its antihypertensive effects, GW0742 reduced heart and kidney weight indices. These results contrast with the lack of effect of PPARβ/δ agonists on cardiac and renal hypertrophy: GW1516 in obese mice (Tian *et al.,* 2012a) or GW0742 in SHR (Zarzuelo *et al.,* 2011). These latter results may be explained by insufficient time (7-10 days and 5 weeks, respectively) to induce morphological regression as compared to the long-term treatment (11 and 13 weeks) followed in the present study.

Previous data showed that chronic GW0742 did not modify (at 30 mg/kg) (Harrington *et al.,* 2007), or increased (6 and 60 mg/kg) (Graham *et al.,* 2005) body weight in mice fed a HFD. Our study shows that mice treated chronically with GW0742 are completely resistant to HFD-induced obesity, and these effects were prevented by GSK0660 indicating a role for PPARβ/δ as previously reported (Wang *et al.,* 2003; Akiyama *et al.,* 2004). The mechanisms whereby PPARβ/δ activation prevents obesity

have been previously addressed (Wang *et al.,* 2003), and involve reduced adiposity, probably due to metabolic changes (Wang *et al.,* 2003), which increased catabolism of circulating TG and prevented lipid accumulation. Whether the cardiovascular changes are secondary to or independent of the decrease in body weight cannot be easily distinguished in this chronic model. It would be expected that the anti-obesity effect induced by GW0742 is important for its protective cardiovascular effects. However, we have reported changes in vascular function in other models unrelated to changes in body fat or body weight (Zarzuelo *et al.,* 2011; Quintela *et al.,*2012; Zarzuelo *et al.,* 2013a) and even in *in vitro* studies (Quintela *et al.,* 2014), suggesting that direct vascular effects may also play a significant role.

The main factors that impair endothelial function in obesity, including increased BP, hyperglycemia, IR, hypertriglyceridemia and systemic inflammation were normalized after PPARβ/δ activation by GW0742. We showed that hepatic mRNA levels of pro-inflammatory cytokines, like TNF-α, and the regulatory protein of inflammatory processes JNK-1, were higher in HFD-fed mice compared to control mice, whereas PPARβ/δ activation reduced these markers of liver inflammation, and consequently improved glucose metabolism. Moreover, GW0742 also restored fat production of adiponectin, an insulin-sensitizing adipokine predominantly secreted by adipocytes, with potent protective effects against endothelial dysfunction (Quiñones *et al.,* 2005). Increased plasma HDL and vascular ABCG1 induced by GW0742 might also play a role in preserving endothelial function in HFD fed mice. Recently, it have been demonstrated that ABCG1 promotes cholesterol efflux from EC to HDL, leading to a redistribution of cholesterol from caveolae to non-cavelolae domains, consequently reducing caveolae cholesterol and the inhibitory interaction of eNOS with Cav-1, resulting in increased eNOS activity (Terasaka *et al.,* 2008; Terasaka *et al.,* 2010). In fact, the improvement endothelial dysfunction induced by GW0742 was accompanied with reduced of eNOS/Cav-1 interaction in HFD fed mice.

A moderate increase of plasma LPS levels has been reported to occur after fat-enriched diet intake, thus revealing the existence of low-grade systemic inflammation in obesity that initiates IR (Cani *et al.,* 2007). In fact, it has been shown that the strategies

that reduce endotoxemia or impair LPS-TLR4 signaling are able to improve glucose homeostasis (Cani *et al.,* 2007; Cani *et al.,* 2008). During obesity induced by HFD feeding, the vasculature is more susceptible than other tissues to the deleterious effects of nutrient overload, inflammation and endothelial dysfunction, including decreased aortic NO levels (Kim *et al.,* 2008). Both, LPS and FFA, such as palmitate, stimulate TLR4 in the vasculature, which resulted in increased NADPH oxidase-dependent O_2^- production and inflammation (Liang *et al.,* 2013; Toral *et al.,* 2014). However, GW0742 was unable to reduce the elevated plasma LPS levels in HFD fed mice. Taken account that this agent abolished endothelial dysfunction and vascular inflammation induced by HFD, we would speculate that PPARβ/δ activation interfered with TLR4 signaling in vascular wall, similarly to that found in others tissues (Haskova *et al.,* 2008; Kapoor *et al.,* 2010). This direct effect in aorta was corroborated by the increased vascular expression of several PPARβ/δ-target genes, such as CPT-1, PDK-4, UCP2 and ABCG1. Furthermore, TLR4 expression was reduced by GW0742 in HFD fed mice. This data might be related to decrease free cholesterol accumulation in the plasma membrane induced by HDL, which leads to reduced levels and signaling of TLR4, as previously found in macrophages (Yvan-Charvet *et al.,* 2008).

In conclusion, GW0742 prevents obesity, hypertension, endothelial dysfunction and the vascular pro-oxidant and pro-inflammatory state in HFD fed mice (Figure 42), showing protective effects of PPARβ/δ activation in early manifestations of atherosclerosis.

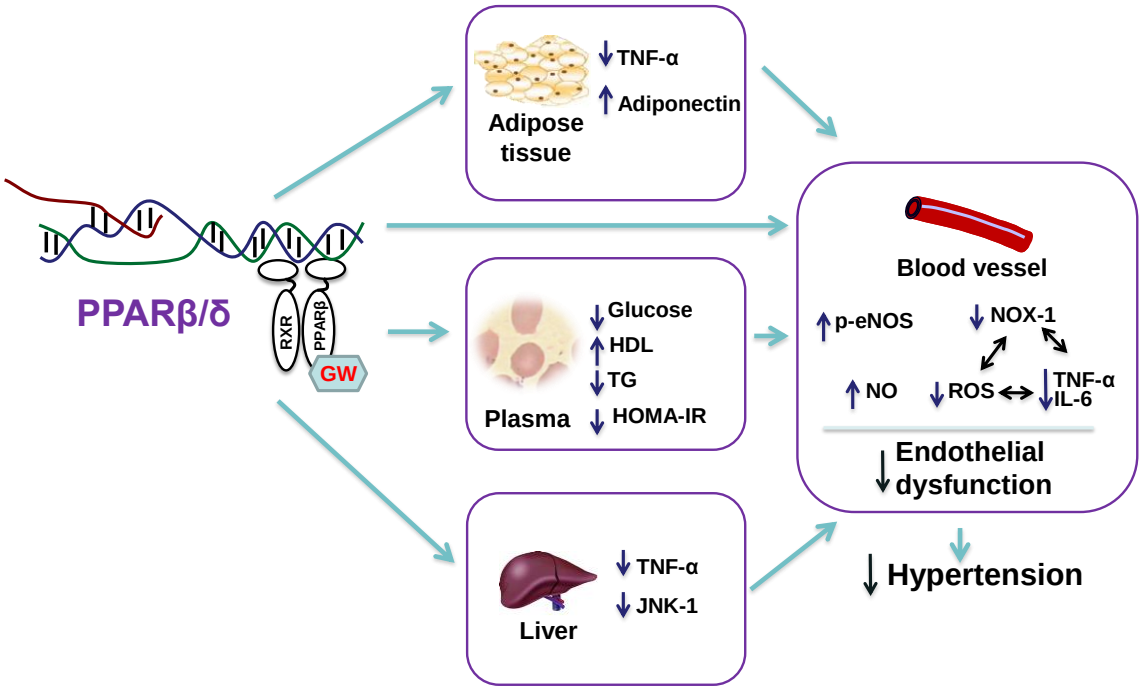

Figure 42. Scheme representing the mechanisms involved in the vascular protective effects of chronic PPARβ/δ activation in diet-induced obesity.

2. Carnitine palmitoyl-transferase-1 up-regulation by PPARβ/δ prevents lipid-induced endothelial dysfunction

Activation of PPARβ/δ has been previously reported to have beneficial effects on endothelial function in obese mice, thus confirming previous studies in diabetic rats (Quintela *et al.,* 2014) and mice (Tian *et al.,* 2012a). Herein, we provide the first evidence that PPARβ/δ activation restores the lipid-induced impairment of endothelium-dependent vasodilation and NO production, acting directly on EC via up-regulation of CPT-1. Moreover, this study points to CPT-1 as a novel therapeutic target in endothelial dysfunction.

All the effects of GW0742 reported in the present study were inhibited by GSK0660, a selective antagonist of PPARβ/δ, confirming the specificity of this drug for this nuclear receptor. Previous studies (Tian *et al.,* 2012a; Quintela *et al.,* 2014), and previous results present in this Doctoral Thesis found that the protective effects on endothelial function in diabetic and obese animals were related to changes in the metabolic profile (reduced plasma TG and IR, and increased plasma HDL). In contrast, the effects of GW0742 in the present study were independent of changes in body weight and plasma levels of lipids or glucose. Moreover, the PPARβ/δ agonist prevented endothelial dysfunction both *in vitro* when induced by palmitate and *in vivo* when induced by a HFD during three weeks.

NO is the main endothelium-dependent vasodilator. The activity of eNOS is regulated by multiple post-transcriptional mechanisms including the phosphorylation of Ser^{1177}, which is mainly regulated by Akt and results in increased enzyme activity, and the phosphorylation of Thr^{495}, which involves PKC among other kinases and inhibits the catalytic activity (Rafikov *et al.,* 2011). NO bioavailability is also strongly dependent on the production of ROS in vascular cells, particularly O_2^-, which rapidly reacts with and inactivates NO.

The relaxant response to the activator of soluble guanylyl cyclase SNP was similar in aortae from control and HFD fed mice, indicating that alterations in the NO sensibility of vascular smooth muscle do not seem to contribute to endothelial dysfunction

induced by lipids. Palmitate and oleic acid inhibit the Akt-dependent phosphorylation of eNOS at Ser^{1177}, reducing NO production, which may contribute to endothelial dysfunction and the occurrence of atherosclerosis (Zanetti *et al.,* 2005; Guo *et al.,* 2008; present results). Additionally, aortae from mice fed a HFD also showed reduced phosphorylation of both eNOS at Ser^{1177} and Akt at Ser^{473} and reduced ACh-induced relaxation. These results indicate reduced basal and stimulated eNOS activity induced by a HFD. However, when the rings were incubated with a high concentration of the eNOS inhibitor L-NAME (> 50 times its IC_{50} value), this relaxation was abolished in rings from all experimental groups, showing that is completely dependent of eNOS-derived NO. GW0742 treatment *in vitro* and *in vivo* prevented the altered responses to ACh, eNOS at Ser^{1177} and NO production induced by lipids, indicating a protective role of this drug on both basal and agonist-induced NO bioactivity.

Endothelial dysfunction induced by palmitate and HFD was also associated with increased production of ROS in vascular cells. In fact, the mitochondrial antioxidant mitoQ and the NADPH oxidase inhibitor apocynin partially prevented the palmitate-induced increase in ROS and the impairment of endothelium-dependent relaxation. The increased NADPH oxidase activity correlated with increased expression of its subunits: NOX-1, NOX-4, $p22^{phox}$ and $p47^{phox}$. Increased ROS may also result from reduced antioxidant enzymes GPx-1, MnSOD and UCP2. Activation of PPARβ/δ with GW0742 prevented the increased ROS levels *in vitro* and *in vivo*. This effect was due to a reduction in both mitochondrial and NADPH oxidase-derived ROS production in the vascular wall. The normalization of ROS also seems to contribute to the restoration of endothelial function.

CPT-1 transports fatty acids into the mitochondria, thus promoting its metabolism via β-oxidation. Up-regulation of CPT-1 seems to play a key role in the protective effects induced by PPARβ/δ activation in endothelial dysfunction evoked by lipids. This is supported by several findings. First, GW0742 produced a large increase in the expression of CPT-1 *in vitro* (MAEC and aortae) and *in vivo*. Second, the effects of GW0742 on ACh relaxation in isolated aortae, and on NO production and ROS levels

in MAEC, were also abolished by the CPT-1 inhibitor etomoxir. Third, down-regulation of CPT-1 also suppressed the effects of GW0742 in NO and ROS levels in MAEC.

Accumulation of fatty acid derivatives, such as DAG, induces endothelial dysfunction in a PKC dependent manner (Shiba *et al.,* 1993; Naruse *et al.,* 2006; Chiasson *et al.,* 2011; Mugabo *et al.,* 2011). PKCα/βII activation leads to endothelial dysfunction by increasing eNOS phosphorylation at Thr^{495}, thus reducing NO production (Graham *et al.,* 2005), and by increasing ROS production from the mitochondria (Wang *et al.,* 2006) and NADPH oxidase (Inoguchi *et al.,* 2000), which decreases NO bioavailability. Likewise, we found that palmitate increased DAG and activation of PKCα/βII. Moreover, PKC inhibition with chelerythrine prevented the reduction in NO and increased ROS in MAEC incubated with palmitate. Interestingly, our findings demonstrate that PPARβ/δ activation by GW0742 prevents palmitate-induced DAG accumulation in MAEC. Our data implicate increased CPT-1 activity in this effect, because DAG levels were restored by the presence of etomoxir. Accordingly, overexpression of CPT-1 in cultured skeletal muscle cells (Bruce *et al.,* 2009; Coll *et al.,* 2010) affords protection against lipid-induced accumulation of DAG. Consistent with the reduction in DAG, GW0742 prevented the increase in PKCα/βII activation and eNOS phosphorylation at Thr^{495} in palmitate-exposed cells. Taken together, the data indicates that as a result of increased mitochondrial transport and oxidation of FFA induced by GW0742, their accumulation in the form of DAG would be reduced. Our data confirm the key role of CPT-1 in the prevention of fatty acid-induced endothelial dysfunction and support the use of GW0742 as a pharmacological tool to prevent DAG accumulation and reduce the vascular alterations derived from this process.

In summary, this study demonstrates that, in lipid-induced endothelial dysfunction, PPARβ/δ activation improves endothelium-dependent relaxation, essentially by preserving the NO-mediated component. This protective effect may be attributable to an up-regulation of CPT-1, which prevented DAG accumulation, thereby impeding PKCα/βII activation and the subsequent eNOS inactivation and ROS production (Figure 43).

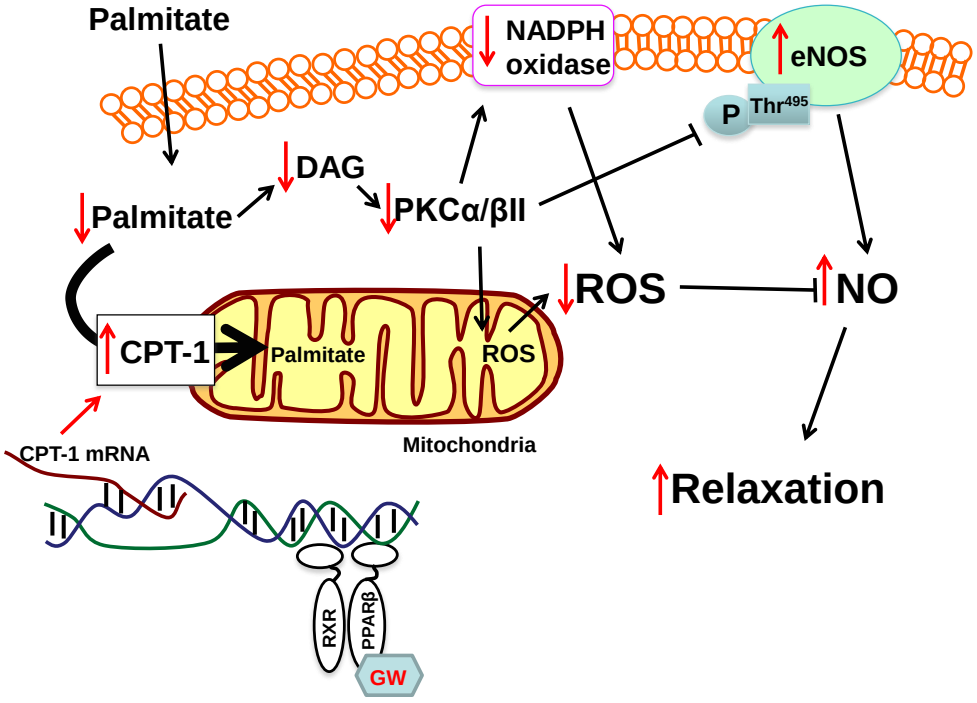

Figure 43. Scheme representing the mechanisms involved in the palmitate-induced impairment of endothelial function and the proposed mechanisms (red arrows) for the protective effect of PPARβ/δ activation.

3. PPARβ/δ activation attenuates palmitate-induced endothelial insulin resistance via carnitine palmitoyl-transferase-1 up-regulation in human endothelial cells

Circulating FFA play a critical role in the induction of IR and endothelial dysfunction. Palmitate is a major component of circulating FFA that evokes oxidative stress and leads to endothelial dysfunction. In this study, we provide the first evidence that PPARβ/δ activation has a protective effect on the lipid-reduced endothelial insulin signaling and NO production through a direct effect on human EC via up-regulation of CPT-1.

IR is characterized by endothelial dysfunction (Kim *et al.,* 2006). The reciprocal relationship between insulin sensitivity and endothelial function is the physiological contributor for the link between metabolism and cardiovascular functions (Jang *et al.,* 2013). Vascular endothelium is an insulin target tissue. In endothelium exists a distinct insulin-signaling pathway leading to eNOS activation and NO production. This pathway involves a series of phosphorylation reactions by the actions of several protein kinases. First, after insulin binding to its receptor at the cell surface, the receptor is activated and can phosphorylate IRS-1 inside the cell, and then phosphorylated IRS-1 binds to and phosphorylates PI3K, and the phosphorylated PI3K then phosphorylates and activates Akt. In the end, Akt directly phosphorylates eNOS at its Ser^{1177}, resulting in increased eNOS activity and NO production (Zeng *et al.,* 2000; Montagnani *et al.,* 2002; Xiao-Yun *et al.,* 2009). In accordance with previous studies (Xiao-Yun *et al.,* 2009; Jang *et al.,* 2013 ; Lu *et al.,* 2013; Wang *et al.,* 2013; Liu *et al.,* 2016), we observed that in HUVEC palmitate inhibited Akt and eNOS phosphorylation without affecting upstream IRS-1, however the mechanisms are not fully characterized. GW0742 treatment prevented the altered response to insulin, phosphorylation of Akt at Ser^{473} and eNOS at Ser^{1177} and NO production induced by lipids, indicating a protective role of this drug on insulin-induced NO bioactivity.

The mitochondrial antioxidant mitoQ and the NADPH oxidase inhibitor apocynin partially prevented the palmitate-induced increase in ROS and the impairment of NO

production. Activation of PPARβ/δ with GW0742 prevented the increased ROS levels in HUVEC. This effect was due to a reduction in both mitochondrial and NADPH oxidase-derived ROS production in the endothelium. The normalization of ROS also seems to contribute to the restoration of NO bioavailability. As previously described, up-regulation of CPT-1 seems to have protective effects induced by PPARβ/δ activation in endothelial dysfunction evoked by lipids. This is supported by several findings. First, GW0742 produced a large increase in the expression of CPT-1 in HUVEC. Second, the effects of GW0742 on insulin-induced NO production, ROS and NADPH activity levels in EC were also abolished by the CPT-1 inhibitor etomoxir, confirming the key role of CPT-1 in the prevention of fatty-acid-induced IR.

In summary, we demonstrated that PPARβ/δ activation, through up-regulation of CPT-1, prevents the palmitate-induced impairment of insulin pathway, leading to increase NO production in HUVEC. This protective effect may be due to CPT-1 overexpression that normalizes ROS production thereby restoring insulin-stimulated IRS-Akt-eNOS signaling (Figure 44).

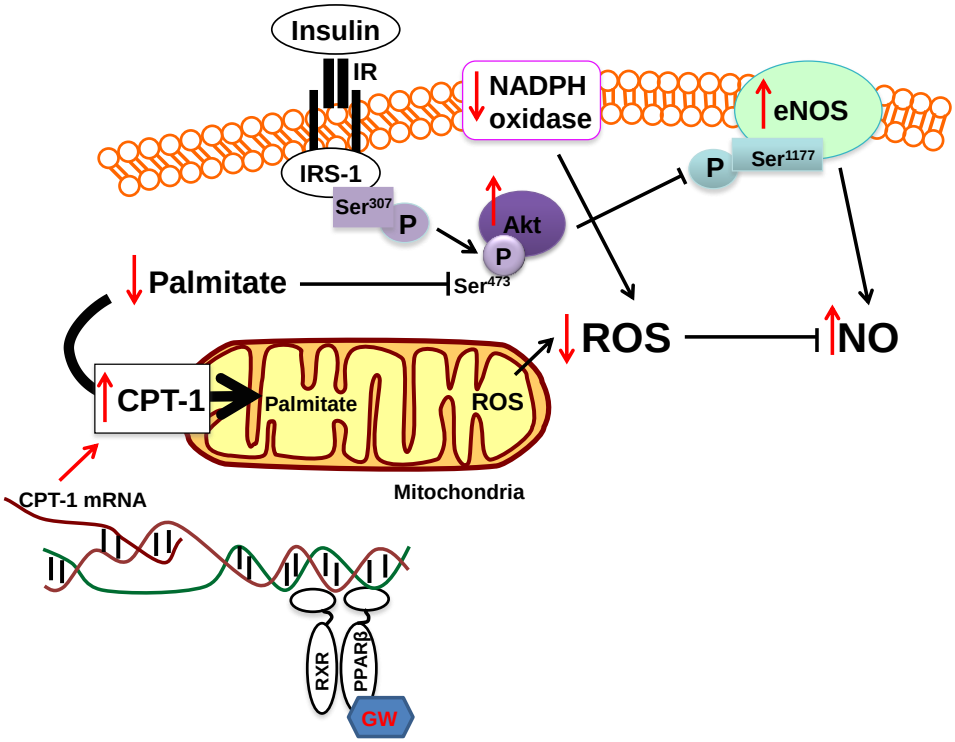

Figure 44. Scheme representing the mechanisms involved in the palmitate-induced impairment of insulin pathway and the proposed mechanisms (red arrows) for the protective effect of PPARβ/δ activation.

4. Role of UCP2 in the protective effects of PPARβ/δ activation on lipopolysaccharides-induced endothelial dysfunction

Activation of PPARβ/δ exhibits anti-inflammatory effects and prevents endothelial dysfunction in experimental models of chronic CVD such as atherosclerosis, diabetes, myocardial ischemia, and hypertension (Graham *et al.,* 2005; Yue *et al.,* 2008; Zarzuelo *et al.,* 2011; Quintela *et al.,* 2012; Tian *et al.,* 2012a; Zarzuelo *et al.,* 2013a; Quintela *et al.,* 2014; present results in this Doctoral Thesis).

Moreover, activation of PPARβ/δ attenuated the multiple organ injury and improved survival in mice with endotoxemia and polymicrobial sepsis (Kapoor *et al.,* 2010). In these acute systemic inflammatory conditions, endothelial dysfunction also plays a key pathophysiological role (Parker and Adams, 1993; Coletta *et al.,* 2014). Herein, we provide the first evidence that PPARβ/δ activation by the highly potent and selective PPARβ/δ agonist GW0742 restores LPS-induced impairment of endothelium-dependent vasodilation and NO production. This is achieved by acting directly on EC via up-regulation of UCP2, with the subsequent reduction of NADPH oxidase activity and ER stress. Therefore, this study points to PPARβ/δ and its target UCP2 as novel therapeutic targets in the treatment of endothelial dysfunction induced by metabolic endotoxemia, such as diabetes or hypertension.

PPARβ/δ was initially reported to regulate glucose and lipid metabolism. In fact, the protective effects of PPARβ/δ on endothelial function in obese animals were related to changes in the systemic metabolic profile, and to direct effects on the endothelium, as a result of CPT-1 up-regulation, without significant changes in plasma levels of LPS. LPS administration *in vivo* does not change glucose tolerance and insulin sensitivity, but induces endothelial dysfunction via TLR4 activation in the vascular wall (Zeuke *et al.,* 2002; Liang *et al.,* 2013). In the present study, we showed that PPARβ/δ activation improves LPS-induced endothelial dysfunction independently of changes in plasma glucose and lipids. In addition, these *in vivo* endothelial protective effects were also confirmed in *in vitro* conditions in MAEC, where glucose and lipid levels were constant.

Endothelium-dependent relaxations to ACh in aorta are attributable exclusively to the production of NO by eNOS, which was confirmed by abolition of the responses with L-NAME. LPS administration *in vivo* impaired these endothelium- and NO-dependent relaxations, while the endothelium-independent relaxant response to SNP were unaffected by LPS. Thus, the functional changes observed in endothelium-dependent relaxation should be attributed to an alteration in NO bioavailability. Similarly, in MAEC, LPS also reduced the NO production stimulated by A23187. GW0742 prevented the changes in NO production induced by LPS, indicating a protective role of this drug on NO bioactivity. All the effects of GW0742 reported herein were inhibited by GSK0660, confirming the involvement of this nuclear receptor. LPS increases ROS production in aorta after *in vivo* administration (Liang *et al.,* 2013; Toral *et al.,* 2014; present results) and in MAEC (Pandian *et al.,* 2005) after 4 h of incubation. This effect was abolished by PEG-SOD, apocynin, mitoQ, and the ER stress alleviator 4-PBA. These results indicate the role of three sources of ROS in EC, namely NADPH oxidase, mitochondria, and ER. In fact, LPS increased the expression of NADPH oxidase subunits NOX-1, NOX-2, $p22^{phox}$ and $p47^{phox}$ in aorta and NOX-2 and NADPH oxidase activity in MAEC. In addition, mitochondrial ROS were also involved in the reduced LPS induced NO production, since mitoQ restored the endothelial NO production stimulated by A23187.

Increased mitochondrial ROS may result from reduced antioxidant enzymes such as UCP2. UCP2 acts as an antioxidant defense in EC, which protects against endothelial function in hypertension (Chan *et al.,* 2009; Ma *et al.,* 2010) and in diet-induced obesity (Tian *et al.,* 2012b). In agreement with previous studies in macrophages (Kizaki *et al.,* 2002; Emre *et al.,* 2007), we found for the first time that acute exposure to LPS down-regulates UCP2 in aorta and MAEC. This reduced expression might be involved in the endothelial dysfunction induced by LPS. In fact, Tian *et al.* (2012b) showed that endothelium dependent relaxations in aorta from UCP2 knockout mice were reduced as compared to control mice. We found that in MAEC with loss of function of UCP2 by inhibition with genipin or by UCP2 knockdown, ROS and NO production were increased and decreased, respectively, showing the critical role of UCP2 in the control of endothelial function. Both siRNA-UCP2 and LPS down-

regulated UCP2. This was followed by an increase in ROS in both cases. However, for a similar down-regulation of UCP2 (siRNA-UCP2 vs LPS) the increase in ROS is higher for LPS, suggesting additional UCP2-independent sources of LPS-induced ROS. Accordingly, LPS still increased ROS in siRNA-UCP2 treated cells. Regarding the pharmacological aspects, GW0742 strongly up-regulated UCP2, which even in the presence of LPS were above baseline levels, which compensates for these additional ROS sources.

In this Thesis, we have confirmed that chronic PPARβ/δ activation increased UCP2 expression in the vasculature. Up-regulation of UCP2 seems to play a key role in the protective effects induced by PPARβ/δ activation in endothelial dysfunction evoked by LPS. This is supported by several findings. First, GW0742 increases the expression of UCP2 *in vitro* and *in vivo*. Second, the protective effects of GW0742 on ACh relaxation in isolated aortae, and on NO production and ROS levels in MAEC were also abolished by the UCP2 inhibitor genipin. Third, down-regulation of UCP2 also suppressed the effects of GW0742 in NO and ROS levels in MAEC.

In human adipocytes, LPS induces ER stress and facilitates IR (Alhusaini *et al.,* 2010). In addition, $TLR4^{-/-}$ mice were protected against HFD-induced ER stress in skeletal muscle, liver and adipose tissue (Pierre *et al.,* 2013). We found that in aorta and EC, LPS also decreased the protein-folding efficiency of ER, initiating a counter regulatory unfolded protein response, involving PERK, ATF-6, and IRE-1α pathways. Previous studies have also implicated ER stress in oxidative stress and endothelial dysfunction (Cheang *et al.,* 2014; Galán *et al.,* 2014). In fact, *ex vivo* culture of mouse aortae with the ER stress inducer tunicamycin impairs endothelium-dependent relaxations and increased O_2^- level (Cheang *et al.,* 2014). In addition, ER stress induction in primary EC from coronary arteries increases ROS production, which was associated with increased NOX-2 and NOX-4 mRNA levels and NADPH oxidase activity (Galán *et al.,* 2014). ER stress seems to be involved on endothelial dysfunction induced by LPS, since the ER stress inhibitor 4-PBA reduced the raise in ROS production and the impaired NO production induced by LPS. GW0742 restored the increased expression of ER stress markers (BiP, PERK, ATF-6, IRE-1α, and CHOP). In

accordance with this, PPARβ/δ-deficient mice exhibited increased ER stress in the heart, and PPARβ/δ activation prevented palmitate- or thapsigargin-induced ER stress in human cardiomyocyte cell line (Palomer *et al.,* 2014), skeletal muscle cells (Salvadó *et al.,* 2014), and tunicamycin-induced ER stress in MAEC (Cheang *et al.,* 2014).

Interestingly, part of anti-inflammatory and antidiabetic effects following PPARβ/δ activation in skeletal muscle cells were dependent on AMPK (Salvadó *et al.,* 2014). In contrast, AMPK-independent effects were described after PPARβ/δ activation in a human cardiomyocyte cell line (Palomer *et al.,* 2014), and in HUVEC (Quintela *et al.,* 2014). In accordance with this, we also found that PPARβ/δ activation prevented endothelial dysfunction induced by LPS in an AMPK-independent manner, since it was unaffected by compound C.

Mitochondria have been previously implicated in regulation of NADPH oxidase. For example, mitochondria depletion in ethidium-treated rabbit aortic smooth muscle cells attenuates NOX-1 expression (Wosniak *et al.,* 2009), and mitochondrial O_2^- contributes to activation of NADPH oxidase in phagocytes cell, by acute activation of NOX-2 (Nazarewicz *et al.,* 2013). In EC, the interplay between mitochondrial and NADPH oxidase-derived O_2^- constitutes a feed-forward cycle in which NOX-2 increases the production of mitochondrial ROS by reverse electron transfer. Enhanced production of mitochondrial ROS further activates the cytoplasmic NADPH oxidase, increasing cellular O_2^- production and diminishing NO bioavailability (Dikalov *et al.,* 2014). In this study, UCP2 seems to play a critical role in controlling NOX-2 expression. Genetic knockdown of UCP2 or UCP2 inhibition increases NOX-2 expression. Conversely, up-regulation of UCP2 by PPARβ/δ activation prevented the increased levels of NOX-2 mRNA and NADPH oxidase activity induced by LPS. Interestingly, these effects were suppressed by genipin, involving UCP2 in this process. NOX-1, NOX-2 and NOX-4 expression has been shown to be up-regulated by ROS in a positive feedback loop involving the Src-kinase signaling pathway (Weaver and Taylor-Fishwick, 2013; Pastori *et al.,* 2015). Accordingly, antioxidants decreased the expression of NOX isoforms. We have not addressed specifically this issue in the present study, but we speculate that

the antioxidant effect of UCP2 may prevent ROS-induced up-regulation of NOX isoforms.

There is also increasing evidence suggesting a potential inter-relationship between alterations in both mitochondria and ER, as mitochondrial dysfunction could participate in activation of the UPR, whereas ER stress could influence mitochondrial function (Rieusset, 2015). The contact points between the ER and mitochondria are the MAM. Mfn2 is a key protein in mitochondrial fusion and it participates in the bridging of mitochondria to the ER. Interestingly, a reduction in ER-mitochondrial crosstalk, achieved by liver-specific ablation of Mfn2, induces mitochondrial dysfunction and ER stress (Lee *et al.,* 2005). Loss of Mfn2 exacerbates all 3 UPR branches (PERK, IRE-1α, and ATF-6). Mfn2 physically interacts with PERK, and deficiency of Mfn2 promotes chronic PERK activation in several cell lines and mouse models (Muñoz *et al.,* 2014). In our study, LPS down-regulated Mfn2 expression in vascular tissue, which was associated with ER stress, since it increased the expression of 3 branches of ER stress. Similarly, UCP2 loss of function in MAEC, induced by genetic knockdown or by genipin, reduced the mRNA levels of Mfn2. Interestingly, UCP2 up-regulation by PPARβ/δ activation restored Mfn2 expression, with the subsequent alleviation of ER stress. These effects induced by GW0742 were suppressed in the presence of the UCP2 inhibitor genipin, showing that ER stress is downstream to mitochondrial dysfunction induced by UCP2 down-regulation.

In conclusion, our study demonstrates that, in LPS-induced endothelial dysfunction, PPARβ/δ activation improves endothelium-dependent relaxation, essentially by preserving the NO-mediated component. This protective effect may be attributable to an up-regulation of UCP2, which reduced mitochondrial ROS production, NADPH oxidase activity, and ER stress with the subsequent protection of NO inactivation (Figure 45).

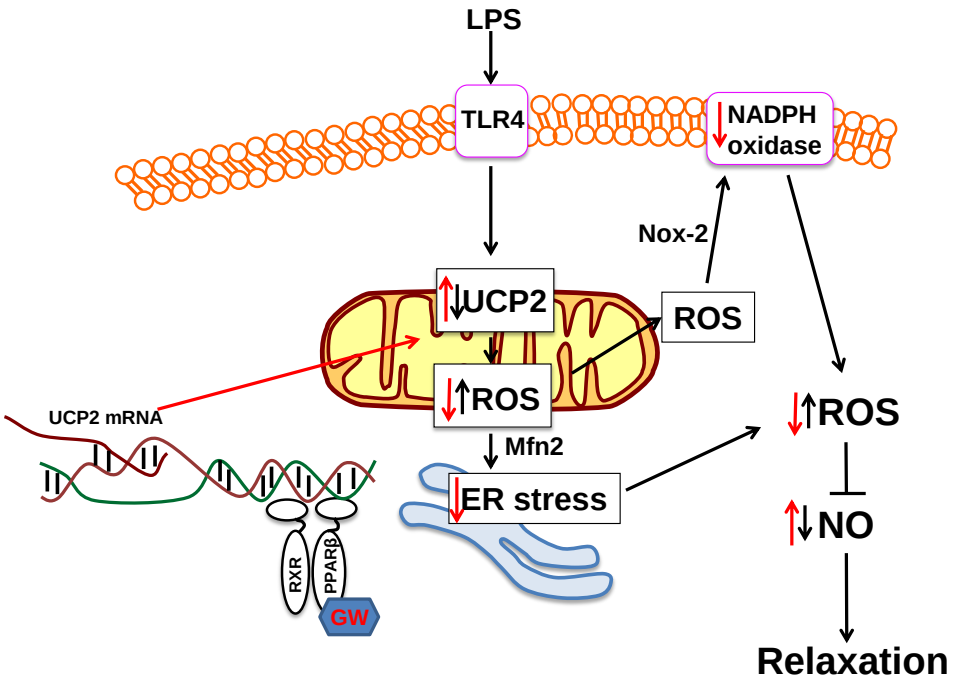

Figure 45. Scheme representing the mechanisms involved in the LPS-induced impairment of endothelial function and the proposed mechanisms (red arrows) for the protective effect of PPARβ/δ activation.

All these experiments indicate that PPARβ/δ activation prevents one of the initial events in the development of atheroma plaque, endothelial dysfunction. Atherogenesis is the pathological basis of CVD (angina, infarction), which is the leading cause of death in patients with MS. The improvement in factors that impair endothelial function, such as systemic metabolic parameters (hyperglycemia, impaired glucose tolerance, HOMA-IR, dyslipidemia, HDL-cholesterol levels), pro-inflammatory cytokines and elevated BP contributes to this protective effect in a situation of obesity. Furthermore, PPARβ/δ activation on the vascular bed (through direct vascular actions) is also involved in the improvement of endothelial dysfunction in MS. Thereby, the increase in oxidation of FFA in endothelium mediated by the PPARβ/δ target gene, CPT-1, improves not only the relaxing response induced via Ca^{2+}-dependent activation of eNOS, but also the production of NO caused by phosphorylation of the eNOS by insulin. Activation of other PPARβ/δ target gene such as UCP2 protects endothelium from the deleterious effect of metabolic endotoxemia.

These findings suggest that PPARβ/δ agonists, as GW0742, possess a therapeutic potential in the prevention of endothelial dysfunction, and consequently of CVD in situations of obesity.

CONCLUSIONS

CONCLUSIONS

1. Chronic PPARβ/δ activation induced by oral GW0742 treatment in HFD-fed mice prevents obesity. It also hinders hypertension and early manifestations of atherosclerosis, like endothelial dysfunction and vascular pro-oxidant and pro-inflammatory status.

2. Pharmacological PPARβ/δ activation *in vivo* and *in vitro* restored the lipid-induced endothelial dysfunction by up-regulation of CPT-1 in MAEC, thus reducing DAG accumulation and the subsequent PKC-mediated ROS production and eNOS inhibition.

3. Pharmacological PPARβ/δ activation *in vitro* prevents palmitate-induced impairment of insulin signaling, which increases insulin-stimulated NO production in HUVEC. This protective effect may be due to CPT-1 over-expression, which normalizes ROS production and restores insulin-stimulated IRS-Akt-eNOS pathway.

4. Pharmacological PPARβ/δ activation *in vivo* and *in vitro* restored the LPS-induced endothelial dysfunction by up-regulation of mitochondrial UCP2, with the subsequent alleviation of ER stress and NADPH oxidase activity, thus reducing intracellular ROS production and increasing NO bioavailability.

REFERENCES

REFERENCES

Ae Park S, Choi MS, Cho SY, Seo JS, Jung UJ, Kim MJ, Sung MK, Park YB, Lee MK. Genistein and daidzein modulate hepatic glucose and lipid regulating enzyme activities in C57BL/KsJ-db/db mice. *Life Sci.* 2006; 79: 1207-13.

Ahirwar AK, Jain A, Singh A, Goswami B, Bhatnagar MK, Bhatacharjee J. The study of markers of endothelial dysfunction in metabolic syndrome. *Horm Mol Biol Clin Investig*. 2015; 24:131-6.

Akiyama TE, Lambert G, Nicol CJ, Matsusue K, Peters JM, Brewer HB Jr, Gonzalez FJ. Peroxisome proliferator-activated receptor beta/delta regulates very low density lipoprotein production and catabolism in mice on a Western diet. *J Biol Chem.* 2004; 279:20874-81.

Alberti KG, Zimmet PZ. Definition, diagnosis and classification of diabetesmellitus and its complications. Part 1: diagnosis and classification of diabetes mellitus provisional report of a WHO consultation. *Diabet Med.* 1998; 15: 539-53.

Alberti KG, Zimmet P, Shaw J; IDF Epidemiology Task Force Consensus Group. The metabolic syndrome--a new worldwide definition. *Lancet.* 2005; 366:1059-62.

Alberti KG, Eckel RH, Grundy SM, Zimmet PZ, Cleeman JI, Donato KA, Fruchart JC, James WP, Loria CM, Smith SC Jr; International Diabetes Federation Task Force on Epidemiology and Prevention; National Heart, Lung, and Blood Institute; American Heart Association; World Heart Federation; International Atherosclerosis Society; International Association for the Study of Obesity. Harmonizing the metabolic syndrome: a joint interim statement of the International Diabetes Federation Task Force on Epidemiology and Prevention; National Heart, Lung, and Blood Institute; American Heart Association; World Heart Federation; International Atherosclerosis Society; and International Association for the Study of Obesity. *Circulation*. 2009; 120:1640-5.

Alessi MC, Juhan-Vague I. PAI-1 and the metabolic syndrome: links, causes, and consequences. *Arterioscler Thromb Vasc Biol.* 2006; 26:2200-7.

Alhusaini S, McGee K, Schisano B, Harte A, McTernan P, Kumar S, Tripathi G. Lipopolysaccharide, high glucose and saturated fatty acids induce endoplasmic reticulum stress in cultured primary human adipocytes: Salicylate alleviates this stress. *Biochem Biophys Res Commun*. 2010; 397:472-8.

Alvarez-Guardia D, Palomer X, Coll T, Serrano L, Rodríguez-Calvo R, Davidson MM, Merlos M, El Kochairi I, Michalik L, Wahli W, Vázquez-Carrera M. PPARβ/δ activation blocks lipid-induced inflammatory pathways in mouse heart and human cardiac cells. *Biochim Biophys Acta.* 2011; 1811:59-67.

Antuna-Puente B, Feve B, Fellahi S, Bastard JP. Adipokines: the missing link

between insulin resistance and obesity. *Diabetes Metab*. 2008; 34:2-11.

Apridonidze T, Essah PA, Iuorno MJ, Nestler JE. Prevalence and characteristics of the metabolic syndrome in women with polycystic ovary syndrome. *J Clin Endocrinol Metab*. 2005; 90: 1929-35.

Arck P, Toth B, Pestka A, Jeschke U. Nuclear receptors of the peroxisome proliferator-activated receptor (PPAR) family in gestational diabetes: from animal models to clinical trials. *Biol Reprod.* 2010; 83:168-76.

Arruda AP, Pers BM, Parlakgül G, Güney E, Inouye K, Hotamisligil GS. Chronic enrichment of hepatic endoplasmic reticulum-mitochondria contact leads to mitochondrial dysfunction in obesity. *Nat Med.* 2014; 20:1427-35.

Asakawa M, Takano H, Nagai T, Uozumi H, Hasegawa H, Kubota N, Saito T, Masuda Y, Kadowaki T, Komuro I. Peroxisome proliferator-activated receptor gamma plays a critical role in inhibition of cardiac hypertrophy in vitro and in vivo. *Circulation.* 2002; 105:1240-6.

Asehnoune K, Strassheim D, Mitra S, Kim JY, Abraham E. Involvement of reactive oxygen species in Toll-like receptor 4-dependent activation of NF-kappa *B. J Immunol.* 2004; 172:2522-9.

Avogaro A, de Kreutzenberg SV. Mechanisms of endothelial dysfunction in obesity. *Clin Chim Acta*. 2005; 360:9-26.

Ay C, Tengler T, Vormittag R, Simanek R, Dorda W, Vukovich T, Pabinger I. Venous thromboembolism--a manifestation of the metabolic syndrome. *Haematologica.* 2007; 92:374-80.

Azhar S. Peroxisome proliferator-activated receptors, metabolic syndrome and cardiovascular disease. *Future Cardiol.* 2010; 6: 657–91.

Balakumar P, Rose M, Singh M. PPAR ligands: are they potential agents for cardiovascular disorders? *Pharmacology*. 2007; 80:1-10.

Balkau B, Charles MA. Comment on the provisional report from the WHO consultation. European Group for the Study of Insulin Resistance (EGIR). *Diabet Med.* 1999; 16: 442-3.

Barlaka E, Galatou E, Mellidis K, Ravingerova T, Lazou A. Role of Pleiotropic Properties of Peroxisome Proliferator-Activated Receptors in the Heart: Focus on the Nonmetabolic Effects in Cardiac Protection. *Cardiovasc Ther.* 2016; 34:37-48.

Barroso E, Rodríguez-Calvo R, Serrano-Marco L, Astudillo AM, Balsinde J, Palomer X, Vázquez-Carrera M. The PPARβ/δ activator GW501516 prevents the down-regulation of AMPK caused by a high-fat diet in liver and amplifies the PGC-1α-Lipin 1-PPARα pathway leading to increased fatty acid oxidation. *Endocrinology*. 2011; 152:1848-59.

Bauersachs J, Widder JD. Endothelial dysfunction in heart failure. *Pharmacol Rep*. 2008; 60:119-26.

Bays HE, Schwartz S, Littlejohn T 3rd, Kerzner B, Krauss RM, Karpf DB, Choi YJ, Wang X, Naim S, Roberts BK. MBX-8025, a

novel peroxisome proliferator receptor-delta agonist: lipid and other metabolic effects in dyslipidemic overweight patients treated with and without atorvastatin. *J Clin Endocrinol Metab.* 2011; 96:2889-97.

Bedard K, Krause KH. The NOX family of ROS-generating NADPH oxidases: physiology and pathophysiology. *Physiol Rev*. 2007; 87:245-313.

Benetti E, Patel NS, Collino M. The role of PPARβ/δ in the management of metabolic syndrome and its associated cardiovascular complications. *Endocr Metab Immune Disord Drug Targets*. 2011; 11:273-84

Benkirane K, Amiri F, Diep QN, El Mabrouk M, Schiffrin EL. PPAR-gamma inhibits ANG II-induced cell growth via SHIP2 and 4E-BP1. *Am J Physiol Heart Circ Physiol.* 2006; 290:H390-7.

Berry DC, Noy N. All-trans-retinoic acid represses obesity and insulin resistance by activating both peroxisome proliferation-activated receptor beta/delta and retinoic acid receptor. *Mol Cell Biol*. 2009; 29:3286-96.

Beyer AM, de Lange WJ, Halabi CM, Modrick ML, Keen HL, Faraci FM, Sigmund CD. Endothelium-specific interference with peroxisome proliferator activated receptor gamma causes cerebral vascular dysfunction in response to a high-fat diet. *Circ Res.* 2008; 103:654-61.

Bishop-Bailey D, Bystrom J. Emerging roles of peroxisome proliferator-activated receptor-beta/delta in inflammation. *Pharmacol Ther.* 2009; 124:141-50.

Boden G. Obesity, insulin resistance and free fatty acids. *Curr Opin Endocrinol Diabetes Obes.* 2011; 18:139-43.

Bocarsly ME, Powell ES, Avena NM, Hoebel BG. High-fructose corn syrup causes characteristics of obesity in rats: increased body weight, body fat and triglyceride levels. *Pharmacol Biochem Behav*. 2010; 97:101-6.

Bonetti PO, Lerman LO, Lerman A. Endothelial dysfunction: a marker of atherosclerotic risk. *Arterioscler Thromb Vasc Biol.* 2003; 23:168-75.

Bourgoin F, Bachelard H, Badeau M, Mélançon S, Pitre M, Larivière R, Nadeau A. Endothelial and vascular dysfunctions and insulin resistance in rats fed a high-fat, high-sucrose diet. *Am J Physiol Heart Circ Physiol.* 2008; 295:H1044-H1055.

Braissant O, Foufelle F, Scotto C, Dauça M, Wahli W. Differential expression of peroxisome proliferator activated receptors (PPARs): tissue distribution of PPAR-alpha, -beta, and gamma in the adult rat. *Endocrinology*. 1996; 137: 354-66.

Brandes RP, Kreuzer J. Vascular NADPH oxidases: molecular mechanisms of activation. *Cardiovasc Res*. 2005; 65:16-27.

Bray GA. The epidemic of obesity and changes in food intake: the Fluoride Hypothesis. *Physiol Behav.* 2004; 82:115-21.

Bray GA, Nielsen SJ, Popkin BM. Consumption of high-fructose corn syrup in beverages may play a role in the epidemic of obesity. *Am J Clin Nutr.* 2004; 79: 537-43

Briones AM, Nguyen Dinh Cat A, Callera GE, Yogi A, Burger D, He Y, Corrêa JW, Gagnon AM, Gomez-Sanchez CE, Gomez-Sanchez EP, Sorisky A, Ooi TC, Ruzicka M, Burns KD, Touyz RM. Adipocytes produce aldosterone through calcineurin-dependent signaling pathways: implications in diabetes mellitus-associated obesity and vascular dysfunction. *Hypertension.* 2012; 59:1069-78.

Bruce CR, Hoy AJ, Turner N, Watt MJ, Allen TL, Carpenter K, Cooney GJ, Febbraio MA, Kraegen EW. Overexpression of carnitine palmitoyl-transferase-1 in skeletal muscle is sufficient to enhance fatty acid oxidation and improve high-fat diet-induced insulin resistance. *Diabetes.* 2009; 58:550-8.

Bruce KD, Byrne CD. The metabolic syndrome: common origins of a multifactorial disorder. *Postgrad Med J*. 2009; 85:614-21.

Brun P, Castagliuolo I, Di Leo V, Buda A, Pinzani M, Palù G, Martines D. Increased intestinal permeability in obese mice: new evidence in the pathogenesis of nonalcoholic steatohepatitis. *Am J Physiol Gastrointest Liver Physiol.* 2007; 292:G518-25.

Boutagy NE, McMillan RP, Frisard MI, Hulver MW. Metabolic endotoxemia with obesity: Is it real and is it relevant? *Biochimie.* 2016; 124:11-20.

Bowie A, O'Neill LA. Oxidative stress and nuclear factor-kappaB activation: a reassessment of the evidence in the light of recent discoveries. *Biochem Pharmacol.* 2000; 59:13-23.

Buettner R, Parhofer KG, Woenckhaus M, Wrede CE, Kunz-Schughart LA, Schölmerich J, Bollheimer LC. Defining high-fat-diet rat models: metabolic and molecular effects of different fat types. *J Mol Endocrinol.* 2006; 36: 485-501.

Burns KA, Vanden Heuvel JP. Modulation of PPAR activity via phosphorylation. *Biochim Biophys Acta.* 2007; 1771:952-60.

Campia U, Tesauro M, Cardillo C. Human obesity and endothelium-dependent responsiveness. *Br J Pharmacol*. 2012; 165:561-73.

Cani PD, Neyrinck AM, Fava F, Knauf C, Burcelin RG, Tuohy KM, Gibson GR, Delzenne NM. Selective increases of bifidobacteria in gut microflora improve high-fat diet-induced diabetes in mice through a mechanism associated with endotoxaemia *Diabetologia*. 2007; 50:2374-83.

Cani PD, Bibiloni R, Knauf C, Waget A, Neyrinck AM, Delzenne NM, Burcelin R. Changes in gut microbiota control metabolic endotoxemia-induced inflam- mation in high-fat diet-induced obesity and diabetes in mice. *Diabetes.* 2008; 57:1470-81.

Cani PD, Possemiers S, Van de Wiele T, Guiot Y, Everard A, Rottier O, Geurts L, Naslain D, Neyrinck A, Lambert DM, Muccioli GG, Delzenne NM. Changes in gut microbiota control inflammation in obese mice through a mechanism involving GLP-2-driven improvement of gut permeability. *Gut.* 2009; 58:1091-103.

Cariou B, Zaïr Y, Staels B, Bruckert E. Effects of the new dual PPAR α/δ agonist GFT505 on lipid and glucose homeostasis

in abdominally obese patients with combined dyslipidemia or impaired glucose metabolism. *Diabetes Care.* 2011; 34:2008-14.

Cariou B, Hanf R, Lambert-Porcheron S, Zaïr Y, Sauvinet V, Noël B, Flet L, Vidal H, Staels B, Laville M. Dual peroxisome proliferator activated receptor α/δ agonist GFT505 improves hepatic and peripheral insulin sensitivity in abdominally obese subjects*. Diabetes Care.* 2013; 36:2923-30.

Chan SH, Wu CA, Wu KL, Ho YH, Chang AY, Chan JY. Transcriptional upregulation of mitochondrial uncoupling protein 2 protects against oxidative stress-associated neurogenic hypertension. *Circ Res.* 2009; 105:886-96.

Chang KC, Liang JT, Tseng CD, Wu ET, Hsu KL, Wu MS, Lin YT, Tseng YZ. Aminoguanidine prevents fructose-induced deterioration in left ventricular-arterial coupling in Wistar rats. *Br J Pharmacol*. 2007; 151: 341-6.

Chavez JA, Summers SA. Characterizing the effects of saturated fatty acids on insulin signaling and ceramide and diacylglycerol accumulation in 3T3-L1 adipocytes and C2C12 myotubes. *Arch Biochem Biophys.* 2003; 419:101-9.

Cheang WS, Fang X, Tian XY. Pleiotropic effects of peroxisome proliferator-activated receptor γ and δ in vascular diseases. *Circ J.* 2013; 77:2664-71.

Cheang WS, Tian XY, Wong WT, Lau CW, Lee SS, Chen ZY, Yao X, Wang N, Huang Y. Metformin protects endothelial function in diet-induced obese mice by inhibition of endoplasmic reticulum stress through 5' adenosine monophosphate-activated protein kinase-peroxisome proliferator-activated receptor δ pathway. *Arterioscler Thromb Vasc Biol.* 2014; 34:830-6.

Chen H, Charlat O, Tartaglia LA, Woolf EA, Weng X, Ellis SJ, Lakey ND, Culpepper J, Moore KJ, Breitbart RE, Duyk GM, Tepper RI, Morgenstern JP. Evidence that the diabetes gene encodes the leptin receptor: identification of a mutation in the leptin receptor gene in db/db mice. *Cell.* 1996; 84:491-5.

Chen R, Liang F, Moriya J, Yamakawa J, Takahashi T, Shen L, Kanda T. Peroxisome proliferator-activated receptors (PPARs) and their agonists for hypertension and heart failure: are the reagents beneficial or harmful? *Int J Cardiol.* 2008; 130:131-9.

Chia PP, Fan SH, Say YH. Screening of Peroxisome Proliferator-Activated Receptors (PPARs) α, γ and α Gene Polymorphisms for Obesity and Metabolic Syndrome Association in the Multi-Ethnic Malaysian Population. *Ethn Dis.* 2015; 25:383-90.

Chiasson VL, Quinn MA, Young KJ, Mitchell BM. Protein kinase CbetaII-mediated phosphorylation of endothelial nitric oxide synthase threonine 495 mediates the endothelial dysfunction induced by FK506 (tacrolimus). *J Pharmacol Exp Ther.* 2011; 337:718-23.

Chistyakov DV, Aleshin S, Sergeeva MG, Reiser G. Regulation of peroxisome proliferator-activated receptor β/δ expression and activity levels by toll-like receptor agonists and MAP kinase inhibitors in rat astrocytes. *J Neurochem.* 2014; 130:563-74.

Chobanian AV, Bakris GL, Black HR, Cushman WC, Green LA, Izzo JL Jr, Jones DW, Materson BJ, Oparil S, Wright JT Jr, Roccella EJ; National Heart, Lung, and Blood Institute Joint National Committee on Prevention, Detection, Evaluation, and Treatment of High Blood Pressure.; National High Blood Pressure Education Program Coordinating Committee.. The Seventh Report of the Joint National Committee on Prevention, Detection, Evaluation, and Treatment of High Blood Pressure: the JNC 7 report. *JAMA.* 2003; 289:2560-72.

Choi YJ, Roberts BK, Wang X, Geaney JC, Naim S, Wojnoonski K, Karpf DB, Krauss RM. Effects of the PPAR-δ agonist MBX-8025 on atherogenic dyslipidemia. *Atherosclerosis.* 2012; 220:470-6.

Cimini A, Benedetti E, Cristiano L, Sebastiani P, D'Amico MA, D'Angelo B, Di Loreto S. Expression of peroxisome proliferator-activated receptors (PPARs) and retinoic acid receptors (RXRs) in rat cortical neurons. *Neuroscience.* 2005; 130:325-37.

Cines DB, Pollak ES, Buck CA, Loscalzo J, Zimmerman GA, McEver RP, Pober JS, Wick TM, Konkle BA, Schwartz BS, Barnathan ES, McCrae KR, Hug BA, Schmidt AM, Stern DM. Endothelial cells in physiology and in the pathophysiology of vascular disorders. *Blood.* 1998; 91:3527-61.

Cnop M, Igoillo-Esteve M, Cunha DA, Ladrière L, Eizirik DL. An update on lipotoxic endoplasmic reticulum stress in pancreatic beta-cells. *Biochem Soc Trans*. 2008; 36:909-15.

Coelho MS, Lopes KL, Freitas Rde A, de Oliveira-Sales EB, Bergasmaschi CT, Campos RR, Casarini DE, Carmona AK, Araújo Mda S, Heimann JC, Dolnikoff MS. High sucrose intake in rats is associated with increased ACE2 and angiotensin-(1-7) levels in the adipose tissue. *Regul Pept.* 2010; 162: 61-7.

Coletta C, Módis K, Oláh G, Brunyánszki A, Herzig DS, Sherwood ER, Ungvári Z, Szabo C. Endothelial dysfunction is a potential contributor to multiple organ failure and mortality in aged mice subjected to septic shock: preclinical studies in a murine model of cecal ligation and puncture. *Crit Care.* 2014; 18:511.

Coll T, Alvarez-Guardia D, Barroso E, Gómez-Foix AM, Palomer X, Laguna JC, Vázquez-Carrera M. Activation of peroxisome proliferator-activated recep-tor-{delta} by GW501516 prevents fatty acid-induced nuclear factor-{kappa}B activation and insulin resistance in skeletal muscle cells. *Endocrinology.* 2010; 151:1560-9.

Collins T, Read MA, Neish AS, Whitley MZ, Thanos D, Maniatis T. Transcriptional regulation of endothelial cell adhesion molecules: NF-kappa B and cytokine-inducible enhancers. *FASEB J.* 1995; 9:899-909.

Contreras C, Sánchez A, García-Sacristán A, Martínez MC, Andriantsitohaina R, Prieto D. Preserved insulin vasorelaxation and up-regulation of the Akt/eNOS pathway in coronary arteries from insulin resistant obese Zucker rats. *Atherosclerosis.* 2011; 217:331-9.

Cook S, Weitzman M, Auinger P, Nguyen M, Dietz WH. Prevalence of a metabolic

syndrome phenotype in adolescents: findings from the third National Health and Nutrition Examination Survey, 1988–1994. *Arch Pediatr Adolesc Med* 2003; 157:821–7.

Cornier MA, Dabelea D, Hernandez TL, Lindstrom RC, Steig AJ, Stob NR, Van Pelt RE, Wang H, Eckel RH. The metabolic syndrome. *Endocr Rev.* 2008; 29: 777-822.

Creager MA, Lüscher TF, Cosentino F, Beckman JA. Diabetes and vascular disease: pathophysiology, clinical consequences, and medical therapy: Part I. *Circulation.* 2003; 108:1527-32.

Dandona P, Aljada A, Chaudhuri A, Mohanty P, Garg R. Metabolic syndrome: a comprehensive perspective based on interactions between obesity, diabetes, and inflammation. *Circulation.* 2005; 111:1448-54.

Daynes RA, Jones DC. Emerging roles of PPARs in inflammation and immunity. *Nat Rev Immunol*. 2002; 2:748-59.

de Brito OM, Scorrano L. Mitofusin 2 tethers endoplasmic reticulum to mitochondria. *Nature.* 2008; 456: 605-10.

De Martin R, Hoeth M, Hofer-Warbinek R, Schmid JA. The transcription factor NF-kappa B and the regulation of vascular cell function. *Arterioscler Thromb Vasc Biol.* 2000; 20:E83-8.

Deji N, Kume S, Araki S, Soumura M, Sugimoto T, Isshiki K, Chin-Kanasaki M, Sakaguchi M, Koya D, Haneda M, Kashiwagi A, Uzu T. Structural and functional changes in the kidneys of high-fat diet-induced obese mice. *Am J Physiol Renal Physiol*. 2009; 296: F118-26.

Dhananjayan R, Koundinya KS, Malati T, Kutala VK. Endothelial Dysfunction in Type 2 Diabetes Mellitus. *Indian J Clin Biochem*. 2016; 31:372-9.

Dikalov SI, Nazarewicz RR, Bikineyeva A, Hilenski L, Lassègue B, Griendling KK, Harrison DG, Dikalova AE. Nox2-induced production of mitochondrial superoxide in angiotensin II-mediated endothelial oxidative stress and hypertension. *Antioxid Redox Signal.* 2014; 20:281-94.

Dikalova AE, Bikineyeva AT, Budzyn K, Nazarewicz RR, McCann L, Lewis W, Harrison DG, Dikalov SI. Therapeutic targeting of mitochondrial superoxide in hypertension. *Circ Res*. 2010; 107:106-16.

Ding G, Cheng L, Qin Q, Frontin S, Yang Q. PPARdelta modulates lipopolysaccharide-induced TNF alpha inflammation signaling in cultured cardiomyocytes. *J Mol Cell Cardiol.* 2006; 40:821-8.

Dong YF, Liu L, Kataoka K, Nakamura T, Fukuda M, Tokutomi Y, Nako H, Ogawa H, Kim-Mitsuyama S. Aliskiren prevents cardiovascular complications and pancreatic injury in a mouse model of obesity and type 2 diabetes. *Diabetologia.* 2010; 53: 180-91.

Doughan AK, Harrison DG, Dikalov SI. Molecular mechanisms of angiotensin II-mediated mitochondrial dysfunction: linking mitochondrial oxidative damage and vascular endothelial dysfunction. *Circ Res.* 2008; 102:488-96.

Dow CA, Lincenberg GM, Greiner JJ, Stauffer BL, DeSouza CA. Endothelial vasodilator function in normal-weight adults with metabolic syndrome. *Appl Physiol Nutr Metab.* 2016; 41:1013-1017.

Dreyer C, Krey G, Keller H, Givel F, Helftenbein G, Wahli W. Control of the peroxisomal beta-oxidation pathway by a novel family of nuclear hormone receptors. *Cell.* 1992; 68:879-87.

Du J, Fan LM, Mai A, Li JM. Crucial roles of Nox2-derived oxidative stress in deteriorating the function of insulin receptors and endothelium in dietary obesity of middle-aged mice. *Br J Pharmacol.* 2013; 170:1064-77.

Du X, Edelstein D, Obici S, Higham N, Zou MH, Brownlee M. Insulin resistance reduces arterial prostacyclin synthase and eNOS activities by increasing endothelial fatty acid oxidation. *J Clin Invest*. 2006; 116:1071-80.

Duan SZ, Usher MG, Mortensen RM. PPARs: the vasculature, inflammation and hypertension. *Curr Opin Nephrol Hypertens.* 2009; 18:128-33.

Duarte S, Arango D, Parihar A, Hamel P, Yasmeen R, Doseff AI. Apigenin protects endothelial cells from lipopolysaccharide (LPS)-induced inflammation by decreasing caspase-3 activation and modulating mitochondrial function. *Int J Mol Sci.* 2013; 14:17664-79.

Dubuc PU. The development of obesity, hyperinsulinemia, and hyperglycemia in ob/ob mice. *Metabolism.* 1976; 25:1567-74.

Duez H, Fruchart JC, Staels B. PPARS in inflammation, atherosclerosis and thrombosis. *J Cardiovasc Risk.* 2001; 8:187-94.

Eckel RH, Alberti KG, Grundy SM, Zimmet PZ. The metabolic syndrome. *Lancet.* 2010; 375:181-3.

Einhorn D, Reaven GM, Cobin RH, Ford E, Ganda OP, Handelsman Y, Hellman R, Jellinger PS, Kendall D, Krauss RM, Neufeld ND, Petak SM, Rodbard HW, Seibel JA, Smith DA, Wilson PW. American College of Endocrinology position statement on the insulin resistance syndrome. *Endocr Pract.* 2003; 9: 237-52.

Eizirik DL, Cardozo AK, Cnop M. The role for endoplasmic reticulum stress in diabetes mellitus. *Endocr Rev.* 2008; 29:42-61.

Emre Y, Hurtaud C, Nübel T, Criscuolo F, Ricquier D, Cassard-Doulcier AM. Mitochondria contribute to LPS-induced MAPK activation via uncoupling protein UCP2 in macrophages. *Biochem J.* 2007; 402: 271-8.

Endemann DH, Schiffrin EL. Endothelial dysfunction. *J Am Soc Nephrol.* 2004; 15:1983-92.

Enser M. Clearing-factor lipase in obese hyperglycaemic mice (ob-ob). *Biochem J.* 1972; 129: 447-53.

Erdei N, Tóth A, Pásztor ET, Papp Z, Edes I, Koller A, Bagi Z. High-fat diet-induced reduction in nitric oxide-dependent arteriolar dilation in rats: role of xanthine oxidase-derived superoxide anion. *Am J Physiol Heart Circ Physiol.* 2006; 291:H2107-15.

Esposito K, Marfella R, Ciotola M, Di Palo C, Giugliano F, Giugliano G, D'Armiento M, D'Andrea F, Giugliano D. Effect of a mediterranean-style diet on endothelial dysfunction and markers of vascular inflammation in the metabolic syndrome: a randomized trial. *JAMA.* 2004; 292:1440-6.

Feige JN, Gelman L, Michalik L, Desvergne B, Wahli W. From molecular action to physiological outputs: peroxisome proliferator-activated receptors are nuclear receptors at the crossroads of key cellular functions. *Prog Lipid Res*. 2006; 45:120-59.

Félétou M, Köhler R, Vanhoutte PM. Endothelium-derived vasoactive factors and hypertension: possible roles in pathogenesis and as treatment targets. *Curr Hypertens Rep.* 2010; 12:267-75.

Fernandes DC, Wosniak J Jr, Pescatore LA, Bertoline MA, Liberman M, Laurindo FR, Santos CX. Analysis of DHE-derived oxidation products by HPLC in the assessment of superoxide production and NADPH oxidase activity in vascular systems. *Am J Physiol Cell Physiol*. 2007; 292:C413-22.

Ford ES, Giles WH, Mokdad AH. Increasing prevalence of the metabolic syndrome among U.S. Adults. *Diabetes Care*. 2004; 27: 2444–9.

Forman BM, Chen J, Evans RM. Hypolipidemic drugs, polyunsaturated fatty acids and eicosanoids are ligands for peroxisome proliferator-activated receptors alpha and delta. *Proc Natl Acad Sci U S A*. 1997; 94:4312-7.

Frost RA, Nystrom GJ, Lang CH. Lipopolysaccharide regulates proinflammatory cytokine expression in mouse myoblasts and skeletal muscle. *Am J Physiol Regul Integr Comp Physiol.* 2002; 283:R698-709.

Galán M, Kassan M, Kadowitz PJ, Trebak M, Belmadani S, Matrougui K. Mechanism of endoplasmic reticulum stress-induced vascular endothelial dysfunction. *Biochim Biophys Acta.* 2014; 1843:1063-75.

Galatou E, Kelly T, Lazou A. The PPARβ/δ agonist GW0742 modulates signaling pathways associated with cardiac myocyte growth via a non-genomic redox mechanism. *Mol Cell Biochem.* 2014; 395:145-54.

Galisteo M, Duarte J, Zarzuelo A. Effects of dietary fibers on disturbances clustered in the metabolic syndrome. *J Nutr Biochem*. 2008; 19:71-84.

Ge F, Zhou S, Hu C, Lobdell H 4th, Berk PD. Insulin- and leptin-regulated fatty acid uptake plays a key causal role in hepatic steatosis in mice with intact leptin signaling but not in ob/ob or db/db mice. *Am J Physiol Gastrointest Liver Physiol.* 2010; 299: G855-66.

Gilde AJ, van der Lee KA, Willemsen PH, Chinetti G, van der Leij FR, van der Vusse GJ, Staels B, van Bilsen M. Peroxisome proliferator-activated receptor (PPAR) alpha and PPARbeta/delta, but not PPARgamma, modulate the expression of genes involved in cardiac lipid metabolism. *Circ Res.* 2003; 92:518-24.

Gómez-Guzmán M, Jiménez R, Sánchez M, Zarzuelo MJ, Galindo P, Quintela AM, López-Sepúlveda R, Romero M, Tamargo J, Vargas F, Pérez-Vizcaíno F, Duarte J.

Epicatechin lowers blood pressure, restores endothelial function, and decreases oxidative stress and endothelin-1 and NADPH oxidase activity in DOCA-salt hypertension. *Free Radic Biol Med.* 2012; 52:70-9.

Gómez-Guzmán M, Jiménez R, Romero M, Sánchez M, Zarzuelo MJ, Gómez-Morales M, O'Valle F, López-Farré AJ, Algieri F, Gálvez J, Pérez-Vizcaino F, Sabio JM, Duarte J. Chronic hydroxychloroquine improves endothelial dysfunction and protects kidney in a mouse model of systemic lupus erythematosus. *Hypertension.* 2014; 64:330-7.

Gonzalez IC, Lamar J, Iradier F, Xu Y, Winneroski LL, York J, Yumibe N, Zink R, Montrose-Rafizadeh C, Etgen GJ, Broderick CL, Oldham BA, Mantlo N. Design and synthesis of a novel class of dual PPARgamma/delta agonists. *Bioorg Med Chem Lett.* 2007; 17:1052-5.

Graham TL, Mookherjee C, Suckling KE, Palmer CN, Patel L. The PPAR delta agonist GW0742X reduces atherosclerosis in LDLR(-/-) mice. *Atherosclerosis.* 2005; 181:29-37.

Grarup N, Albrechtsen A, Ek J, Borch-Johnsen K, Jørgensen T, Schmitz O, Hansen T, Pedersen O. Variation in the peroxisome proliferator-activated receptor delta gene in relation to common metabolic traits in 7,495 middle-aged white people. *Diabetologia.* 2007; 50:1201-8.

Grewal AS, Beniwal M, Pandita D, Sekhon BS, Lather V. Recent Updates on Peroxisome Proliferator-Activated Receptor δ Agonists for the Treatment of Metabolic Syndrome. *Med Chem.* 2016; 12:3-21.

Griendling KK, Sorescu D, Lassègue B, Ushio-Fukai M. Modulation of protein kinase activity and gene expression by reactive oxygen species and their role in vascular physiology and pathophysiology. *Arterioscler Thromb Vasc Biol.* 2000; 20:2175-83.

Gruber HJ, Mayer C, Meinitzer A, Almer G, Horejsi R, Möller R, Pilz S, März W, Gasser R, Truschnig-Wilders M, Mangge H. Asymmetric dimethylarginine (ADMA) is tightly correlated with growth in juveniles without correlations to obesity related disorders. *Exp Clin Endocrinol Diabetes*. 2008; 116:520-4.

Grundy SM, Brewer HB Jr, Cleeman JI, Smith SC Jr, Lenfant C; National Heart, Lung, and Blood Institute; American Heart Association. Definition of metabolic syndrome: report of the National Heart, Lung, and Blood Institute/American Heart Association conference on scientific issues related to definition. *Arterioscler Thromb Vasc Biol.* 2004; 24: e13-8.

Grundy SM, Cleeman JI, Daniels SR, Donato KA, Eckel RH, Franklin BA, Gordon DJ, Krauss RM, Savage PJ, Smith SC Jr, Spertus JA, Costa F; American Heart Association; National Heart, Lung, and Blood Institute. Diagnosis and management of the metabolic syndrome: an American Heart Association/National Heart, Lung, and Blood Institute Scientific Statement. *Circulation*. 2005; 112:2735-52.

Grundy SM. Metabolic syndrome pandemic. *Arterioscler Thromb Vasc Biol*. 2008; 28:629-36.

Grundy SM. Pre-diabetes, metabolic syndrome, and cardiovascular risk. *J Am Coll Cardiol.* 2012; 59:635-43.

Grundy SM. Metabolic syndrome update. *Trends Cardiovasc Med.* 2016; 26: 364-73.

Guo WX, Yang QD, Liu YH, Xie XY, Wang-Miao, Niu RC. Palmitic and linoleic acids impair endothelial progenitor cells by inhibition of Akt/eNOS pathway. *Arch Med Res*. 2008; 39:434-42.

Gupta RA, Wang D, Katkuri S, Wang H, Dey SK, DuBois RN. Activation of nuclear hormone receptor peroxisome proliferator-activated receptor-delta accelerates intestinal adenoma growth. *Nat Med.* 2004; 10:245-7.

Gustot T, Lemmers A, Moreno C, Nagy N, Quertinmont E, Nicaise C, Franchimont D, Louis H, Devière J, Le Moine O. Differential liver sensitization to toll-like receptor pathways in mice with alcoholic fatty liver. *Hepatology*. 2006; 43:989-1000.

Hamblin M, Chang L, Fan Y, Zhang J, Chen YE. PPARs and the cardiovascular system. *Antioxid Redox Signal*. 2009; 11:1415-52.

Harrington LS, Moreno L, Reed A, Wort SJ, Desvergne B, Garland C, Zhao L, Mitchell JA. The PPARbeta/delta agonist GW0742 relaxes pulmonary vessels and limits right heart hypertrophy in rats with hypoxia-induced pulmonary hypertension. *PLoS One.* 2010; 5:e9526.

Harrington WW, S Britt C, G Wilson J, O Milliken N, G Binz J, C Lobe D, R Oliver W, C Lewis M, M Ignar D. The effect of PPAR alpha, PPAR delta, PPAR gamma, and PPARpan agonists on body weight, body mass, and serum lipid profiles in diet-induced obese AKR/J mice. *PPAR Res.* 2007; 2007:97125.

Haskova Z, Hoang B, Luo G, Morgan LA, Billin AN, Barone FC, Shearer BG, Barton ME, Kilgore KS. Modulation of LPS-induced pulmonary neutrophil infiltration and cytokine production by the selective PPARbeta/delta ligand GW0742. *Inflamm Res.* 2008; 57:314-21.

Héliès-Toussaint C, Gambert S, Roller P, Tricot S, Lacour B, Grynberg A. Lipid metabolism in human endothelial cells. *Biochim Biophys Acta*. 2006; 1761:765-74.

Hetz C, Martinon F, Rodriguez D, Glimcher LH. The unfolded protein response: integrating stress signals through the stress sensor IRE1α. *Physiol Rev*. 2011; 91: 1219-43.

Hotamisligil GS. Inflammation and metabolic disorders. *Nature.* 2006; 444:860-7**.**

Hotamisligil GS. Endoplasmic reticulum stress and the inflammatory basis of metabolic disease. *Cell*. 2010; 140: 900-17.

Hsu CL, Wu CH, Huang SL, Yen GC. Phenolic compounds rutin and o-coumaric acid ameliorate obesity induced by high-fat diet in rats. *J Agric Food Chem*. 2009; 57: 425-31.

Huang W, Metlakunta A, Dedousis N, Zhang P, Sipula I, Dube JJ, Scott DK, O'Doherty RM. Depletion of liver Kupffer cells prevents the development of diet-induced hepatic steatosis and insulin resistance. *Diabetes.* 2010; 59: 347-57.

Hummasti S, Hotamisligil GS. Endoplasmic reticulum stress and inflammation in obesity and diabetes. *Circ Res.* 2010; 107: 579-91.

Iglarz M, Touyz RM, Viel EC, Paradis P, Amiri F, Diep QN, Schiffrin EL. Peroxisome proliferator-activated receptor-alpha and receptor-gamma activators prevent cardiac fibrosis in mineralocorticoid-dependent hypertension. *Hypertension.* 2003; 42:737-43.

Inoguchi T, Li P, Umeda F, Yu HY, Kakimoto M, Imamura M, Aoki T, Etoh T, Hashimoto T, Naruse M, Sano H, Utsumi H, Nawata H. High glucose level and free fatty acid stimulate reactive oxygen species production through protein kinase C-dependent activation of NAD(P)H oxidase in cultured vascular cells. *Diabetes.* 2000; 49:1939-45.

Jang HJ, Ridgeway SD, Kim JA. Effects of the green tea polyphenol epigallocatechin-3-gallate on high-fat diet-induced insulin resistance and endothelial dysfunction. *Am J Physiol Endocrinol Metab*. 2013; 305:E1444-51.

Jay MA, Ren J. Peroxisome proliferator-activated receptor (PPAR) in metabolic syndrome and type 2 diabetes mellitus. *Curr Diabetes Rev.* 2007; 3:33-9.

Jericó C, Knobel H, Montero M, Ordoñez-Llanos J, Guelar A, Gimeno JL, Saballs P, López-Colomés JL, Pedro-Botet J. Metabolic syndrome among HIV-infected patients: prevalence, characteristics, and related factors. *Diabetes Care.* 2005; 28: 132-7.

Jiao P, Ma J, Feng B, Zhang H, Diehl JA, Chin YE, Yan W, Xu H. FFA-induced adipocyte inflammation and insulin resistance: involvement of ER stress and IKKβ pathways. *Obesity (Silver Spring).* 2011, 19: 483-91.

Jiménez R, Sánchez M, Zarzuelo MJ, Romero M, Quintela AM, López-Sepúlveda R, Galindo P, Gómez-Guzmán M, Haro JM, Zarzuelo A, Pérez-Vizcaíno F, Duarte J. Endothelium-dependent vasodilator effects of peroxisome proliferator-activated receptor beta agonists via the phosphatidyl-inositol-3 kinase-Akt pathway. *J Pharmacol Exp Ther.* 2010; 332:554-61.

Johnson AR, Milner JJ, Makowski L. The inflammation highway: metabolism accelerates inflammatory traffic in obesity. *Immunol Rev.* 2012; 249:218-38.

Kadowaki H, Nishitoh H. Signaling pathways from the endoplasmic reticulum and their roles in disease. *Genes (Basel*). 2013; 4: 306-33.

Kapoor A, Shintani Y, Collino M, Osuchowski MF, Busch D, Patel NS, Sepodes B, Castiglia S, Fantozzi R, Bishop-Bailey D, Mota-Filipe H, Yaqoob MM, Suzuki K, Bahrami S, Desvergne B, Mitchell JA, Thiemermann C. Protective role of peroxisome proliferator-activated receptor-β/δ in septic shock. *Am J Respir Crit Care Med.* 2010; 182:1506-15.

Kars M, Yang L, Gregor MF, Mohammed BS, Pietka TA, Finck BN, Patterson BW, Horton JD, Mittendorfer B, Hotamisligil GS, Klein S. Tauroursodeoxycholic acid may improve liver and muscle but not adipose tissue insulin sensitivity in obese men and women. *Diabetes*. 2010;59: 1899–905.

Kassan M, Galán M, Partyka M, Saifudeen Z, Henrion D, Trebak M, Matrougui K. Endoplasmic reticulum stress is involved in cardiac damage and vascular endothelial dysfunction in hypertensive mice. *Arterioscler Thromb Vasc Biol.* 2012; 32:1652-61.

Kaur J. A comprehensive review on metabolic syndrome. *Cardiol Res Pract*. 2014; 2014:943162.

Kawasaki N, Asada R, Saito A, Kanemoto S, Imaizumi K. Obesity-induced endoplasmic reticulum stress causes chronic inflammation in adipose tissue. *Sci Rep*. 2012; 2:799.

Kersten S, Wahli W. Peroxisome proliferator activated receptor agonists. *EXS*. 2000; 89:141-51.

Khan O, Riazi S, Hu X, Song J, Wade JB, Ecelbarger CA. Regulation of the renal thiazide-sensitive Na-Cl cotransporter, blood pressure, and natriuresis in obese Zucker rats treated with rosiglitazone. *Am J Physiol Renal Physiol.* 2005; 289:F442-50.

Khashab MA, Liangpunsakul S, Chalasani N. Nonalcoholic fatty liver disease as a component of the metabolic syndrome. *Curr Gastroenterol Rep.* 2008; 10: 73-80.

Khera A, Vega GL, Das SR, Ayers C, McGuire DK, Grundy SM, de Lemos JA. Sex differences in the relationship between C-reactive protein and body fat. *J Clin Endocrinol Metab.* 2009; 94:3251-8.

Kim F, Tysseling KA, Rice J, Pham M, Haji L, Gallis BM, Baas AS, Paramsothy P, Giachelli CM, Corson MA, Raines EW. Free fatty acid impairment of nitric oxide production in endothelial cells is mediated by IKKbeta. *Arterioscler Thromb Vasc Biol.* 2005; 25:989-94.

Kim F, Pham M, Luttrell I, Bannerman DD, Tupper J, Thaler J, Hawn TR, Raines EW, Schwartz MW. Toll-like receptor-4 mediates vascular inflammation and insulin resistance in diet-induced obesity. *Circ Res.* 2007; 100:1589-96

Kim F, Pham M, Maloney E, Rizzo NO, Morton GJ, Wisse BE, Kirk EA, Chait A, Schwartz MW. Vascular inflammation, insulin resistance, and reduced nitric oxide production precede the onset of peripheral insulin resistance. *Arterioscler Thromb Vasc Biol.* 2008; 28:1982-8.

Kim HJ, Ham SA, Kim MY, Hwang JS, Lee H, Kang ES, Yoo T, Woo IS, Yabe-Nishimura C, Paek KS, Kim JH, Seo HG. PPARδ coordinates angiotensin II-induced senescence in vascular smooth muscle cells through PTEN-mediated inhibition of superoxide generation. *J Biol Chem.* 2011a; 286:44585-93.

Kim HJ, Ham SA, Paek KS, Hwang JS, Jung SY, Kim MY, Jin H, Kang ES, Woo IS, Kim HJ, Lee JH, Chang KC, Han CW, Seo HG. Transcriptional up-regulation of antioxidant genes by PPARδ inhibits angiotensin II-induced premature senescence in vascular smooth muscle cells. *Biochem Biophys Res Commun.* 2011b; 406:564-9.

Kim JA, Montagnani M, Koh KK, Quon MJ. Reciprocal relationships between insulin resistance and endothelial dysfunction: molecular and pathophysiological mechanisms. *Circulation* 2006; 113:1888-904.

Kim SM, Rico CW, Lee SC, Kang MY. Modulatory Effect of Rice Bran and Phytic Acid on Glucose Metabolism in High Fat-Fed C57BL/6N Mice. *J Clin Biochem Nutr*. 2010; 47:12-7.

Kizaki T, Suzuki K, Hitomi Y, Taniguchi N, Saitoh D, Watanabe K, Onoé K, Day NK, Good RA, Ohno H. Uncoupling protein 2 plays an important role in nitric oxide production of lipopolysaccharide-stimulated macrophages. *Proc Natl Acad Sci USA.* 2002; 99:9392-7.

Kobayashi M, Inoue K, Warabi E, Minami T, Kodama T. A simple method of isolating mouse aortic endothelial cells. *J Atheroscler Thromb.*2005; 12:138-42.

Kobayasi R, Akamine EH, Davel AP, Rodrigues MA, Carvalho CR, Rossoni LV. Oxidative stress and inflammatory mediators contribute to endothelial dysfunction in high-fat diet-induced obesity in mice. *J Hypertens.* 2010; 28:2111-9.

Kojda G, Harrison D. Interactions between NO and reactive oxygen species: pathophysiological importance in atherosclerosis, hypertension, diabetes and heart failure. *Cardiovasc Res*. 1999; 43:562-71.

Kostapanos MS, Florentin M, Elisaf MS, Mikhailidis DP. Hemostatic factors and the metabolic syndrome. *Curr Vasc Pharmacol.* 2013; 11:880-905.

Kota BP, Huang TH, Roufogalis BD. An overview on biological mechanisms of PPARs. *Pharmacol Res.* 2005; 51:85-94.

Kraja AT, Province MA, Arnett D, Wagenknecht L, Tang W, Hopkins PN, Djoussé L, Borecki IB. Do inflammation and procoagulation biomarkers contribute to the metabolic syndrome cluster? *Nutr Metab (Lond).* 2007; 4:28.

Krauss S, Zhang CY, Lowell BB. The mitochondrial uncoupling-protein homologues. *Nat Rev Mol Cell Biol.* 2005; 6:248-61.

Kubota T, Kubota N, Kumagai H, Yamaguchi S, Kozono H, Takahashi T, Inoue M, Itoh S, Takamoto I, Sasako T, Kumagai K, Kawai T, Hashimoto S, Kobayashi T, Sato M, Tokuyama K, Nishimura S, Tsunoda M, Ide T, Murakami K, Yamazaki T, Ezaki O, Kawamura K, Masuda H, Moroi M, Sugi K, Oike Y, Shimokawa H, Yanagihara N, Tsutsui M, Terauchi Y, Tobe K, Nagai R, Kamata K, Inoue K, Kodama T, Ueki K, Kadowaki T. Impaired insulin signaling in endothelial cells reduces insulin-induced glucose uptake by skeletal muscle. *Cell Metab.* 2011; 13:294-307.

Kwaśniewska M, Kozińska J, Dziankowska-Zaborszczyk E, Kostka T, Jegier A, Rębowska E, Orczykowska M, Leszczyńska J, Drygas W. The impact of long-term changes in metabolic status on cardiovascular biomarkers and microvascular endothelial function in middle-aged men: a 25-year prospective study. *Diabetol Metab Syndr*. 2015; 7:81.

Lagou V, Scott RA, Manios Y, Chen TL, Wang G, Grammatikaki E, Kortsalioudaki C, Liarigkovinos T, Moschonis G, Roma-Giannikou E, Pitsiladis YP. Impact of peroxisome proliferator-activated receptors gamma and delta on adiposity in toddlers and preschoolers in the GENESIS Study. *Obesity (Silver Spring).* 2008; 16:913-8.

Laugerette F, Alligier M, Bastard JP, Drai J, Chanséaume E, Lambert-Porcheron S, Laville M, Morio B, Vidal H, Michalski MC. Overfeeding increases postprandial endotoxemia in men: Inflammatory outcome may depend on LPS transporters LBP and sCD14. *Mol Nutr Food Res.* 2014; 58:1513-8.

Laurindo FR, Fernandes DC, Santos CX. Assessment of superoxide production and NADPH oxidase activity by HPLC analysis of dihydroethidium oxidation products. *Methods Enzymol*. 2008; 441:237-60.

Lê KA, Tappy L. Metabolic effects of fructose. *Curr Opin Clin Nutr Metab Care.* 2006; 9:469-75.

Lee CH, Chawla A, Urbiztondo N, Liao D, Boisvert WA, Evans RM, Curtiss LK. Transcriptional repression of atherogenic inflammation: modulation by PPARdelta. *Science.* 2003; 302:453-7.

Lee CH, Olson P, Hevener A, Mehl I, Chong LW, Olefsky JM, Gonzalez FJ, Ham J, Kang H, Peters JM, Evans RM. PPARdelta regulates glucose metabolism and insulin sensitivity. *Proc Natl Acad Sci USA.* 2006; 103:3444-9.

Lee H, Ham SA, Kim MY, Kim JH, Paek KS, Kang ES, Kim HJ, Hwang JS, Yoo T, Park C, Kim JH, Lim DS, Han CW, Seo HG. Activation of PPARδ counteracts angiotensin II-induced ROS generation by inhibiting rac1 translocation in vascular smooth muscle cells. *Free Radic Res.* 2012; 46:912-9.

Lee KU, Lee IK, Han J, Song DK, Kim YM, Song HS, Kim HS, Lee WJ, Koh EH, Song KH, Han SM, Kim MS, Park IS, Park JY. Effects of recombinant adenovirus-mediated uncoupling protein 2 overexpression on endothelial function and apoptosis. *Circ Res.* 2005; 96:1200-7.

Lei F, Zhang XN, Wang W, Xing DM, Xie WD, Su H, Du LJ. Evidence of anti-obesity effects of the pomegranate leaf extract in high-fat diet induced obese mice. *Int J Obes (Lond).* 2007; 3: 1023-9.

Leibowitz MD, Fiévet C, Hennuyer N, Peinado-Onsurbe J, Duez H, Bergera J, Cullinan CA, Sparrow CP, Baffic J, Berger GD, Santini C, Marquis RW, Tolman RL, Smith RG, Moller DE, Auwerx J. Activation of PPARdelta alters lipid metabolism in db/db mice. *FEBS Lett.* 2000; 473:333-6.

Lenna S, Han R, Trojanowska M. Endoplasmic reticulum stress and endothelial dysfunction. *IUBMB Life*. 2014; 66:530-7.

Leo CH, Hart JL, Woodman OL. Impairment of both nitric oxide-mediated and EDHF-type relaxation in small mesenteric arteries from rats with streptozotocin-induced diabetes. *Br J Pharmacol*. 2011; 162:365-77.

Levin D, Bell S, Sund R, Hartikainen SA, Tuomilehto J, Pukkala E, Keskimäki I, Badrick E, Renehan AG, Buchan IE, Bowker SL, Minhas-Sandhu JK, Zafari Z, Marra C, Johnson JA, Stricker BH, Uitterlinden AG, Hofman A, Ruiter R, de Keyser CE, MacDonald TM, Wild SH, McKeigue PM, Colhoun HM; Scottish Diabetes Research Network Epidemiology Group.; Diabetes and Cancer Research Consortium.. Pioglitazone and bladder cancer risk: a multipopulation pooled,

cumulative exposure analysis. *Diabetologia*. 2015; 58:493-504.

Lewis JD, Habel LA, Quesenberry CP, Strom BL, Peng T, Hedderson MM, Ehrlich SF, Mamtani R, Bilker W, Vaughn DJ, Nessel L, Van Den Eeden SK, Ferrara A. Pioglitazone Use and Risk of Bladder Cancer and Other Common Cancers in Persons With Diabetes. *JAMA.* 2015; 314:265-77.

Li H, Forstermann U. Pharmacological prevention of eNOS uncoupling. *Curr Pharm Des.* 2014; 20:3595-606.

Liang CF, Liu JT, Wang Y, Xu A, Vanhoutte PM. Toll-like receptor 4 mutation protects obese mice against endothelial dysfunction by decreasing NADPH oxidase isoforms 1 and 4. *Arterioscler Thromb Vasc Biol*. 2013; 33:777-84.

Liao JK. Linking endothelial dysfunction with endothelial cell activation. *J Clin Invest.* 2013; 123:540-1.

Libby P, Ridker PM, Maseri A. Inflammation and atherosclerosis. *Circulation.* 2002; 105:1135-43.

Licata G, Argano C, Di Chiara T, Parrinello G, Scaglione R. Obesity: a main factor of metabolic syndrome? *Panminerva Med.* 2006; 48:77-85.

Lim JS, Mietus-Snyder M, Valente A, Schwarz JM, Lustig RH. The role of fructose in the pathogenesis of NAFLD and the metabolic syndrome. *Nat Rev Gastroenterol Hepatol*. 2010; 7: 251-64.

Lima VV, Giachini FR, Choi H, Carneiro FS, Carneiro ZN, Fortes ZB, Carvalho MH, Webb RC, Tostes RC. Impaired vasodilator activity in deoxycorticosterone acetate-salt hypertension is associated with increased protein O-GlcNAcylation. *Hypertension.* 2009; 53:166-74.

Liu G, Li X, Li Y, Tang X, Xu J, Li R, Hao P, Sun Y. PPARδ agonist GW501516 inhibits PDGF-stimulated pulmonary arterial smooth muscle cell function related to pathological vascular remodeling. *Biomed Res Int.* 2013;2013:903947.

Liu KG, Lambert MH, Leesnitzer LM, Oliver W Jr, Ott RJ, Plunket KD, Stuart LW, Brown PJ, Willson TM, Sternbach DD. Identification of a series of PPAR gamma/delta dual agonists via solid-phase parallel synthesis. *Bioorg Med Chem Lett.* 2001; 11:2959-62.

Liu Z, Jiang C, Zhang J, Liu B, Du Q. Resveratrol inhibits inflammation and ameliorates insulin resistant endothelial dysfunction via regulation of AMP-activated protein kinase and sirtuin 1 activities. *J Diabetes.* 2016; 8:324-35.

Lu Y, Qian L, Zhang Q, Chen B, Gui L, Huang D, Chen G, Chen L. Palmitate induces apoptosis in mouse aortic endothelial cells and endothelial dysfunction in mice fed high-calorie and high-cholesterol diets. *Life Sci*. 2013; 92:1165-73.

Lu YC, Yeh WC, Ohashi PS. LPS/TLR4 signal transduction pathway. *Cytokine.* 2008; 42:145-51.

Lumeng CN, Saltiel AR. Inflammatory links between obesity and metabolic disease. *J Clin Invest.* 2011; 121:2111-7.

Ma S, Ma L, Yang D, Luo Z, Hao X, Liu D, Zhu Z. Uncoupling protein 2 ablation exacerbates high-salt intake-induced vascular dysfunction. *Am J Hypertens.* 2010; 23:822-8.

Ma Y, Brewer JW, Diehl JA, Hendershot LM. Two distinct stress signaling pathways converge upon the CHOP promoter during the mammalian unfolded protein response. *J Mol Biol.* 2002; 318:1351-65.

Mackenzie LS, Lione L. Harnessing the benefits of PPARβ/δ agonists. *Life Sci.* 2013; 93:963-7.

Malhotra A, Kang BP, Cheung S, Opawumi D, Meggs LG. Angiotensin II promotes glucose-induced activation of cardiac protein kinase C isozymes and phosphorylation of troponin I. *Diabetes.* 2001; 50:1918-26.

Maloney E, Sweet IR, Hockenbery DM, Pham M, Rizzo NO, Tateya S, Handa P, Schwartz MW, Kim F. Activation of NF-kappaB by palmitate in endothelial cells: a key role for NADPH oxidase-derived superoxide in response to TLR4 activation. *Arterioscler Thromb Vasc Biol*. 2009; 29:1370-5.

Mandard S, Patsouris D. Nuclear control of the inflammatory response in mammals by peroxisome proliferator-activated receptors. *PPAR Res.* 2013; 2013:613864.

Mark AL, Shaffer RA, Correia ML, Morgan DA, Sigmund CD, Haynes WG. Contrasting blood pressure effects of obesity in leptin-deficient ob/ob mice and agouti yellow obese mice. *J Hypertens*. 1999; 17: 1949-53.

Martinez SC, Tanabe K, Cras-Méneur C, Abumrad NA, Bernal-Mizrachi E, Permutt MA. Inhibition of Foxo1 protects pancreatic islet beta-cells against fatty acid and endoplasmic reticulum stress-induced apoptosis. *Diabetes*. 2008; 57:846-59.

Massiera F, Barbry P, Guesnet P, Joly A, Luquet S, Moreilhon-Brest C, Mohsen-Kanson T, Amri EZ, Ailhaud G. A Western-like fat diet is sufficient to induce a gradual enhancement in fat mass over generations. *J Lipid Res.* 2010; 51:2352-61.

Matsuzawa Y, Funahashi T, Kihara S, Shimomura I. Adiponectin and metabolic syndrome. *Arterioscler Thromb Vasc Biol.* 2004; 24:29-33.

Mazzon E, Cuzzocrea S. Role of TNF-alpha in ileum tight junction alteration in mouse model of restraint stress. *Am J Physiol Gastrointest Liver Physiol*. 2008; 294:G1268-80.

McVeigh GE, Cohn JN. Endothelial dysfunction and the metabolic syndrome. *Curr Diab Rep*. 2003; 3:87-92.

Meigs JB, Wilson PW, Nathan DM, D'Agostino RB Sr, Williams K, Haffner SM. Prevalence and characteristics of the metabolic syndrome in the San Antonio Heart and Framingham Offspring Studies. *Diabetes.* 2003; 52:2160-7.

Meshkani R, Adeli K. Hepatic insulin resistance, metabolic syndrome and cardiovascular disease. *Clin Biochem*. 2009; 42:1331-46.

Miatello R, Vázquez M, Renna N, Cruzado M, Zumino AP, Risler N. Chronic administration of resveratrol prevents

biochemical cardiovascular changes in fructose-fed rats. *Am J Hypertens*. 2005; 18: 864-70.

Michalik L, Desvergne B, Wahli W. Peroxisome-proliferator-activated receptors and cancers: complex stories. *Nat Rev Cancer*. 2004; 4:61-70.

Minamiyama Y, Bito Y, Takemura S, Takahashi Y, Kodai S, Mizuguchi S, Nishikawa Y, Suehiro S, Okada S. Calorie restriction improves cardio-vascular risk factors via reduction of mitochondrial reactive oxygen species in type II diabetic rats. *J Pharmacol Exp Ther.* 2007; 320:535-43.

Mombouli JV, Vanhoutte PM. Endothelial dysfunction: from physiology to therapy. *J Mol Cell Cardiol*. 1999; 31:61-74.

Montagnani M, Ravichandran LV, Chen H, Esposito DL, Quon MJ. Insulin receptor substrate-1 and phosphoinositide-dependent kinase-1 are required for insulin-stimulated production of nitric oxide in endothelial cells. *Mol Endocrinol.* 2002; 16:1931-42.

Moraes LA, Swales KE, Wray JA, Damazo A, Gibbins JM, Warner TD, Bishop-Bailey D. Nongenomic signaling of the retinoid X receptor through binding and inhibiting Gq in human platelets. *Blood.* 2007; 109:3741-4.

Morse SA, Zhang R, Thakur V, Reisin E. Hypertension and the metabolic syndrome. *Am J Med Sci.* 2005; 330:303-10.

Mugabo Y, Mukaneza Y, Renier G. Palmitate induces C-reactive protein expression in human aortic endothelial cells. Relevance to fatty acid-induced endothelial dysfunction. *Metabolism.* 2011; 60:640-8.

Muñoz JP, Ivanova S, Sánchez-Wandelmer J, Martínez-Cristóbal P, Noguera E, Sancho A, Díaz-Ramos A, Hernández-Alvarez MI, Sebastián D, Mauvezin C, Palacín M, Zorzano A. Mfn2 modulates the UPR and mitochondrial function via repression of PERK. *EMBO J*. 2014; 32:2348-61.

Naruhn S, Meissner W, Adhikary T, Kaddatz K, Klein T, Watzer B, Müller-Brüsselbach S, Müller R. 15-hydroxyeicosatetraenoic acid is a preferential peroxisome proliferator-activated receptor beta/delta agonist. *Mol Pharmacol.* 2010; 77:171-84.

Naruse K, Rask-Madsen C, Takahara N, Ha SW, Suzuma K, Way KJ, Jacobs JR, Clermont AC, Ueki K, Ohshiro Y, Zhang J, Goldfine AB, King GL. Activation of vascular protein kinase C-beta inhibits Akt-dependent endothelial nitric oxide synthase function in obesity-associated insulin resistance. *Diabetes.* 2006; 55:691-8.

Nazarewicz RR, Dikalova AE, Bikineyeva A, Dikalov SI. Nox2 as a potential target of mitochondrial superoxide and its role in endothelial oxidative stress. *Am J Physiol Heart Circ Physiol.* 2013; 305:H1131-40.

Neels JG, Grimaldi PA. Physiological functions of peroxisome proliferator-activated receptor β. *Physiol Rev.* 2014; 94:795-858.

Nishikawa T, Araki E. Impact of mitochondrial ROS production in the pathogenesis of diabetes mellitus and its

complications. *Antioxid Redox Signal.* 2007; 9:343-53**.**

Noronha BT, Li JM, Wheatcroft SB, Shah AM, Kearney MT. Inducible nitric oxide synthase has divergent effects on vascular and metabolic function in obesity. *Diabetes.* 2005; 54:1082-9.

Oh YS, Lee YJ, Park EY, Jun HS. Interleukin-6 treatment induces beta-cell apoptosis via STAT-3-mediated nitric oxide production. *Diabetes Metab Res Rev*. 2011; 27:813-9.

Oishi Y, Manabe I, Tobe K, Ohsugi M, Kubota T, Fujiu K, Maemura K, Kubota N, Kadowaki T, Nagai R. SUMOylation of Krüppel-like transcription factor 5 acts as a molecular switch in transcriptional programs of lipid metabolism involving PPAR-delta. *Nat Med.* 2008; 14:656-66.

Oliver WR Jr, Shenk JL, Snaith MR, Russell CS, Plunket KD, Bodkin NL, Lewis MC, Winegar DA, Sznaidman ML, Lambert MH, Xu HE, Sternbach DD, Kliewer SA, Hansen BC, Willson TM. A selective peroxisome proliferator-activated receptor delta agonist promotes reverse cholesterol transport. *Proc Natl Acad Sci USA*. 2001; 98:5306-11.

Olson EJ, Pearce GL, Jones NP, Sprecher DL. Lipid effects of peroxisome proliferator-activated receptor-δ agonist GW501516 in subjects with low high-density lipoprotein cholesterol: characteristics of metabolic syndrome. *Arterioscler Thromb Vasc Biol.* 2012; 32:2289-94.

Ooi EM, Watts GF, Sprecher DL, Chan DC, Barrett PH. Mechanism of action of a peroxisome proliferator-activated receptor (PPAR)-delta agonist on lipoprotein metabolism in dyslipidemic subjects with central obesity. *J Clin Endocrinol Metab.* 2011; 96:E1568-76.

Oyekan A. PPARs and their effects on the cardiovascular system. *Clin Exp Hypertens.* 2011; 33:287-93.

Ozcan U, Cao Q, Yilmaz E, Lee AH, Iwakoshi NN, Ozdelen E, Tuncman G, Gorgun C, Glimcher LH, Hotamisligil GS. Endoplasmic reticulum stress links obesity, insulin action, and type 2 diabetes. *Science*. 2004; 306:457- 61.

Ozcan U, Yilmaz E, Ozcan L, Furuhashi M, Vaillancourt E, Smith RO, Gorgun CZ, Hotamisligil GS. Chemical chaperones reduce ER stress and restore glucose homeostasis in a mouse model of type 2 diabetes. *Science.* 2006; 313:1137- 40.

Palomer X, Capdevila-Busquets E, Botteri G, Salvadó L, Barroso E, Davidson MM, Michalik L, Wahli W, Vázquez-Carrera M. PPARβ/δ attenuates palmitate-induced endoplasmic reticulum stress and induces autophagic markers in human cardiac cells. *Int J Cardiol.* 2014; 174:110-8.

Panchal SK, Brown L. Rodent models for metabolic syndrome research*. J Biomed Biotechnol*. 2011; 2011:351982.

Pandian RP, Kutala VK, Liaugminas A, Parinandi NL, Kuppusamy P. Lipopolysaccharide-induced alterations in oxygen consumption and radical generation in endothelial cells. *Mol Cell Biochem.* 2005; 278:119-27.

Parker JL, Adams HR. Selective inhibition of endothelium-dependent vasodilator

capacity by Escherichia coli endotoxemia. *Circ Res.* 1993; 72:539-51.

Pastori D, Pignatelli P, Carnevale R, Violi F. Nox-2 up-regulation and platelet activation: Novel insights. *Prostaglandins Other Lipid Mediat.* 2015; 120:50-5.

Patel J, Iyer A, Brown L. Evaluation of the chronic complications of diabetes in a high fructose diet in rats. *Indian J Biochem Biophys*. 2009; 46:66-72.

Patel MS, Korotchkina LG. Regulation of the pyruvate dehydrogenase complex. *Biochem Soc Trans*. 2006; 34:217-22.

Peters JM, Gonzalez FJ, Müller R. Establishing the Role of PPARβ/δ in Carcinogenesis. *Trends Endocrinol Metab.* 2015; 26:595-607.

Pierce GL, Lesniewski LA, Lawson BR, Beske SD, Seals DR. Nuclear factor-{kappa}B activation contributes to vascular endothelial dysfunction via oxidative stress in overweight/obese middle-aged and older humans. *Circulation.* 2009; 119:1284-92.

Pierre N, Deldicque L, Barbé C, Naslain D, Cani PD, Francaux M. Toll-like receptor 4 knockout mice are protected against endoplasmic reticulum stress induced by a high-fat diet. *PLoS One.* 2013; 8:e65061.

Piqueras L, Reynolds AR, Hodivala-Dilke KM, Alfranca A, Redondo JM, Hatae T, Tanabe T, Warner TD, Bishop-Bailey D. Activation of PPARbeta/delta induces endothelial cell proliferation and angiogenesis. *Arterioscler Thromb Vasc Biol*.2007; 27:63-9.

Planavila A, Laguna JC, Vázquez-Carrera M. Nuclear factor-kappaB activation leads to down-regulation of fatty acid oxidation during cardiac hypertrophy. *J Biol Chem.* 2005; 280:17464-71.

Pollock CB, Rodriguez O, Martin PL, Albanese C, Li X, Kopelovich L, Glazer RI. Induction of metastatic gastric cancer by peroxisome proliferator-activated receptor δ activation. *PPAR Res.* 2010; 2010:571783.

Portaluppi F, Boari B, Manfredini R. Oxidative stress in essential hypertension. *Curr Pharm Des*. 2004; 10:1695-8.

Pothiwala P, Jain SK, Yaturu S. Metabolic syndrome and cancer. *Metab Syndr Relat Disord.* 2009; 7:279-88.

Prasad A, Quyyumi AA. Renin-angiotensin system and angiotensin receptor blockers in the metabolic syndrome. *Circulation.* 2004; 110:1507-12.

Prewitt RL, Rice DC, Dobrian AD. Adaptation of resistance arteries to increases in pressure. *Microcirculation.* 2002; 9:295-304.

Quintela AM, Jiménez R, Gómez-Guzmán M, Zarzuelo MJ, Galindo P, Sánchez M, Vargas F, Cogolludo A, Tamargo J, Pérez-Vizcaíno F, Duarte J. Activation of peroxisome proliferator-activated receptor-β/-δ (PPARβ/δ) prevents endothelial dysfunction in type 1 diabetic rats. *Free Radic Biol Med.* 2012; 53:730-41.

Quintela AM, Jiménez R, Piqueras L, Gómez-Guzmán M, Haro J, Zarzuelo MJ, Cogolludo A, Sanz MJ, Toral M, Romero M, Pérez-Vizcaíno F, Duarte J. PPARβ activation restores the high glucose-

induced impairment of insulin signalling in endothelial cells. *Br J Pharmacol.* 2014; 171:3089-102.

Quiñones MJ, Nicholas SB, Lyon CJ. Insulin resistance and the endothelium. *Curr Diab Rep.* 2005; 5:246-53.

Quyyumi AA. Endothelial function in health and disease: new insights into the genesis of cardiovascular disease. *Am J Med.* 1998; 105:32S-39S.

Rafikov R, Fonseca FV, Kumar S, Pardo D, Darragh C, Elms S, Fulton D, Black SM. eNOS activation and NO function: structural motifs responsible for the posttranslational control of endothelial nitric oxide synthase activity. *J Endocrinol.* 2011; 210:271-84.

Rainbolt TK, Saunders JM, Wiseman RL. Stress-responsive regulation of mitochondria through the ER unfolded protein response. *Trends Endocrinol Metab.* 2014; 25:528-37.

Ramachandran U, Kumar R, Mittal A. Fine tuning of PPAR ligands for type 2 diabetes and metabolic syndrome. *Mini Rev Med Chem*. 2006; 6:563-73.

Ratziu V, Harrison SA, Francque S, Bedossa P, Lehert P, Serfaty L, Romero-Gomez M, Boursier J, Abdelmalek M, Caldwell S, Drenth J, Anstee QM, Hum D, Hanf R, Roudot A, Megnien S, Staels B, Sanyal A; GOLDEN-505 Investigator Study Group. Elafibranor, an Agonist of the Peroxisome Proliferator-Activated Receptor-α and -δ, Induces Resolution of Nonalcoholic Steatohepatitis Without Fibrosis Worsening. *Gastroenterology.* 2016; 150:1147-1159.

Rieck M, Wedeken L, Müller-Brüsselbach S, Meissner W, Müller R. Expression level and agonist-binding affect the turnover, ubiquitination and complex formation of peroxisome proliferator activated receptor beta. *FEBS J*. 2007; 274:5068-76.

Rieusset J. Contribution of mitochondria and endoplasmic reticulum dysfunction in insulin resistance: Distinct or interrelated roles? *Diabetes Metab*. 2015; 41:358-68.

Risérus U, Sprecher D, Johnson T, Olson E, Hirschberg S, Liu A, Fang Z, Hegde P, Richards D, Sarov-Blat L, Strum JC, Basu S, Cheeseman J, Fielding BA, Humphreys SM, Danoff T, Moore NR, Murgatroyd P, O'Rahilly S, Sutton P, Willson T, Hassall D, Frayn KN, Karpe F. Activation of peroxisome proliferator-activated receptor (PPAR) delta promotes reversal of multiple metabolic abnormalities, reduces oxidative stress, and increases fatty acid oxidation in moderately obese men. *Diabetes.* 2008; 57:332-9.

Rival Y, Benéteau N, Taillandier T, Pezet M, Dupont-Passelaigue E, Patoiseau JF, Junquéro D, Colpaert FC, Delhon A. PPARalpha and PPARdelta activators inhibit cytokine-induced nuclear translocation of NF-kappaB and expression of VCAM-1 in EAhy926 endothelial cells. *Eur J Pharmacol*. 2002; 435:143-51.

Roberts CK, Vaziri ND, Wang XQ, Barnard RJ. Enhanced NO inactivation and hypertension induced by a high-fat, refined-carbohydrate diet. *Hypertension.* 2000; 36:423-9.

Roberts CK, Barnard RJ, Sindhu RK, Jurczak M, Ehdaie A, Vaziri ND. A high-fat, refined-carbohydrate diet induces

endothelial dysfunction and oxidant/antioxidant imbalance and depresses NOS protein expression. *J Appl Physiol (1985).* 2005; 98:203-10.

Roberts CK, Barnard RJ, Sindhu RK, Jurczak M, Ehdaie A, Vaziri ND. Oxidative stress and dysregulation of NAD(P)H oxidase and antioxidant enzymes in diet-induced metabolic syndrome. *Metabolism.* 2006; 55:928-34.

Rodríguez-Calvo R, Serrano L, Coll T, Moullan N, Sánchez RM, Merlos M, Palomer X, Laguna JC, Michalik L, Wahli W, Vázquez-Carrera M. Activation of peroxisome proliferator-activated receptor beta/delta inhibits lipopolysaccharide-induced cytokine production in adipocytes by lowering nuclear factor-kappaB activity via extracellular signal-related kinase 1/2. *Diabetes*. 2008; 57:2149-57.

Romero M, Jiménez R, Toral M, León Gómez E, Gómez-Gúzman M, Sánchez M, Zarzuelo MJ, Rodríguez-Gómez I, Rath G, Tamargo J, Pérez-Vizcaíno F, Dessy C, Duarte J. Vascular and Central Activation of Peroxisome Proliferator-Activated Receptor-β Attenuates Angiotensin II-Induced Hypertension: Role of RGS-5. *J Pharmacol Exp Ther.* 2016; 358:151-63.

Sahai A, Malladi P, Pan X, Paul R, Melin-Aldana H, Green RM, Whitington PF. Obese and diabetic db/db mice develop marked liver fibrosis in a model of nonalcoholic steatohepatitis: role of short-form leptin receptors and osteopontin. *Am J Physiol Gastrointest Liver Physiol.* 2004; 287: G1035-43.

Salvadó L, Barroso E, Gómez-Foix AM, Palomer X, Michalik L, Wahli W, Vázquez-Carrera M. PPARβ/δ prevents endoplasmic reticulum stress-associated inflammation and insulin resistance in skeletal muscle cells through an AMPK-dependent mechanism. *Diabetologia.* 2014; 57:2126-35.

Salvadó L, Palomer X, Barroso E, Vázquez-Carrera M. Targeting endoplasmic reticulum stress in insulin resistance. *Trends Endocrinol Metab.* 2015; 26: 438-48.

Samad F, Ruf W. Inflammation, obesity, and thrombosis. *Blood.* 2013; 122:3415-22.

Sanchez M, Lodi F, Vera R, Villar IC, Cogolludo A, Jimenez R, Moreno L, Romero M, Tamargo J, Perez-Vizcaino F, Duarte J. Quercetin and isorhamnetin prevent endothelial dysfunction, superoxide production, and overexpression of p47phox induced by angiotensin II in rat aorta. *J Nutr.* 2007; 137:910-5.

Sanchez-Siles AA, Ishimura N, Rumi MA, Tamagawa Y, Ito S, Ishihara S, Nabika T, Kinoshita Y. Administration of PPARβ/δ agonist reduces copper-induced liver damage in mice: possible implications in clinical practice. *J Clin Biochem Nutr.* 2011; 49:42-9.

Sansbury BE, Cummins TD, Tang Y, Hellmann J, Holden CR, Harbeson MA, Chen Y, Patel RP, Spite M, Bhatnagar A, Hill BG. Overexpression of endothelial nitric oxide synthase prevents diet-induced obesity and regulates adipocyte phenotype. *Circ Res.* 2012; 111:1176-89.

Santos M, Shah AM. Alterations in cardiac structure and function in hypertension. *Curr Hypertens Rep.* 2014; 16:428.

Santuré M, Pitre M, Marette A, Deshaies Y, Lemieux C, Larivière R, Nadeau A, Bachelard H. Induction of insulin resistance by high-sucrose feeding does not raise mean arterial blood pressure but impairs haemodynamic responses to insulin in rats. *Br J Pharmacol*. 2002; 137: 185-96.

Scheuner D, Song B, McEwen E, Liu C, Laybutt R, Gillespie P, Saunders T, Bonner-Weir S, Kaufman RJ. Translational control is required for the unfolded protein response and in vivo glucose homeostasis. *Mol Cell.* 2001; 7:1165–76.

Schiffrin EL, Amiri F, Benkirane K, Iglarz M, Diep QN. Peroxisome proliferator-activated receptors: vascular and cardiac effects in hypertension. *Hypertension*. 2003; 42:664-8.

Sebastián D, Herrero L, Serra D, Asins G, Hegardt FG. CPT I overexpression protects L6E9 muscle cells from fatty acid-induced insulin resistance. *Am J Physiol Endocrinol Metab.* 2007; 292:E677-86.

Sebastián D, Hernández-Alvarez MI, Segalés J, Sorianello E, Muñoz JP, Sala D, Waget A, Liesa M, Paz JC, Gopalacharyulu P, Orešič M, Pich S, Burcelin R, Palacín M, Zorzano A. Mitofusin 2 (Mfn2) links mitochondrial and endoplasmic reticulum function with insulin signaling and is essential for normal glucose homeostasis. *Proc Natl Acad Sci USA.* 2012; 109:5523-8.

Schinzari F, Iantorno M, Campia U, Mores N, Rovella V, Tesauro M, Di Daniele N, Cardillo C. Vasodilator responses and endothelin-dependent vasoconstriction in metabolically healthy obesity and the metabolic syndrome. *Am J Physiol Endocrinol Metab.* 2015; 309:E787-92.

Shapiro A, Mu W, Roncal C, Cheng KY, Johnson RJ, Scarpace PJ. Fructose-induced leptin resistance exacerbates weight gain in response to subsequent high-fat feeding. *Am J Physiol Regul Integr Comp Physiol*. 2008; 295: R1370-5.

Sharma N, Okere IC, Barrows BR, Lei B, Duda MK, Yuan CL, Previs SF, Sharov VG, Azimzadeh AM, Ernsberger P, Hoit BD, Sabbah H, Stanley WC. High-sugar diets increase cardiac dysfunction and mortality in hypertension compared to low-carbohydrate or high-starch diets. *J Hypertens.* 2008; 26: 1402-10.

Sharma NK, Das SK, Mondal AK, Hackney OG, Chu WS, Kern PA, Rasouli N, Spencer HJ, Yao-Borengasser A, Elbein SC. Endoplasmic reticulum stress markers are associated with obesity in nondiabetic subjects. *J Clin Endocrinol Metab.* 2008; 93:4532–541.

Shearer BG, Billin AN. The next generation of PPAR drugs: do we have the tools to find them? *Biochim Biophys Acta.* 2007; 1771:1082–93.

Shen KP, Lin HL, Chang WT, An LM, Chen IJ, Wu BN. Suppression of inflammatory response and endothelial nitric oxide synthase downregulation in hyperlipidaemic C57BL/6J mice by eugenosedin-A. *J Pharm Pharmacol.* 2011; 63:860-8.

Shi H, Kokoeva MV, Inouye K, Tzameli I, Yin H, Flier JS. TLR4 links innate immunity and fatty acid-induced insulin resistance. *J Clin Invest.* 2006; 116:3015-25.

Shi Y, Vanhoutte PM. Oxidative stress and COX cause hyper-responsiveness in vascular smooth muscle of the femoral

artery from diabetic rats. *Br J Pharmacol.* 2008; 154:639-51.

Shiba T, Inoguchi T, Sportsman JR, Heath WF, Bursell S, King GL. Correlation of diacylglycerol level and protein kinase C activity in rat retina to retinal circulation. *Am J Physiol.* 1993; 265:E783-93.

Shimasaki Y, Pan N, Messina LM, Li C, Chen K, Liu L, Cooper MP, Vita JA, Keaney JF Jr. Uncoupling protein 2 impacts endothelial phenotype via p53-mediated control of mitochondrial dynamics. *Circ Res.* 2013; 113:891-901.

Silver AE, Beske SD, Christou DD, Donato AJ, Moreau KL, Eskurza I, Gates PE, Seals DR. Overweight and obese humans demonstrate increased vascular endothelial NAD(P)H oxidase-p47(phox) expression and evidence of endothelial oxidative stress. *Circulation.* 2007; 115:627-37.

Skogsberg J, McMahon AD, Karpe F, Hamsten A, Packard CJ, Ehrenborg E; West of Scotland Coronary Prevention Study. Peroxisome proliferator activated receptor delta genotype in relation to cardiovascular risk factors and risk of coronary heart disease in hypercholesterolaemic men. *J Intern Med.* 2003; 254:597-604.

Smeets PJ, Teunissen BE, Willemsen PH, van Nieuwenhoven FA, Brouns AE, Janssen BJ, Cleutjens JP, Staels B, van der Vusse GJ, van Bilsen M. Cardiac hypertrophy is enhanced in PPAR alpha-/- mice in response to chronic pressure overload. *Cardiovasc Res*. 2008; 78: 79-89.

Somers MJ, Burchfield JS, Harrison DG. Evidence for a NADH/NADPH oxidase in human umbilical vein endothelial cells using electron spin resonance, *Antioxid Redox Signal*. 2000; 2:779-87.

Song MJ, Kim KH, Yoon JM, Kim JB. Activation of Toll-like receptor 4 is associated with insulin resistance in adipocytes. *Biochem Biophys Res Commun.* 2006; 346:739-45.

Sprecher DL. Lipids, lipoproteins, and peroxisome proliferator activated receptor-delta. *Am J Cardiol.* 2007; 100:n20-4.

Steinberg HO, Paradisi G, Hook G, Crowder K, Cronin J, Baron AD. Free fatty acid elevation impairs insulin-mediated vasodilation and nitric oxide production. *Diabetes.* 2000; 49:1231-8.

Sutherland LN, Capozzi LC, Turchinsky NJ, Bell RC, Wright DC. Time course of high-fat diet-induced reductions in adipose tissue mitochondrial proteins: potential mechanisms and the relationship to glucose intolerance. *Am J Physiol Endocrinol Metab.* 2008; 295: E1076-83.

Symons JD, McMillin SL, Riehle C, Tanner J, Palionyte M, Hillas E, Jones D, Cooksey RC, Birnbaum MJ, McClain DA, Zhang QJ, Gale D, Wilson LJ, Abel ED. Contribution of insulin and Akt1 signaling to endothelial nitric oxide synthase in the regulation of endothelial function and blood pressure. *Circ Res.* 2009; 104:1085-94.

Szmitko PE, Wang CH, Weisel RD, de Almeida JR, Anderson TJ, Verma S. New markers of inflammation and endothelial cell activation: Part I. *Circulation*. 2003;108:1917-23.

Takada I, Yu RT, Xu HE, Lambert MH, Montana VG, Kliewer SA, Evans RM, Umesono K. Alteration of a single amino acid in peroxisome proliferator-activated receptor-alpha (PPAR alpha) generates a PPAR delta phenotype. *Mol Endocrinol.* 2000; 14:733-40**.**

Takata Y, Liu J, Yin F, Collins AR, Lyon CJ, Lee CH, Atkins AR, Downes M, Barish GD, Evans RM, Hsueh WA, Tangirala RK. PPAR delta-mediated antiinflammatory mechanisms inhibit angiotensin II-accelerated atheroscle- rosis. *Proc Natl Acad Sci USA.* 2008; 105:4277-82.

Tam CS, Viardot A, Clément K, Tordjman J, Tonks K, Greenfield JR, Campbell LV, Samocha-Bonet D, Heilbronn LK. Short-term overfeeding may induce peripheral insulin resistance without altering subcutaneous adipose tissue macrophages in humans. *Diabetes.* 2010; 59:2164-70.

Tanaka T, Yamamoto J, Iwasaki S, Asaba H, Hamura H, Ikeda Y, Watanabe M, Magoori K, Ioka RX, Tachibana K, Watanabe Y, Uchiyama Y, Sumi K, Iguchi H, Ito S, Doi T, Hamakubo T, Naito M, Auwerx J, Yanagisawa M, Kodama T, Sakai J. Activation of peroxisome proliferator-activated receptor delta induces fatty acid beta-oxidation in skeletal muscle and attenuates metabolic syndrome. *Proc Natl Acad Sci USA.* 2003; 100:15924-9.

Tappy L, Lê KA. Metabolic effects of fructose and the worldwide increase in obesity. *Physiol Rev.* 2010; 90: 23-46

Tenenbaum A, Motro M, Fisman EZ, Adler Y, Shemesh J, Tanne D, Leor J, Boyko V, Schwammenthal E, Behar S. Effect of bezafibrate on incidence of type 2 diabetes mellitus in obese patients. *Eur Heart J.* 2005a; 26:2032-8.

Tenenbaum A, Motro M, Fisman EZ, Tanne D, Boyko V, Behar S. Bezafibrate for the secondary prevention of myocardial infarction in patients with metabolic syndrome. *Arch Intern Med*. 2005b; 165:1154-60.

Terasaka N, Yu S, Yvan-Charvet L, Wang N, Mzhavia N, Langlois R, Pagler T, Li R, Welch CL, Goldberg IJ, Tall AR. ABCG1 and HDL protect against endothelial dysfunction in mice fed a high-cholesterol diet. *J Clin Invest*. 2008; 118:3701-13.

Terasaka N, Westerterp M, Koetsveld J, Fernández-Hernando C, Yvan-Charvet L, Wang N, Sessa WC, Tall AR. ATP-binding cassette transporter G1 and high-density lipoprotein promote endothelial NO synthesis through a decrease in the interaction of caveolin-1 and endothelial NO synthase. *Arterioscler Thromb Vasc Biol.* 2010; 30:2219-25.

Teunissen BE, Smeets PJ, Willemsen PH, De Windt LJ, Van der Vusse GJ, Van Bilsen M. Activation of PPARdelta inhibits cardiac fibroblast proliferation and the transdifferentiation into myofibroblasts. *Cardiovasc Res.* 2007; 75:519-29.

Thorp E, Li G, Seimon TA, Kuriakose G, Ron D, Tabas I. Reduced apoptosis and plaque necrosis in advanced atherosclerotic lesions of Apoe-/- and Ldlr-/- mice lacking CHOP. *Cell Metab.* 2009; 9:474-81.

Tian XY, Wong WT, Wang N, Lu Y, Cheang WS, Liu J, Liu L, Liu Y, Lee SS, Chen ZY, Cooke JP, Yao X, Huang Y. PPARδ activation protects endothelial

function in diabetic mice. *Diabetes.* 2012a; 61:3285-93.

Tian XY, Wong WT, Xu A, Lu Y, Zhang Y, Wang L, Cheang WS, Wang Y, Yao X, Huang Y. Uncoupling protein-2 protects endothelial function in diet-induced obese mice. *Circ Res.* 2012b; 110:1211-6.

Toral M, Gómez-Guzmán M, Jiménez R, Romero M, Sánchez M, Utrilla MP, Garrido-Mesa N, Rodríguez-Cabezas ME, Olivares M, Gálvez J, Duarte J. The probiotic Lactobacillus coryniformis CECT5711 reduces the vascular pro-oxidant and pro-inflammatory status in obese mice*. Clin Sci (Lond).* 2014; 127:33-45.

Tran LT, Yuen VG, McNeill JH. The fructose-fed rat: a review on the mechanisms of fructose-induced insulin resistance and hypertension. *Mol Cell Biochem*. 2009; 332: 145-59.

Tschudi MR, Mesaros S, Lüscher TF, Malinski T. Direct in situ measurement of nitric oxide in mesenteric resistance arteries. Increased decomposition by superoxide in hypertension. *Hypertension.* 1996; 27:32-5.

Tuncman G, Hirosumi J, Solinas G, Chang L, Karin M, Hotamisligil GS. Functional in vivo interactions between JNK1 and JNK2 isoforms in obesity and insulin resistance. *Proc Natl Acad Sci USA.* 2006; 103:10741-6.

Turnbaugh PJ, Ley RE, Mahowald MA, Magrini V, Mardis ER, Gordon JI. An obesity-associated gut microbiome with increased capacity for energy harvest. *Nature*. 2006; 444:1027-31.

Turnbaugh PJ, Hamady M, Yatsunenko T, Cantarel BL, Duncan A, Ley RE, Sogin ML, Jones WJ, Roe BA, Affourtit JP, Egholm M, Henrissat B, Heath AC, Knight R, Gordon JI. A core gut microbiome in obese and lean twins. *Nature*. 2009; 457:480-4.

Usuda D, Kanda T. Peroxisome proliferator-activated receptors for hypertension. *World J Cardiol.* 2014; 6:744-54.

Van den Bergh A, Vanderper A, Vangheluwe P, Desjardins F, Nevelsteen I, Verreth W, Wuytack F, Holvoet P, Flameng W, Balligand JL, Herijgers P. Dyslipidaemia in type II diabetic mice does not aggravate contractile impairment but increases ventricular stiffness. *Cardiovasc Res*. 2008; 77:371-9.

Vanhoutte PM, Miller VM. Heterogeneity of endothelium dependent responses in mammalian blood vessels. *J Cardiovasc Pharmacol.* 1985;7 Suppl 3:S12-23.

Vanhoutte PM, Shimokawa H, Tang EH, Feletou M. Endothelial dysfunction and vascular disease. *Acta Physiol (Oxf).* 2009; 196:193-222.

Vázquez-Carrera M. Unraveling the Effects of PPARβ/δ on Insulin Resistance and Cardiovascular Disease. *Trends Endocrinol Metab.* 2016; 27:319-34.

Vila E, Salaices M. Cytokines and vascular reactivity in resistance arteries. *Am J Physiol Heart Circ Physiol.* 2005; 288:H1016-21.

Vogel RA, Corretti MC, Plotnick GD. Effect of a single high-fat meal on endothelial

function in healthy subjects. *Am J Cardiol*. 1997; 79:350-4.

Wadosky KM, Willis MS. The story so far: post-translational regulation of peroxisome proliferator-activated receptors by ubiquitination and SUMOylation. *Am J Physiol Heart Circ Physiol.* 2012; 302:H515-26.

Wagner N, Jehl-Piétri C, Lopez P, Murdaca J, Giordano C, Schwartz C, Gounon P, Hatem SN, Grimaldi P, Wagner KD. Peroxisome proliferator-activated receptor beta stimulation induces rapid cardiac growth and angiogenesis via direct activation of calcineurin. *Cardiovasc Res.* 2009; 83:61-71.

Wallace JM, Schwarz M, Coward P, Houze J, Sawyer JK, Kelley KL, Chai A, Rudel LL. Effects of peroxisome proliferator-activated receptor alpha/ delta agonists on HDL-cholesterol in vervet monkeys. *J Lipid Res.* 2005; 46:1009-16.

Wan J, Jiang L, Lü Q, Ke L, Li X, Tong N. Activation of PPARdelta up-regulates fatty acid oxidation and energy uncoupling genes of mitochondria and reduces palmitate-induced apoptosis in pancreatic beta-cells. *Biochem Biophys Res Commun.* 2010; 391: 1567-72.

Wang Q, Cheng XL, Zhang DY, Gao XJ, Zhou L, Qin XY, Xie GY, Liu K, Qin Y, Liu BL, Qin MJ. Tectorigenin attenuates palmitate-induced endothelial insulin resistance via targeting ROS-associated inflammation and IRS-1 pathway. *PLoS One.* 2013; 8:e66417.

Wang Y, Biswas G, Prabu SK, Avadhani NG. Modulation of mitochondrial metabolic function by phorbol 12-myristate 13-acetate through increased mitochondrial translocation of protein kinase Calpha in C2C12 myocytes. *Biochem Pharmacol.* 2006; 72:881-92.

Wang YX, Lee CH, Tiep S, Yu RT, Ham J, Kang H, Evans RM. Peroxisome-proliferator-activated receptor delta activates fat metabolism to prevent obesity. *Cell.* 2003; 113:159-70.

Watt MJ, Southgate RJ, Holmes AG, Febbraio MA. Suppression of plasma free fatty acids upregulates peroxisome proliferator-activated receptor (PPAR) alpha and delta and PPAR coactivator 1alpha in human skeletal muscle, but not lipid regulatory genes. *J Mol Endocrinol.* 2004; 33:533-44.

Weaver JR, Taylor-Fishwick DA. Regulation of NOX-1 expression in beta cells: a positive feedback loop involving the Src-kinase signaling pathway. *Mol Cell Endocrinol*. 2013; 369:35-41.

Weisberg SP, Hunter D, Huber R, Lemieux J, Slaymaker S, Vaddi K, Charo I, Leibel RL, Ferrante AW Jr. CCR2 modulates inflammatory and metabolic effects of high-fat feeding. *J Clin Invest.* 2006; 116:115-24.

Weiss R, Dziura J, Burgert TS, Tamborlane WV, Taksali SE, Yeckel CW, Allen K, Lopes M, Savoye M, Morrison J, Sherwin RS, Caprio S. Obesity and the metabolic syndrome in children and adolescents. *N Engl J Med*. 2004; 350:2362-74.

Wieser V, Moschen AR, Tilg H. Inflammation, cytokines and insulin resistance: a clinical perspective. *Arch Immunol Ther Exp.* 2013; 61:119-25.

Wigg SJ, Tare M, Tonta MA, O'Brien RC, Meredith IT, Parkington HC. Comparison of effects of diabetes mellitus on an EDHF-dependent and an EDHF-independent artery. *Am J Physiol Heart Circ Physiol*. 2001; 281:H232-40.

Winzell MS, Wulff EM, Olsen GS, Sauerberg P, Gotfredsen CF, Ahrén B. Improved insulin sensitivity and islet function after PPARdelta activation in diabetic db/db mice. *Eur J Pharmacol.* 2010; 626: 297-305.

Wojtala A, Bonora M, Malinska D, Pinton P, Duszynski J, Wieckowski MR. Methods to monitor ROS production by fluorescence microscopy and fluorometry. *Methods Enzymol.* 2014; 542:243-62.

Wosniak J Jr, Santos CX, Kowaltowski AJ, Laurindo FR. Cross-talk between mitochondria and NADPH oxidase: effects of mild mitochondrial dysfunction on angiotensin II-mediated increase in Nox isoform expression and activity in vascular smooth muscle cells. *Antioxid Redox Signal.* 2009; 11:1265-78.

Xiao-Yun X, Zhuo-Xiong C, Min-Xiang L, Xingxuan H, Schuchman EH, Feng L, Han-Song X, An-Hua L. Ceramide mediates inhibition of the AKT/eNOS signalling pathway by palmitate in human vascular endothelial cells. *Med Sci Monit.* 2009; 15:BR254-61.

Xu H, Hertzel AV, Steen KA, Wang Q, Suttles J, Bernlohr DA. Uncoupling lipid metabolism from inflammation through fatty acid binding protein-dependent expression of UCP2. *Mol Cell Biol.* 2015; 35:1055-65.

Xu HE, Lambert MH, Montana VG, Parks DJ, Blanchard SG, Brown PJ, Sternbach DD, Lehmann JM, Wisely GB, Willson TM, Kliewer SA, Milburn MV. Molecular recognition of fatty acids by peroxisome proliferator activated receptors. *Mol Cell.* 1999; 3:397-403.

Xu J, Zhou Q, Xu W, Cai L. Endoplasmic reticulum stress and diabetic cardiomyopathy. *Exp Diabetes Res.* 2012; 2012: 827971.

Xu Y, Etgen GJ, Broderick CL, Canada E, Gonzalez I, Lamar J, Montrose-Rafizadeh C, Oldham BA, Osborne JJ, Xie C, Shi Q, Winneroski LL, York J, Yumibe N, Zink R, Mantlo N. Design and synthesis of dual peroxisome proliferator-activated receptors gamma and delta agonists as novel euglycemic agents with a reduced weight gain profile. *J Med Chem.* 2006; 49:5649-52.

Youssef J, Badr M. Peroxisome proliferator-activated receptors and cancer: challenges and opportunities. *Br J Pharmacol.* 2011; 164:68-82.

Yue TL, Nerurkar SS, Bao W, Jucker BM, Sarov-Blat L, Steplewski K, Ohlstein EH, Willette RN. In vivo activation of peroxisome proliferator-activated receptor-delta protects the heart from ischemia/reperfusion injury in Zucker fatty rats. *J Pharmacol Exp Ther.* 2008; 325:466-74.

Yvan-Charvet L, Welch C, Pagler TA, Ranalletta M, Lamkanfi M, Han S, Ishibashi M, Li R, Wang N, Tall AR. Increased inflammatory gene expression in ABC transporter-deficient macrophages: free cholesterol accumulation, increased

signaling via toll-like receptors, and neutrophil infiltration of atherosclerotic lesions. *Circulation.* 2008; 118:1837-47.

Zanetti M, Barazzoni R, Stebel M, Roder E, Biolo G, Baralle FE, Cattin L, Guarnieri G. Dysregulation of the endothelial nitric oxide synthase-soluble guanylate cyclase pathway is normalized by insulin in the aorta of diabetic rat. *Atherosclerosis.* 2005; 181:69-73.

Zarzuelo MJ, Jiménez R, Galindo P, Sánchez M, Nieto A, Romero M, Quintela AM, López-Sepúlveda R, Gómez-Guzmán M, Bailón E, Rodríguez-Gómez I, Zarzuelo A, Gálvez J, Tamargo J, Pérez-Vizcaíno F, Duarte J. Antihypertensive effects of peroxisome proliferator-activated receptor-β activation in spontaneously hypertensive rats. *Hypertension.* 2011; 58:733-43.

Zarzuelo MJ, Gómez-Guzmán M, Jiménez R, Quintela AM, Romero M, Sánchez M, Zarzuelo A, Tamargo J, Pérez-Vizcaíno F, Duarte J. Effects of peroxisome proliferator-activated receptor-β activation in endothelin-dependent hypertension. *Cardiovasc Res.* 2013a; 99:622-31.

Zarzuelo MJ, López-Sepúlveda R, Sánchez M, Romero M, Gómez-Guzmán M, Ungvary Z, Pérez-Vizcaíno F, Jiménez R, Duarte J. SIRT1 inhibits NADPH oxidase activation and protects endothelial function in the rat aorta: implications for vascular aging. *Biochem Pharmacol.* 2013b; 85:1288-96.

Zeng G, Nystrom FH, Ravichandran LV, Cong LN, Kirby M, Mostowski H, Quon MJ. Roles for insulin receptor, PI3-kinase, and Akt in insulin-signaling pathways related to production of nitric oxide in human vascular endothelial cells. *Circulation.* 2000; 101:1539-45.

Zeuke S, Ulmer AJ, Kusumoto S, Katus HA, Heine H. TLR4-mediated inflammatory activation of human coronary artery endothelial cells by LPS. *Cardiovasc Res.* 2002; 56:126-34.

Zhang H, Pi R, Li R, Wang P, Tang F, Zhou S, Gao J, Jiang J, Chen S, Liu P. PPARbeta/delta activation inhibits angiotensin II-induced collagen type I expression in rat cardiac fibroblasts. *Arch Biochem Biophys.* 2007; 460:25-32.

Zielonka J, Kalyanaraman B. Hydroethidine and MitoSOX-derived red fluorescence is not a reliable indicator of intracellular superoxide formation: another inconvenient truth. *Free Radic Biol Med.* 2010; 48:983-1001.

Zimmet P, Alberti KG, Shaw J. Global and societal implications of the diabetes epidemic. *Nature.* 2001; 414:782-7.